INVESTIGATIONS OF TELOMERE MAINTENANCE IN DNA DAMAGE RESPONSE DEFECTIVE CELLS AND TELOMERASE IN BRAIN TUMOURS

A thesis submitted for the degree of Doctor of Philosophy

by

Erik Cabuy

Brunel
UNIVERSITY
WEST LONDON

Division of Biosciences
School of Health Sciences and Social Care

November 2004

Abstract

Telomeres are nucleoprotein complexes located at the end of chromosomes. They have an essential role in protecting chromosome ends. Telomerase or ALT (alternative lengthening of telomeres) mechanisms maintain telomeres by compensating natural telomeric loss.

We have set up a flow-FISH method and using mouse lymphoma cell lines we identified unexpectedly the presence of subpopulations of cells with different telomere lengths. Subpopulations of cells with different telomere lengths were also observed in a human ALT and non-ALT cell line. Differences in telomere length between subpopulations of cells were significant and we term this phenomenon TELEFLUCS (TElomere LEngth FLUctuations in Cell Subpopulations).

By applying flow-FISH we could successfully measure telomere lengths during replicative senescence in human primary fibroblasts with different genetic defects that confer sensitivity to ionising radiation (IR). The results from this study, based on flow-FISH and Southern hybridisation measurements, revealed an accelerated rate of telomere shortening in radiosensitive fibroblasts. We also observed accelerated telomere shortening in murine *BRCA1* deficient cells, another defect conferring radiosensitivity, in comparison with a *BRCA1* proficient cell line. We transiently depleted BRCA1 by siRNAs in two human mammary epithelial cell lines but could not find changes in telomere length in comparison with control cells. Cytological evidence of telomere dysfunction was observed in all radiosensitive cell lines. These results suggest that mechanisms that confer sensitivity to IR may be linked with mechanisms that cause telomere dysfunction. Furthermore, we have been able to show that human ALT positive cell lines show dysfunctional telomeres as detected by either the presence of DSBs at their telomeres or cytogenetic analysis and usually cells with dysfunctional telomeres are sensitive to IR.

Finally, we assessed hTERT mRNA splicing variants and telomerase activity in brain tumours, which exhibit considerable chromosome instability suggesting that DNA repair mechanisms may be impaired. We demonstrated that high levels of hTERT mRNAs and telomerase activity correlate with proliferation rate. The presence of hTERT splice variants did not strictly correlate with absence of telomerase activity but hTERT spliced transcripts were observed in some telomerase negative brain tumours suggesting that hTERT splicing may contribute to activation of ALT mechanisms

Publications arising from this thesis

Cabuy E, Newton C, and Slijepcevic P, Role of BRCA1 in telomere maintenance in mammary epithelial cells and telomere function in ALT cells. In preparation

Glaviano A., Nayak V, Cabuy E, Slijepcevic P, Yin Z, Newson R, Rubio M, and Case CP, hTERT partially protects against metal ion induced genomic instability. Submitted

Cabuy E, Newton C, Joksic G, Woodbine L, Koller B, Jeggo PA and Slijepcevic P, Accelerated telomere shortening and telomere abnormalities in radiosensitive cell lines. Radiation Research, In press

Haines J, Johnson V, Pack K, Suraweera N, Slijepcevic P, Cabuy E, Coster M, Ilyas M, Wilding J, Sieber O, Bodmer W, Tomlinson I, and Silver A, Genetic basis of variation in adenoma multiplicity in Apc in $Apc^{Min/+}$ $Mom1^{S}$ mice. Proc. Natl. Acad. Sci 2005: 102:2868-2873

Cabuy E, Newton C, Roberts T, Newbold R, and Slijepcevic P, Identification of subpopulations of cells with different telomere lengths in mouse and human cell lines by flow FISH. Cytometry 2004; 62A:150-161

Cabuy E and de Ridder L, Telomerase activity and expression of telomerase reverse transcriptase (hTERT) correlated with cell proliferation in meningiomas and malignant brain tumors *in vivo.* Virchows Archive (International Journal of Pathology) 2001; 439: 176-184

Foreword

Early in the nineties, when I was an instrument engineer in process automation for the chemical industry, I took a sabbatical year and embarked on a world trip to visit treasures of nature. It revived the passion that I had for biology when I was only a boy and so I decided to go back studying again. When I finished my master's degree in Zoology in 1997 at the University of Ghent, Belgium my scientific research career started with a detailed anatomical study of the craniomorphology of the clariid catfish *Gymnallabes typus*. A comparison of this species with their less anguilliform relatives revealed an evolutionary trend in the reduction of the osteocranium and a spectacular enlargement of the jaw muscles. This work was done in collaboration with the Institute of Zoology, Ghent University and the Ichthyology department of the Royal Museum for Central Africa, Tervuren, Belgium and I have published this in the Journal of Morphology (Cabuy et al., 1999).

Shortly afterwards, I created the first three-dimensional reconstruction of an ant organ, the spermatheca of an *Odontomachus* ant queen, using Surfdriver software and ray-tracing rendered in Asymetrix 3D F/X at the Zoological Institute of the University of Leuven, Belgium.

In April 1999, I started working as a research fellow and teaching assistant at the University of Ghent, Faculty of Medicine, Belgium. My research was focused on telomerase and alternative splicing of hTERT mRNA in benign versus malignant brain tumours. I was also involved in two short-term research projects. The first one at the University of Bologna, Italy, where I cloned the full coding sequence of the cDNA of human β1,4 N-acetylgalactosaminyl transferase from differentiated human colon carcinoma Caco2 cells (Cabuy et al., 2002; EMBL/GenBank/DDBJ databases locus AF510036), which led to a publication in the Journal of Biochemistry (Presti LL, Cabuy E et al., 2003). This was followed by a project at the International Agency for Research on Cancer (IARC), in Lyon, France where I worked on the positional cloning of genes responsible for heritable thyroid cancers (NMTC1 and TCO). All these different work experiences and the variation of the research subjects were equally important to acquire experience and flexibility in different research fields and have been crucial in allowing me to complete this thesis. However, the main part of research presented in this thesis started later in September 2002, when Dr. Predrag Slijepcevic gave me the opportunity to work on telomere maintenance at the Institute of Cancer Genetics and Pharmacogenomics, Brunel University.

This thesis summarises the main results of telomeres and telomerase in cellular DNA damage response and in brain tumours. Research in collaboration with Dr. Patrick Case (Bristol Implant Research Centre, University of Bristol) and Dr. Andrew Silver (Colorectal Cancer Unit, St Marks Hospital, London) research group during the fulfilment of this thesis have been omitted in this thesis.

The content of this thesis have not been presented for the award of a degree at this or any other university. The data are the original work of the author except where indicated.

Acknowledgement

I could count on the help of many people, to whom I owe a debt of thanks. First and foremost, I am grateful to Dr. Predrag Slijepcevic. He encouraged me, and offered me all the opportunities to explore new paths under his expert supervision, and gave me the opportunity to complete my PhD. I also thank him for his constructive comments on the draft version of this thesis. I would like to thank Dr. Minoru Koi for acting as co-supervisor. Thanks also go to Dr. Mariann Rand-Weaver, current Director of the Department of Biosciences, for co-supporting my PhD and early submission of this thesis and approval to include previous research from Ghent University, Belgium. Special thanks go to Christine Newton for her excellent assistance in the cell culture lab work, anaphase and metaphase cell preparations. Dr. Terry Roberts was happy to share his real-time PCR TRAP assay abilities with me for the analysis of telomerase activity and I am equally grateful to him for introducing me to playing golf. I also would like to thank my former colleague Hui-Pak Wong and all present colleagues at the Institute of Cancer Genetics and Pharmacogenomics. Alison Marriott and Rana Hasan kindly provided a sample of the PC3 and 21NT pBabe hTERT cell lines. Denise May kindly took care of the orders. Margaret Kruger, former secretary of the Institute and my current landlady, was very helpful in providing me with a quiet place to work and she encouraged me throughout the project. I also would like to thank Dr. Sayori Wada, now working at the Department of Biochemistry, Kyoto prefectural University of Medicine, Japan for her support throughout my stay at Brunel University.

I am grateful to Dr. Penelope Jeggo, University of Sussex, Brighton for supplying the human fibroblast cell lines, Dr. Beverly Koller, University of North Carolina at Chapel Hill, USA for donating the mouse embryonic stem cell lines, and Dr. Silvia Baccetti, McMaster University, Canada for providing the derivative WI-38

VA13/2RA+hTERT cell line. Dr. Maria Blasco and Dr. Andrés Canela Rodriguez have been most helpful and demonstrated flow-FISH on mouse lymphoma cells at the National Centre of Biotechnology, Madrid. The TFL-Telo program was kindly provided by Dr. Peter Lansdorp, British Columbia Cancer Research Center, Vancouver, Canada.

I want to extent my gratitude to my former colleagues at the Institute of Histology, University Ghent, Belgium. I am grateful to Prof. Dr. Leo de Ridder, head of the institute, for having given me the opportunity to start research on brain cancer under his expert supervision. I would like to mention my ex-colleagues Prof. Dr. Anne Vral, Prof. Dr. Ria Cornelissen, Dr. Sylvie Mione, and Prof. Dr. Bert Thierens with whom I spent weekly progress meetings. I enjoyed the amusing coffee breaks and extraordinary Christmas parties with all other members of staff: Roger de Vos, Nelly François, Leen Pieters, Ans Baeyens, Willy Braeckman, Yvonne Van Dooren, and Marie Dobbelaere. In particular, I would like to thank Leen Pieters for processing paraffin embedded slides, Nelly François for assistance in the cell culture lab work, and Roger De Vos for solving various technically related problems. Prof. Dr. Katharina D'Herde kindly provided samples of human meninges. Thanks also to Dr. Karel Dhaene from the Laboratory of Pathology, University Hospital of Antwerp for guiding me into the initial steps of PCR. I was honoured to work with the following neurosurgeons who kindly provided me with tumour samples and introduced me to their skills in brain surgery: Dr. Jacques Caemaert, Dr. Tom Vandekerckhove, and Dr. Jean-Pierre Kalala Okito of the University Hospital; and Dr. Dirk de Ridder and Dr. Luc De Waele of the St. Lucas Hospital in Ghent, Belgium.

And last but not least, I would like to express my gratitude to Rita Cuypers for her support during my studies in engineering (electromechanics), science (zoology) and research.

The work was performed for this thesis by a grant to Dr. Predrag Slijepcevic from the Department of Health (RRX97), UK and EC Euratom (Figh-CT-2002-00217). The University of Ghent, Faculty of Medicine, Laboratory of Anatomy, Embryology, Histology and Medial Physics, Belgium supported Chapter 6 of this thesis.

Abbreviations

ALT	alternative lengthening of telomeres
AT	ataxia-telangiectasia
ATM	ataxia-telangiectasia, mutated
APB	ALT-associated PML nuclear body
APS	ammonium persulfate
ATCC	American type culture collection
bp	base pair
BRCA1 (2)	breast cancer gene 1 (2)
BrdU	5-bromo-2'deoxyuridine
BSA	bovine serum albumin
cDNA	complementary DNA
CHAPS	3-[(3-Cholamidopropyl)dimethylamminio]-1-propanesulfonate
CLDT	chromatids lacking detectable telomere
CO-FISH	chromosome-orientation fluorescence in situ hybridisation
DAB	diaminobenzidine
DAPI	4', 6-diamidino-2-phenylindole
DEPC	diethyl pyrocarbonate
DIG	digoxigenin
DMEM	dulbecco's modified eagle's medium
DMSO	dimethylsulfoxide
DNA-PK	DNA-dependent protein kinase
DNA-PKcs	DNA-dependent protein kinase catalytic subunit
DSBs	double strand breaks
DTT	dithiotreitol
dUTP	deoxyuridinetriphosphate
ECTF	extra chromosomal telomeric fragments
EDTA	ethylenediaminetetraacetic acid
EGF	epidermal growth factor
ELISA	enzyme-linked immunosorbent assay
EtBr	ethidiumbromide
FA	fanconi anemia
FITC	fluorescein isothiocyanate
flow-FISH	flow cytometric FISH
GBM	glioblastoma multiforme
Gy	Gray (unit of dosage of radiation)
HBSS	hepes buffered saline solution
H-E	hematoxylin eosin
HEPES	n-2-hydroxyethylpiperazine-n'-2-ethanesulfonic acid
HMEC	human mammary epithelial cells
HPA	hybridisation protection assay
HR	homologous recombination
HRP	horseradish peroxidase
hTERC	human telomerase RNA component
hTERT	human telomerase reverse transcriptase
IR	Ionising radiation
kDa	kilo Daltons
LI	labelling index
LY-R	L5178Y mouse radioresistant lymphoma cells
LY-S	L5178Y mouse radiosensitive cells
MEBM	mammary epithelial basal medium
MEF	mouse embryonic fibroblast
MMLV	moloney murine leukaemia virus
MOLT-4	human T lymphoblastic leukaemia

NHEJ	non-homologous end-joining
NBS	nijmegen breakage syndrome
NHR	non-homologous recombination
OD	optical densitometry
PAGE	polyacrylamide gel electrophoresis
PARP	poly (ADP-ribose) polymerase
PBS	phosphate buffered saline
PCNA	proliferating cell nuclear antigen
PD	population doublings
PI	propidium iodide
PML	promyelocytic leukaemia
PMSF	phenylmethylsulfonylfluoride
PNA	peptide nucleic acid
Q-FISH	quantitative fluorescence in situ hybridisation
RNase	RNA nuclease
rpm	revolutions per minute
RT	room temperature
RT-PCR	reverse transcriptase polymerase chain reaction
scid	severe combined immunodeficiency
SD	standard deviation
SDS	sodium dodecyl sulfate
SE	standard error of mean
siRNA	small interfering RNA
SSA	single-strand annealing
SSC	sodium chloride sodium citric acid
TAE	tris acetic acid + ethylenediaminetetra acetic acid
TBE	tris boric acid + ethylenediaminetetra acetic acid
TBS	tris buffered saline
hTERT	human catalytic subunit of telomerase
TdT	terminal deoxynucleotidyl transferase)
TE	tris-EDTA
TEMED	N,N,N',N'-tetramethylethylenediamine
hTR	human RNA subunit of telomerase
TFI	telomere fluorescence intensity
TR	Texas red
TRAP-assay	telomeric repeat amplification protocol
Tris	tris(hydroxymethyl)methyl-2-aminoethane-sulfonic acid
TRF	terminal restriction fragment
TRF1	telomeric repeat binding factor 1
TRF2	telomeric repeat binding factor 2
TRITC	tetramethylrhodamine isothiocyanate
TUNEL	terminal deoxynucleotidyl transferase [TdT]-mediated deoxyuridinetriphosphate [dUTP] nick end labelling
Tween-20	polyxyethylene-sorbitan monolaurate
V(D)J	variable (diversity) joining (recombination)
WHO	world health organisation
XP	xeroderma pigmentosum
XRCC	X-ray cross complementing

Table of Contents

List of tables

List of figures

CHAPTER 1

GENERAL INTRODUCTION

1.1 Introduction

Eukaryotic cells have intricate networks of mechanisms designed to protect chromosomal and genomic stability. These include mechanisms that sense, signal and repair DNA damage, mechanisms responsible for cell-cycle checkpoint control and also mechanisms that control apoptosis (Shiloh and Lemann, 2004). An appropriate collective name for these mechanisms is “DNA damage response”. It is becoming increasingly clear that telomeres, specialized structures at chromosome ends, play a role in DNA damage response either directly or indirectly. Here, we will review telomere biology, assess the importance of telomeres in DNA damage response and discuss the role of telomerase in brain tumorigenesis.

1.2 Structure and function of telomeres

Telomeres are long repetitive nucleotide sequences at the ends of chromosomes. In normal human cells, the telomeres contain up to 15kb of tandem

repeats of a G rich hexanucleotide TTAGGG. When DNA replicates, one strand is replicated by leading-strand DNA synthesis and the other by lagging-strand synthesis. Owing to the replication properties of mammalian polymerases it has been thought in the past that two strands of telomeric DNA will have different terminal structures immediately following replication: the leading-strand telomere will be blunt-ended and the lagging-strand telomere will have a 3' overhang (see conventional model in Figure 1.1.). The size of this 3' overhang should be equivalent to the size of an RNA primer i.e. 8-12 base pairs (bp). The loss of these 8-12 bp, which must occur in each cell cycle, is also known as the end replication problem (Olovnikov, 1973). However, measurements of telomere length in dividing cells revealed a much greater loss, 50-150 bp/cell division (Harley et al., 1990). Therefore, additional mechanisms must be responsible for this loss and experimental evidence indicate that an exonucleolytic activity will modify telomeric DNA in a way that both strands of newly replicated DNA will have single-strand overhangs the size of which is ~ 200 bp (Makarov et al., 1997; McElligot and Wellinger, 1997; see also revised model in Figure 1.1).

Telomere erosion is cumulative. It is thought that this telomere shortening process ultimately limits the capacity of a cell to divide (Olovnikov, 1973), and acts as a powerful tumour suppressor mechanism. It eventually produces an altered telomere structure, which either activates a DNA damage response (d'Adda di Fagagna et al., 2003; Takai et al., 2003), or leads to repair-mediated chromosome rearrangements causing dicentric (fused) chromosomes. Therefore, gradual telomere shortening in normal human somatic cells during consecutive rounds of replication eventually leads to critically short telomeres that induce replicative senescence *in vitro* and *in vivo* (Harley et al., 1990; Lindsey et al., 1991).

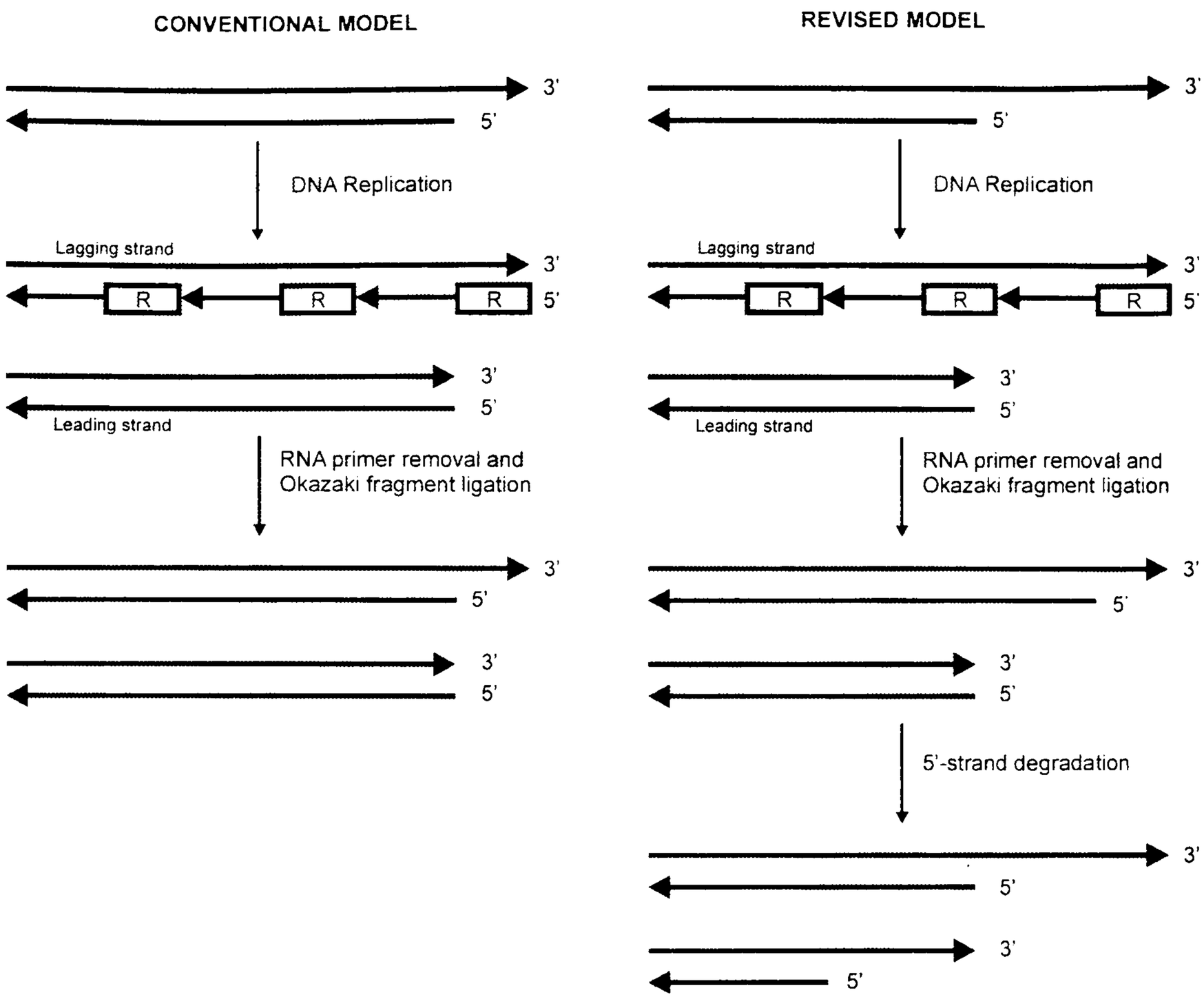

Figure 1.1 Schematic overview of the end replication problem during DNA replication by DNA-dependent DNA polymerases (adapted from Slijepcevic, 1998). Because an RNA primer (R) primes synthesis of the lagging strand, removal of the RNA primer leaves a gap of 8-12 bp (conventional model) (Wright et al., 1997). However, degradation of the 5' ends by exonuclease activity shortens the strand further (Wellinger et al., 1996, Makarov et al., 1997) (revised model).

The telomeric DNA forms a loop structure, which effectively hides the end of chromosomal DNA from DNA damage recognition mechanisms. A G-rich overhang at the extreme 3'-end of each DNA strand which is approximately 200 ± 75 nucleotides long serves as a substrate for proteins in telomere replication and participates in the formation of the t- and D-loop structures (Griffith et al., 1999; Munoz-Jordan et al., 2001). The G-rich overhang has the ability to fold backwards and bond with one of the two duplex telomere strands forming a t-loop and the free 3'-end inserts between the two strands, forming a minor D-loop (Figure 1.2). Free 3'-end may be recognised as DNA strand breaks that can activate the checkpoints of the DNA repair apparatus,

which probably could initiate the process of cellular senescence and apoptosis. Thus, the loop structures sequester the free 3'-ends, preventing DNA damage and activation of repair signals and therefore provide stability to the chromosome. This structure critically depends on a telomere binding protein TRF2, but is maintained by many other proteins (see section 1.3). This structure is also thought to be dynamic, as several proteins need to access the extreme terminus of linear DNA (Bryan et al., 1997).

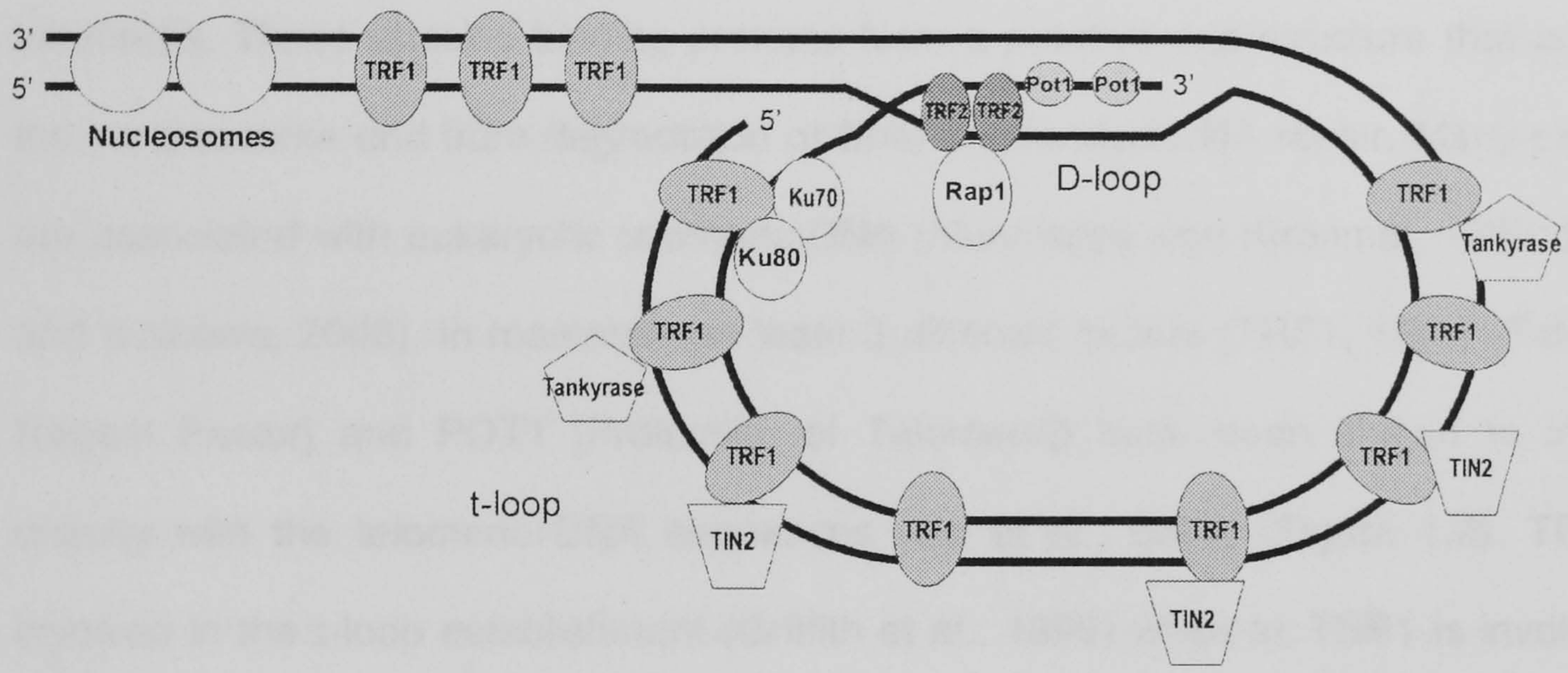

Figure 1.2 Model for mammalian telomere structure (adapted from Kanoh and Ishikawa, 2003; Niedle and Parkinson, 2003). Human telomeres consist of up to 15 kbp of double-stranded DNA, which at the extreme end bends backward to form a loop structure (t-loop). The G-strand overhang invades part of its upstream sequence to form a D-loop. Most of the telomere is packaged into nucleosomes, but at the extreme end a few 100 bp of telomeric DNA is associated with TRF1 and TRF2. TRF1 forms complexes with two other telomeric proteins, TIN2 and Tankyrase. TRF2 recruits RAP1. In addition to the Ku proteins shown here, the MRE11-RAD50-NBS1 complex that are involved in double-stranded DNA repair is also localised at telomeres (Rhodes et al., 2002). The single stranded G-rich overhang binds POT1.

The primary role of telomeres is to protect chromosome ends from aberrant chromosomal recombination, end-to-end fusions, and DNA degradation (Blackburn, 1991). They protect chromosome ends from accidental chromosome breakage that would otherwise trigger DNA damage response mechanisms and promote cell-cycle arrest and DNA repair. In addition to the physical protection of chromosome ends,

eukaryotic telomeres have important roles in cellular processes including chromatin organisation and control of cell proliferation (Hackett et al., 2001).

1.3 Telomere binding proteins

An important aspect of telomere structure and function is the interaction of the repeat sequences with specific binding proteins and associated factors, which are essential for both the regulation of telomere length and the capping function of telomeres. These specific binding proteins form a putative cap structure that protects the chromosome end from degradation or from unintended DNA repair. Many proteins are associated with eukaryotic telomeric DNA (Muniyappa and Kironmai, 1998; Kanoh and Ishikawa, 2003). In mammals, at least 3 different factors (TRF1, TRF2 [Telomere Repeat Factor] and POT1 [Protection of Telomere]) have been shown to interact directly with the telomeric DNA sequences (Liu et al., 2004) (Figure 1.2). TRF2 is involved in the t-loop establishment (Griffith et al., 1999) whereas TRF1 is involved in the control of telomere length homeostasis (van Steensel and de Lange, 1997). Four additional telomere-associated proteins (TIN2 [TRF1-Interacting Nuclear protein 2], RAP1 [Repressor Activator Protein 1], TANK1 and TANK2 [TANKyrase]) are also localised at telomeres but through their binding with above mentioned three proteins (Ye and de Lange, 2004). Other proteins, involved in DNA repair including the MRE11-RAD50-NBS1 (MRN) complex or the DNA-dependent protein kinase complex composed of Ku (DNA end binding subunit) and DNA-PKcs (catalytic subunit) are also present at telomeres (Song et al., 2000; Wu et al., 2000; Zhu et al., 2000; reviewed in Bailey and Goodwin, 2004). Some of these proteins have effects on telomere length, the structure of G-rich overhangs and can affect other cell phenotypes. Other genes involved in telomere maintenance include genes encoding telomerase associated proteins (hTERT and hTERC) and other DNA repair proteins RAD54, RAD51D, ERCC1/XPF (for recent reviews see Chan and Blackburn, 2002; Wei et al., 2002; Blasco & Hahn. 2003; Slijepcevic, 2004).

Expression of truncated forms of TRF1 and its interacting factor TIN2 induce inappropriate telomere elongation in telomerase-positive cells (van Steensel and de Lange, 1997; Kim et al., 1999; Smogorzewska et al., 2000). Inhibition of TRF2 in cultured cells results in "deprotection" of chromosome ends and covalently fused telomeres (van Steensel et al., 1998). Additionally, loss of TRF2 function can lead to growth arrest and ATM/p53 mediated apoptosis (van Steensel et al., 1998; Karlseder et al., 1999). Both TRF1 and TRF2 are characterised as negative regulators of telomere length i.e. overexpression of either results in gradual length decline (van Steensel and de Lange, 1997; Smogorzewska et al., 2000). Telomere binding proteins are therefore critical regulators of telomere length and essential components of the protective structures that are formed at the chromosome ends.

1.4 Telomere maintenance by telomerase

In most organisms complete replication of telomeres is accomplished by telomerase, a specialised reverse transcriptase that was first isolated from the ciliate *Tetrahymena* (Greider and Blackburn, 1985). Telomerase, or telomere terminal transferase, is a ribonucleoprotein that adds telomeric repeats onto chromosomal ends by using the RNA template complementary to the $(TTAGGG)_n$ repeats (Blackburn, 1991; Feng et al., 1995). Its occurrence is widely conserved in eukaryotes, as revealed by phylogenetic comparison. For many years it was assumed since the first report on telomerase activity in cancer (Kim et al., 1994) that normal human somatic cells lack telomerase activity. However, a recent study suggested that normal human somatic cells such as fibroblasts may show low telomerase activity as revealed by immunological detection of telomerase catalytic component in these cells (Masutomi et al., 2003; see also Chapter 6). In contrast, high telomerase activity has been detected in most human cancers (Kim and Wu, 1997; Meeker and Coffey, 1997; reviewed in Dhaene et al., 2000), suggesting a role for telomerase in providing a proliferative capacity to cells, which is a requirement for progression towards malignancy.

Telomerase is also detected in stem cells, during embryonic development (Ulaner and Guidice, 1997; Ulaner et al., 1998), and in adult germ-line tissues (Wright et al., 1996). It has been hypothesized that cell senescence can be overcome by upregulation of telomerase (Blackburn, 1991; Feng et al., 1995; Kim and Wu, 1997). Experiments by Bodnar et al. (1998) confirmed that this is the case.

The length of telomeres and G-rich overhangs and the levels of the telomerase subunits are indirect indicators of the enzyme function that can be assessed in various samples. Telomeres are thought to control the expression of subtelomeric genes, a phenomenon known as telomere position effect (Baur et al., 2001), and therefore paradoxically this might affect the expression of telomerase itself, which is located at the extreme end of chromosome 5p in humans (Meyerson et al., 1997; Kilian et al., 1997). Most studies have implicated telomerase in the maintenance of stable telomere length although telomere length can, in some cases, be maintained in the absence of telomerase by mechanisms referred to as alternative lengthening of telomeres (ALT), which is discussed in section 1.5.

1.4.1 Telomerase components

Telomerase is a large complex, with an estimated molecular mass of over 1000 kDa (Schnapp et al., 1998). *In vitro*, 2 components are absolutely essential for the telomerase activity: hTERT (hTERCT, hEST) the human reverse transcriptase (Kilian et al., 1997, Nakayama et al., 1998) and hTERC (TER, hTR), the RNA template (Feng et al., 1995; Weinrich et al., 1997). However, telomerase has been found to have several additional components, including two heat shock proteins (HSP90 and HSP23) and the telomerase-associated protein hTEP1 that assists in the function of telomerase (Harrington et al., 1997). HSP90 functions as an activator of telomerase catalytic activity, but the precise function of hTEP1 is unclear. While hTEP1 is not required for telomerase activity, it is thought to function as a structure component, contributing to the stability of the telomerase protein-RNA complex (Kickhoefer et al., 2001). In normal

cells hTERC is constitutively expressed but hTERT was found to be absent or low in many studies (Meyerson et al., 1997; Kanaya et al., 1998; Ramakrishnan et al., 1998; Kyo et al., 1999; Takakura et al., 1998 Dhaene et al., 2000). However, a recent study suggests that a good-quality antibody can detect hTERT in human primary fibroblasts (Masutomi et al., 2003). In most tumours over-expression of hTERT is accompanied by an increase in telomerase activity. hTERC and hTERT are indispensable for telomerase activity, and expression of these subunits *in vitro* leads to the formation of a functional telomerase enzyme (Counter et al., 1992; Weinrich et al., 1997; Nakayama et al., 1998).

1.4.1.1 hTERC (human TElomerase RNA Component)

hTERC, the RNA component of the telomerase complex, acts as the template for telomere elongation. In *in vitro* reconstitution experiments, hTERC RNA was one of the 2 components essential in obtaining telomerase activity (Weinrich et al., 1997). The *hTERC* gene was cloned and was located on human chromosome 3q26.3 (Feng et al., 1995). This single-copy gene does not contain any introns.

Expression of hTERC RNA, as analysed by RT-PCR, showed that this component is widely expressed in both tumour and non-tumour tissues (Feng et al., 1995; Yi et al., 2001). Thus, it was concluded that hTERC was not essential for telomerase reactivation. However, using *in situ* hybridisation, other investigators observed that hTERC expression is up-regulated in tumour tissues (Heine et al., 1998; Soder et al., 1998). A weak expression in some normal renal parenchymal cells, gastric mucosa epithelial cells, smooth muscle cells, Schwann cells of peripheral nerves and activated lymphocytes was occasionally detected (Heine et al., 1998; Paradis et al., 1999; Hiyama et al., 1999). However, RT-PCR for hTERC is error prone, as the absence of introns make it impossible to distinguish the cDNA-based PCR product from the genomic DNA-based product. It is therefore necessary to perform a DNase I digestion of RNA preparations to overcome this problem. Using this technique, hTERC

expression was found to be correlated with telomerase activity in colorectal cancer (Yan et al., 2001), indicating that this gene might play a role during the process of telomerase reactivation.

In humans, the mature hTERC transcript is 451 nucleotides long and lacks a polyA tail. The RNA contains a template region of 11 nucleotides 5'-CUAACCCUAAC-3' located in the 5' extremity. Although hTERC RNA sequences are phylogenetically divergent, their secondary structures have been found to be similar from ciliates to vertebrates (Chen et al., 2000). Recent studies reported the presence of a classical small nucleolar RNA (snoRNA) structure called H/ACA box (Mitchell et al., 1999). This motif consists of a hairpin-hinge-hairpin-ACA-tail. The H/ACA structure is essential for accumulation of hTERC RNA *in vivo* (Mitchell and Collins, 2000). Several proteins, including dyskerin or snoRNP recognise this sequence and may be involved in the RNA stability. This role can be provided by a heterologous H/ACA domain when substituting hTERC H/ACA domain (Mitchell et al., 1999). Moreover, the H/ACA motif is also crucial for telomerase activity *in vivo*, a role which can not be replaced by a heterologous domain. Furthermore, 2 other elements in the H/ACA 5' neighbour hairpin (HS1 also called CR4-CR5) are also required for the hTERT-hTERC interaction *in vivo* (Mitchell and Collins., 2000; Bachand et al., 2001; Chen et al., 2002). Finally, a pseudoknot has been also found to play a role in hTERC RNA stability (Gilley and Blackburn, 1999).

1.4.1.2 hTERT (human TElomerase Reverse Transcriptase)

hTERT is the catalytic subunit of telomerase and harbours the reverse transcriptase activity. Presence of this subunit was first suggested in 1989 in crude nuclear HeLa fractions in which the activity of the human telomerase was identified (Morin, 1989). Using sequences derived from *Saccharomyces cerevisiae* and *Euplotes aediculatus* catalytic subunits, the corresponding human cDNA was isolated in 1997 (Kilian et al., 1997; Meyerson et al., 1997). However, the genomic sequence and the

gene organisation were only characterised in 1999 by several groups (Cong et al., 1999; Horikawa et al., 1999; Takakura et al., 1999; Wick et al., 1999). The single-copy *hTERT* gene is composed of 16 exons and 15 introns spanning more than 40 kb. Using fluorescence *in situ* hybridisation (FISH), the *hTERT* gene was localised on human chromosome 5p15.33, very close to the telomere (Meyerson et al., 1997; Bryce et al., 2000). The *hTERT* gene encodes a 127 kDa protein of 1132 amino acids (Meyerson et al., 1997). This protein is almost exclusively localised in the nucleus (Harrington et al., 1997). hTERT protein presents a telomerase-specific motif (T), followed by 7 conserved RT (Reverse Transcriptase) motifs (1 and 2, A-E) , forming a finger-palm-thumb structure (Lingner et al., 1997; Nakamura et al., 1997).

Phylogenetic studies showed that the reverse transcriptase subunit is very well conserved from protozoa to humans, including plants. The RT motifs are also shared by viruses and retroelements, indicating that the use of telomerase to maintain telomere length might be ancient (Nakamura and Cech, 1998). RT motifs are very important for the reverse transcriptase activity as mutations in amino acids in these motifs prevented telomerase activity (Harrington et al., 1997; Weinrich et al., 1997; Nakayama et al., 1998). Through these motifs, hTERT protein recognises the RNA template and reversibly transcribes the telomeric motif, which leads to telomere elongation. In the basic mechanism, the telomerase complex is located at the 3' extremity of the leading strand. hTERC is correctly positioned through its sequences adjacent to the template region. Elongation is then performed by the catalytic subunit hTERT, until the end of the template region. Following this step, the complex is translocated and repositioned on the newly synthesised DNA, in order to continue telomere elongation. Finally, the lagging strand is replicated by DNA polymerases. The region containing the RT motifs has also been shown to bind hTP1 protein, independent of the hTERC binding (Beattie et al., 2000).

Telomerase adds telomeric repeats on to the ends of chromosomes, thus maintaining their length despite continued cell division. It is postulated that, at crisis,

critical telomere shortening results in end-to-end fusions and chromosome breakage–fusion cycles that cause marked chromosomal abnormalities and apoptosis (Londoño-Vallejo, 2004). Expression of telomerase would avoid this catastrophic series of events. This model is supported by the demonstration that forced expression of telomerase allows maintenance of telomere length and increases the replicative lifespan of some cell types without a crisis period (Zhu et al., 1999). However, events additional to forced hTERT expression might be required to gain full telomerase activity and cell immortalisation. Nevertheless, telomerase expression might be a critical step in the immortalisation process during oncogenesis. In telomerase-null yeast, increased mutation rates and genomic instability were observed, suggesting that telomerase can prevent chromosomal instability (Hackett et al., 2001). Lack of telomerase in mouse leads to chromosomal instability (Blasco et al., 1997).

1.4.2 Regulation of telomerase activity

The current picture of telomerase regulation is complex. Enzyme activity is likely to be controlled at several levels, with multiple pathways converging to modulate the functional activity of the holoenzyme. Although the story is far from complete, several regulatory pathways have already been implicated in the normal and aberrant activity of telomerase in human cells. Extensive evidence from expression studies suggests that *hTERC* and *hTERT* are regulated on a transcriptional level and that this regulation is a major deterministic factor governing the activation of telomerase activity in normal and cancer cells. Although much remains to be clarified, cloning of the promoter regions for the genes encoding *hTERC* and *hTERT* has enabled the identification of several positive and negative regulators of telomerase transcription (Ducrest et al., 2002).

Telomerase activity can be reconstituted *in vitro* from its two essential subunits, hTERC and hTERT, although the enzyme exists in its active form at the telomere as a highly ordered multi-subunit complex. The structure of the holoenzyme therefore

represents another level at which telomerase activity is likely to be regulated. Some of the constituent proteins that contribute to the complex have intrinsic regulatory functions, such as the poly (ADP-ribose)polymerase (PARP) domain of tankyrase, a protein identified as interacting with the telomeric-repeat-binding factor TRF1 at the telomere. PARP activity is a major mechanism for post-translational regulation of nuclear proteins involved in a variety of cellular functions such as the DNA damage response. It is now clear that these other post-translational signalling events acting directly on hTERT or on other proteins involved in the complex play a role in regulation of telomerase activity. The phosphorylation status of hTERT is also involved in modulation of the catalytic activity of telomerase: both protein phosphatase 2A and the c-Abl tyrosine kinase act as negative regulators of telomerase function, whereas protein kinase C (PKC) and the Akt protein kinase upregulate activity. Previous studies have shown that c-Myc stimulates hTERT transcription through the binding sites located on the *hTERT* promoter (Zhou and Liu, 2003; Wang and Zhu, 2004). Recently, evidence has been provided that the BRCA1 protein binds to the c-Myc protein, turns off the transcription of *hTERT*, and prevents incidental cellular immortalisation (Li et al., 2002; Xiong et al., 2003; Zhou and Liu, 2003).

Transcription of eukaryotic genes produces mRNA precursors, which must be processed by RNA splicing, precisely removing the introns and joining together the exons, before the spliced mRNA is exported to the cytoplasm for translation. Splicing of mRNA precursors is carried out by complex particles called spliceosomes, which are assembled from several small nuclear ribonucleoprotein components (snoRNPs) and contain about 100 different proteins. These post-transcriptional mechanisms could play a role in regulating telomerase activity. Kilian et al. (1997) identified several splice variants of the hTERT transcript that are expected to be inactive due to truncations or mutations in domains essential for catalytic activity. The hTERT alternative splicing transcripts include a deletion variant lacking conserved residues from the catalytic core component of the protein (Kilian et al., 1997). This hTERT splice variant, termed

hTERT α, has been identified as a dominant negative inhibitor of telomerase activity (Colgin et al., 2000; Yi et al., 2000). It is expressed in normal and developing tissues (Ulaner et al., 1997) and it appears conceivable that it may be expressed in some ALT cell lines or tumour tissues. Repetitive hTERT α- inhibits telomerase activities in telomerase-positive cells, which results in telomere shortening and chromosome end-to-end fusions (Colgin et al., 2000). These results suggest a possible role for hTERT splice variants in the regulation of telomerase activity. The function of the remaining splice variants of hTERT is still unclear; it is generally accepted that these cannot play a role in the activation of telomerase, since they lack key reverse transcriptase or C-terminal sequences as a result of open reading frame shifts and premature stop codons (Wick et al., 1999). It might be of much interest to examine more precisely the role that alternative splicing might play in the regulation of telomerase activity, particularly in ALT cell lines.

1.5 Alternative lengthening of telomeres

Several distinct strategies for telomere length maintenance have evolved in eukaryotes. As we have seen, telomeres can be elongated independently of the rest of the genome by telomerase. Although telomerase appears responsible for telomere maintenance in most cases, telomerase activity is not detected by the standard TRAP (telomeric repeat amplification protocol) assay in ~ 5-10% of human cancers (Kim et al., 1994) and the mechanism by which these cells acquire telomere elongation is not fully understood. Therefore, telomerase cannot be the only mechanism of telomere maintenance.

Drosophila melanogaster and related dipterans employ retrotransposons in telomere maintenance instead of telomerase (Mason and Biessmann, 1995). Homologous recombination (see section 1.6.2) is used for telomere elongation in the mosquito *Anopheles gambiae* (Roth et al., 1997). In the case of telomerase-defective yeast, rare survivors are able to elongate their telomeres via recombination events that

are dependent on the DNA double-strand break repair gene *RAD52* (Lundblad and Blackburn, 1993; Teng and Zakian, 1999). Similarly, homologous recombination was proposed in humans as a mechanism to elongate telomeres by the formation of intertelomeric, T-loop (to allow the 3' extremity to copy itself), and rolling circle and integration of extrachromosomal telomeric repeats (Yeager et al., 1999; Reddel et al., 2001; Henson et al., 2002; Tomaska et al., 2004). Homologous recombination is also a leading candidate mechanism for telomere lengthening (Henson et al., 2002) known as ALT (Bryan et al., 1995; 1997).

Telomere morphology and function in ALT cells appear to differ significantly from cells with telomerase activity (Ford et al., 2001; Perrem et al., 2001; Scheel et al., 2001). The existence of ALT has been deduced from the observation of heterogeneous and elongated telomeres in the absence of detectable telomerase (Murane et al., 1994). ALT tumours and some *in vitro* immortalised cell lines have telomeres that are highly heterogeneous in length, ranging from 3 kb to 50 kb (Bryan et al., 1997; Grobelny et al., 2000), a range notably higher than the maximum length in non-neoplastic somatic tissues (~10-15 kb in humans). Analysis using Q-FISH revealed strong telomeric signals in some chromosomes and its complete absence in other chromosomes (Ford et al., 2001; Lansdorp et al., 1997; Perrem et al., 2001; Scheel et al., 2001). The occurrence of elongated and shortened telomeres and signal-free chromosome ends could give rise to chromosomal end-to-end associations and breakage-fusion-bridge cycles, resulting in an increased number of complex non-reciprocal chromosomal rearrangements (McClintock, 1941).

Another potential useful morphological marker of ALT is ALT-associated PML (promyelocytic leukaemia) bodies (APBs) (Yeager et al., 1999). APBs are unique because of their association with telomeric DNA in ALT cells as revealed by fluorescence *in situ* hybridisation (FISH) or the immunological detection of TRF1 and TRF2. APBs contain PML, MRE11, NBS1, RAD50, and BLM that normally exist in PML bodies. In promyelocytic leukaemia, the PML protein forms a fusion protein with retinoic

acid receptor α (RARα) due to a chromosome 15;17 translocation, which disrupts PML bodies (de Thé et al., 1991). In addition, APBs contain the telomere-associating protein RAP1 and the recombination proteins RAD51, RAD52, and BRCA1, which are not normally present in PML bodies (Yeager et al., 1999; Naka et al., 2002; Wu et al., 2000; 2003). Nabetani et al. (2004) reported that hRAD9, hHUS1, hRAD1, and hRAD17 are also constitutive components of APBs. Furthermore, 5-bromo-2'deoxyuridine (BrdU) incorporation was detected at the NBS1 foci in a small fraction of growing ALT cells, suggesting that DNA is synthesised at APBs (Wu et al., 2000). These nuclear bodies probably function in the process of telomere lengthening through recombination, because they appear at exactly the same time as the activation of the ALT mechanism during cell immortalisation, and because these nuclear bodies include RPA, RAD51, and RAD52 (Yeager et al., 1999). APB bodies can be found in 5% of interphase nuclei and it would therefore appear feasible to detect them by immunohistochemistry. Evidence of APBs is provided by co-localisation of PML with either TRF1 and/or TRF2 (Yeager et al., 1999).

ALT has been found in a subset of *in vitro* immortalised and tumour-derived cell lines as well as in spontaneous human tumours (Reddel et al., 2001). The types of tumours and tumour cell lines in which ALT has been observed include, ovarian epithelium (Grobelny et al., 2000), osteosarcoma (Scheel et al., 2001), glioblastoma (Hakin-Smith et al., 2003), and renal cell carcinoma (Mehle et al., 1996). Although it was not mentioned by the authors, ALT was probably also present in one case of malignant meningiomas (case 30) showing no telomerase activity and telomere length greater than 25kbp (Chen et al., 2000). Genetic changes known to promote ALT activation include transformation of cells with SV-40 or human papillomavirus (HPV) oncogenes and spontaneous loss of the tumour suppressors p53 and $p16^{INK4a}$ (Bryan et al., 1995).

Notably, not all tumours without telomerase activity have ALT-like telomeres (Bryan et al.. 1997). Perhaps some of these findings reflect tumours that presented

clinically before immortalisation. Therefore, not all of the approximately 10% telomerase-negative tumours display the telomere morphology characteristic of ALT. However, the possibility that there are other mechanisms independent of telomerase and that do not exhibit the ALT pattern of telomere morphology cannot be excluded. Some telomerase-positive tumours were shown to have elongated and heterogeneous telomeres, which could indicate a coexistence of ALT and telomerase activity (Bryan et al., 1997; Reddel et al., 2001). Coexistence of ALT and telomerase has been described in three recent studies (Cerone et al., 2001; Grobelny et al., 2001; Perrem et al., 2001). So far, no extensive surveys for ALT in human tumours have been carried out, but a variety of malignant human tumours may exhibit ALT (Bryan et al., 1997; Mehle et al., 1996; Scheel et al., 2001). Cell lines with ALT phenotype are being used in an ongoing study of which the first results are described in Chapter 6.

1.6 Telomeres and DNA damage response

The evidence is accumulating that telomeres may be involved in DNA damage response. For example, mice lacking functional telomerase, the enzyme that synthesizes telomeric DNA, are radiosensitive (Wong et al., 2000, Goytisolo et al., 2000). In addition, ataxia telangiectasia patients, characterized by altered DNA damage response, show altered telomere maintenance (Metcalfe et al., 1996). Similarly, several genetically deficient strains of mice including *Ku*$^{-/-}$, *PARP*$^{-/-}$ and scid (severe combined immunodeficiency) mice show defective DNA damage response and altered telomere maintenance (Hande et al., 1999; d'Adda di Faggagna et al.; 1999, Samper et al., 2000). Also yeast and *Caenorhabditis elegans* mutants with altered telomeres have defective DNA damage responses (Boulton and Jackson 1996, Ahmed and Hodgkin 2000). Taken together these results argue that telomere maintenance is a part of the DNA damage response machinery. This possibility is strengthened by recent studies showing an inverse correlation between chromosomal radiosensitivity and telomere length in a group of 29 breast cancer patients (McIlrath et al., 2001) or a larger group of

different cancer patients (Wu et al., 2003). In this section we will review the role of telomeres in DNA damage response, especially how the cell's response to DNA breakage is linked with telomere maintenance.

1.6.1 Telomeres and repair of DNA double strand breaks (DSBs)

DNA double strand breaks (DSBs) are the most lethal form of DNA damage. They occur in response to ionising radiation (IR), to chemotherapeutic or radiomimetic agents (e.g. bleomycin, mitomycin C, cisplatinum, methylmethanesulfonate), as well as to endogenous free radicals, the by-products of oxidative metabolism. DSBs also arise as a consequence of natural processes, such as V(D)J recombination (a lymphoid specific process required for gene rearrangement and maturation of T and B cells), and as a consequence of normal cellular metabolism. If not repaired prior to DNA replication or mitosis, DSBs can induce cell death. If misrepaired, DSBs have the potential to lead to chromosome translocations, genomic instability and cancer predisposition. The mechanisms responding to DSBs include pathways of DNA repair, cell cycle checkpoint arrest and apoptosis (Jeggo and Concannon, 2001). Cell cycle checkpoint controls may serve to prevent cells from initiating critical steps, such as DNA replication and mitosis in the presence of DSBs. There are two major pathways for the repair of DSBs in mammalian cells, namely homologous recombination (HR) and non-homologous end joining (NHEJ). Telomere maintenance is linked with both pathways as indicated by telomere dysfunction and changes in telomere length regulation in the absence of proteins involved in HR and NHEJ (see below).

1.6.2 Homologous recombination (HR)

HR repairs a DSB in one DNA molecule by using a second, homologous molecule as a template for DNA synthesis and repair, thereby enabling coding information lost at the site of the break to be retrieved (Figure 1.3). HR, therefore, has the potential to be a highly accurate and efficient pathway for repairing DSBs. HR is

important during and following DNA replication, when a sister chromatid is present as a template for repair.

In the early steps of HR processing (Figure 1.3), the MRE11-RAD50-NBS1 (MRN) heterotrimeric complex will initially process the DSB. The MRN complex, which has exonuclease and endonuclease functions, acts to produce and expose single stranded tailed DNA (Rattray and Symington, 1995).

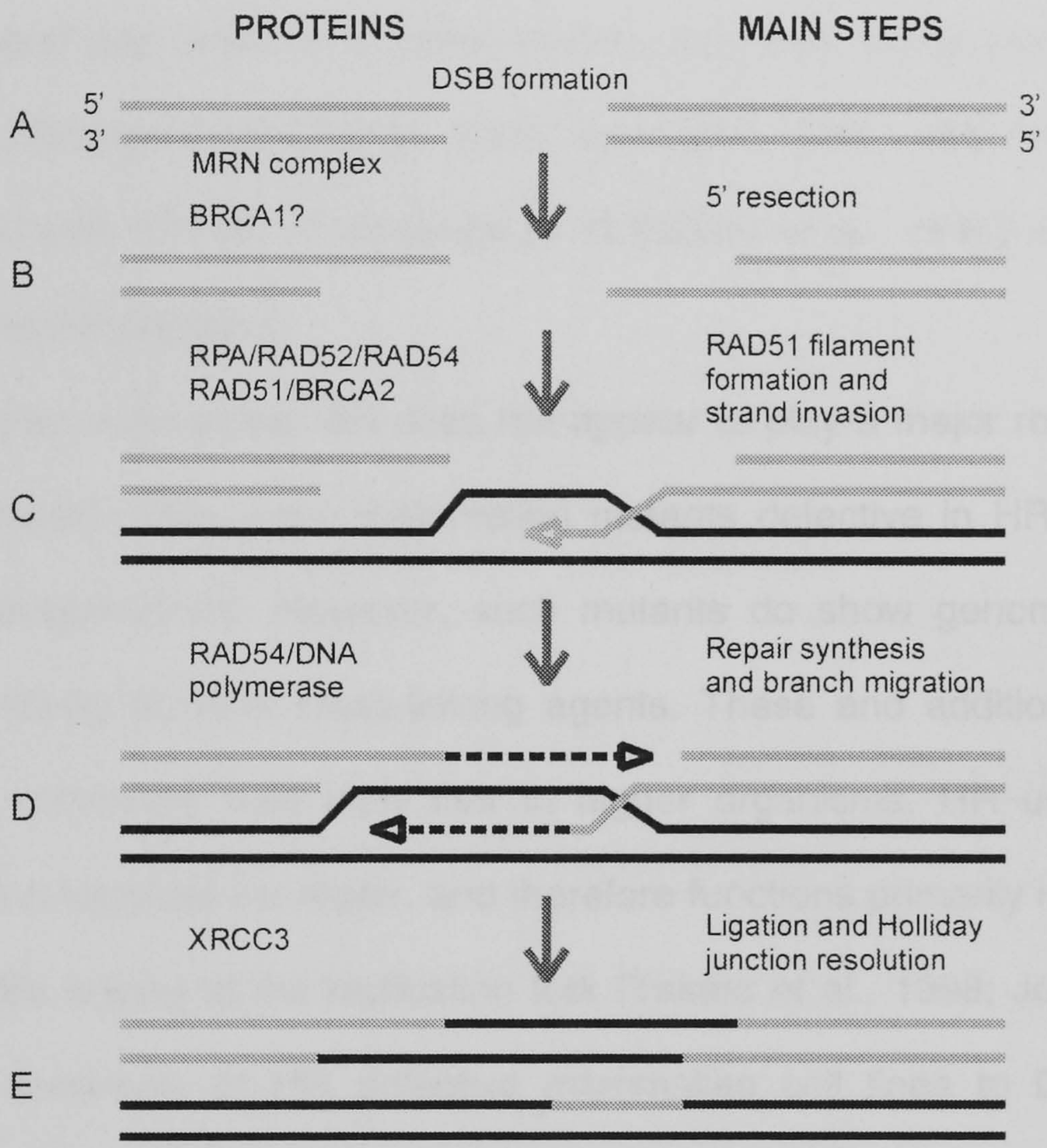

Figure 1.3 Schematic representation of homologous recombination repair of DNA double-strand break adapted from Thacker (2004). (**A**) DSB recognition and the ends are nucleolytically processed by the MRN complex. (**B**) 3' Single-stranded tails are formed by resection of break ends and are coated with RAD51. (**C**) Displacement of single-stranded binding protein RPA (replication protein A) with the assistance of RAD52 and RAD51 like proteins. A 3' end molecule (grey) invades an unbroken (black) molecule, displacing a strand (D-loop) that acts as a repair template. (**D**) RAD54 has both pre- and post-invasion roles to facilitate the opening up of DNA. (**E**) The cross stranded structures are resolved by XRCC3 and a RAD51 like heterodimer.

This complex is also involved in non-homologous end joining (NHEJ) (see next section) (Petrini, 1999). In the next step of HR processing RAD51 with the aid of BRCA2 and RAD54 will bind the exposed single stranded DNA and invade the broken DNA into the adjacent sister chromatid to search for homologous sequences (Yang et al., 2002). This invasion displaces the non-complementary intact strand, forming a D-loop, which enlarges as new DNA synthesis progresses across the break site. Once the adjacent DNA strands are paired at the homologous sequence, DNA polymerases will enter to fill the damaged gap, and the resulting Holliday junctions will be resolved to complete the process (Thompson and Schild, 2002; Symington, 2002). BRCA1 has been shown to co-localise with RAD51 in response to IR (Scully et al., 1997) and might also be involved in the HR pathway.

In higher eukaryotes, HR does not appear to play a major role in the repair of radiation induced DSBs since mammalian mutants defective in HR display at most, only mild radiosensitivity. However, such mutants do show genomic instability and marked sensitivity to DNA cross-linking agents. These and additional findings have lead to the commonly held view that in higher organisms, HR uses only a sister chromatid as a template for repair, and therefore functions primarily in late S/G_2 phase to repair DSBs arising at the replication fork (Takata et al., 1998; Johnson and Jasin, 2001). The sensitivity of HR defective mammalian cell lines to DNA cross-linking agents is therefore probably due to the generation of DSBs at the replication fork following attempts to replicate past DNA cross-links.

1.6.3 Non-homologous end joining (NHEJ)

The potentially more significant pathway for repair of radiation-induced DSBs in mammalian cells is DNA non-homologous end-joining (NHEJ) (for a review see Lieber et al., 2004). This type of end-joining does not require homologies between the two recombining molecules and is distinct from the well-characterised homologous

recombination pathway (Figure 1.4). NHEJ is active throughout the cell cycle, including late S and G_2 of the cell cycle (Takata et al., 1998).

Five core proteins have been identified that function in NHEJ in higher organisms (Pasta and Blasiak, 2003). Three of these constitute a complex termed DNA dependent protein kinase (DNA-PK), namely the two subunits of the heterodimeric Ku protein (Ku70 and Ku80) and a large catalytic subunit, termed DNA-dependent protein kinase subunit (DNA-PKcs).

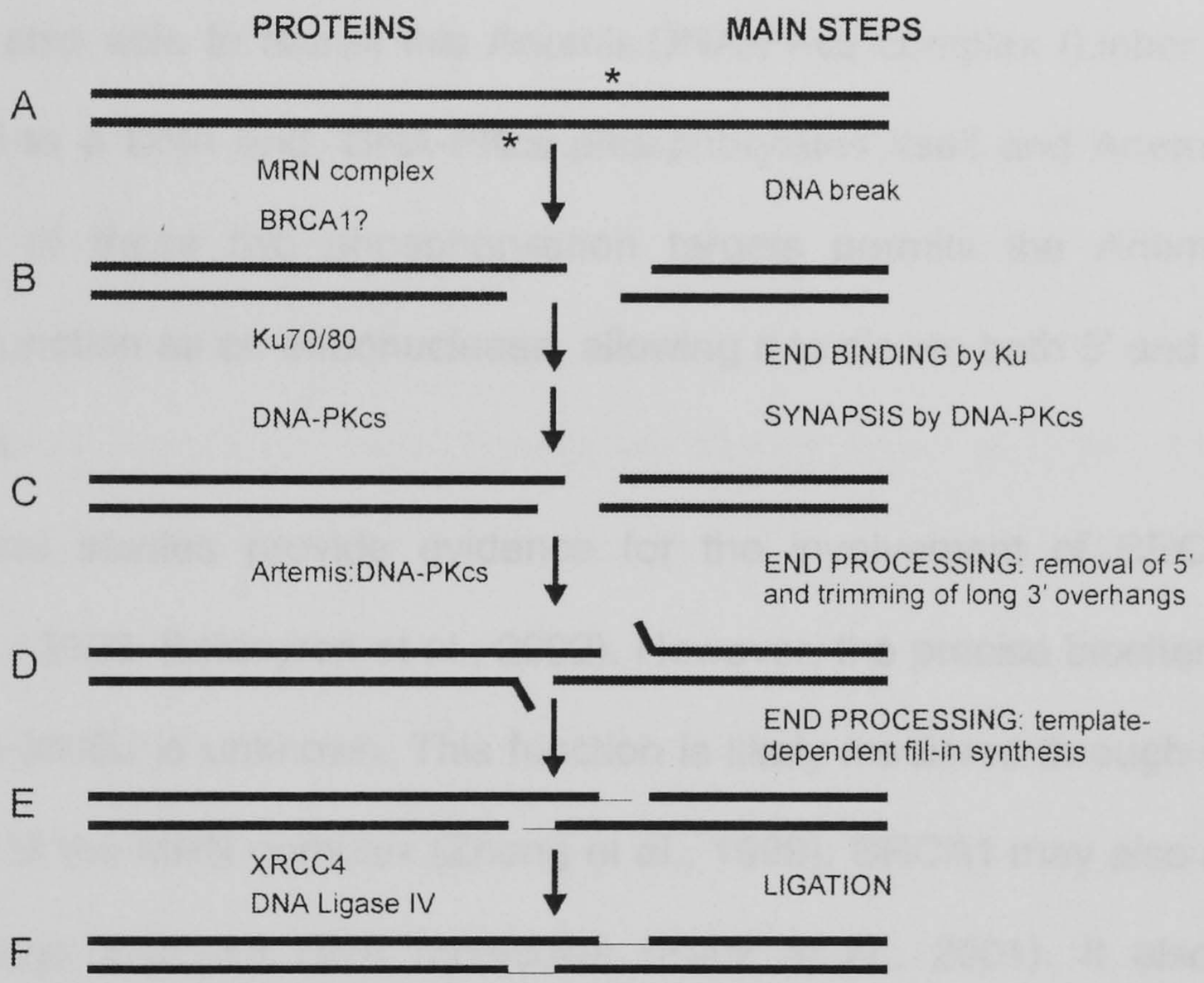

Figure 1.4 The steps and proteins in the non-homologous end-joining pathway (adapted from Lieber et al., 2004). (**A**) When a double-stranded DNA break occurs, MRE11 processes the DNA ends by 3'-5' endonucleolytic activity enhanced by the presence of RAD50 and NBS1. Next, Ku binds to the DNA ends. (**B**) The second step is the recruitment of the nuclease DNA PKcs, which holds the ends in proximity to permit subsequent repair to proceed and to align the two ends. (**C**) This step can be referred to as synapsis. (**D**) For complex DNA ends, as would be generated by ionising radiation, there is often need for nucleolytic processing. If so, Artemis:DNA-PKcs are likely to carry out processing. (**E**) The next step is to fill in the gaps by polymerases. (**F**) Ligation is the final step and is done by the XRCC4:DNA ligase IV complex.

Ku has strong affinity for double stranded DNA ends, and when DNA bound, Ku recruits and activates DNA-PKcs. The remaining two proteins, XRCC4 and DNA ligase IV are required for the subsequent rejoining step. They co-associate strongly but are not associated with DNA-PK in undamaged cells (Lees-Miller and Meek, 2003). They are also defective in their ability to undergo V(D)J recombination demonstrating that NHEJ also functions during this process.

In eukaryotic cells, some fraction of the DNA-PKcs population of molecules is bound to the Artemis protein in a very stable complex (Ma et al., 2002). Ku is presumably also able to recruit this Artemis:DNA-PKcs complex (Lieber et al., 2004). Once bound to a DNA end, DNA-PKcs phosphorylates itself and Artemis (Ma et al., 2002). One of these two phosphorylation targets permits the Artemis:DNA-PKcs complex to function as an endonuclease, allowing it to cleave both 5' and 3' overhangs of any length.

Several studies provide evidence for the involvement of BRCA1 in NHEJ (Zhong et al., 2002; Baldeyron et al., 2002). However, the precise biochemical function of BRCA1 in NHEJ is unknown. This function is likely mediated through its interaction with RAD50 of the MRN complex (Zhong et al., 1999). BRCA1 may also act like DNA-PKcs to bridge adjacent DNA molecules (Paull et al., 2001). It also inhibits the nucleolytic processing ability of the MRN complex (Paull et al., 2001), suggesting that BRCA1 regulates the function of the MRN complex to prevent extensive DNA end processing.

1.7 DSB repair and telomere maintenance

As shown in section 1.6.2 RAD54 is a RAD51-interacting DNA-dependent ATPase involved in homologous DNA pairing (Mazin et al., 2003). By using *RAD54*-defective mice Jaco et al. (2003) provided evidence for the role of this gene product in telomere length maintenance and telomere capping. *RAD54* deficiency in mice resulted in a significant loss of telomeric sequences, suggesting that RAD54 is important for

telomere length maintenance in mice (Jaco et al., 2003). This result suggests that HR participates in telomere length maintenance or that RAD54 has a role in telomere protection. An increase in end-to-end fusions in *RAD54* deficient cells is consistent with a role for this protein in telomere capping (Jaco et al., 2003). Tarsounas et al. (2004) reported that RAD51d, a paralog of RAD51 and a key component in HR (Baumann et al., 1996), is also involved in telomere maintenance. Using telomerase positive *RAD51d*$^{-/-}$ *TRP*$^{-/-}$ primary mouse embryonic fibroblasts (MEFs) they demonstrated telomere shortening and elevated levels of end-to-end chromosome fusions, a signature of telomere dysfunction, compared with wild type MEFs.

Proteins involved in DNA DSB repair by NHEJ include Ku70, Ku80 and DNA-PKcs (Pasta and Blasiak, 2003) as shown in section 1.6.3. Knockout mutations in any of these three genes in mice cause spontaneous end-to-end fusions of chromosomes, an indication of impaired telomere capping function (Bailey et al., 1999; Goytisolo et al., 2001). It was also demonstrated that inactivation of Ku in mice causes either telomere elongation (Samper et al., 2000) or telomere shortening in primary MEFs (d'Adda di Fagagna et al., 2001). Furthermore, inactivation of one allele of the gene encoding Ku80 in human cells resulted in telomere shortening (Myung et al., 2004). However, inactivation of DNA-PKcs in mice did not cause any effect on telomere length but it did affect telomere capping function (Goytisolo et al., 2001). In scid mice, which are natural DNA-PKcs mutants, telomeres are abnormally elongated and also lack the capping function (Hande et al., 1999). The use of a DNA-PKcs kinase inhibitor induced chromosomal end-to-end fusions demonstrating that the telomere end-protection role of DNA-PK requires its kinase activity (Bailey et al., 2004). These results establish that Ku and DNA-PK, including its kinase activity, play a critical role in telomere capping in mammalian cells.

Taken together, above results suggest that DSB repair proteins are required to prevent end-to-end chromosome fusions. In addition, telomere fusions resulting from inhibition of TRF2 are generated by DNA ligase IV-mediated NHEJ (Smogorzewska et

al., 2002) suggesting further that DSB repair proteins actively participate in chromosome stability maintenance through their interplay with telomeres. In line with these observations, it has been speculated that dysfunctional telomeres will behave as DNA DSBs. The experimental evidence for this possibility was recently obtained in two independent studies (d'Adda di Fagagna et al., 2003; Takai et al., 2003). It is clear from these studies that telomere dysfunction generated either by cell-senescence associated telomere shortening (Bakkenist et al., 2004) or TRF2 defect (Takai et al., 2003) cause DNA damage response that resemble the cell response to external agents that cause DSBs. For example, a protein that specifically detects the sites of DSBs, γ-H2AX, co-localises with dysfunctional telomeres (Takai et al., 2003; Bakkenist et al., 2004) thus formally proving that indeed dysfunctional telomeres are interpreted by the cell DNA damage response machinery as DSBs.

There is another line of evidence supporting the view that DSB repair mechanisms and processing of DSBs, particularly through NHEJ, are inextricably linked. One way for cells to respond to telomere dysfunction is through end-to-end chromosome fusions i.e. these fusions will eliminate DSBs. Chromosome fusion junctions from cells with dysfunctional telomeres have been isolated from *S. cerevisiae* (Hackett et al., 2001) and mice (Hemann et al., 2001). The structures of these fusion junctions are strikingly similar, suggesting the possibility of a common mechanism for their formation in yeast and mammals. Fusion junctions from both organisms contain 0-10 bp of microhomology, characteristic of a non-homologous end-joining mechanism. These fusions involve the loss of all telomeric and some subtelomeric sequences. The loss of sequence suggests that the mechanism of fusion might be an error-prone DNA repair pathway i.e. NHEJ.

1.8 Telomere maintenance in disorders that are associated with defective DNA damage responses

Chromosome aberrations, genomic instability and cancer predisposition are the hallmarks of a number of syndromes in which the defective genes play an important role in recognising, signalling and/or repairing DNA damage, DNA processing, cell cycle regulation, apoptosis and/or telomeric maintenance (Klapper et al., 2001; Surrallés et al., 2004). Defects in any of these genes can lead to cancer predisposition and to a number of clinical defects. These syndromes share various features at the clinical and cellular level that can be explained in most cases by interactions and molecular links among them, creating a network of pathways involved in DNA damage response.

Some of the telomere binding proteins are very important for their dual function as they also participate in different DNA damage response pathways that altogether cross-talk in a complex network of tumour suppressor pathways (Surrallés et al., 2004). A deficiency in any of these proteins leads to serious disorders of genetic instability ultimately leading to cancer predisposition. Syndromes with DNA damage response defects that also affect telomere maintenance are briefly discussed below. Primary fibroblast cell lines originating from patients with DNA damage response syndromes were used in this study (see Chapter 4).

1.8.1 The role of ATM in telomere maintenance

Ataxia-telangiectasia (AT) is a rare, autosomal-recessive inherited disorder characterised by neurological deterioration, immunodeficiency, spontaneous chromosomal instability, hypersensitivity to IR, predisposition to cancer, particularly T cell leukaemia and lymphoma, and premature ageing (Metcalfe et al., 1996). The gene responsible for AT is *ATM* (ataxia-telangiectasia mutated). ATM activates a number of pathways, which involve either DNA repair or cell cycle checkpoint control (Kastan and Lim, 2000). The fact that ATM is associated with phosphorylated H2AX foci (γ-H2AX) is

consistent with a major role for ATM in the early detection of DSBs and subsequent induction of cellular responses (Fernandez-Capetillo et al., 2004).

Shorter telomeres and higher frequency of chromosome end fusions were found in patients suffering from AT (Pandita et al., 1995; 1996). This was confirmed by Metcalfe et al. (1996) and Hande et al. (2001). In addition, it has also been reported that the ATM protein interacts with TRF1, one of the telomere binding proteins (Kishi et al., 2001). However, there is still no evidence that ATM is directly involved in telomere maintenance. The defective telomere metabolism in AT cells is most likely the result of mechanisms that indirectly affect telomere maintenance. This has been illustrated by mild chronic oxidative stress induced by hydrogen peroxide, which increased the rate of telomere shortening in AT cells (Tchirkov and Lansdorp, 2003). *ATM* deficient mice show high incidence of extra-chromosomal telomeric fragments (Hande et al., 2001).

1.8.2 The role of FA genes in telomere maintenance

Fanconi anemia (FA) also belongs to a group of chromosome instability diseases. FA is an autosomal recessive disease of childhood characterised by progressive bone marrow failure that often evolves towards acute leukaemia. FA can be caused by mutations in at least eight different genes (Tischkowitz and Hodgson, 2003; Seal et al., 2003). These FA genes correspond to subtypes *FA-A*, *B*, *C*, *D1*, *D2*, *E*, *FA*, and *G* (reviewed in Joenje and Patel, 2001). Data strongly suggest that the gene causing FA-D1 is *BRCA2* (Seal et al., 2003). Interaction pathways have been established, both between the FA proteins and other proteins involved in DNA damage repair, such as ATM, BRCA1 and BRCA2, thereby providing a link with other disorders in which defective DNA damage repair is a feature (Tischkowitz and Hodgson, 2003).

Accelerated telomere shortening in peripheral blood mononuclear cells was found in FA patients (Ball et al., 1998; Leteurtre et al., 1999; Hanson et al., 2001; Callén et al., 2002). Adelfalk et al. (2001) demonstrated that telomeric DNA is continuously lost at a higher rate in FA fibroblasts compared to healthy controls.

Accelerated shortening of telomeres could be explained by a hematopoietic stem cell undergoing a higher than normal number of cell divisions to generate mature end cells, but a recent study has shown that, in addition to replicative shortening, there is also a higher rate of breakage at telomeric sequences in FA cells, suggesting a defect in telomere maintenance (Callén et al., 2002). The molecular mechanisms leading to telomere shortening in FA cells, however, are still unknown. Consistent with telomere breakage as an alternative mechanism of telomere shortening, recent investigations have shown accumulation of breaks at telomeres after oxidative stress in human fibroblasts *in vitro* (Oikawa and Kawanishi, 1999; von Zglinicki et al., 2000; von Zglinicki, 2002) and DNA repair at telomeres is defective (Lansdorp, 2000). It is known that FA cells are highly impaired in their response to oxidative stress (Joenje and Patel, 2001).

1.8.3 The role of NBS1 in telomere maintenance

Nijmegen breakage syndrome (NBS) is a rare human disease displaying chromosome instability, radiosensitivity, cancer predisposition, immunodeficiency, and other defects (Weemaes et al., 1981; van der Burgt et al., 1996; Iijima et al., 2004). Cells established from patients are defective in their responses to DSBs induced by IR, thus showing an increased frequency of chromosomal aberrations (Weemaes et al., 1994). NBS is caused by a mutation or a defectiveness in the *NBS1* gene and the majority of the patients are homozygous for the same mutation in exon 6 of the *NBS1* gene, resulting in premature truncation of the protein (Varon et al., 1998). The gene that is affected in these patients, *NBS1*, encodes a protein called nibrin or p95 (Girard et al., 2000). Nibrin is a key regulator of the MRE11 and RAD50 protein complex, the so called MRN complex, involved in the repair and processing of double-strand breaks (DSBs) (Carney et al., 1998; Petrini, 1999; Iijima et al., 2004). NBS1 is also localised to telomere ends in association with the telomere-binding proteins TRF1 and TRF2 (Zhu et al., 2000; Wu et al., 2000). Ranganathan et al. (2001) have shown that blood cells

from NBS patients have shorter telomeres in comparison to normal individuals. Likewise, they observed shortened telomeres in cultured NBS fibroblasts that exhibit a premature growth cessation. Ranganathan et al. (2001) suggested that NBS1 might contribute to telomere elongation by showing that co-expression of intact NBS1 and hTERT in two NBS fibroblast strains resulted in increased telomere lengths compared with the parental populations. However, Siwicki et al. (2003) provided evidence that telomere length maintenance is possible in the absence of a full-length NBS1 protein in human T lymphocytes with high telomerase activity.

NBS1 is also included in the APBs (Wu et al., 2000; Naka et al., 2002). In ALT cells, clear NBS1 foci can be observed in the nucleus from G_1-G_2-phase, and they co-localise with the PML bodies (Iijima et al., 2004). However, the PML bodies co-localise with telomeres only during G_2-phase, suggesting that the APBs might be formed only when they act during telomere maintenance. The NBS1 complex, localises at ALT-independent PML nuclear bodies and could be a reservoir of repair-related proteins, which then translocate to a damaged DNA site in response to DSBs (Iijima et al., 2004). Thus, these nuclear bodies could not only be involved in telomere maintenance when they are located on telomeres, but function also in response to DNA damage.

1.9 Telomerase activity in benign versus malignant brain tumours

A large body of evidence accumulated over the last 15 years clearly implicates telomeres and telomerase in carcinogenesis. One of our interests is how telomerase is regulated in malignant brain tumours in comparison with their benign counterparts. Brain tumours are diverse in terms of their malignancy and can originate in all different places of the brain determining their phenotypic and genotypic outcome. Brain tumours exhibit considerable chromosome instability (El-Zein et al., 1999; Hui et al. 2001; Sawyer et al., 2003), suggesting that DNA repair mechanisms are impaired or that genetic susceptibility may lead to defects in DNA damage response pathways. In this

section the meningiomas as generally benign and the glioblastomas as highly malignant tumours of the brain are briefly discussed.

Meningiomas are generally slow growing tumours attached to the dura mater and composed of neoplastic meningothelial cells. These tumours arise from arachnoid cells that form the middle layer of the meninges, the arachnoid mater (Whittle et al., 2004) (Figure 1.5).

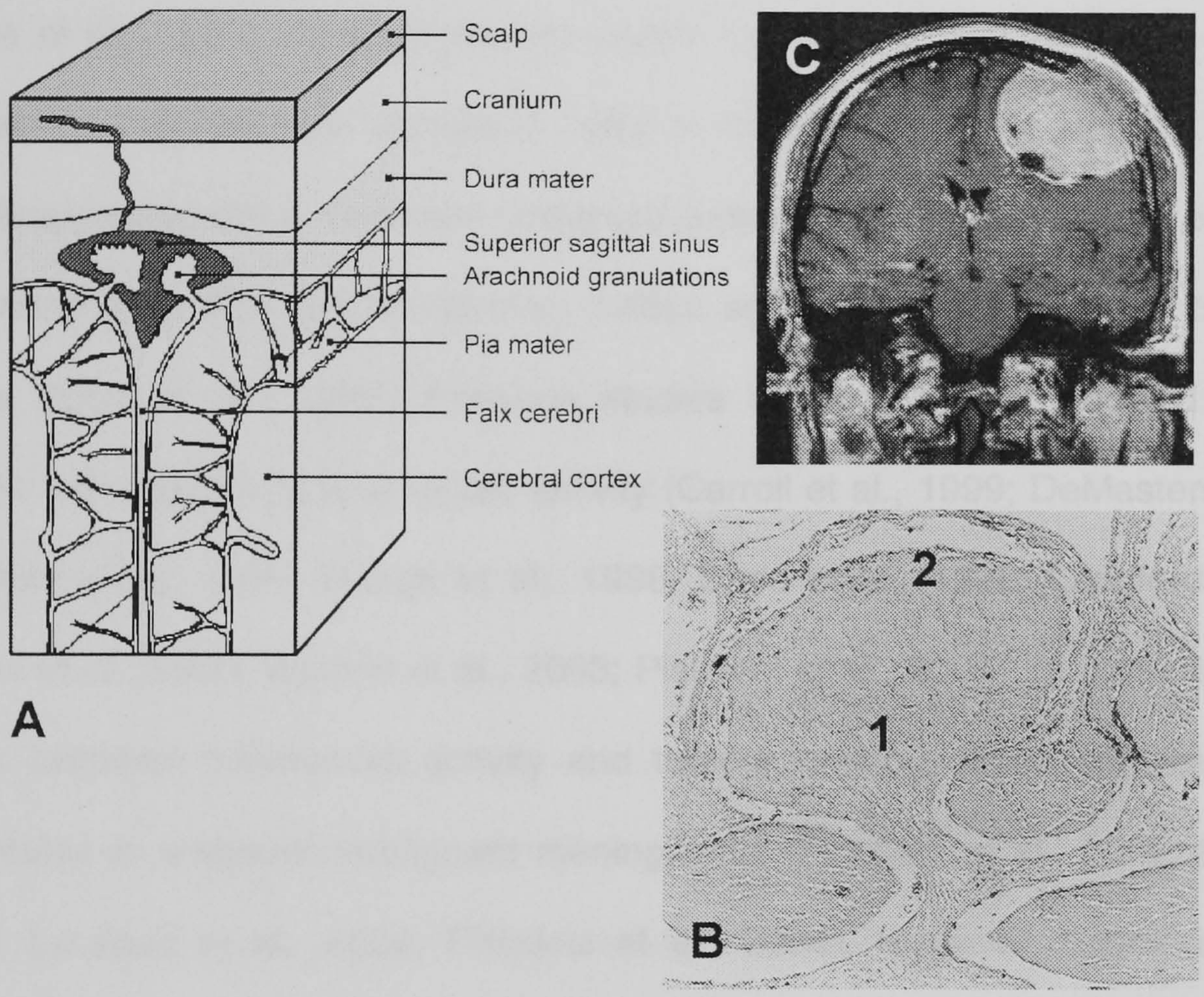

Figure 1.5 Meningiomas. Schematic overview of meninges and arachnoid granulations (**A**) (drawing adapted from Clinical Anatomy for Medical Students, Lippincott William and Wilkins, 7th Edition); Detail from a histological slide showing a cross section of an archnoid granulation (**1**) and arachnoid cap cells (**2**) (meninges provided by Prof. Dr. Katharina D'Herde, University Ghent) (**B**); Sagittal image of a MR acquisition showing a meningioma attached to the dura mater (case 25, Table 2.3) (**C**).

Microscopically, meningiomas have a varied but characteristic histopathologic appearance, the diversity of which forms the basis for the pathologic classification of meningiomas (for a review see Whittle et al., 2004). Most meningiomas are benign in nature. In atypical meningiomas, certain features that may be seen by light microscopy

show an increased tumour aggressiveness and increased likelihood for recurrence. Loss of architectural pattern, high cellularity, increased mitotic figures, necrosis, prominent nucleoli, and nuclear pleomorphism are identified as histologic parameters. In general, cellular proliferation increases from benign to atypical to anaplastic (malignant) meningioma. Meningiomas are known to be induced by even a low dose of IR (Kleinschmidt and Lillehei, 1995). Radiation-induced meningiomas are more commonly atypical or aggressive, and multifocal, show higher proliferation indices (Musa et al., 1995). Flow cytometric studies have demonstrated approximately equal numbers of diploid and aneuploid cells in meningioma tumours, and have shown significant correlations between aneuploid tumours and features such as recurrence, pleomorphism, high cellular density, mitotic activity and infiltration of brain and soft tissue (Cruz et al., 1993). Previous studies of meningiomas showed contradicting results with regards to telomerase activity (Carroll et al., 1999; DeMasters et al., 1997; Falchetti et al., 1999, Hiraga et al., 1998, Sano et al., 1998; Langford et al., 1997; Simon et al., 2000; Boldrini et al., 2003; Pistolesi et al., 2004). In general a correlation exists between telomerase activity and tumour grading, since enzymatic activity is detectable in anaplastic/malignant meningiomas (Falchetti et al., 2002; Boldrini et al., 2003; Leuraud et al., 2004; Pistolesi et al., 2004). However, telomerase was also detected in benign meningiomas (Langford et al., 1997; Simon et al., 2000; Falchetti et al., 2002).

Glioblastoma multiforme (GBM) is the most common malignant tumour of neuroepithelial origin in the human brain. This neoplasm is highly proliferative. Glioblastoma is composed of poorly differentiated neoplastic astrocytes. Histopathological features include cellular polymorphism, nuclear atypia, brisk mitotic activity, vascular thrombosis, microvascular proliferation and necrosis. They have an abnormal DNA content determined by flow cytometry, which could reflect aneuploidy (Ehemann et al., 1999). Gene amplification occurs frequently in glioblastomas (Fischer et al., 2002). They may develop from diffuse astrocytomas WHO grade II (World Health

Organisation classification; Kleihues and Cavenee, 2000) or anaplastic astrocytomas, but more frequently, they manifest after a short clinical history *de novo*, without evidence of a less malignant precursor lesion. In malignant gliomas, telomerase activity is very often detected (Langford et al., 1997; DeMasters et al., 1997; Sallinen et al., 1997; Sano et al., 1998; Falchetti et al., 1999; Kleinschmidt-DeMasters et al., 2000; Harada et al., 2000). In malignant gliomas, telomerase is positive in 10 to 100% of anaplastic astrocytomas and in 26 to 100% of glioblastoma. Although the ratio of telomerase-positive cells in gliomas varies, most of the reports show that the incidence of telomerase expression is closely correlated with malignancy. By contrast, neither normal brain tissues (DeMasters et al., 1997; Huang et al., 1999; Harada et al., 2000; Cabuy and de Ridder, 2001), nor the meninges (Cabuy and de Ridder, 2001) express telomerase activity.

1.10 The aim and outline of the PhD project

The first task of the PhD project was to set-up a flow-FISH technique for telomere length measurement in our laboratory and verify its accuracy on a new Beckman coulter EPICS XL cytometer. This is a relatively new, accurate and fast technique with a good potential for further improvements towards a multicolour FISH (Baerlocher and Lansdorp, 2003). During these studies we discovered the phenomenon we termed TELEFLUCS (TElomere LEngth FLUctuations in Cell Subpopulations) and demonstrated the importance of flow-FISH in telomere analysis (Chapter 3).

The next aim was to assess whether flow-FISH could be used to measure telomere length in radiosensitive fibroblast cell lines (Chapter 4). So far, flow-FISH was used almost exclusively in cells of hematopoietic origin (Scheding et al., 2003; Van Ziffle et al., 2003; Rigolin et al., 2004). Given a potential link between telomere maintenance and radiosensitivity (Slijepcevic, 2004) and the role of telomeres in DSB repair (Mills et al., 1999; Martin et al., 1999) we hypothesized that telomere shortening

may be a consequence of radiosensitivity (McIlrath et al., 2001). Since the cellular capacity to respond to IR is proportional to their ability to repair DSBs we investigated telomere maintenance in mouse cell lines deficient in DSB repair. This part of the project is relevant for elucidating the genetic basis of radiosensitivity.

Since many genes involved in DNA damage response also affect telomere maintenance we wanted to test whether the *BRCA1* (breast cancer 1, early onset) gene may participate, directly or indirectly, in telomere maintenance (Chapter 5). This hypothesis stems from two recent studies implicating *BRCA1* in telomerase regulation (Xiong et al., 2003) and in ALT cell telomere maintenance (Wu et al., 2003). To investigate this we used small interfering RNA (siRNA) oligonucleotides in two mammary epithelial cell lines and assessed DNA damage indicators, chromosome abnormalities and telomere lengths up to 11 days post-transfection. We also analysed telomere maintenance and interactions of *BRCA1* with some other DNA damage response factors (γ-H2AX) in a panel of 4 human ALT cell lines.

Finally, we evaluated hTERT mRNA expression and telomerase activity in benign versus malignant brain tumours (Chapter 6). Brain tumours exhibit considerable chromosome instability (El-Zein et al., 1999; Sawyer et al., 2003), suggesting that also DNA repair mechanisms might be impaired in brain tumours and telomere dysfunction. This part of the project was focused on the relationship between alternative splicing of hTERT mRNA, telomerase activity and cell proliferation in brain tumours.

CHAPTER 2

MATERIALS AND METHODS

2.1 Cell lines and tissue culture conditions

2.1.1 Human cell lines

2.1.1.1 Human primary fibroblast cell lines

Primary fibroblast cell lines (Table 2.1) derived from 9 patients with defects in various DNA damage response pathways were provided by Dr. P. A. Jeggo, University of Sussex, Brighton. Normal fibroblasts were purchased from the Coriell Cell Repository, Camden, USA. Human fibroblast cell lines were cultured in Dulbecco's Modified Eagle Medium (D-MEM) supplemented with 100 U/mL of penicillin and 0.1 mg/mL of streptomycin, 2 mM L-glutamine, 0.1 mM non essential amino acids and 15% foetal bovine serum (FBS) at 37°C under 5% CO_2 (all reagents were from Gibco, Invitrogen, NY, USA). Cells were subcultured 1:3 by gentle trypsinisation and medium was changed twice a week until cells failed to double within two weeks.

Table 2.1 Human primary fibroblast cell lines used in this study. Cells lines were obtained from DNA damage response defective patients who over-responded to IR (ionising radiation) therapy. Note that the PD number represents an estimated PD at which cells were received. Mitomycin is an alkylating agent, which forms interstrand and/or intrastrand crosslinks.

Cell line	Syndrome	Defective protein	PD No.	Clinical Sensitivity	Cellular Sensitivity	Reference
AT1BR	Ataxia telangiectasia	ATM	10	IR	IR	Taylor et al., 1975
AT6BR	Ataxia telangiectasia	ATM variant	10	IR	IR	Girard et al., 2002
347BR	Nijmegen breakage	NBS1 (Nibrin)	14	IR	IR	Girard et al., 2000
425BR	Fanconi anaemia	FA-A	3	IR	Mitomycin C	Marcou et al., 2001
180BR	LIG4	DNA ligase IV	6	IR	IR	Riballo et al., 1999
46BR	LIG1	DNA ligase I	10	IR	IR	Barnes et al., 1992
CJ179	Radiosensitive scid	Artemis	10	IR	IR	Jeggo, unpublished results
2BN	Unknown NHEJ factor	Unknown	8	IR	IR	Dai et al., 2003
XP14BR	Xeroderma pigmentosum	XP-C	8	IR, UVB, UVC	IR, UVB, UVC	Rogers et al., 2000
GM09503	normal	none	2	normal	normal	http://coriell.umdnj.edu/
GM08399	normal	none	6	normal	normal	http://coriell.umdnj.edu/
GM04505	normal	none	5	normal	normal	http://coriell.umdnj.edu/

Table 2.2 *BRCA1* and *BRCA2* deficient lymphoblastoid and embryonic mouse stem cell lines and their controls.

Cell line	Species	Defect	Clinically Affected
GM00893	human	normal	No
GM01954	human	normal	No
GM00536	human	normal	No
GM00607	human	normal	No
GM14090	human	*BRCA1*$^{+/-}$	Yes
GM13705	human	*BRCA1*$^{+/-}$	Yes
GM14170	human	*BRCA2*$^{+/-}$	Yes
GM14622	human	*BRCA2*$^{+/-}$	Yes
E14	mouse	normal	-
408	mouse	*BRCA1*$^{-/-}$	-

2.1.1.2 Human lymphoblastoid cell lines

Normal human lymphoblastoid cell lines and lymphoblastoid cell lines derived from carriers of *BRCA1*$^{+/-}$ and *BRCA2*$^{+/-}$ mutations (Table 2.2) were purchased from the Coriell Cell Repository, Camden, USA. The cells were grown as a suspension culture in RPMI 1640 medium containing 10% FBS, 100 U/mL of penicillin and 0.1 mg/mL of streptomycin. Lymphoblastoid cells were subcultured depending on the cell culture density.

MOLT-4 cells (T lymphoblast) were purchased from American Type Culture Collection (ATCC) Cat. No. CRL-1582 (Rockville, MD). The MOLT-4 cell line was grown in RPMI 1640 medium supplemented with 10% FBS, 2 mM L-glutamine, 1.5 g/L sodium bicarbonate, and 10 mM HEPES at 37 °C in a humidified atmosphere of 5% CO_2 and 95% air at cell densities between 5 x 10^4 and 2 x 10^6/mL. Cultures were maintained by addition or replacement of fresh medium. Viable cells were counted by 0.2% trypan blue exclusion method with a Neubauer hemocytometer.

Macrophages from blood samples (kindly donated by Prof. Dr. Ann Vral, Ghent University, Belgium) were used as negative controls in immunocytochemistry hTERT assays.

2.1.1.3 Human epithelial cell lines

Human Hela cells (cervix epithelial adenocarcinoma) were purchased from ATCC (Cat. No. CCL-2, Rockville, MD) and grown in Eagle Minimum Essential Medium (EMEM) with 2mM L-glutamine, 1.5 g/L sodium bicarbonate, 0.1 mM non-essential amino acids, and 1.0 mM sodium pyruvate, and 10 % FBS in a humidified atmosphere of 5% CO_2 at 37°C.

The breast epithelial cell line MCF10A was obtained from the ATCC (Cat. No. CRL-10317, Rockville, MD). These cells are not tumorigenic in immunosuppressed mice, but form colonies in semisolid medium. MCF10A human breast epithelial cells were cultured in mammary epithelial basal medium (MEBM) supplemented with 0.4%

bovine pituitary extract, 0.5 μg/mL hydrocortisone, 5 μg/mL insulin, 20 ng/mL EGF (Cambrex Co, NJ, USA). Antibiotics and cholera toxin were omitted. Cells were incubated at 37 °C with 5% CO_2 and passaged if they reach no more than 80% confluence. Routine trypsinisation of cells was achieved by aspirating the medium and rinsing the cell monolayer with 30mM Hepes Buffered Saline Solution (HBSS) and adding1 mL of Trypsin-EDTA (0.025% - 0.01 %) to 25cm^2 culture flasks. The flasks were kept at 37 °C until the cells had dispersed (~15 min) and the cells centrifuged at 900 x g for 4 minutes. Trypsin was neutralized by the addition of 1 mL of Trypsin Neutralising Solution (TNS) (all products from Clonetics, Cambrex, Wakersville, USA). The resulting cell pellet was resuspended in the appropriate volume of complete medium and seeded in a tissue culture flask. Cells were cryopreserved in culture medium containing 7.5% DMSO.

The breast adenocarcinoma cell line MCF7 obtained from the European Collection of Cell Cultures (ECACC, Cat No. 86012803) was grown in EMEM (Sigma-Aldrich) supplemented with 2mM Glutamine, 1% non-essential amino acids, 10% FBS and 5 μg/mL insulin. Cells were cryopreserved in 90% FBS and 10% DMSO.

The breast cancer cell line HCC1937, which has a truncated, non-functional BRCA1 and which has defective IR-induced S-phase and G_2-M checkpoints, was cultured in RPMI 1640 (Gibco/BRL) supplemented with 15% FBS at 37°C in a humidified atmosphere containing 5% CO_2. This cell line is heterozygous for the BRCA1 5382C mutation, whereas the primary tumour cell line is homozygous for the same mutation. The cell line was a gift from Dr M. Zdzienicka, University of Leiden.

Primary human mammary epithelial cell line (HMEC) Bre-80 (kindly donated by Prof. Rob Newbold) was used in control experiments. The cells were maintained in MEBM, supplemented with 10 μg/mL EGF in a buffered bovine serum albumin (BSA) solution, 5 μg/mL bovine insulin, 0.5 μg/mL hydrocortisone, and 5% bovine pituitary extract. Cells were incubated at 37 °C with 5% CO_2. Cells were passed prior to confluence using 0.05% trypsin/EDTA solution (Life Technologies).

The breast cancer line 21NT pBabe hTERT was used as a positive control for BRCA1 and hTERT in RT-PCR experiments. The cells were cultured in MEM alfa medium supplemented with 10 % FBS, 0.5 µg/mL hydrocortisone, 1 µg/mL insulin, and 12.5 ng/mL EGF (Cambrex Co, NJ, USA). Cells were passaged prior to confluence using 0.05% trypsin/EDTA solution (Life Technologies).

The prostate adenocarcinoma cell line PC-3 (ATCC, Cat. No. CRL-1435) was cultured in Ham's F12K medium with 2 mM L-glutamine adjusted to contain 1.5 g/L sodium bicarbonate and 10% FBS in an atmosphere with 5% CO_2. Proteins from this cell line were used to set up a calibration curve for the real-time PCR TRAP assay.

2.1.1.4 Human ALT cell lines

The lung fibroblast cell line WI-38 (ECACC, Cat. No. 90020107) and WI-38 VA13/2RA (ECACC, Cat. No. 85062512), derived from the SV40-transformed WI-38, and the lung adenocarcinoma SK-LU-1 cell line (ECACC, Cat. No. 93120835) were grown in EMEM (Sigma-Aldrich) supplemented with 2mM Glutamine, 1% non-essential amino acids, and 10% FBS. The derivative WI-38 VA13/2RA+hTERT was obtained from Dr. Silvia Baccetti, McMaster University, Canada and grown in the same culture conditions.

The human osteosarcoma cell line U2-OS (ECACC, Cat. No. 92022711) and G-292 (ECACC Cat. No. 90110522) were grown in McCoy's 5a culture medium supplemented with 1.5mM Glutamine and 10% FBS.

All cells were cryopreserved in 90% FBS and 10% DMSO.

2.1.2 Mouse cell lines

2.1.2.1 Mouse embryonic stem cells

Mouse embryonic stem (ES) cells (wild type and mutant *BRCA1*$^{-/-}$ obtained from B. Koller, University of North Carolina at Chapel Hill) were propagated and maintained as described previously (Snouwaert et al., 1999). Undifferentiated ES cells were

cultured at 37°C in an atmosphere with 5% CO_2, on gelatine-coated dishes in KnockOut D-MEM medium supplemented with 20% KnockOut serum replacement, 2 mM L-glutamine, 0.001% β-mercaptoethanol (Sigma-Aldrich, MO, USA), 1000 U/mL ESGRO (Chemicon, CA, USA), 10 U/mL penicillin, and 10 µg/mL streptomycin (all purchased, except were stated, from Gibco, Invitrogen, NY, USA). Medium was changed every 3 days and cells subcultured initially at the ratio 1:2 and the ratio progressively increased up to 1:8.

2.1.2.2 Mouse lymphoma cells

Mouse lymphoma LY-R (radio-resistant) and LY-S (radio-sensitive) cells were grown in suspension under standard tissue culture conditions using RPMI 1640 medium and 10% FBS supplemented with 100 U/mL of penicillin and 0.1 mg/mL of streptomycin. Cells were subcultured at the ratio 1:10 every 2-3 days. Mouse lymphoma LY-R and LY-S cells were used as a reference to extrapolate the telomere fluorescence values from fibroblasts into kb. LY-R and LY-S showed previously to have telomere lengths of 48 and 7kb, respectively (McIlrath et al., 2001).

2.1.2.3 Irradiation of mouse lymphoma cells

Mouse lymphoma cells were grown to about 60% confluence in RPMI before irradiation. LY-R/S cells were irradiated with 2.0 and 5.0 Gy of γ rays using a ^{60}Co source with a dose rate of 0.25 Gy/min. After irradiation the cells were immediately transferred to an incubator to recover for 2 h before harvesting for flow-FISH analysis.

2.1.3 Brain tumour samples and handling

2.1.3.1 Brain tumour biopsies

Multiple tissue samples, when possible from different locations in brain tumours, were collected by the author during open brain surgery of 32 patients. Table 2.3 shows the clinical data and histopathological diagnosis. The group consisted of 21 female

patients and 11 male patients, with ages ranging from 1.5 to 88 years. All cases under study came from total surgical removal of tumours from between 2000-2001. No chemotherapy or radiotherapy was administered before surgery. Prior therapeutic embolisation, which can cause extensive necrosis, was carried out on the tumours of two patients (case no. 25 and 28). Informed consent was obtained for the use of brain tissue and for access to medical records for research purposes.

Table 2.3 Clinical data and histopathological diagnosis of 32 brain tumours.
[a] All samples were frozen immediately except for *, which were frozen 2-4 h after tumour resection; [b] oedematous brain tissue present in samples from *; M: male; F: female.

Case No. [a]	Age	Sex	Diagnosis [b]	Recurrence
1	72	F	meningothelial meningioma	
2	28	F	meningothelial meningioma	
3*	88	F	transitional meningioma	
4	75	F	transitional meningioma	
5	62	F	angiomatous meningioma	
6	64	F	meningiothelial meningioma	
7	44	F	meningiothelial meningioma	
8	74	M	meningiothelial meningioma	
9	34	M	acoustic schwannoma	
10	37	F	pituitary adenoma	
11	3	F	medulloblastoma	
12	33	F	astrocytoma	2nd
13	52	F	glioblastoma multiforme	
14*	1.5	M	ependymoma	
15*	41	F	glioblastoma multiforme*	
16*	30	F	astrocytoma*	
17	69	M	atypical meningioma	
18	77	M	meningothelial meningioma	
19	70	F	meningiothelial meningioma	
20	73	F	meningiothelial meningioma	
21	56	F	meningiothelial meningioma	
22	69	F	meningiothelial meningioma	
23*	9	F	medulloblastoma*	2nd
24	58	M	glioblastoma multiforme	
25	70	M	transitional meningioma	
26	64	F	fibrous meningioma	
27	80	F	atypical meningiomas	3th
28	46	F	transitional meningioma	
29*	64	M	glioblastoma multiforme	
30	46	M	psammomatous meningioma	
31	40	M	transitional meningioma	
32	75	M	glioblastoma multiforme	

The tumours were classified according to WHO criteria (Kleiheus and Cavenee, 2000) by neuropathologists at the University Hospital and the St Lucas Hospital (Ghent, Belgium). The tumours comprised 20 meningiomas, 18 of which were benign and two atypical, one acoustic schwannoma, one pituitary adenoma, eight gliomas, and two medulloblastomas. All biopsies were divided into approximately 125 mm^3 pieces and a total of 121 samples were immediately frozen and stored separately in liquid nitrogen under RNase-free conditions. This procedure was carried within half an hour after surgery, except for six samples (case no. 3, 14-16, 23 and 29), which were frozen in liquid nitrogen 2-4 hours after surgery. Dura mater and arachnoid tissue could also be obtained from case 2 for *in vitro* cell culture. The histological identity of multiple formalin fixed specimens of each tumour was checked by microscopy of serial sections stained with hematoxylin-eosin and Masson trichrome.

2.1.3.2 Brain tumour derived cell cultures

Twenty-one primary cell cultures derived from collected brain tumour tissues were grown in Hanks modification of Eagles medium (HMEM) supplemented with 10% FBS and 50 µg/mL streptomycin, 50 U/mL penicillin and Fungizone. Subconfluent cells grown on 13 mm diameter Thermanox coverslips (Nunc) in medium were washed with PBS and then fixed with 4°C acetone for 3 min.

The human glioblastoma cell line U251 was established from a glioblastoma multiforme tumour and grown in DMEM supplemented with 10% FBS and 4mM glutamine, 50 U/mL penicillin, and 50 µg/mL streptomycin. This cell line was used as a positive control in experimental TRAP assay and RT-PCR.

2.1.4 Mycoplasma

All cell lines were tested negative for Mycoplasma contamination as detected by PCR ELISA (Roche Diagnostics, Mannheim, Germany) (see section 2.14).

2.1.5 Calculation of population doublings

When recording the phase of a cell population, age should be expressed as a population doubling, rather than passage number. The term "passage" is often used to indicate the age of cell cultures. However, it indicates only the number of trypsinisation steps performed during the culture period. It is therefore inadequate for describing the age of a culture because trypsinisation can be performed at different split ratios.

Since one population doubling (PD) means doubling the number of cells as a group, the relationship between PD and dilution factor is defined as follows:

2^n = dilution factor (where n = PD)

If the logarithm of both sides is taken and rearranged:

log 2^n = log(dilution factor)

n (PD) = log(dilution factor)/log 2 = log(dilution factor)/0.301

This formula was used when for each passage number the dilution factor was known. Otherwise the cell PDs were calculated using the following formula:

$PD = (\text{Log } N_1/\text{Log2}) - (\text{Log}N_0/\text{Log2})$

where N_0 is the cell number at the beginning and N_1 is the cell number at the end of the cell culture period. In order to determine the concentration of the cells, a Neubauer haemocytometer was used.

2.2 Reverse transcription-PCR (RT-PCR)

2.2.1 RT-PCR analysis of BRCA1 and hTERT

2.2.1.1 RNA isolation and reverse transcription

Total cell RNA was extracted from monolayers using NucleoSpin RNA II (Macherey-Nagel GmbH & Co., Düren, Germany), according to the manufacturer's instructions. Briefly, cells were lysed by incubation in a solution containing large amounts of chaotropic ions. This lysis buffer immediately inactivates RNases and adsorbs RNA to a silica membrane. Contaminating DNA, which is also bound to the

silica membrane, is removed by a DNase I solution. Simple washing steps with two different buffers remove salts, metabolites and macromolecular cellular components. Pure RNA is finally eluted under low ionic strength conditions with RNase-free water. The RNA concentration was determined by A_{260} using an Eppendorf BioPhotometer. Aliquots of 1 μg RNA were reverse transcribed using M-MLV reverse transcriptase (Promega) at 10,000 units/mL. Aliquots of cDNA corresponding to 0.5 μg of original RNA were used for PCR amplification. RNA integrity was initially checked on a 1% agarose gel by judging the presence of the 18S and 28S ribosomal RNA bands (Figure 2.1).

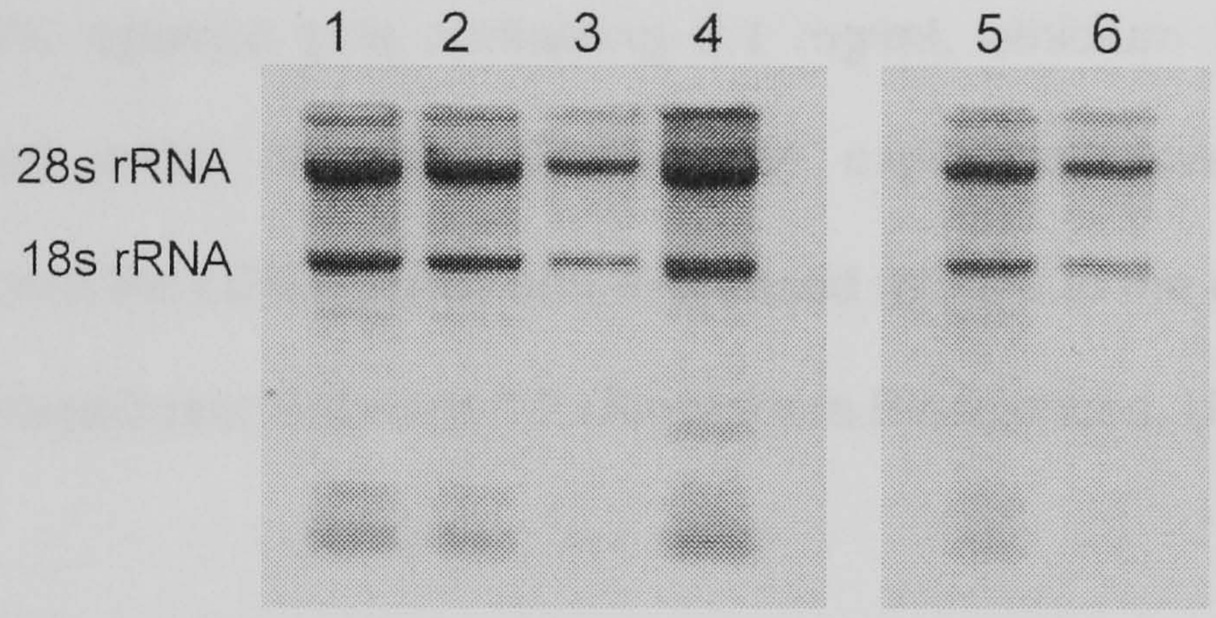

Figure 2.1 Extracted RNA quality control of brain tumours and mammary epithelial cells. Lane 1: meningioma; Lane 2: glioblastoma; Lane 3: medulloblastoma; Lane 4: astrocytoma; Lane 5: MCF10A and Lane 6: MCF7

2.2.1.2 PCR

The cDNA samples were amplified in a 20 μL reaction mixture containing buffer (10mM Tris-HCl, 50mM KCl, and 0.1% Triton), 200 μM dNTP's, 1 U of Taq polymerase, and 0.2 μM of primers.

The 285bp segment amplified from *BRCA1* is located from positions 5239 to 5524 in the published cDNA sequence (GenBank accession number U15595, submitted by Mike et al., 1994). DNA was first denatured for 1.5 min at 94°C, then amplified using cycles of 1 min at 94°C, 45 sec at 50°C and 1 min at 72°C, with a final 7 min incubation at 72°C.

Primers for hTERT were used to amplify a region including the specific T-motif of hTERT to generate a 145 bp fragment. DNA was first denatured for 1.5 min at 94°C, then amplified using cycles of 30 sec at 94°C, 35 sec at 58°C and 30 sec at 72°C, with a final 7 min incubation at 72°C.

β-actin was amplified as a control, resulting in a 764bp product located from positions 265-1028. The cycle number was adjusted so that all reactions fell within the linear range of product amplification.

The sense and antisense PCR primer pairs (5' to 3' direction) and expected product sizes are listed in Table 2.4. PCR products were analysed by electrophoresis through 1.5% agarose gels containing 0.1 mg/mL ethidium bromide and gels were photographed under UV light. The mRNA expression levels were quantified by densitometry of the cDNA bands and expressed relative to the control gene (β-actin) by using the ImageQuant Software 5.2 (Amersham Biosciences, USA).

2.2.2 RT-PCR analysis of telomerase transcripts in brain tumours

2.2.2.1 RNA isolation and reverse transcription

Total RNA was obtained from 72 frozen brain tumour samples using Tri-reagent (Sigma-Aldrich), in accordance with the manufacturer's protocol. During dissection care was taken (macroscopically) to avoid areas with necrosis and excessive blood infiltration. Brain tissues were homogenised in 200-500 µl Tri-reagent in microtubes and matching disposable pestles. This product, a mixture of guanidine thiocyanate and phenol in a mono-phase solution, effectively dissolves DNA, RNA, and protein on homogenisation or lysis of tissue samples. After adding chloroform and centrifuging, the mixture separates into 3 phases: an aqueous phase containing the RNA, the interphase containing DNA and an organic phase containing the proteins. The RNA in the supernatant was precipitated with isopropanol, washed with 75% ethanol, allowed to air dry for 30 min. and dissolved in double distilled water at 4°C. The RNA concentration was determined by A_{260} using an Eppendorf BioPhotometer. RNA

integrity was initially checked on a 1% agarose gel by judging the presence of the 18S and 28S ribosomal RNA bands (Figure 2.1).

First-strand synthesis (reverse transcription, RT) was carried out from total RNA in a volume of 20 µL at 37°C for 1 h with MMLV-reverse transcriptase using random hexamers, followed by inactivation of the MMLV enzyme by incubation at 95°C for 5 min (all reagents from Promega). The RNA yield ranged between 0.4 and 1.2µg/µl and approximately 1 µg RNA was processed for RT.

2.2.2.2 PCR

The cDNA samples were amplified in a 20 µL reaction mixture containing buffer (10mM Tris-HCl, 50mM KCl, and 0.1% Triton), 50 µM dNTP's, 1 U of Taq polymerase, and 0.2 µM of primers. We used a nested PCR approach with primers according to the cDNA sequences as reported by Kilian et al. (1997) and Ulaner and colleagues (Ulaner et al., 1998; 2000) (see also Figure 6.1; Table 2.4).

Table 2.4 Overview of primer sequences used in this study.

Gene	Forward Primer	Reverse Primer	Product size (bp)
BRCA1	5'-GATTTGACGGAAACATCTTAC-3'	5'-CCAGCATCAGTAGTATGA-3'	236
BRCA1	5'-TTGCGGGAGGAAAATGGGTAGTTA-3'	5'-TGTGCCAAGGGTGAATGATGAAA-3'	285
BRCA1	5'-ATGCTGAATGAG-CAT-GATTTT-3'	5'-AGAGTGCTACACTGTCCAAC-3'	351
TERT	5'-TTCCTGCACTGGCTGATGA-3'	5'-GTGTCTGGAGCAAGTTGCAA-3'	126
TERT	5'-CGGAAGAGTGTCTGGAGCAA-3'	5'-GGATGAAGCGGAGTCTGGA-3'	146
TERT	5'-AGTTCCTGCACTGGCTGATGAGT-3'	5'- CTCGGCCCTCTTTTCTCTGCG -3'	328
TERT	5'-GCCTGAGCTGTACTTTGTCAA-3')	5'-CGCAAACAGCTTGTTCTCCATGTC-3'	457
TERC	5'-CTAACCCTAACTGAGAAGGGCGTAG-3'	5'-GAAGGCGGCAGGCCGAGGCTTTTCC-3'	103
TS/PS	5'-AATCCGTCGAGCAGAGTT-3'	5'-GCGCGG $[CTTACC]_3$ CTAACC-3'	TRAP
β-actin	5'-GGGAATTCAAAACTGGAACGGTGAAGG-3'	5'-GGAAGCTTATCAAAGTCCTCGGCCACA-3'	98
β-actin	5'-CAGGTCATCACCATTGGCAATGAGC-3'	5'-CGGATGTCCACGTCACACTTCATGA-3'	135

Primers hTERT-1784S (5'-CGGAAGAGTGTCTGGAGCAA-3') and hTERT-1928A (5'-GGATGAAGCGGAGTCTGGA-3') were used to amplify a region including the specific T-motif of hTERT to generate a 145 bp fragment. The reaction mixtures were heated at 94°C for 30 sec, followed by 33 cycles of 94°C for 20 sec, 68°C for 40 sec and 72°C for 30 sec. Primers 774 (5'-GGGAATTCAAAACTGGAACGGTGAAGG-3') and 775 (5'-GGAAGCTTATCAAAGTCCTCGGCCACA-3') were added at 72°C of cycle 13 for β-actin internal control.

Primers hTERT-2164S (5'-GCCTGAGCTGTACTTTGTCAA-3') and hTERT-2620A (5'-CGCAAACAGCTTGTTCTCCATGTC-3') were used to amplify a sequence between the two reverse transcriptase motifs A and B' of hTERT, to generate a 457 bp fragment. The reaction mixtures were heated at 94°C for 30 sec, followed by 35 cycles of 94°C for 25 sec, 68°C for 50 sec and 72 °C for 50 sec. Primers 774 and 775 were added at 72°C of cycle 15 for β-actin internal control.

Primers hTERC-46S (5'-CTAACCCTAACTGAGAAGGGCGTAG-3') and hTERC-148A (5'-GAAGGCGGCAGGCCGAGGCTTTTCC-3') were used to amplify a hTERC region to generate a 103 bp fragment. The reaction mixtures were heated at 94°C for 30 sec, followed by 28 cycles of 94°C for 20 sec, 68°C for 40 sec and 72°C for 30 sec. Primers 5899 (5'-CAGGTCATCACCATTGGCAATGAGC-3') and 5900 (5'-CGGATGTCCACGTCACACTTCATGA-3') were added at 72°C of cycle 9 for β-actin internal control.

Amplified products were electrophoresed on 4-20% polyacrylamide gels (Novex, Belgium) and visualized with SYBR-Green I nucleic acid gel stain by use of an UV-transilluminator. Double-checks were performed on most samples. Amplification of β-actin cDNA was used to confirm cDNA synthesis and integrity in each sample and the leukaemia cell line Molt-4 was used as a positive control. Some confluent, slow growing cell cultures of meningiomas (cases 5, 7, 9, 17, and 20) were also tested for telomerase expression.

2.3 Telomere length measurement

2.3.1 Terminal restriction fragment (TRF) telomere length analysis

Telomeric hexanucleotide repeats $(TTAGGG)_n$ in humans and some sub-telomeric DNA sequence, do not contain restriction sites. Digestion of genomic DNA with restriction enzymes such as HinfI, reduces the majority of genomic DNA to small fragments, whilst the terminal chromosome fragment remains whole. This fragment, containing an undisclosed length of sub telomeric DNA in addition to the terminal section of hexameric repeats, is termed the terminal restriction fragment (TRF). The average size of the TRF, when separated by agarose gel electrophoresis, can be measured by Southern blotting and hybridisation to an isotope end labelled telomeric oligonucleotide primer, $(TTAGGG)_4$, and detected by autoradiography or Phosphorimager. Telomeric DNA, which is constantly eroded during DNA replication, appears as a smear when analysed, indicating the characteristically heterogeneous telomere population. This technique is commonly used to determine variation in telomere length.

2.3.1.1 Telomere amount length assay

2.3.1.1.1 Extraction of DNA

Exponentially growing monolayer cells were collected by scraping with a rubber policeman, washed two times with PBS and frozen at –80°C upon retrieval. Genomic DNA from frozen fibroblasts was extracted as described by Sambrook et al. (1989). In brief, cells were lysed by incubating at 37°C for 30 min in 10 mM Tris-HCl, pH 8.0, 20 mM EDTA, 0.5% SDS, 20 µg/mL DNase free RNase. Poteinase K (100 µg/mL) (Sigma, St. Louis, MO) was then added and the mixture was incubated at 48°C overnight. The mixture was extracted with 1 volume of phenol, chloroform/isoamyl alcohol. The genomic DNA in the supernatant was precipitated with 2 volumes 100% ethanol/0.1 volume of 3 M sodium acetate (pH 5.2), washed with 70% ethanol, allowed to air dry

for 30 min, and dissolved in double distilled water overnight at 4°C. The DNA concentration was determined by A_{260} using an Eppendorf BioPhotometer.

2.3.1.1.2 Preparation of ^{32}P-labelled telomere probe

The telomere probe $(TTAGGG)_4$ (Sigma-Genosys) was end-labelled with ^{32}P. Briefly, 75 ng of $(TTAGGG)_4$ oligonucleotide was incubated with the forward reaction buffer (Gibco BRL), 35 µCi γ-^{32}P-ATP (Pharmacia Biotech) and 10 units Polynucleotide T4 Kinase (Gibco BRL) for 30 min at 37°C. The labelled probe was purified using QIAquick Nucleotide Removal kit (QIAGEN).

2.3.1.1.3 Telomere amount and length assay (TALA)

Aliquots (2.5 µg) of DNA were digested with the restriction enzymes, i.e., 10 units each of Hinf I, Hha I, Hae III in ReACT2 buffer (all from Gibco BRL), overnight at 37°C. Complete cutting was confirmed by electrophoresis of 5µl of DNA digests on 1% agarose gels. The digested DNA was mixed with 1.5ng ^{32}P-labeled probe in the ReACT 2 buffer. The mixture was denatured at 98°C for 6 min, hybridised at 55°C for 40 min, and further cooled to 4°C for at least 5 min. The unhybridised excess probe and digested non-telomeric DNA fragments were separated from the hybridised telomeres by gel electrophoresis on a 0.7% agarose gel for 6 h at 90 volts in 1X TBE. The gel was then dried in a heater. The dried gel was transferred on a filter, covered with plastic wrap film and exposed to a phosphorimager screen for at least 6 h. The resulting autoradiograph was captured using a phosphorimager, and the intensity of the signal was determined using ImageQuantNT software (Molecular Dynamics, Sunyvale, CA). The average signal was calculated as the average of the signal found in the background areas. The telomere amount was calculated as total intensity of the telomeric signal using the area under curve method minus the background signal. The mean telomere length was defined as length corresponding to the position where 50% of the total signal occurred. Data calculation and statistical analysis were performed

using the Microsoft Excel program. This method was executed successfully but the next non-isotopic method was preferred to eliminate safety issues associated with the handling of radioactive isotopes as the telomeric probe is labelled with digoxigenin (DIG) (see below).

2.3.1.2 Non-radioactive chemiluminescent assay to determine telomere length

2.3.1.2.1 Extraction of DNA and enzyme digestion

Exponentially growing monolayer cells were collected by scraping with a rubber policeman, washed two times with PBS and frozen at –80°C until required. Genomic DNA from frozen fibroblasts was extracted as described by Sambrook et al. (1989). In brief, cells were lysed by incubating at 37°C for 30 min in 10 mM Tris-HCl, pH 8.0, 20 mM EDTA, 0.5% SDS, 20 µg/mL DNase free RNase. Poteinase K (100 µg/mL) (Sigma, St. Louis, MO) was then added and the mixture was incubated at 48°C overnight. The mixture was extracted with 1 volume of phenol, chloroform/isoamyl alcohol. The genomic DNA in the supernatant was precipitated with 2 volumes 100% ethanol/0.1 volume of 3 M sodium acetate (pH 5.2), washed with 70% ethanol, allowed to air dry for 30 min, and dissolved in double distilled water overnight at 4°C. The DNA concentration was determined by A_{260} using an Eppendorf BioPhotometer. A 6 µg sample of genomic DNA from each cell culture was digested overnight with a RsaI/HinfI restriction enzyme mixture (Roche Diagnostics, Mannheim, Germany) at 37°C.

2.3.1.2.2 Electrophoresis and hybridisation of digested DNA

Digested DNA was subjected to 0.8% agarose gel electrophoresis in 1x TAE buffer. The gels were stained with ethidium bromide prior to hybridisation to indicate that the samples were loaded evenly. Two digoxigenin (DIG) size markers were run on each gel to test uniformity of DNA migration rate across the gel. The gel was then depurinated for 5-10 min in 0.25M HCl, denatured for 30 min in 0.5 M NaOH, 1.5 M NaCl, and neutralized for 30 min in 0.5 M Tris-HCl, 3 M NaCl (pH 7.5). Upward

capillary transfer was used to transfer the DNA from the gel to a positively charged nylon membrane and fixed with UV. Hybridisation was carried out with a 3'-end DIG-labelled d(TAGGG)$_4$ at 42°C for 3h. Stringency washes were carried out by washing membranes two times in 2xSSC/0.1% SDS and in 0.2xSSC/0.1% SDS at room temperature. Chemiluminescent detection was performed by virtue of alkaline metabolising CDP-Star as recommended by the manufacturer (Roche Diagnostics, Mannheim, Germany).

2.3.1.2.3 Computing densitometry

Exposure of a chemiluminiscent detection film (Roche) to the membrane revealed telomere lengths as smears ranging from 2 to more than 21 kb. The films were scanned with a densitometer and using ImageQuant software 5.2 (Amersham Biosciences, USA) the telomere signal in each lane was quantified in a grid object, defined as a single column with 30 rows (see Figure 2.2). This grid was placed over the lanes corresponding to the molecular size markers and telomere lane, and recorded. These data were transferred to a spreadsheet Excel (Microsoft) and quantitation was performed by integrating volume. Interpolating molecular sizes for each row were determined by plotting the row number, 1 – 30, against the log10(molecular size) for the molecular size ladder, and fitting a best (least squares) line. The average labelled TRF length in each lane was calculated in Excel as the mean of the optical density above background using the formula $L=\Sigma(OD_i)/\Sigma(OD_iL_i)$, where OD_i and L_i are the signal intensity and TRF length (in base pairs; bp) respectively at position i on the gel image. The samples underwent one to three replicate experiments, and the experimental errors were found to be within 5%.

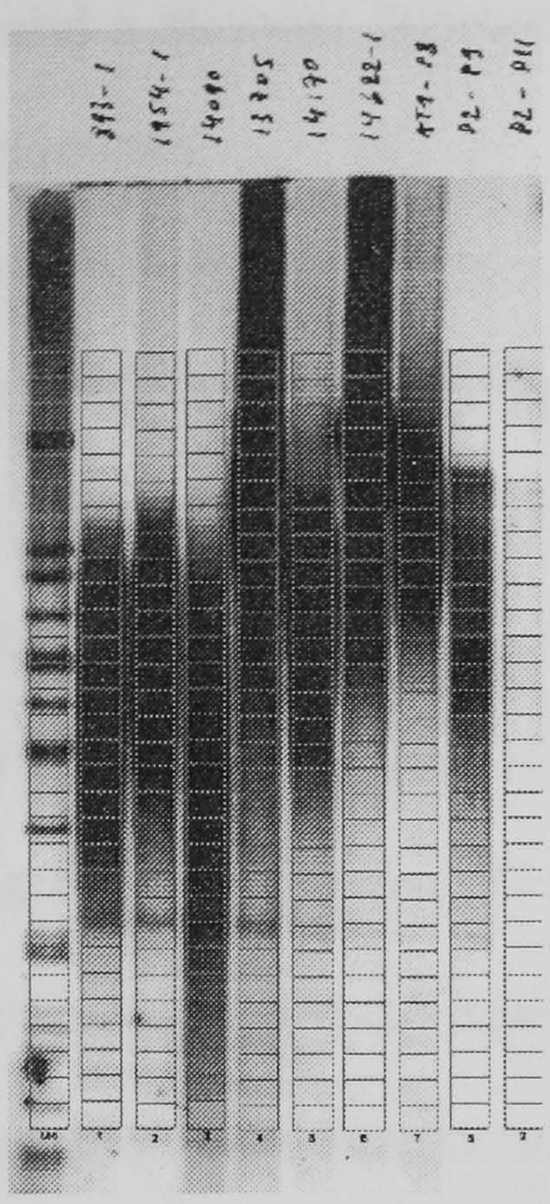

Figure 2.2 Image of a typical gel used to measure telomere lengths. The lane on the left side shows the molecular size marker. Gel profiles were read in a densitometer and collected in a grid, data were transferred to Excel spreadsheet for analysis. Telomeric sizes are then calculated as described in the text.

2.3.2 Telomere length determination by flow-FISH

The average telomere length in cells was measured by flow cytometry as described previously with minor modifications (Rufer et al., 1998). Cells were washed in phosphate-buffered saline (PBS), centrifuged, the supernatant discarded and $5x10^5$ cells were resuspended in 500 µl of hybridisation mixture containing 70% deionised formamide, 20mM Tris buffer pH 7, 1% BSA and 0.3 µg/mL FITC conjugated $(C_3TA_2)_3$ peptide nucleic acid (PNA) probe (Applied Biosystems, MA, USA).

PNA probes contain an uncharged glycine backbone rather than the charged phosphate-ribose/deoxyribose backbone of traditional oligonucleotide probes. The PNA probe hybridises to complementary DNA in low ionic strength solutions that do favour reannealing of the target strands. PNA-DNA interactions are more stable than DNA-DNA or RNA-RNA interactions under hybridisation conditions. This property yields

more reproducible results and a stronger fluorescent signal than can be obtained with conventional DNA oligonucleotides.

Samples were heat-denatured for 10 min at 80°C and left to hybridise for 2h in the dark at room temperature. Samples without PNA probe were used as negative control. Excess probe was then washed away twice in a wash solution containing 70% formamide, 10 mM Tris buffer (pH 7), 0.1% BSA and 0.1% Tween-20, centrifuged for 5 min at RT at 3000 rpm and again washed twice in PBS, 0.1% BSA and 0.1% Tween-20 and centrifuged for 5 min at RT at 2000 rpm. The cells were then incubated in 500 µl PBS, 0.1% BSA, 10 µg/mL RNAse A and 0.1 µg/mL propidium iodide (PI) for 1 h at 4°C prior to the analysis. All samples were stored on ice until analysis by flow cytometry. Flow cytometric analysis was performed on fresh and frozen samples using a Beckman coulter EPICS XL equipped with a single laser and a 4 colour (FITC, PE, ECD/PI and PeCy5) detection system (Becton Dickinson, USA). The size and internal granularity were described by the forward scatter and side scatter, respectively. The FITC signal was detected in the FL1 channel and the propidium iodide fluorescence in the FL3 channel with no compensation set on the instrument. Polyploid cells were eliminated prior to cell cycle analysis because they were recorded next to the G_2/M peak position. Apoptotic and necrotic cells were identified and measured on the PI fluorescence histogram as a hypodiploid peak, as described previously (Nicoletti et al., 1991).

List mode data from 20,000 un-gated events were collected in each experiment and evaluated using Expo32 ADC Analysis software (Coulter corporation, USA). In order to obtain the best CV (coefficient of variation), the flow rate was kept below 150 events/sec. Mean telomere fluorescence intensity (TFI) was calculated as the difference between the mean fluorescence FL1 channel of electronically gated G_0/G_1 cells and the control samples. The performance of the instrument was monitored before analysis by using Flow-Check fluorospheres (Beckman Coulter).

The conversion of TFI units into bp was performed using the formula $y = 4.13x + 2.56$ ($R^2=1$). This formula was obtained following telomere length correlation analysis

in LY-R and LY-S cells, which have telomere lengths of 49 and 7 kb, respectively (McIlrath et al., 2001), by two independent methods, flow-FISH and Q-FISH (quantitative-FISH). This formula was validated using telomere length values from six established human lymphoblastoid cell lines determined by Southern blot and flow-FISH.

2.4 Telomeric repeat amplification protocol (TRAP) assay

The PCR based TRAP (telomeric repeat amplification protocol) assay for telomerase activity was performed essentially as described (Kim et al., 1994) except that there is no incorporation of radioactive nucleotides, use of wax barrier nor end-labelling of primers. Cell lysates were prepared using the CHAPS detergent lysis method and 0.7 µg of total protein was used in each assay. The protein concentration of lysates was measured using Bio-Rad protein assay kit. Amplification products were separated on a 10% non-denaturing polyacrylamide gel, stained with SYBR-green I (Molecular Probes) and visualized using a UV-transilluminator.

2.4.1 Assay for telomerase activity

The TRAP assay measures enzymatic activity of telomerase if it is present. In the first step of the reaction, telomerase adds a number of telomeric repeats (GGTTAG) onto the 3' end of a substrate oligonucleotide (TS). In the second step, the extracted products are amplified by PCR using the TS and ACX (reverse) primers. Following the PCR amplification the reactions are electrophoresed on an acrylamide gel, and if telomerase products are present, they are visible as a 6 bp ladder of products with 6 base increments starting at 50 nucleotides: 50, 56, 62, 68 etc. upon staining of the gel with a fluorescent dye. Additionally, each reaction mixture contains a primer (K1) and a template (TSK1) for amplification of a 36 bp internal standard. Incorporation of this internal positive control makes it possible to quantify telomerase activity more accurately and to identify false-negative samples that contain Taq

polymerase inhibitors. Since telomerase is a ribonucleoprotein, precautions against contamination with RNases were always taken, as well as conventional precautions against contamination with PCR products.

2.4.2 Lysis of cells and tissues

Frozen brain tumour samples were homogenized in 200-600 µL ice-cold extraction buffer [10 mM Tris-HCl (pH 7.5), 1 mM $MgCl_2$, 1 mM EGTA, 0.1 mM benzamidine, 0.5% CHAPS, 5 mM β-mercaptoethanol, 10% glycerol], depending on the size of the tumour sample. After 30 minutes of incubation on ice, lysates were centrifuged at 12,000 g for 20 minutes at 4°C, and 40-200 µL of each supernatant was collected.

2.4.3 Measurement of protein concentration

Protein content in each lysate was measured by the Bradford assay (Bio-Rad laboratories) by using BSA as a standard ($y=0.612 + 0.014$; $R^2=0.99$) and adjusted to 2 µg/µL. The OD_{595} of samples were measured on an Eppendorf BioPhotometer. Aliquots of 40 µL protein extracts were frozen in liquid nitrogen, which were used only once.

2.4.4 Telomerase and PCR reaction

Telomerase enzymatic activity was determined in 49 samples using the TRAP protocol of the TRAPeze Telomerase Detection Kit (Intergen) with minor modifications. Briefly, 0.7 µg of protein extract was incubated in 20 µL of reaction mixture containing 1x TRAP reaction buffer, 50 µM dNTPs, 0.45 µL TS primer (5'-AATCCGTCGAGCAGA GTT-3'), 0.45 µL Primer Mix (RP primer 5'-GCGCGG $[CTTACC]_3$CTAACC-3' (manufacturer's communication), K1 primer and TSK1 template for internal control), and 1U of Taq DNA Polymerase at 30°C for 30 min for telomerase-mediated extension

of the TS primers. Reaction mixtures were subjected to 33 cycles using the following conditions: 94°C for 40 sec, 59°C for 30 sec, and 72°C for 30 sec.

2.4.5 Electrophoresis

Ten microlitres of each PCR reaction was analysed by electrophoresis on 10% polyacrylamide-urea gels (Novex) and visualized with SYBR-Green I nucleic acid gel stain by means of an UV-transilluminator. High telomerase activity is defined as more than six incremental TRAP products. All samples were repeated twice to validate our findings.

2.4.6 Internal PCR standard for TRAP assay

The inclusion of an internal control, a synthetic DNA construct added to all samples and which is amplified with the TS and RP primers to generate a 36-bp product, aided the detection of false-negatives which can result from the presence of PCR inhibitors in the extracts. The immortal cell lines Hela (human cervix carcinoma), U251 (human glioblastoma) and Molt-4 (human T lymphoblastic leukaemia) showed telomerase activity and expressed all alternative splice products of hTERT mRNA. In all further experiments Molt-4 was ultimately used as a positive control, because of ease of cell culture production. As a negative control, cDNA was replaced by lysis buffer.

2.5 Real-Time Quantitative TRAP assay (RTQ-TRAP)

2.5.1 Assay for telomerase activity

A real-time quantitative TRAP (RTQ-TRAP) system has been developed (Hou et al., 2001; Wege et al., 2003) by combining a real-time PCR technique with the conventional TRAP method. RTQ-PCR, designed to avoid the deficiencies of conventional PCR. uses the ABI PRISM 7900HT Sequence Detection System (PE Applied Biosystems). The fluorescent dye SYBR Green is capable of binding to the

double-stranded amplicons and generating fluorescence signals in a PCR reaction. This allows the amount of PCR products to be determined based on fluorescence produced during the extension step of each cycle in a closed tube.

2.5.2 Protein extraction

Cells (1-2 x 10^6) were lysed in 50 µl of CHAPS buffer containing RNase inhibitor and incubated at 4°C for 30 min. The lysate was then centrifuged at 12,000 g for 30 min at 4°C, and the supernatant was collected. The protein concentration was measured using the Coomassie (Bradford) Protein Assay (Pierce Biotechnology, USA) by using BSA as a standard ($y=0.007x + 0.7126$; $R^2=0.897$) and adjusted to 250 ng/µL. The OD_{595} of samples were measured on an Eppendorf BioPhotometer.

2.5.3 RTQ-TRAP assay

The total volume of the reaction mixture was 25 µl and contained 1x SYBR Green PCR master mix (P/N 4309155, PE Applied Biosystems), 0.1µg of primer TS (5'-AATCCGTCGAGCAGAGTT-3') and 0.05 µg of primer ACX (5'-GCGCGG$(CTTACC)_3$ CTAACC-3'). The PCR was performed in a 96 well microtiter plate on an ABI PRISM 7900HT Sequence Detector System. The reaction mixture was first incubated at 25°C for 20 min to allow the telomerase in the protein extracts to elongate the TS primer by adding TTAGGG repeat sequences. The PCR was then started at 95°C for 10 min, followed by a 35-cycle amplification (95°C for 20s, 60°C for 30s, and 72°C for 90s). SYBR Green, a fluorescence dye, is known to bind double-stranded DNA. When new amplicons were produced, SYBR Green bound to them at once and generated fluorescence signals, which were collected and analysed with the Sequence Detector software (Version 2.1; PE Applied Biosystems) during the late step of each cycle. The fluorescence threshold was calculated as 10 SD of the baseline fluorescence intensity at the default setting of 3-15 cycles. Quantification of telomerase activity in unknown samples is extrapolated from the standard curve and threshold cycle C_t. PC3 cells

(prostate adenocarcinoma cell line) were used to set up a standard calibration curve. All samples were run in triplicates, TSR8 oligonucleotide template and MCF10 cells were used as a positive control and the lysis buffer was used as a negative control.

2.6 Transfection of human cells with small interfering RNAs

2.6.1 Principles of siRNA interference

RNA interference (RNAi) is a sequence-specific posttranscriptional gene silencing mechanism, which is triggered by double-stranded RNA and causes degradation of mRNAs homologous in sequence to the dsRNA. Although RNAi has been observed in a wide range of eukaryotes, including plants, protist, filamentous fungi, and vertebrate animals, it has only recently become possible to silence human genes in cultured somatic cells. The detection of RNAi in somatic mammalian cells has been hampered by the presence of a number of dsRNA-triggered pathways that mediate non-specific suppression of gene expression. dsRNA is a potent inducer of type I interferon (IFN) synthesis and is the activator of two clases of IFN-induced enzymes: PKR, the dsRNA-dependent protein kinase, and 2',5'-oligoadenylate synthetases, whose products activate the latent ribonuclease RNase L. These non-specific responses to dsRNA are not triggered by dsRNA shorter than 30 bp including siRNA duplexes that resemble in length and structure the natural processing products from long dsRNAs. The most predominant processing products are duplexes of 21- and 22nt RNAs with symmetric 2-nt 3' overhangs, which are also the most efficient mediators of mRNA degradation.

2.6.2 Procedure of siRNA interference

The small interfering RNAs (siRNA) target sequence of *BRCA1* used is: AAG GAA CCU GUC UCC ACA AAG UU (Bruun et al., 2003). The siSTABLE siRNA duplex was synthesized by Dharmacon Research and provided as a purified and annealed

duplex (Technical Bulletin, Dharmacon Research). Transfection was carried out using Oligofectamine (Invitrogen) following the protocol recommended by Invitrogen.

Briefly, MCF10A and MCF7 cells were grown in T25 flasks until they reached ~ 70% confluence and 4 hours before transfection cells were given fresh culture medium. For each T25 flask, 10 µl of 75 µM stock of siSTABLE siRNA duplex was mixed with 500 µl of Opti-MEM (Invitrogen) while in a separate tube 25 µl of oligofectamine was mixed with 500 µl of Opti-MEM and incubated at room temperature for 5 min. The lipofectamine solution was mixed with the diluted siSTABLE siRNA duplex and incubated at room temperature for 20 min. The lipofectamine-siRNA complex was added drop wise to the cells in 4mL culture medium including serum and incubated at 37°C.

MCF10A and MCF7 cells were also grown on Thermanox coverslips in 24 well plates. For each coverslip, 1 µl of 75 µM stock of siSTABLE siRNA duplex was mixed with 50 µl of Opti-MEM (Invitrogen) while in a separate tube 2 µl of oligofectamine was mixed with 50 µl of Opti-MEM. The two solutions were then gently combined and added to cells in 500 µl culture medium including serum. Cells without siRNA were mock-transfected with lipofectamine. The medium was changed after 48h and cells were harvested after 0-11 days.

2.7 Western blotting

2.7.1 Protein isolation

Cells were scraped from flasks (MCF10A) and petri-dishes (MCF7), centrifuged and washed with ice-cold PBS then lysed on ice for 15 min in lysis buffer. The aim was to find a method that would solubilise all the target antigen (hTERT and BRCA1) in a form that is immunoreactive and undegraded. Therefore, different lysis buffers were examined e.g. single detergent lysis buffers based on Triton XP-100 or Igepal CA-630 (formerly called NP-40) and the triple detergent RIPA lysis buffer, which contains three

detergents. The RIPA lysis buffer was finally chosen to extract proteins: 50mM Tris-HCl pH 8, 150mM NaCl, 1% Igepal CA-630, 0.5% sodiumdeoxycholate, 0.1% SDS supplemented with protease inhibitor mix (Roche, Mannheim, Germany) and 1mM PMSF (phenylmethylsulfonylfluoride). Cell debris was removed from extracts by centrifugation at 13,000 g for 5 min. The protease inhibitor from Roche inhibits a broad spectrum of serine, cysteine and metalloproteases as well as calpains. PMSF is an irreversible protease inhibitor of trypsin-like serine proteases. It causes sulfonylation of the active-site serine residues.

2.7.2 Protein concentration measurement

Concentrations of proteins were determined by using the Bio-Rad DC protein assay. This is a colorimetric assay based on the reaction of protein with an alkaline copper tartrate solution and Folin reagent. This assay was applied because compounds like SDS, Triton X-100, or 2% Igepal, which were used in testing several protein lysis buffers, are compatible with the Bio-Rad DC Protein Assay. A standard curve of optical density against increasing protein concentration was established for each protein sample using serial dilutions of bovine gamma globulin and a Coomassie blue-based dye reagent (Biorad). The protein absorbance was measured on a Hitachi U-1100 spectrophotometer set at 750 nm (located in students teaching laboratory).

2.7.3 SDS-PAGE electrophoresis

hTERT and BRCA1 protein expression levels were determined in MCF cells transfected with siRNA BRCA1, as explained above, and harvested at different times (0-11 days). Aliquots of protein (50 μg/lane) stored at –20°C were mixed with denaturing 5x SDS-PAGE sample buffer (0.25MTris-HCL pH 6.8, 8% SDS, 30% glycerol, 0.2% Bromophenol blue, 5% β-mercaptoethanol) and denatured by heating at 90 °C for 4 min. A 30% acrylamide/methylene bisacrylamide solution was used to prepare a 6% running gel and a 5% stacking gel (6 and 5%, respectively for BRCA1;

10 and 5%, respectively for hTERT) prepared with standard Laemmli solutions. Hundred micrograms of protein per lane was loaded onto the gel and SDS-PAGE was carried out using a Biorad Mini-Protein II electrophoresis cell for 30 min at 100 V and then for 45 min at 150 V at 4 °C. In each experiment, equal aliquots of total cellular protein were electrophoresed. A high range molecular weight marker (Biorad) was run on each gel.

2.7.4 Immunoblotting

Proteins were transferred to Hybond-P membranes (Amersham Biosciences) in a mini trans-blot electrophoresis transfer cell (BioRad) for 1 h at 180 mA at 4 °C and blocked for 1 hour in 5% non-fat dry milk, 0.1% Tween-TBS.

All antibodies used in this study are shown in Table 2.5. To detect BRCA1 and hTERT proteins, blots were incubated overnight at 4°C. BRCA1 was detected using a mouse monoclonal antibody Ab-4 (Oncogene) at a concentration of 2µg/mL or a rabbit polyclonal antibody C-20 (Santa Cruz Biotechnology, CA, USA) at a dilution of 1:200. hTERT was detected using L-20 (Santa Cruz). This antibody is an affinity purified goat polyclonal antibody, mapping near the amino terminus of TERT of mouse origin

The blots were then rinsed in TBS with 0.1% Tween for 2x10 min and incubated at RT for 1 hour with a secondary peroxidase (BRCA1: goat anti-mouse IgG at a dilution of 0.2 µg/mL or with a secondary peroxidase goat anti-rabbit IgG at a dilution of 1:5000; hTERT: chicken/donkey anti-goat IgG at a dilution of 1:5000). The immunoblots were rinsed for 3x10 min with 0.1% T-TBS.

Blotted proteins were visualized using the enhanced chemiluminiscence (ECL+Plus) detection reagents (Amersham Biosciences). A monoclonal anti β-actin AC-15 (Sigma, MI. USA) at a dilution of 1:5000 was used to confirm siRNA BRCA1 transfection efficiency and equal protein loading to each well. A dual colour marker (Cat No. 161-0374, BioRad) was used as a molecular size standard. The blotted membrane was exposed to Lumi-Film Chemiluminiscent detection film (Roche). The protein bands

were quantitated by densitometry using the ImageTool Software 3.0 (The University of Texas Health Science Center, San Antonino, USA) and the values were expressed relative to β-actin as a control. The total protein content on the membrane was checked by Coomassie blue staining.

Table 2.5 Overview of antibodies used for Western blotting (WB) and immunocytochemistry (IHC). M: monoclonal; P: polyclonal

Antibody	Cat. No.	Type	Source	Application
BRCA1 (Ab-1)	OP92	M	Oncogene	IHC
BRCA1 (Ab-4)	OP107	M	Oncogene	WB
BRCA1 (C-20)	sc-642	P	Santa Cruz	WB
γ-H2A.X (Ser139)	05-636	M	Upstate Biotechnology	IHC
Ki-67	NCL-KI67-MM1	M	Novocastra	IHC
Ki-67	A0047	P	Dako	IHC
PCNA (PC10)	sc-56	M	Santa Cruz	IHC
Nucleolin - C23 (MS-3)	sc-8031	M	Santa Cruz	IHC
TERT (L-20)	sc-7214	P	Santa Cruz	WB
TERT (H-231)	sc-7212	P	Santa Cruz	IHC
TRF1 (C-19)	sc-1977	P	Santa Cruz	IHC
TRF2 (N-20)	sc-8528	P	Santa Cruz	IHC
PML (PG-M3)	sc-966	M	Santa Cruz	IHC
PML (A-20)	sc-9863	P	Santa Cruz	IHC
β-Actin (AC-15)	A5441	M	Sigma	WB
goat anti-mouse IgG HRP	DC02L	-	Oncogene	WB
goat anti-rabbit IgG HRP	sc-2004	-	Santa Cruz	WB
donkey anti-goat IgG HRP	sc-2020	-	Santa Cruz	WB
rabbit anti-goat IgG biotinylated	BA-5000	-	Vector Laboratories	IHC
goat anti-mouse IgG FITC	F5262	-	Sigma	IHC
donkey ant-goat IgG FITC	sc-2024	-	Santa Cruz	IHC
donkey anti-goat IgG TR	sc-2783	-	Santa Cruz	IHC
donkey ant-goat IgG TRITC	sc-2094	-	Santa Cruz	IHC
chicken anti-mouse IgG FITC	sc-2989	-	Santa Cruz	IHC
chicken anti-mouse IgG TR	sc-3924	-	Santa Cruz	IHC
chicken anti-mouse IgG TRITC	sc-2861	-	Santa Cruz	IHC

2.8 Immunocytochemistry

2.8.1 Single immunofluorescence detection of γ-H2AX, BRCA1, PML, and TRF1/2

Immunofluorescent staining was performed on 1:1 methanol/acetone-fixed cells on Thermanox coverslips or on poly-L-lysine-coated slides (Sigma), fixed for 15 min at room temperature in a 4% paraformaldehyde-buffered solution, and permeabilised with 0.1% Triton X-100 for 10 min at 4°C. For list of antibodies see Table 2.5. Cells were blocked in 0.5% BSA in PBS and incubated with 2µg/mL mouse monoclonal anti-phospho-histone H2AX (Upstate, NY, USA), 1:100-500 mouse monoclonal anti-BRCA1 (Oncogene Research, CA, USA), mouse monoclonal anti-PML, mouse monoclonal anti-TRF1 and TRF2 (Santa Cruz) in blocking buffer for 1 hour at room temperature or performed overnight at 4°C. Cells were then washed and incubated with a species-specific secondary IgG FITC-, TRITC- or Texas Red-conjugated antibody (Sigma and Santa Cruz) at 1:100-500 for 1 hour at room temperature. Cells were then washed in PBS several times and covered with Vectashield mounting medium (Vector Laboratories, CA, USA) containing 1.5 µg/mL DAPI. Slides were viewed using a Zeiss fluorescence Axioplan2 imaging microscope and digitally scanned.

2.8.2 Double immunofluorescence detection of TRF2 with PML, γ-H2AX, and BRCA1

Cells were spread onto poly-L-lysine-coated slides. For the simultaneous visualization of TRF2-PML, TRF2-γ-H2AX, and TRF2-BRCA1 foci, cells were fixed as mentioned in previous section. Cell preparations were blocked for 1 h in 10% FBS/PBS, rinsed, and incubated with primary antibodies. Double staining with antibodies was performed for 1 hour at room temperature or overnight at 4°C in PBS/1% BSA, whereas species-specific FITC-, TRITC-, or Texas Red-conjugated secondary antibodies were applied for 1 h at room temperature followed by counterstaining for 5 min at room temperature with 0.5 µg/mL DAPI. Slides were mounted in Vectashield (Vector Labs, USA) and analysed by fluorescence microscopy. All primary antibodies

were used at 1 : 300-600 dilutions, whereas the secondary antibodies were employed at a 1 : 500 dilution. At least 100 nuclei were examined, showing at least one foci, which were scored at a magnification of 400x using a fluorescence microscope. Parallel samples, incubated either with serum or only with the secondary antibody, confirmed that the observed fluorescence pattern was not attributable to artefacts.

2.8.3 Immunocytochemistry on paraffin embedded brain tumour tissues

Eighty-five paraffin-embedded tissues of 32 intracranial tumours were used for the cell proliferation assessment. Sections of 3 μm thickness, adjacent to H&E and Masson trichrome sections, were heated in sodium citrate buffer (10 mM; pH 6.0) for 10 minutes in a microwave oven for high temperature antigen unmasking. The endogenous peroxidase activity was blocked by 3% H_2O_2 in Tris-Buffered Saline (TBS) buffer, pH 7.6 for 5 min.

A three-step SABC method was used. Sections were first incubated with the monoclonal antibody Ki-67 (Novocastra NCL-Ki-67-MM1) at a dilution of 1:100. Subsequently, sections were incubated with biotinylated rabbit anti-mouse, 1:200 in TBS for 30 min, followed by the third incubation step with streptavidin-biotin-peroxidase complex, 1:200 for 30 min. Visualization of the complex was realized with diaminobenzidine (DAB) and sections were counterstained with haematoxylin. Epidermis tissue and Molt-4 cells were applied as positive controls, whereas brain tissue was used as negative control. Ki-67 labelling indices (LI) were calculated as mean percentage values by counting nuclei of tumour cells in three 0.22 mm^2 areas of a single tumour, each area consisting of 500 to 1800 neoplastic cells depending on the tumour type.

2.8.4 Immunocytochemistry on brain tumour cell cultures

2.8.4.1 Immunocytochemistry of Ki-67, hTERT, PCNA and Nucleolin

Cells were either grown on Thermanox coverslips or fixed and dropped on slides. For preparation of droplet slides, T25 cell cultures were trypsinised and centrifuged at 900 rpm for 4 min. The cell pellets were resuspended in 10 mL of hypotonic buffer (75mM KCl) and placed in a 15 mL tube at RT for 15 min. This was followed by fixation (9:1:10, formaldehyde:acetic acid:Ringer buffer) for 5 min on ice. Cells were centrifuged at 900 rpm for 4 min and resuspended again in 10 mL fixative, followed by 5 min incubation on ice and centrifugation. Fixative was changed in 70% ethanol. Cells were immediately dropped on slides and processed. Cells on coverslips were washed three times with cold PBS then fixed by treatment with acetone at 4°C for 3 minutes.

Cells were incubated with primary antibody solutions for 1 hour at room temperature with a monoclonal Ki-67 (NCL-Ki-67-MM1, Novocastra), polyclonal Ki-67 (A 0047, Dako, UK), rabbit polyclonal hTERT antibody (H231 and L-20, Santa Cruz Biotechnology), PCNA (PC10, Novocastra, UK), and Nucleolin (C23, Santa Cruz, USA) at 1:100 at room temperature for 1.5 h. After washing three times in PBS, cells were incubated with biotinylated secondary antibodies at 1:200 for 30 minutes at room temperature. Cells were then washed three times with PBS and once with water then stained with DAB or AEC+ substrate chromogen (Dako), and counterstained with Haematoxylin or toluidine mounted onto glass slides in aqueous mounting medium (Faramount, Dako). Slides were viewed using a Zeiss Axiolab microscope and digitally scanned using a Pixera Professional camera. Images were collected using a 40 or a 100x oil-immersion lens and were edited in Adobe Photoshop 5.5 and CorelDraw10.

2.8.4.2 Double immunocytochemsitry of Ki-67 with hTERT

Cells on coverslips were washed three times with PBS then fixed by treatment with acetone at 4°C for 3 minutes or with 50% methanol/acetone for 2 min at room temperature. Coverslips were blocked in 0.5% BSA/PBS. Co-staining for Ki-67 and hTERT was carried out using a 1:100 dilution of the monoclonal Ki-67 (NCL-Ki-67-MM1, Novocastra) and the rabbit polyclonal TERT antibody (L-20, Santa Cruz Biotechnology). After washing three times in PBS, cells were incubated in a 1:100 dilution of the FITC rabbit anti-mouse IgG (Dako) and the Texas Red goat anti-rabbit IgG secondary antibodies. Dilutions were established by preliminary titration. Cells were then washed three times with PBS and once with water then mounted onto glass slides in 10% DABCO and 1 μg/mL DAPI or propidiumiodide (PI). Slides were viewed with Vectashield mounting medium (Vector) using a Leica DMRB fluorescence microscope. Images were collected using a 100x oil-immersion lens and were edited in Adobe Photoshop 5.5 and CorelDraw10. Images were photographed using a Leitz orthomat camera or digitally scanned with a Pixera camera.

2.9 Fluorescence *in situ* hybridisation (FISH) of telomeres

In order to obtain metaphases, 0.1 μg/mL colcemid (Demecolcine, Sigma) was added 2 hours prior to harvesting to exponentially growing cell cultures. Cells were centrifuged at 1200 rpm for 4 min followed by 30 min hypotonic pre-treatment with 75mM KCl then fixation in 3:1 methanol:acetic acid solution. Cell suspensions were dropped onto clean glass slides and aged at 55°C overnight. The slides were washed in PBS and fixed in 4% formaldehyde for 2 minutes. After a second wash in PBS, the metaphases were incubated in 1 mg/mL pepsin solution (Sigma) in acidified water (1 mM hydrochloric acid) at 37°C for 10 min. The slides were then briefly washed in PBS, fixed in 4% formaldehyde for 2 min, and dehydrated through 70%, 90%, and 100% ethanol. Metaphase spreads were hybridised with a 6 μl/mL FITC or Cy3-conjugated PNA probe $(C_3T_2A)_3$ (Applied Biosystems, MA, USA) in 700 μl deionised formamide, 5

µl blocking reagent (10% in maleic acid), 50 µl $MgCl_2$ buffer (2.5M $MgCl_2$, 9 mM Na_2HPO_4, pH 7), 10 µl TRIS (1 M, pH 7.2), and 152 µl deionised water, as described in Zijlmans et al. (1997). The slides were denatured at 72°C for 2 min and incubated for 2 h at room temperature in the dark. The slides were washed in 70% formamide (15 min) and in PBS, and dehydrated in ethanol before counterstaining with DAPI. Images of metaphase and interphase cells were obtained on a Zeiss Axioplan working station equipped with a CCD camera (Photometrics) and Smartcapture 2 software (Digital Scientific) using fixed time exposure of 0.3 sec and magnification of 400x and 1000x. Only the objects on the same planar focus were chosen for analysis. The total telomere fluorescence intensity per cell was determined using ImageQuant software (version 5.0 Molecular Dynamics, USA). The average signal was calculated as a total intensity of the telomeric signal using the area under curve method minus the background signal. The accuracy of the method was verified by comparing TFI values of LY-R cells generated by this method and TFI values of the same cells generated by conventional Q-FISH. To test for the presence of cell subpopulations with different telomere lengths the following method was applied. TFI of each individual cell was compared with remaining 14 cells (a total of 15 cells is typically analysed in Q-FISH measurements) on the basis of grouping cells into clusters in which TFI values of individual cells do not differ by > 50% from any other cell in the cluster. For example, if TFI of a single cell is 1,000 any cell that has 50% more or less fluorescence (the range 500-1500) will become part of that cell cluster. This method is referred to as cell clustering. The presence of two cell clusters with statistically significant differences in the average TFI values is consistent with two subpopulations of cells with different telomere lengths.

2.10 Combined immunofluorescence and FISH (Immuno-FISH)

Cells were grown, fixed, and permeabilised as described previously. First, detection of γ-H2AX foci by immunofluorescence was performed. Digital images of cells with γ-H2AX foci were captured and coordinates were noted. Next, the FISH method,

described in previous section, was applied with a Cy3-conjugated PNA probe $(C_3T_2A)_3$ (Applied Biosystems, MA, USA), followed by standard formamide and SSC washes. Cells were counterstained with DAPI in fluorescence antifade medium. Digital images of cells with γ-H2AX foci and telomere signals were edited in CorelDraw or layered on top of each other by use of Photoshop software.

2.11 Cytogenetic analysis

2.11.1 Anaphase bridge analysis

For anaphase bridge analysis, cells were cultured on Thermanox plastic coverslips (Nunc, NY, USA) in 24-well plates or on poly-L-lysine-coated slides in the appropriate culture medium. Cells were treated with or without cytochalasin B. Cytochalasin B depoplymerise (eliminates) actin and therefore maintains the two daughter nuclei in the same cytoplasm by inhibition of cytokinesis which makes it more easy to detect anaphase bridges. Fibroblasts were harvested at different passages, mammary epithelial cells before and during different stages of BRCA1 siRNA transfection and fixed with methanol:acetic acid (3:1). Slides were stained with 10% Giemsa or DAPI and a total of 100-200 cells were scored for the presence of anaphase bridges.

2.11.2 Metaphase chromosome analysis

Cell monolayers were grown in 25 and 75 cm^2 flasks until 80-90% confluency and then treated for 2-6 hours at 37°C by addition of 20µl of demecolcine (colcemid) solution (10µg/mL in HBSS, Sigma-Aldrich) to the culture. The culture medium and PBS wash were retained during trypsinisation and combined with the harvested cells, which were then centrifuged at 400 g in a 50 mL tube for 8 min. The cell pellets were resuspended in 10 mL of hypotonic buffer (75mM KCl) and placed in a 15 mL tube at 37°C for 12 min. This was followed by addition of 1 mL of ice cold fixative (3:1, methanol:acetic acid) and a 5 min incubation on ice. Cells were centrifuged again at

400 g for 8 min and resuspended twice in 10 mL fixative, followed by 5 min incubation on ice and centrifugation. Preparations were stored in 15 mL fixative at -20°C.

2.12 AgNOR silver staining

Representative sections of the resected brain tumours were selected for the AgNOR silver staining technique. Four-micron unstained sections were obtained from these areas to perform the stain. The modified AgNOR silver staining technique introduced by Ploton et al. (1982) was used. The tissues were deparaffinised in several changes of xylene and descending alcohol concentrations, followed by rehydration in several changes of ultrapure distilled water. The tissues were then incubated in acid alcohol (3 parts ethanol : 2 parts acetic acid) for 5 min and several times rinsed in ultrapure distilled water. The sections were then incubated with silver nitrate solution in a dark humidified chamber for 30 min. The silver staining solution consisted of two parts of a 50% solution of silver nitrate and one part 2% gelatine in 1% formic acid solution. The sections were then incubated with a 10% solution of sodium thiosulfate solution for 5 min, washed in distilled water, dehydrated in graded alcohol, xylene and coverslipped.

2.13 TUNEL apoptotic cell detection in paraffin-embedded tissues

In the TUNEL assay, the enzyme terminal deoxynucleotide transferase (TdT) adds fluorescently-labelled dUTP onto broken DNA strands. TUNEL (terminal deoxynucleotidyl transferase [TdT]-mediated deoxyuridinetriphosphate [dUTP] nick end labelling) assay was performed as described by the manufacturer (Promega, MA, USA). Briefly, paraffin embedded tumour tissues (5µm paraffin sections) were deparaffinised in toluene, washed in ethanol 100% and then rehydrated by sequentially immersing slides through graded ethanol washes for 3 minutes each at room temperature. Tissues were permeabilized with 20µg/mL proteinase K for 10 minutes at room temperature. The tissue sections were refixed in 4% paraformaldehyde solution

in PBS for 5 minutes at room temperature. The sections were equilibrated with 100µl of equilibration buffer (200mM potassium cacodylate pH 6.6, 25mM Tris-HCL pH 6.6, 0.2mM DTT, 0.25mg/mL BSA and 2.5mM cobalt chloride) for 10 minutes. Tissues were incubated with TdT (Terminal deoxynucleotidyl Transferase) enzyme reaction mixture (TdT enzyme, biotinylated nucleotide mix, and equilibration buffer) at 37°C for 1 hour inside a humidified chamber to allow end-labelling reaction to occur. The reaction was terminated in 2x SSC for 15 minutes and washed in PBS for 2x5 minutes. Immersing the slides in 0.3% hydrogen peroxidase for 3 minutes at room temperature blocked endogenous peroxidase. Tissue sections were incubated for 30 minutes in streptavidin HRP solution at a dilution of 1:500, washed in PBS and incubated for 10 minutes in DAB chromogen solution. Slides were stained with H-E and mounted in Canada balsem.

HL-60 cells were used as a positive control by treating them with DNase I to cause DNA fragmentation. For negative controls, sections were incubated without TdT enzyme.

2.14 PCR ELISA for detection of Mycoplasma

A photometric enzyme immunoassay was used for the detection of PCR-amplified DNA of Mycoplasma in cell cultures according to the manufacturer (Roche Diagnostics GmbH, Mannheim, Germany). Briefly, cells were centrifuged and lysed in an alkaline lysis solution then neutralised. A conserved Mycoplasma-specific region of the DNA was amplified in the presence of a digoxigenin-labelled dUTP (DIG-dUTP). The DIG-labelled amplicon was denatured by NaOH treatment. The single stranded PCR product was hybridised to a biotin labelled capture probe and immobilised on streptavidin coated microtiter plate wells. The immobilised amplicon was detected by means of an antibody to digoxigenin coupled to horseradish peroxidase (anti-DIG-POD) and a sensitive peroxidase substrate.

2.15 Statistical Analysis

The Mann-Whitney U test and the two-tailed Student's t-test were applied to compare the mean ± standard error (S.E.) or standard deviation (S.D.) values. A P-value < 0.05 was considered as statistically significant. Linear regression correlation was analysed by the Spearman rank correlation coefficient.

CHAPTER 3

IDENTIFICATION OF SUBPOPULATIONS OF CELLS WITH DIFFERENT TELOMERE LENGTHS IN MOUSE AND HUMAN CELL LINES BY FLOW-FISH

3.1 Introduction

Telomeres are specialized protective structures at chromosome ends, which undergo dynamic changes in each cell cycle (Blackburn, 2000). Telomere dynamics involves mechanisms of telomere degradation, as well as mechanisms of telomere renewal. Telomere degradation results from the end replication problem (Olovnikov, 1973), exonuclease activity (Wellinger et al., 1996) and DNA breakage within telomeric sequences due to oxidative damage (von Zglinicki, 2002). Telomere renewal is achieved either through the activity of telomerase or recombination mechanisms known as the ALT (alternative lengthening of telomeres) pathway (Blackburn, 2000). The interplay between opposing mechanisms of degradation and renewal is usually mediated by telomere binding proteins (Smogorzewska et al., 2000). These proteins regulate telomerase in either a positive or negative fashion on the basis of telomere length information (Smogorzewska et al., 2000). Mechanisms that regulate ALT are not clear at present.

In normal human somatic cells telomere degradation mechanisms are dominant and after a limited number of divisions cells will eventually reach telomere-mediated senescence, which can be recognized by the formation of nuclear foci comprising dysfunctional telomeres and numerous DNA damage response factors (d'Adda di Fagagna, 2003). In human immortalized cell lines telomere length is generally stable suggesting that in these cells an equilibrium exists between telomere degradation and telomere renewal (Blackburn, 2000).

There is far less information about the status of telomere length in primary versus immortalized mouse cell lines. However, results exist for various normal mouse strains, which indicate much longer and more heterogeneous telomeres in comparison with human cells (Zijlmans et al., 1997). It is noteworthy that in many genetically modified mouse strains telomeres are either significantly shorter or longer in comparison with wild type animals. For example, telomeres in telomerase deficient mice shorten gradually in each successive generation (Blasco et al., 1997). In contrast, telomeres in scid (severe combined immunodeficiency) mice, which have defective DNA-PK, an enzyme involved in DNA double-strand break repair (see section 1.6.3), are abnormally elongated (Hande et al., 1999). Interestingly, mice deficient in Ku, another protein involved in DNA double strand break repair (see section 1.6.3), show either shorter or elongated telomeres in comparison with wild type animals (d'Adda di Fagagna et al., 2001; Samper et al., 2000). Therefore, telomere length in mouse cells appears to fluctuate more than telomere length in human cells possibly as a result of mouse telomeres being naturally long.

The assessment of telomere dynamics is critically dependent on telomere length measurement techniques. Several techniques are available including Southern blot analysis, quantitative fluorescence *in situ* hybridisation (Q-FISH), flow-FISH, hybridisation protection assay (HPA), quantitative PCR and single telomere length analysis (STELA). Each technique has advantages and limitations. For example, Southern hybridisation and flow-FISH can determine average telomere length whereas

Q-FISH provides information about telomere length in individual chromosomes. Unlike Southern blot, the HPA quantifies the telomeric repeats and does not include subtelomeric regions (Nakamura et al., 1999; Freulet-Marriere et al., 2004). Another method to measure average telomere lengths is quantitative PCR (Förstemann et al., 2000; Cawthon, 2002). Quantitative PCR, which is inherently sensitive and accurate, has been hampered by the lack of appropriate primer binding sites (Förstemann et al., 2000; Cawthon, 2002). In addition to Q-FISH, which can measure the length of telomeres from individual chromosomes, a new elegant method called STELA was recently developed by Baird et al. (2003). However, in contrast to Q-FISH, which measures all telomeres, so far STELA was used to measure telomeres in only XpYp chromosome at a time. A distinctive advantage of flow-FISH over other techniques is that it can accurately identify sub-populations of cells with different telomere length in a given cell population. For example, pioneering flow-FISH experiments revealed that different subpopulations of human peripheral blood lymphocytes have different telomere lengths (Rufer et al., 1998).

The first aim of this study was to set up the flow-FISH method in our laboratory and assess its accuracy in comparison with other methods in particular Southern blot and Q-FISH. We used a pair of mouse lymphoma cell lines with well defined telomere lengths as calibration standard for flow-FISH and unexpectedly identified the presence of subpopulations of cells with different telomere lengths in several cell lines. Results of this analysis are described in detail below.

3.2 Results

3.2.1 Establishment of flow-FISH protocol for telomere length measurement

The first task in this study was to set up the flow-FISH method in our laboratory. Initially, the flow-FISH technique was applied on mouse lymphoma LY-R and LY-S cells. These cells have well defined telomere lengths as determined by Q-FISH in one of our earlier studies i.e. LY-R cells have, on average, 7-8 times longer telomeres than LY-S cells (McIlrath et al., 2001). Telomeres in LY-S cells are ~ 7 kb whereas telomeres in LY-R cells are ~ 50 kb long (McIlrath et al., 2001). Given that one cell line has short telomeres and the other one long telomeres, these cell lines can potentially be used as calibration standards for flow-FISH. An example of LY-R cells hybridised with a telomeric PNA probe before flow-FISH analysis is shown in Figure 3.1. Our flow-FISH measurements of telomere fluorescence intensities (TFIs) indicated a good agreement with Q-FISH. For example, in several independent experiments we observed Q-FISH-like differences in TFIs between LY-R and LY-S cells (results not shown; for flow-FISH profiles of LY-R and LY-S cells see below). This is in line with results generated in the laboratory of our collaborator, Dr. Maria Blasco, where LY-R and LY-S cells are used routinely as calibration standards for flow-FISH (Samper et al., 2002; Espejel et al., 2002; Franco et al., 2004). Because results of TFI measurements in LY-R and LY-S cells were highly reproducible we generated a calibration curve for the conversion of TFI into base pairs (bp) of DNA using published Q-FISH results (McIlrath et al., 2001) and our own flow-FISH measurement in LY-R and LY-S cells (Figure 3.2). Therefore, the conversion of TFI values from any cell line into bp of telomere length can be carried out using the formula $y = 4.13 x + 2.56$ (Figure 3.2 A). To test the formula we performed a correlation analysis of telomere length measurement between the classical Southern blot method and flow-FISH measurements generated for six human lymphoblastoid cell lines. This analysis revealed a good correlation with the R^2-value of 0.90 (Figure 3.2 B).

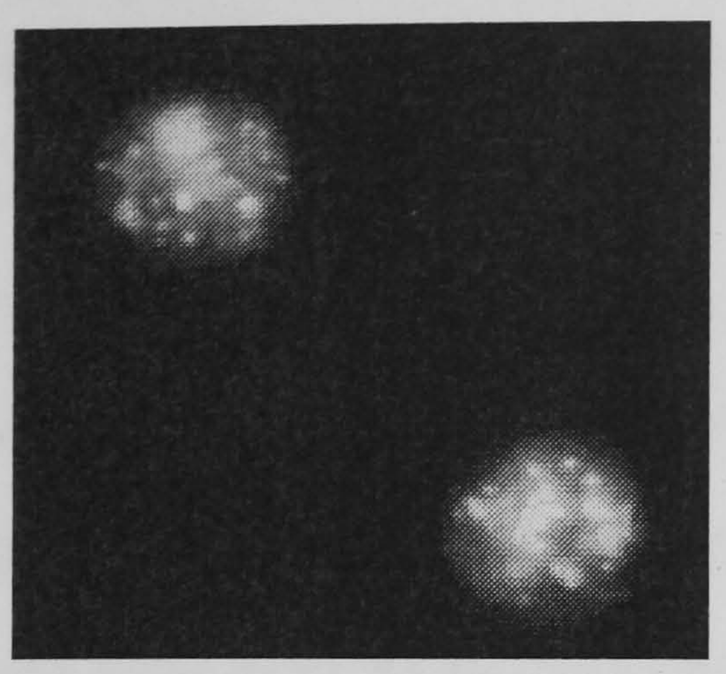

Figure 3.1 LY-R cells floating in PBS buffer hybridised with a FITC conjugated $(C_3TA_2)_3$ PNA probe and the nuclei counterstained with propidium iodide (PI) ready for flow-FISH analysis.

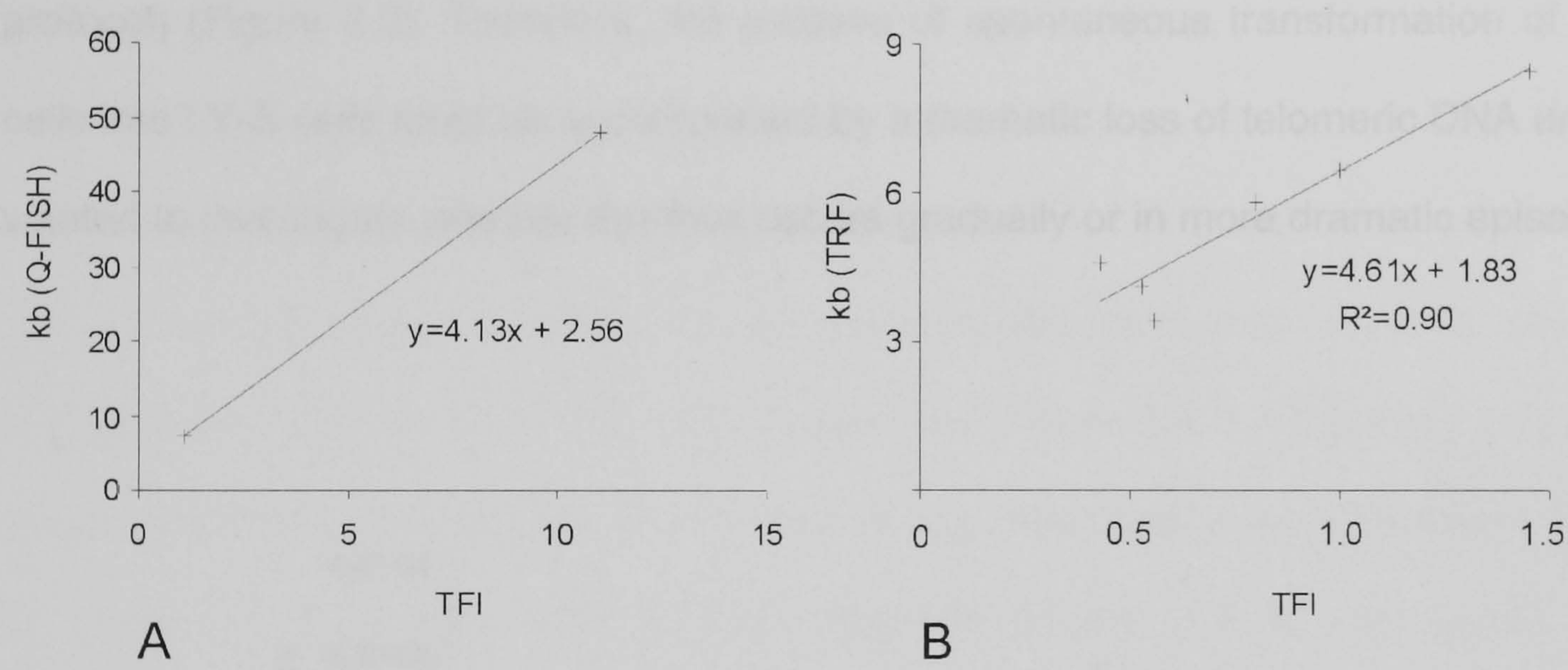

Figure 3.2 (**A**) A calibration curve generated using published Q-FISH results (McIlrath et al., 2001) and our own flow-FISH measurements (TFI) in LY-R and LY-S cells. (**B**) Correlation analysis of telomere length using flow-FISH and Southern hybridisation in six lymphoblastoid cell lines (for the list of cell lines see table 2.2).

3.2.2 Telomere length dynamics in mouse lymphoma cell lines

Above results indicate that the flow-FISH method generates highly reproducible results in our hands and that these results are remarkably similar to those produced in the laboratory of our collaborator Dr. Maria Blasco. Therefore, we wanted to assess telomere dynamics in LY-R and LY-S cells over time using flow-FISH. Assessment of telomere dynamics in these cells is interesting for a specific reason described below. The mouse lymphoma cell line, LY-S, shows extreme sensitivity to ionising radiation

(IR), in contrast to the parental cell line, LY-R, which has normal sensitivity to IR (Alexander and Mikulski, 1961). The process of transformation of LY-R cells into LY-S cells is spontaneous and occurs after prolonged *in vitro* culture. Sensitivity of LY-S cells to IR results from impaired repair of DNA double strand breaks (DSBs) although many known DSB repair components in LY-S cells are normal (McIlrath et al., 2001). As mentioned above LY-R cells have much longer telomeres (~ 50 kb) than LY-S cells (~ 7 kb (McIlrath et al., 2001). This difference in telomere length is not due to differences in telomerase activity i.e. both cell lines showed similar levels of telomerase activity as was verified by RTQ-TRAP (real-time quantitative telomeric repeat amplification protocol) (Figure 3.3). Therefore, the process of spontaneous transformation of LY-R cells into LY-S cells must be accompanied by a dramatic loss of telomeric DNA and we wanted to investigate whether this loss occurs gradually or in more dramatic episodes.

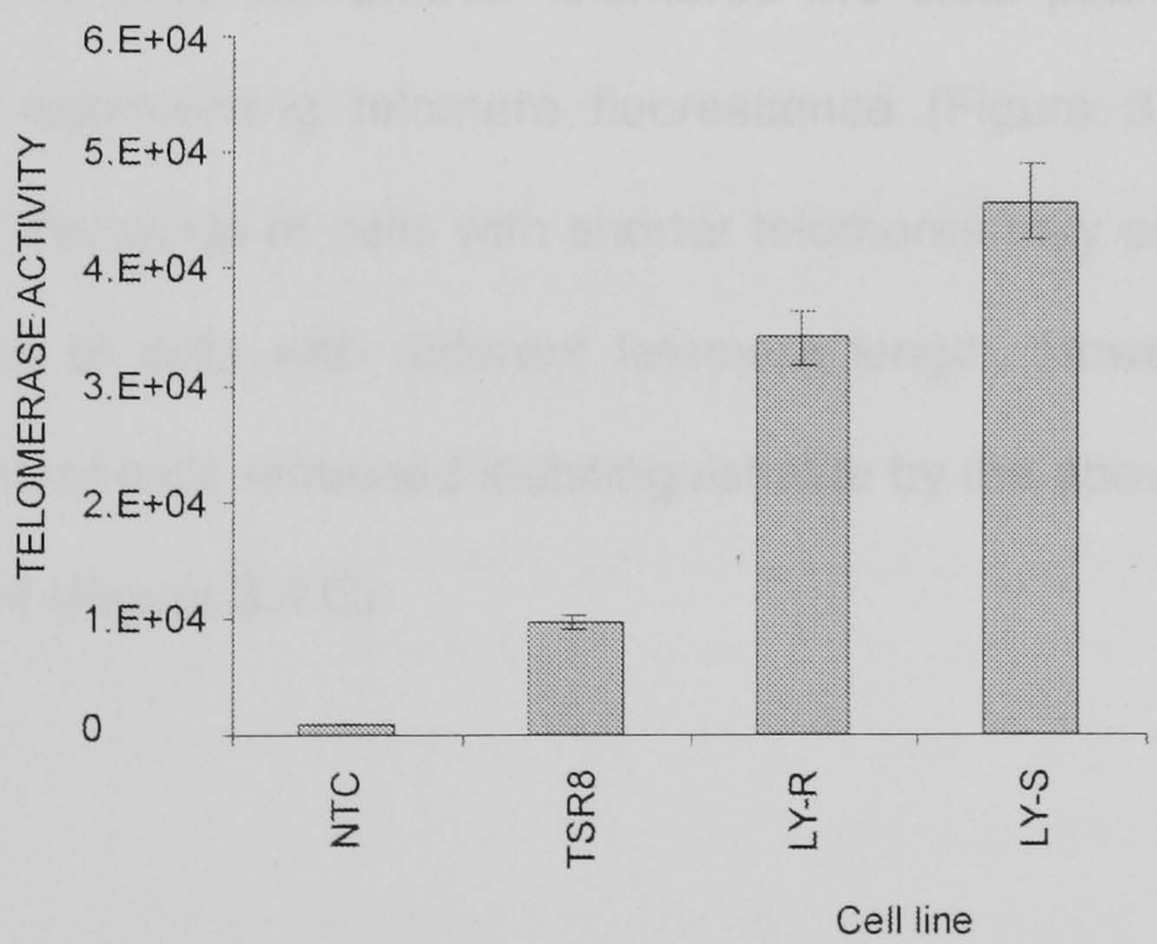

Figure 3.3 Telomerase activity as determined by RTQ-TRAP in LY-S and LY-R cells. Pooled results are shown (n=6) indicating telomerase activity as a percentage relative to that found in the prostate adenocarcinoma cell line PC-3. NTC: negative control; TSR8 oligonucleotide template: positive control.

The above two cell lines were grown for ~ 80 population doublings (PDs) and telomere length was monitored by flow-FISH after, on average, each 9 PDs. LY-R cells had expected telomere length and flow-FISH parameters indicated the presence of a single cell population up to PD ~ 20 (Figures 3.4 A and C). However, after ~ 20 PDs two subpopulations of cells were identified within the LY-R cell line, one of which had telomere length similar to the original population of LY-R cells, but the remaining subpopulation had significantly shortened telomeres in comparison to the original population of LY-R cells (Figures 3.4 B and C). We estimated that the subpopulation of cells with longer telomeres had average length of 43.0 kb whereas the subpopulation with shorter telomeres had average length of 16.6 kb.

Subpopulations of cells with different telomere lengths were defined by two parameters: (**i**) detection of two or more separate peaks on the FL 1 (FITC) channel representing telomere fluorescence in gated G_0/G_1 cells and (**ii**) two separate populations of cells in a FL1 vs. FL3 dot plot (see Figure 3.4 B left panel). Within the subpopulation of cells with shorter telomeres two clear peaks were identified on the FL1 channel representing telomere fluorescence (Figure 3.4 B, third panel). This suggests that the group of cells with shorter telomeres may consist of two overlapping subpopulations of cells with different telomere length. However, these two putative subpopulations of cells remained indistinguishable by the above criteria until the end of the experiment (Figure 3.4 C).

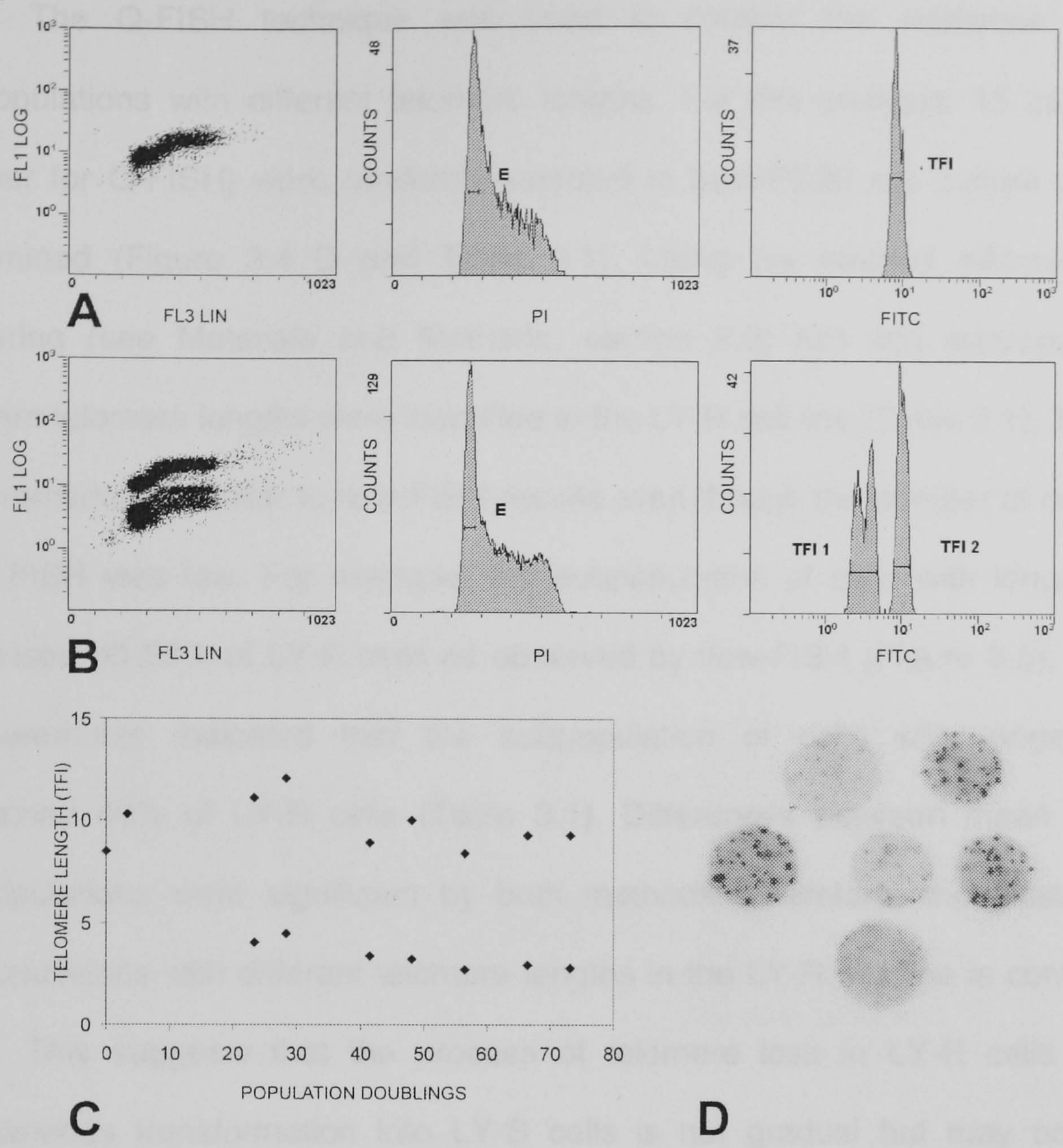

Figure 3.4 (**A**) A typical flow-FISH profile of LY-R cells at the beginning of the experiment. A dot-plot profile in the first box represents a combination of FL3 channel [the DNA content, excluding subG_0/G_1 peaks and polyploid cells, after staining nuclei with PI (propidium iodide)] and FL1 channel [the telomere fluorescence after FITC (fluorescein isothyocianate) staining]. One single population of cells was distinguished at PDs <20 as indicated by the presence of a single group of cells in the dot-plot or a single peak on the FL1 channel (FITC). Histograms in second and third box show PI and FITC profiles separately. (**B**) A gate (E) was drawn in G_0/G_1 of the cell cycle distribution histogram to obtain a histogram of telomere fluorescence for the gated region. Two cell subpopulations with different telomere lengths were distinguished at PDs >20 as indicated on FL3 vs. FL1 dot plot (two groups of cells) and in the FITC histogram (two separate peaks). (**C**) Subpopulations of cells with different telomere lengths at PDs 1-73. A dot represents one cell subpopulation. (**D**) Q-FISH image of LY-R interphase cells. Note clear differences in telomere fluorescence intensity between three middle cells and cells at the periphery of the image.

The Q-FISH technique was used to confirm the existence of two cell subpopulations with different telomere lengths. For this analysis, 15 cells (standard number for Q-FISH) were randomly selected in post-PD20 cell culture and TFI was determined (Figure 3.4 D and Table 3.1). Using the method referred to as cell clustering (see Materials and Methods, section 2.9) two cell subpopulations with different telomere lengths were identified in the LY-R cell line (Table 3.1). These results were remarkably similar to flow-FISH results even though the number of cells analysed by Q-FISH was low. For example, the subpopulation of cells with longer telomeres comprised 30-60% of LY-R cells as observed by flow-FISH (Figure 3.5), and Q-FISH measurements indicated that the subpopulation of cells with longer telomeres comprised 40% of LY-R cells (Table 3.1). Differences between mean TFIs of two subpopulations were significant by both methods. Therefore, the existence of cell subpopulations with different telomere lengths in the LY-R cell line is confirmed by Q-FISH. This suggests that the process of telomere loss in LY-R cells during their spontaneous transformation into LY-S cells is not gradual but may occur in rapid episodes after which telomere length remains stable for a long time (Figure 3.4 C).

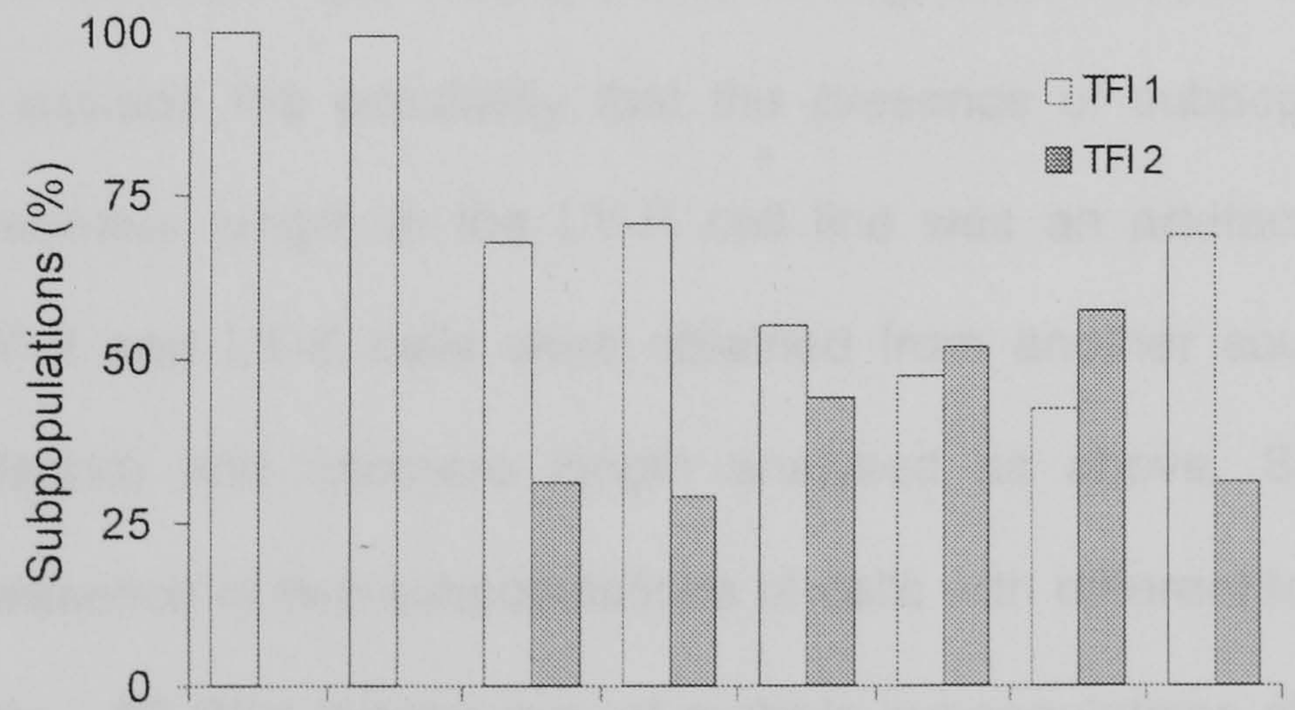

Figure 3.5 Telomere length dynamics in LY-R cells. Percentages are shown for subpopulations of cells with average telomere length 43.0 kb (TFI 1) and 16.6 kb (TFI 2), respectively.

Table 3.1 Telomere fluorescence intensity (TFI) in LY-R cells in arbitrary units as measured by Q-FISH. A cell cluster represents a group of cells in which TFI values do not differ by >50%. For example cell number 8 belongs to the cluster of cells 1-8. Cell clusters in bold represent two subpopulations of cells with significantly different average telomere lengths ($p<0.01$, t-test).

Cell Number	TFI	Cell cluster	Mean	S.E.
1	1803	1-4		
2	1875	1-5		
3	2106	1-7		
4	2356	1-7		
5	2788	**1-8**	2552.6	459.4
6	2893	**1-8**		
7	2903	**1-8**		
8	3697	**1-8**		
9	6142	2-8		
10	7167	8-14		
11	7822	8-15		
12	8001	**9-15**	8077.0	226.1
13	8599	**9-15**		
14	8941	**9-15**		
15	9867	**9-15**		

In contrast to LY-R cells, analysis of telomere fluorescence in LY-S cells by flow-FISH showed a single cell population throughout the experiment (Figure 3.6).

To exclude the possibility that the presence of subpopulations of cells with different telomere length in the LY-R cell line was an artefact associated with cell culture, LY-R and LY-S cells were obtained from another source (laboratory of M. Blasco, Madrid) and telomere length analysed as above. Similarly, this analysis revealed presence of two subpopulations of cells with different telomere lengths in LY-R cells after ~ 50 PDs but the lack of multiple subpopulations of cells in the LY-S cell line (Figure 3.7).

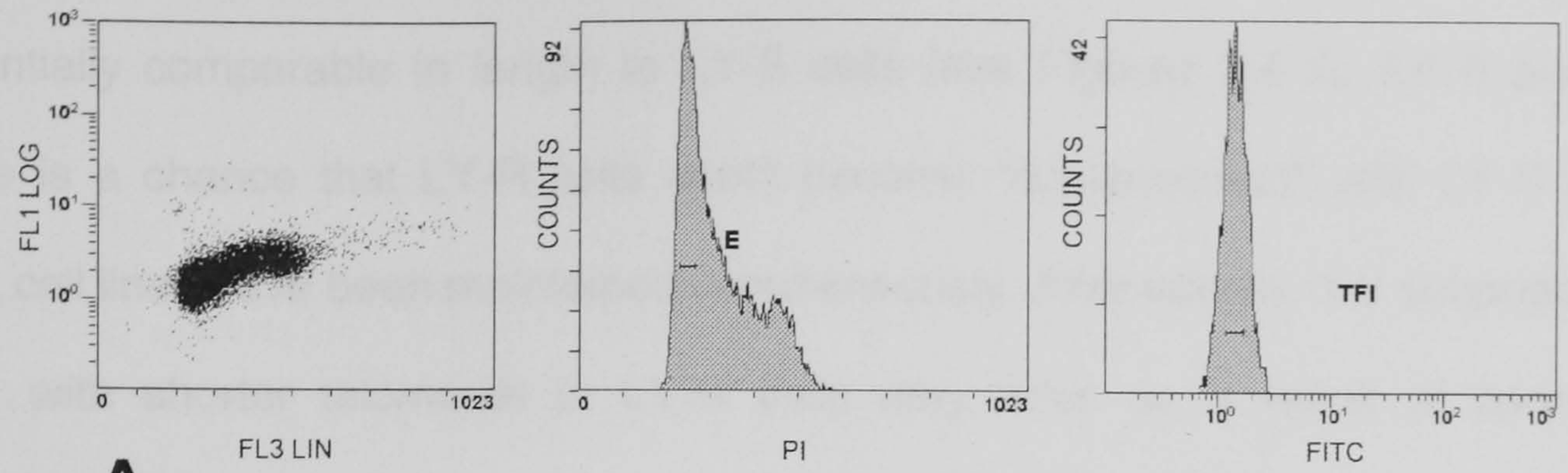

Figure 3.6 A typical flow cytometry profile of LY-S cells (**A**) and analysis of subpopulations of cells with different telomere lengths at PDs 1-73 (**B**). One single population was distinguished on FL3 vs. FL1 dot-plot and in the FL1 (FITC) histogram.

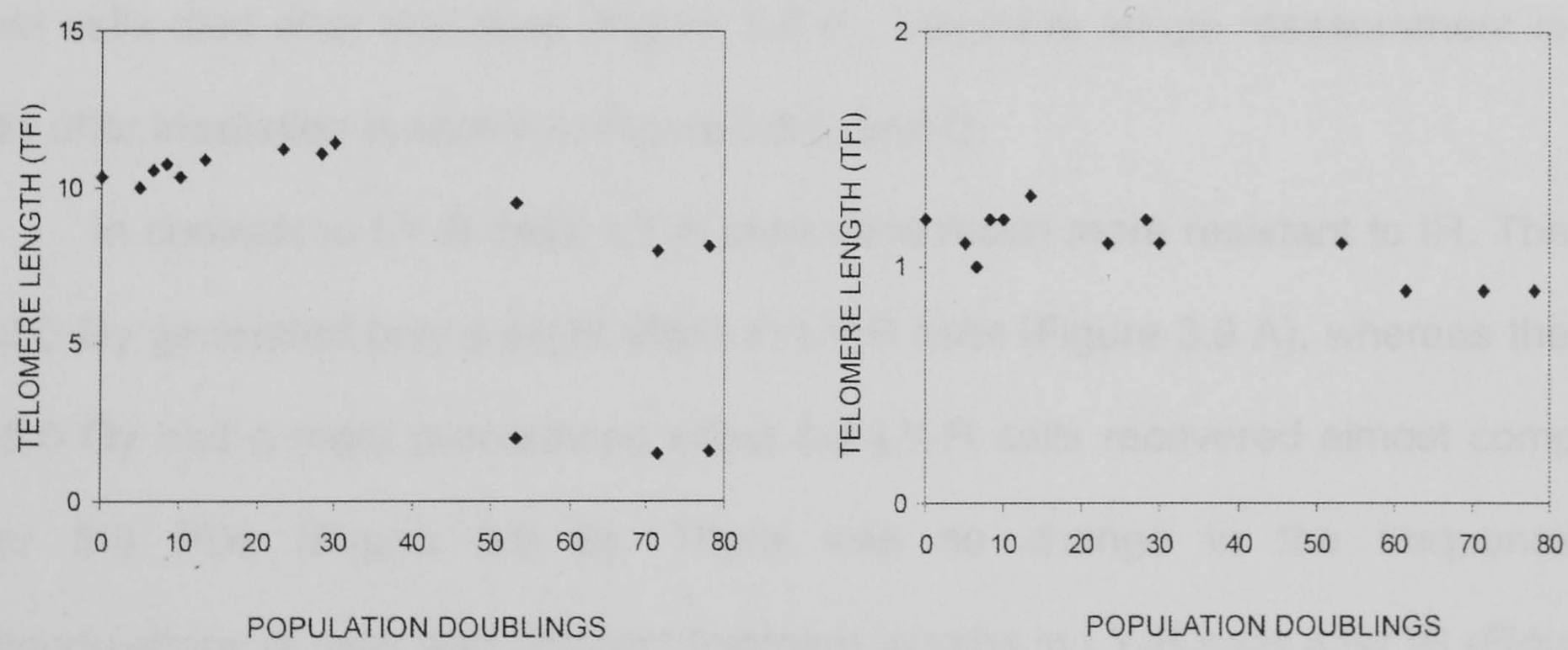

Figure 3.7 Two subpopulations of cells at PDs >50 in the LY-R cell line (**A**) and single population in the LY-S cell line (**B**). LY-R and LY-S cells for this analysis were obtained from the laboratory of Dr. Maria Blasco.

Since telomeres in some subpopulations of LY-R cells were short and potentially comparable in length to LY-S cells (see Figures 3.4 C, 3.6 B and 3.7 A) there is a chance that LY-R cells could become "contaminated" with LY-S because both cell lines have been maintained simultaneously. Alternatively, the subpopulation of cells with shorter telomeres in LY-R cells may arise as a result of spontaneous transformation, which eventually results in LY-S cells (McIlrath et al., 2001). To exclude these possibilities, both LY-R and LY-S cells were irradiated with 2.0 and 5.0 Gy gamma rays and flow cytometry parameters and telomere length monitored before and after irradiation. IR induces cell killing either through apoptosis or necrosis and these events can be identified by flow cytometry. Frequencies of apoptotic and necrotic cells induced by IR were expected to be higher in radiosensitive LY-S cells than in LY-R cells. The dose of 2.0 Gy induced high levels of apoptotic and necrotic cells in the LY-S cell line and as a result the frequency of proliferating cells was markedly reduced (Figure 3.8 A). However, after approximately 2-3 PDs LY-S cells recovered and frequencies of apoptotic, necrotic and proliferating cells returned to almost normal levels (Figure 3.8 A). The dose of 5.0 Gy had much greater effect on LY-S cells and most cells died after this dose (Figure 3.8 B). Telomere length measurement in LY-S cells after irradiation is shown in Figure 3.8 C and D.

In contrast to LY-S cells, LY-R cells were much more resistant to IR. The dose of 2.0 Gy generated only a slight effect in LY-R cells (Figure 3.9 A), whereas the dose of 5.0 Gy had a more pronounced effect but LY-R cells recovered almost completely after 2-3 PDs (Figure 3.9 B). There was no change in the frequencies of subpopulations of cells with different telomere lengths in LY-R cells after IR (Figure 3.9 C and D) thus excluding the possibility that the observed subpopulations of cells with different telomere lengths in LY-R cells may be the result of contamination with LY-S cells or that the new subpopulation of cells is sensitive to radiation. Similar results were found in the second source (laboratory of Dr. Maria Blasco) of LY-R and LY-S cells (Figure 3.10).

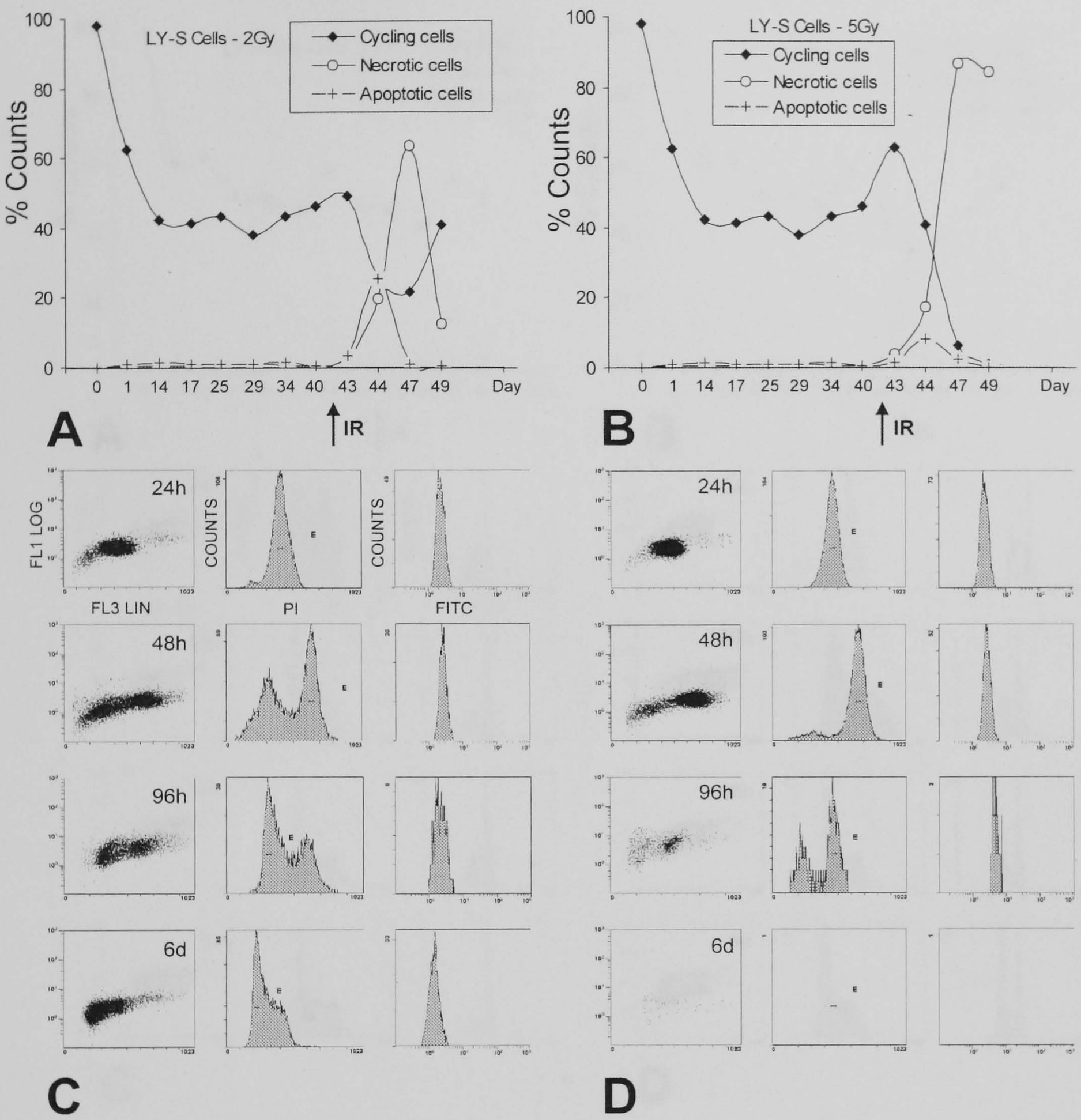

Figure 3.8 Flow cytometric counts for cycling (proliferating), apoptotic and necrotic cells in the LY-S cell line following the dose of 2.0 Gy (**A**) and 5.0 Gy (**B**). IR (ionising radiation) was administered at day 42 as indicated by arrows. Telomere length measurements in LY-S cells (24h, 48h, 96h, and 6 days) after irradiation with 2.0 Gy (**C**) and 5.0 Gy (**D**).

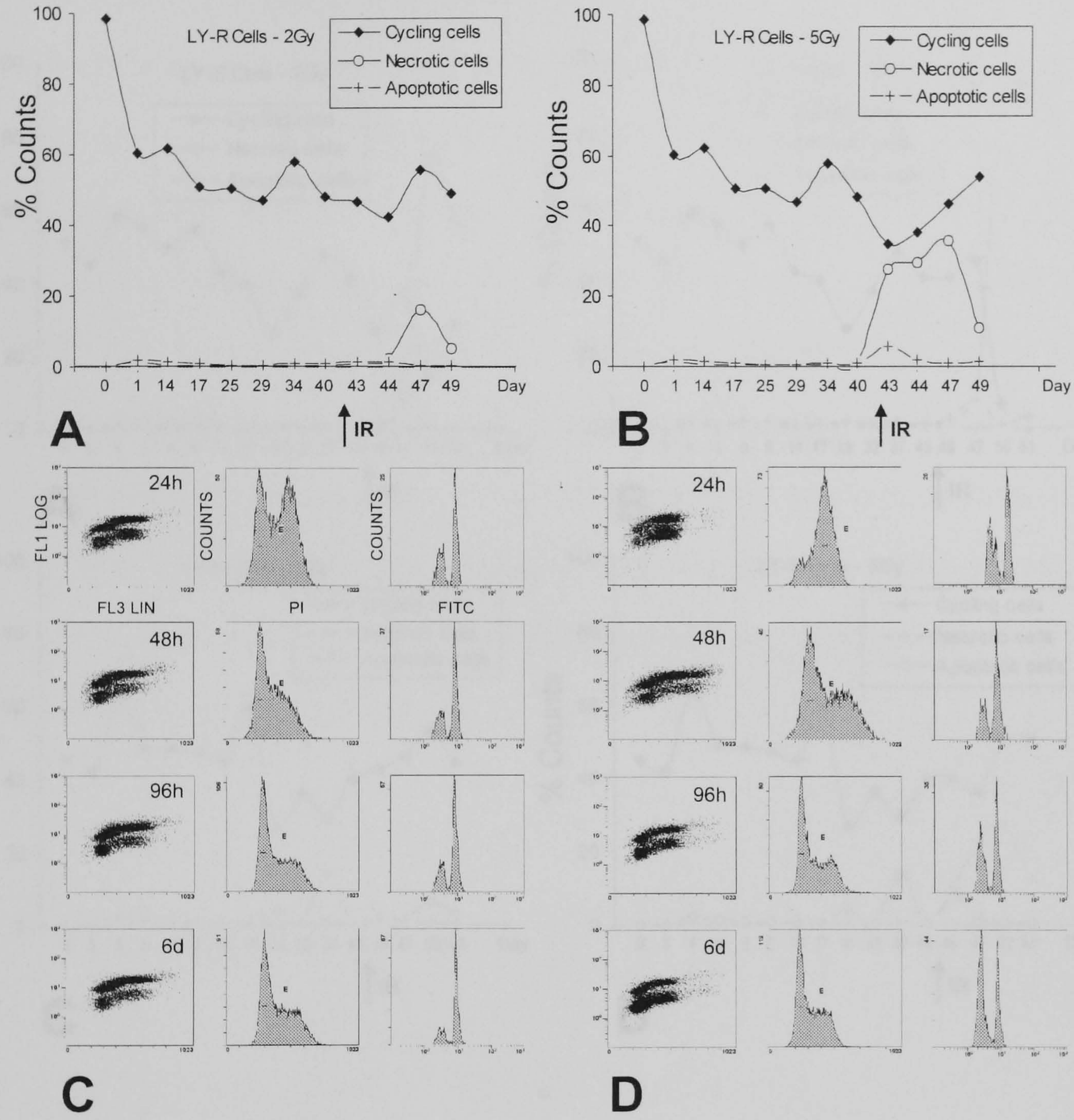

Figure 3.9 Flow cytometric counts for cycling (proliferating), apoptotic and necrotic cells in LY-R cells following the dose of 2.0 Gy (**A**) and 5.0 Gy (**B**). IR (ionising radiation) was administered at day 42 as indicated by arrows. Telomere length measurements in LY-R cells (24h, 48h, 96h, and 6 days) after irradiation with 2.0 Gy (**C**) and 5.0 Gy (**D**).

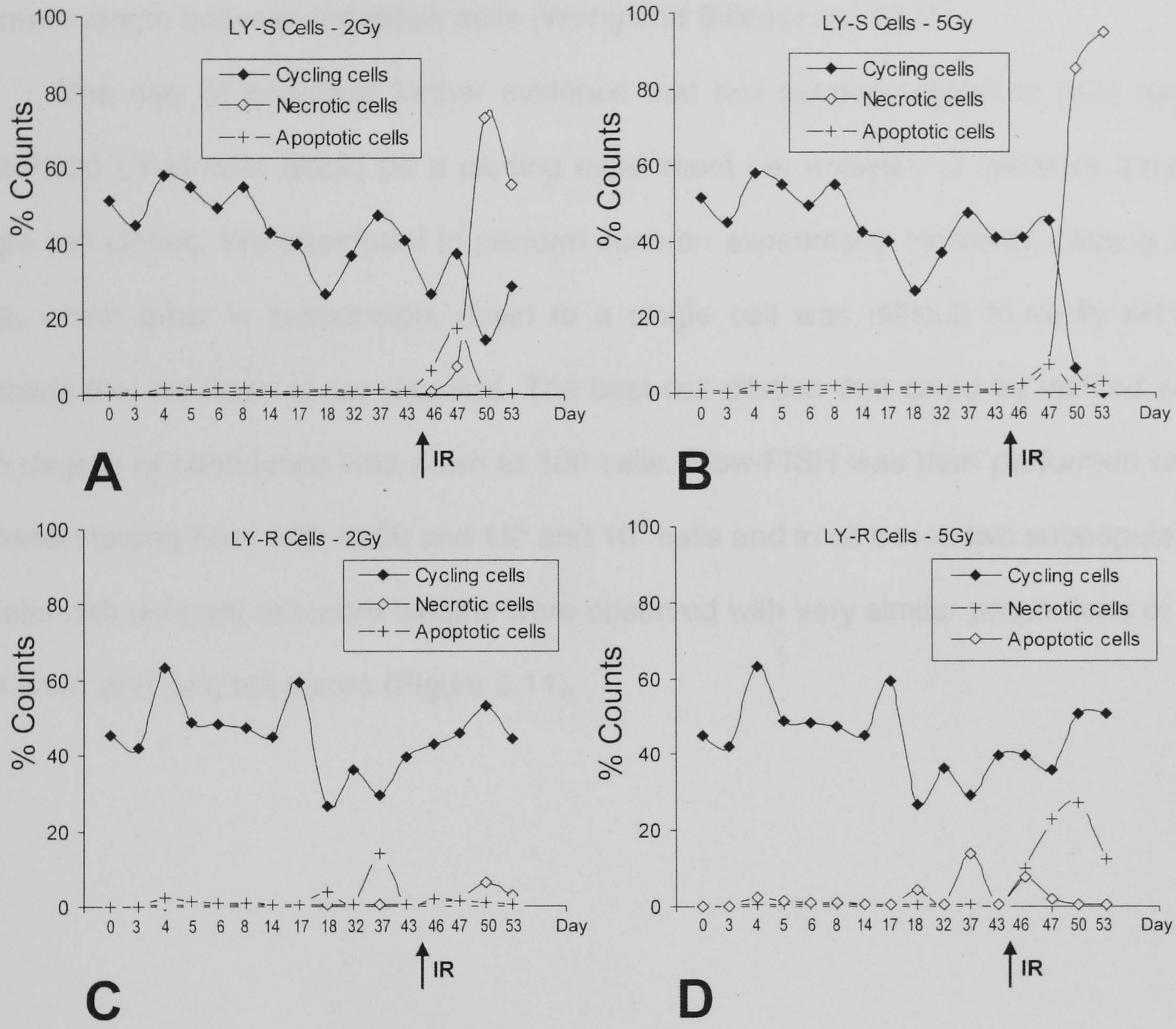

Figure 3.10 Flow cytometric counts for cycling (proliferating), apoptotic and necrotic cells in LY-S cells following the dose of 2.0 Gy (**A**) and 5.0 Gy (**B**) and in LY-R cells following the dose of 2.0 Gy (**C**) and 5.0 Gy (**D**). IR (ionising radiation) was administered at day 45 as indicated by arrows. LY-R and LY-S cells for this experiment were obtained from Dr. Maria Blasco's laboratory.

Therefore, we conclude that the LY-R cell line contains subpopulations of cells with different telomere lengths. This conclusion is in line with published Q-FISH measurements of telomere size in LY-R cells, which indicated several-fold differences in the average telomere length between individual cells (Wong and Slijepcevic, 2004).

One way of providing further evidence that two subpopulations of cells exist in post-PD20 LY-R cells would be a cloning experiment i.e. analysis of telomere length in single cell clones. We attempted to perform such an experiment. However, diluting LY-R cells, which grow in suspension, down to a single cell was difficult to verify with the methods that we have at our disposal. The best cell dilution that could be verified with a high degree of confidence was down to 100 cells. Flow-FISH was then performed on the material starting from 100, 1000 and 10^5 and 10^6 cells and in all cases two subpopulations of cells with different telomere lengths were observed with very similar proportions of cells with short and long telomeres (Figure 3.11).

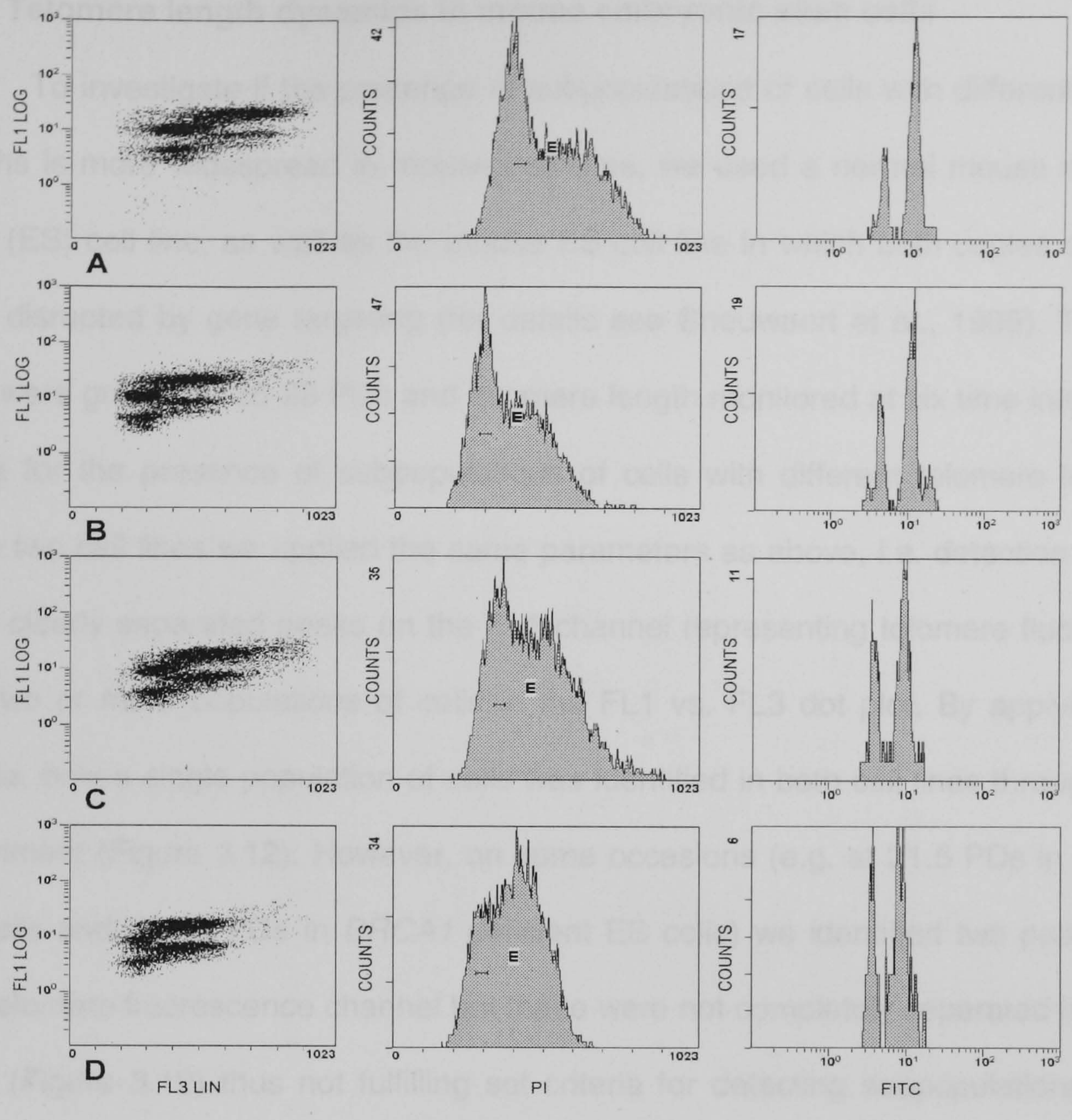

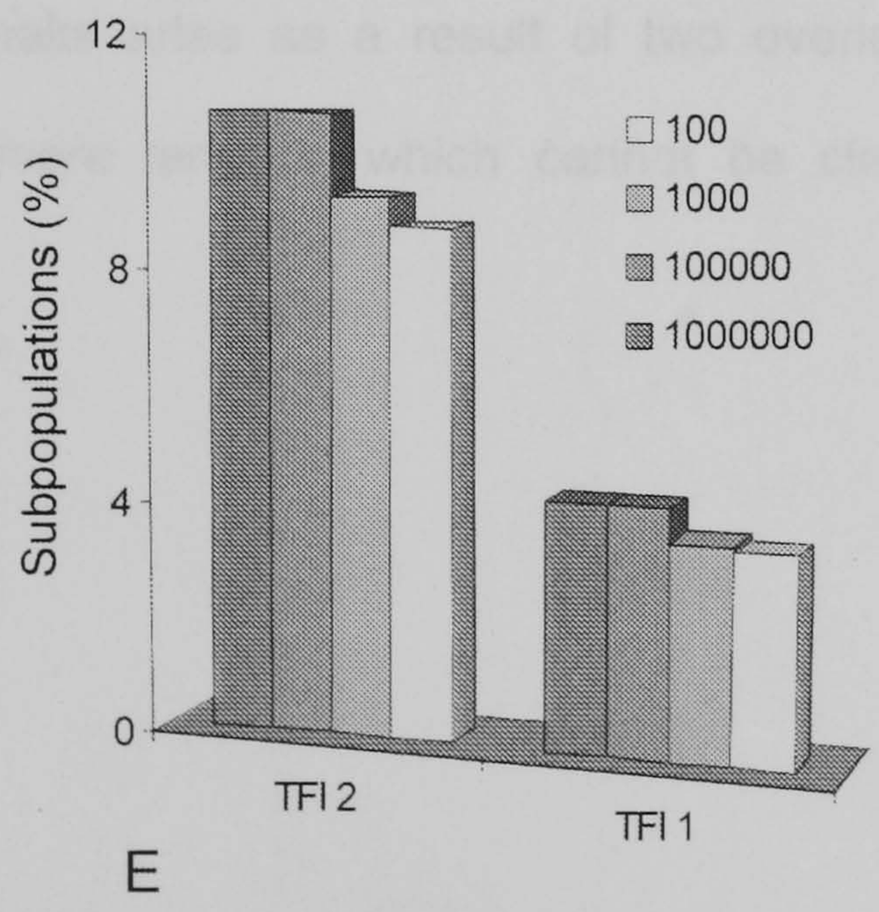

Figure 3.11 LY-R cells revealed two subpopulations after one week of cell culture starting with 10^6 cells (**A**); 10^5 cells (**B**); 10^3 cells (**C**); and <100 cells (**D**). The mean telomere length for subpopulation TFI 1 was 43.4 kb and for subpopulation TFI 2 was 19.0 kb. Interestingly, percentages of cells in G_2/M cell cycle phase increase from A to D in histograms of middle panel.

3.2.3 Telomere length dynamics in mouse embryonic stem cells

To investigate if the presence of subpopulations of cells with different telomere lengths is more widespread in mouse cell lines, we used a normal mouse embryonic stem (ES) cell line, as well as the mouse ES cell line in which both copies of *BRCA1* were disrupted by gene targeting (for details see Snouwaert et al., 1999). These cell lines were grown for 25-28 PDs and telomere length monitored at six time intervals. To check for the presence of subpopulations of cells with different telomere lengths in these two cell lines we applied the same parameters as above, i.e. detection of two or more clearly separated peaks on the FL1 channel representing telomere fluorescence and two or more populations of cells in the FL1 vs. FL3 dot plot. By applying these criteria, only a single population of cells was identified in both cell lines throughout the experiment (Figure 3.12). However, on some occasions (e.g. at 21.5 PDs in wild type ES cells and at 7.2 PDs in *BRCA1* deficient ES cells) we identified two peaks in the FL1 telomere fluorescence channel but these were not completely separated from each other (Figure 3.12) thus not fulfilling set criteria for detecting subpopulations of cells with different telomere length (see above). However, the possibility cannot be excluded that these peaks arise as a result of two overlapping subpopulations of cells with different telomere lengths, which cannot be clearly detected using the flow-FISH method.

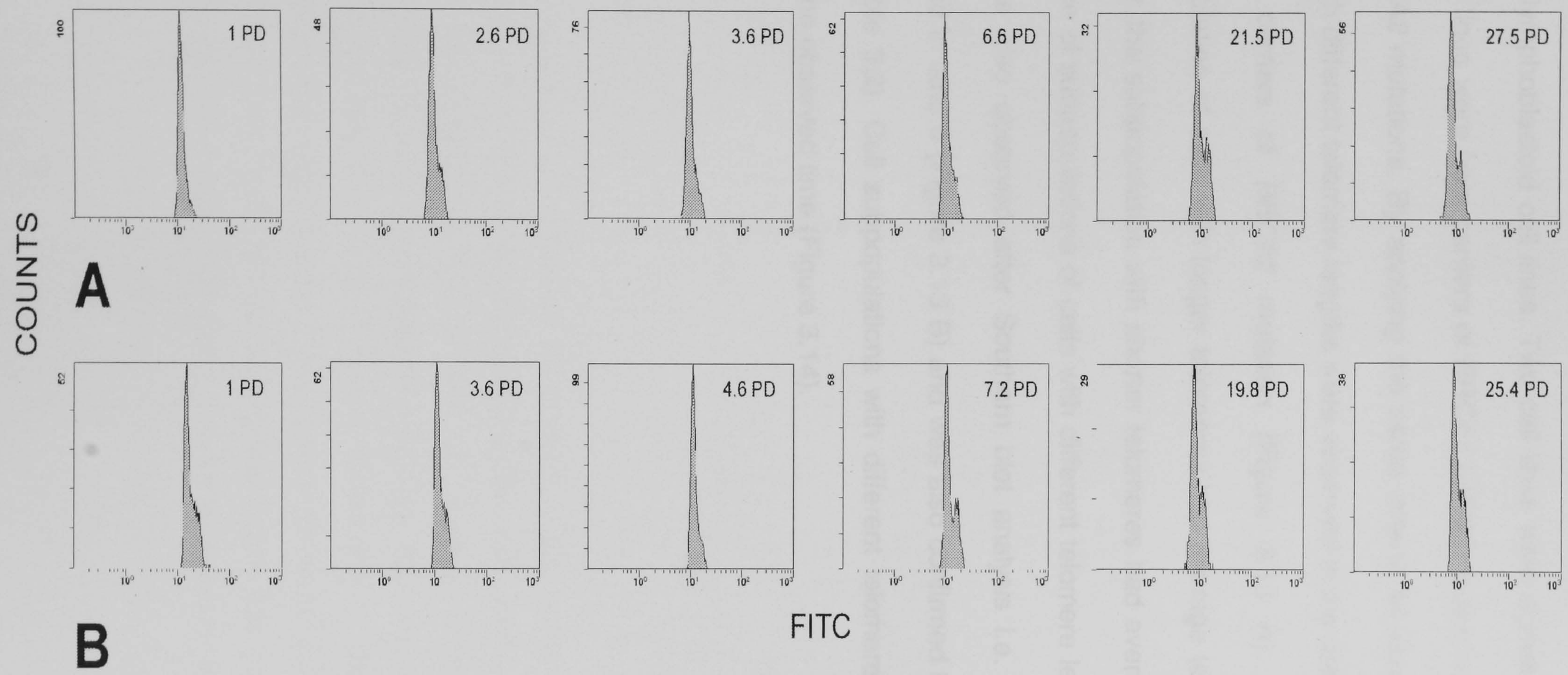

Figure 3.12 Telomere fluorescence measurements at different PDs in normal mouse ES cells (**A**) and ES cells in which *BRCA1* was inactivated (**B**).

3.2.4 Telomere length dynamics in human non-ALT cell lines

To investigate if subpopulations of cells with different telomere lengths exist within human cell lines, we investigated telomere length by flow-FISH in six different human lymphoblastoid cell lines. Two cell lines were derived from normal individuals, two cell lines were from carriers of *BRCA1* mutations and remaining two from carriers of *BRCA2* mutations. By applying the same criteria as above two subpopulations of cells with different telomere lengths were observed in the cell line, GM14622, from one of the carriers of *BRCA2* mutation (Figure 3.13 A). We estimated that the subpopulation of cells with longer telomeres had average telomere length of 18.5 kb, whereas the subpopulation with shorter telomeres had average length of 6.7 kb. The presence of subpopulations of cells with different telomere length in the GM14622 cell line was also observed after Southern blot analysis i.e. the bi-modal distribution observed in lane 6 (Figure 3.13 B) and was also confirmed by Q-FISH (Figure 3.13 C and Table 3.2). Cell subpopulations with different telomere lengths remained stable during the observed time (Figure 3.14).

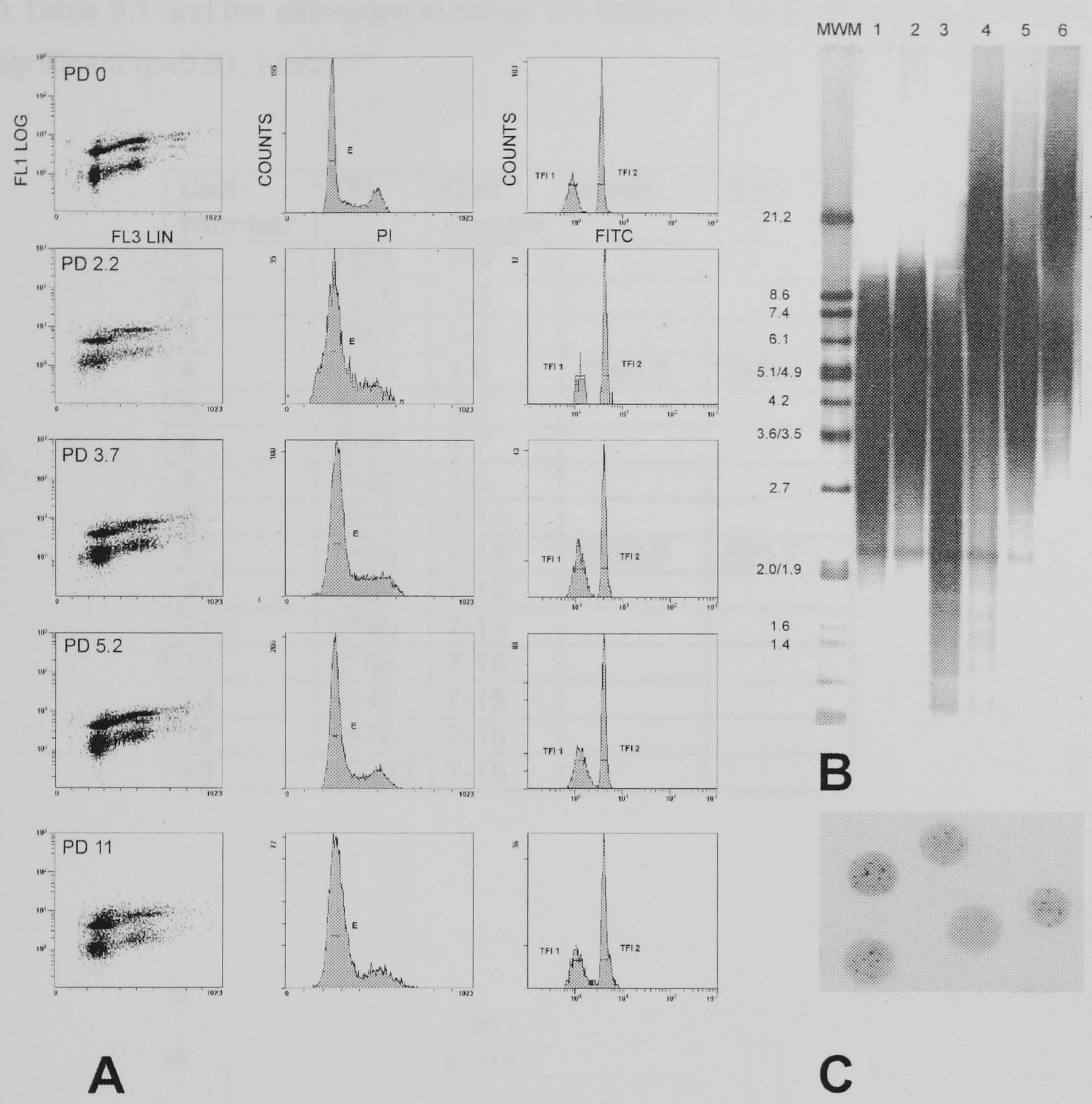

Figure 3.13 (**A**) Flow cytometry parameters in the human lymphoblastoid cell line, GM14622, from a *BRCA2* carrier. Note the presence of two cell subpopulations on the FL1:FL3 dot plot and on a FITC channel. (**B**) Southern blot analysis of telomere length in six different human lymphoblastoid cell lines. Cell lines from Lane 1 - Lane 6:1: GM00893; 2: GM01945; 3: GM14090; 4: GM13705; 5: GM14170 and 6: GM14622. MWM: molecular weight marker. * the bulk of telomeric signal was concentrated in a narrow smear around 21 kb and in a smear below this point. (**C**) A FISH image of interphase GM14622 cells with clearly identifiable different telomere signal intensities.

Table 3.2 Telomere fluorescence intensity (TFI) in GM14622 cells in arbitrary units as detected by Q-FISH. Two subpopulations of cells (cell clusters in bold) are defined as in Table 3.1 and the difference in mean TFI between two subpopulations is statistically significant ($p<0.01$, t-test).

Cell Number	TFI	Cell cluster	Mean	S.E.
1	1376	1-3		
2	1678	1-3		
3	1987	1-4		
4	2724	**1-6**	2395.8	348.9
5	3015	2-6		
6	3595	3-7		
7	5122	4-8		
8	6618	6-14		
9	7858	**7-15**	8258.3	520.7
10	8367	**7-15**		
11	8760	**7-15**		
12	8766	**7-15**		
13	8942	**7-15**		
14	9670	**7-15**		
15	10222	**7-15**		

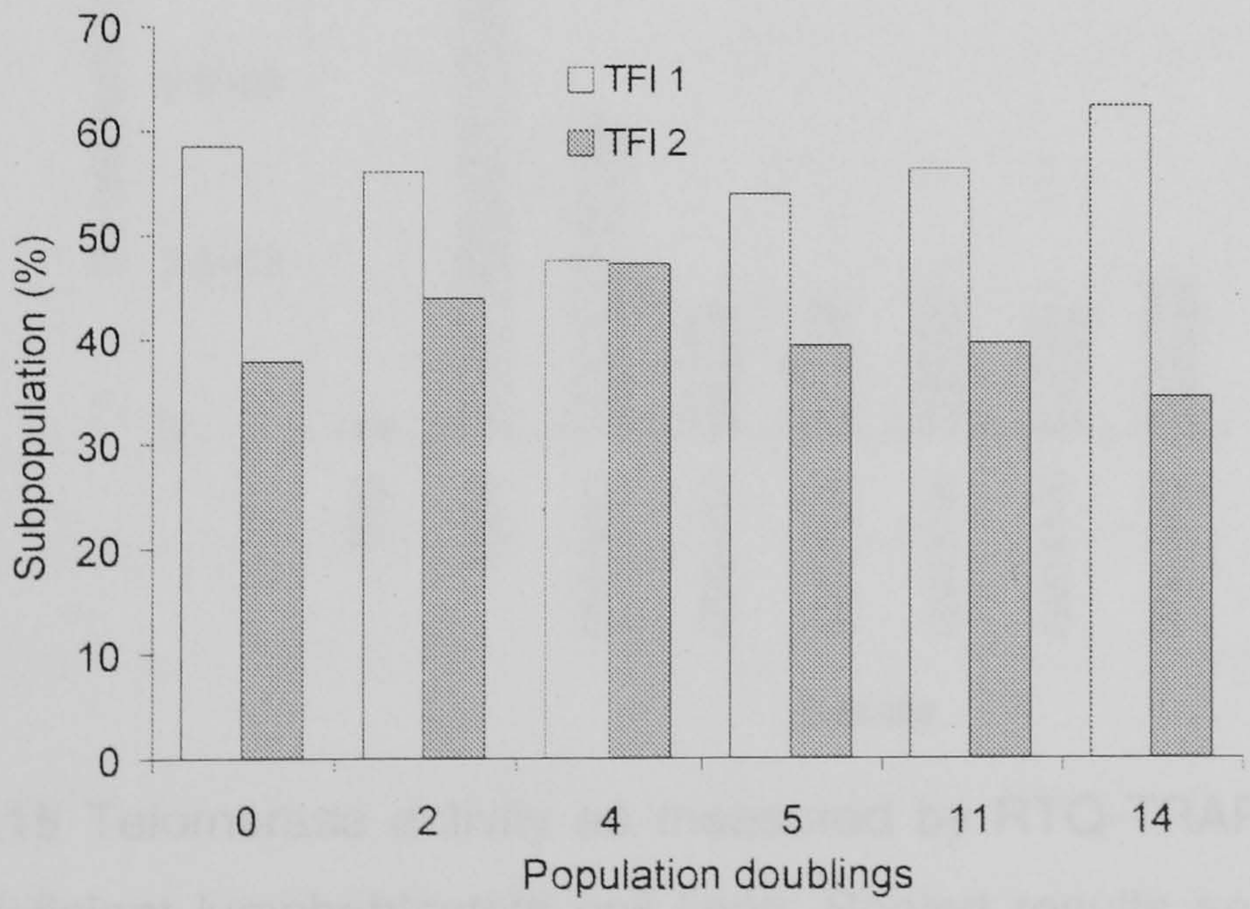

Figure 3.14 Telomere length dynamics in the human lymphoblastoid cell line GM14622. Percentages of cells from two different subpopulations (TFI 1 and TFI 2). Average telomere length for TFI 1 was 18.5 kb and for TFI 2 was 6.7 kb.

The GM14622 cell line had unusually long telomeres, on average 3 times longer than telomeres in the rest of cell lines (data not shown). Examination of telomere length by Southern blot analysis confirmed that this cell line had extremely long telomeres and the majority of telomeric signal was concentrated in a narrow smear around 21 kb (Figure 13 B). This pattern is similar to the pattern usually observed in ALT positive cells (Grobelny et al., 2000). However, examination of telomeres in metaphase GM14622 cells did not reveal telomere heterogeneity in individual chromosomes typical of ALT cells (data not shown). In addition, all six lymphoblastoid cell lines showed low/moderate levels of telomerase activity as was detected by RTQ-TRAP (Figure 3.15) suggesting that the GM14622 cell line is not an ALT cell line i.e. ALT cells usually lack detectable telomerase activity.

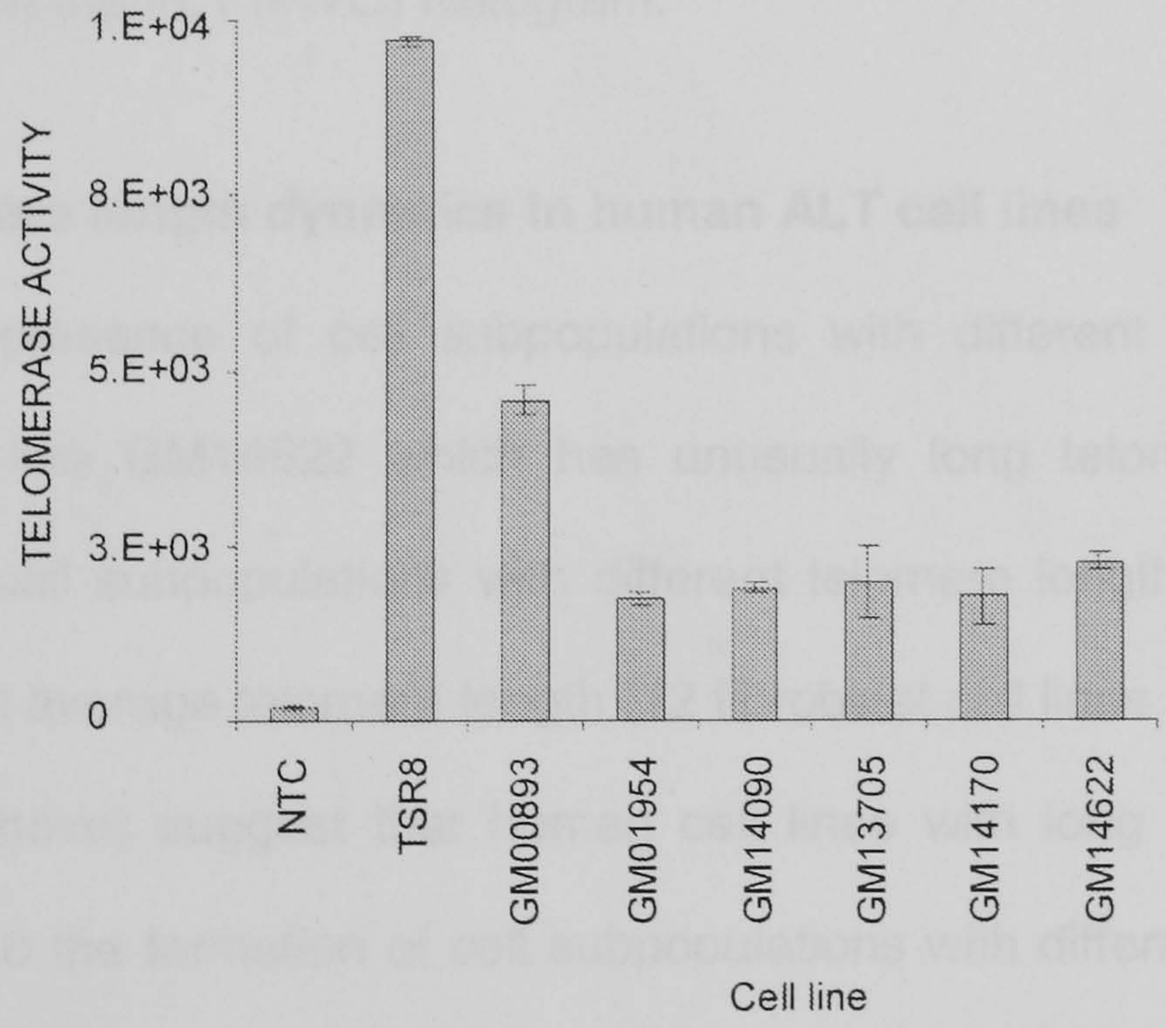

Figure 3.15 Telomerase activity as measured by RTQ-TRAP in normal, *BRCA1* and *BRCA2* deficient lymphoblastoid cell lines. Pooled results are shown (n=6) indicating telomerase activity as a percentage of the prostate adenocarcinoma cell line PC-3 telomerase activity. NTC: negative control; TSR8 oligonucleotide template: positive control.

We have also analysed telomere length in three normal primary fibroblast cell lines and primary fibroblast cell lines from nine patients with different DNA damage response defects. We observed only a single population of cells in all analysed fibroblast cell lines (Figure 3.16).

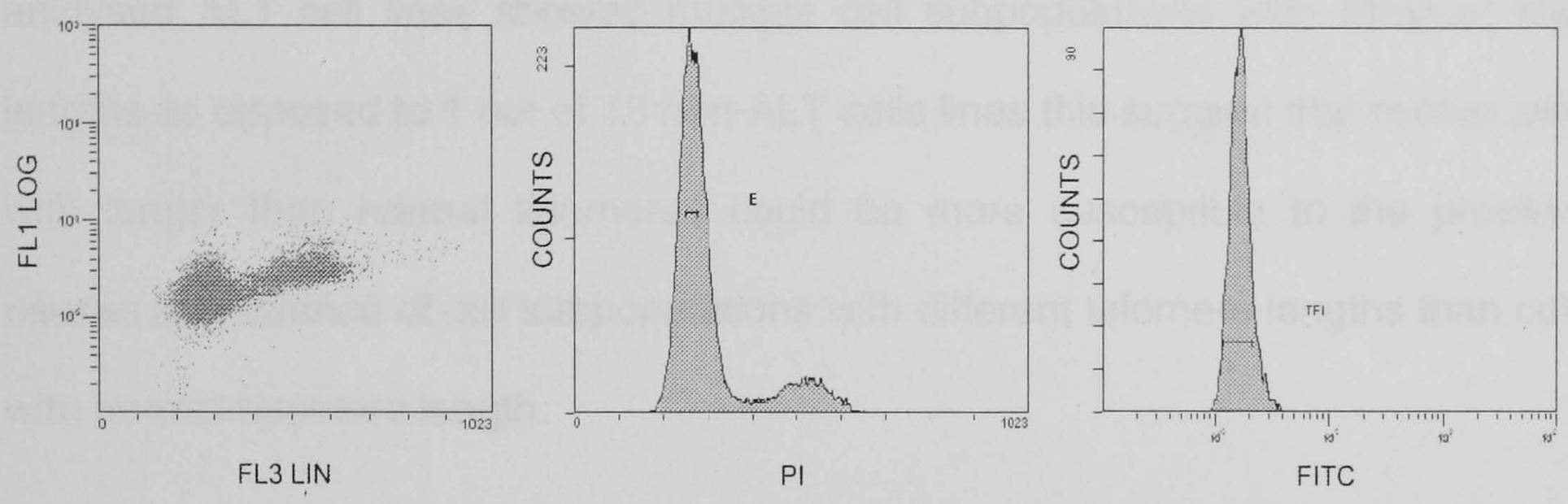

Figure 3.16 A representative example of a flow cytometry dot-plot and histograms obtained by flow-FISH analysis of telomere length in fibroblasts, in this case a normal fibroblast cell line (GM09503). One single population was distinguished on FL3 vs. FL1 dot plot and in the FL1 (FITC) histogram.

3.2.5 Telomere length dynamics in human ALT cell lines

The presence of cell subpopulations with different telomere lengths in the human cell line GM14622 which has unusually long telomeres and the complete absence of cell subpopulations with different telomere lengths in 18 human cell lines with a typical average telomere length (12 fibroblast cell lines and 6 lymphoblastoid cell lines, see above) suggest that human cell lines with long telomeres may be more susceptible to the formation of cell subpopulations with different telomere lengths than cell lines with normal telomere length. This possibility can be tested by analysing human ALT cell lines. ALT cell lines show great telomere length heterogeneity and significantly longer telomeres than human non-ALT cell lines (Henson et al., 2002). For this purpose four verified ALT cell lines were used: U2-OS; WI-38 VA13/2RA; SK LU1; and G-292 (Henson et al., 2002). By applying the same criteria as above we observed three cell subpopulations with different telomere lengths in the U2-OS cell line (Figure

3.17). These three subpopulations with average telomere lengths 23.7, 39.8 and 64.3 kb remained stable for at least 20 PDs (Figure 3.18). Q-FISH analyses confirmed the existence of three cell subpopulations with different telomere lengths in this cell line (results not shown). We did not observe subpopulations of cells with different telomere lengths in the remaining three ALT cell lines (Figure 3.19). Given that 1 out of 4 analysed ALT cell lines showed multiple cell subpopulations with different telomere lengths as opposed to 1 out of 18 non-ALT cells lines this suggest that human cell lines with longer than normal telomeres could be more susceptible to the process that causes appearance of cell subpopulations with different telomere lengths than cell lines with normal telomere length.

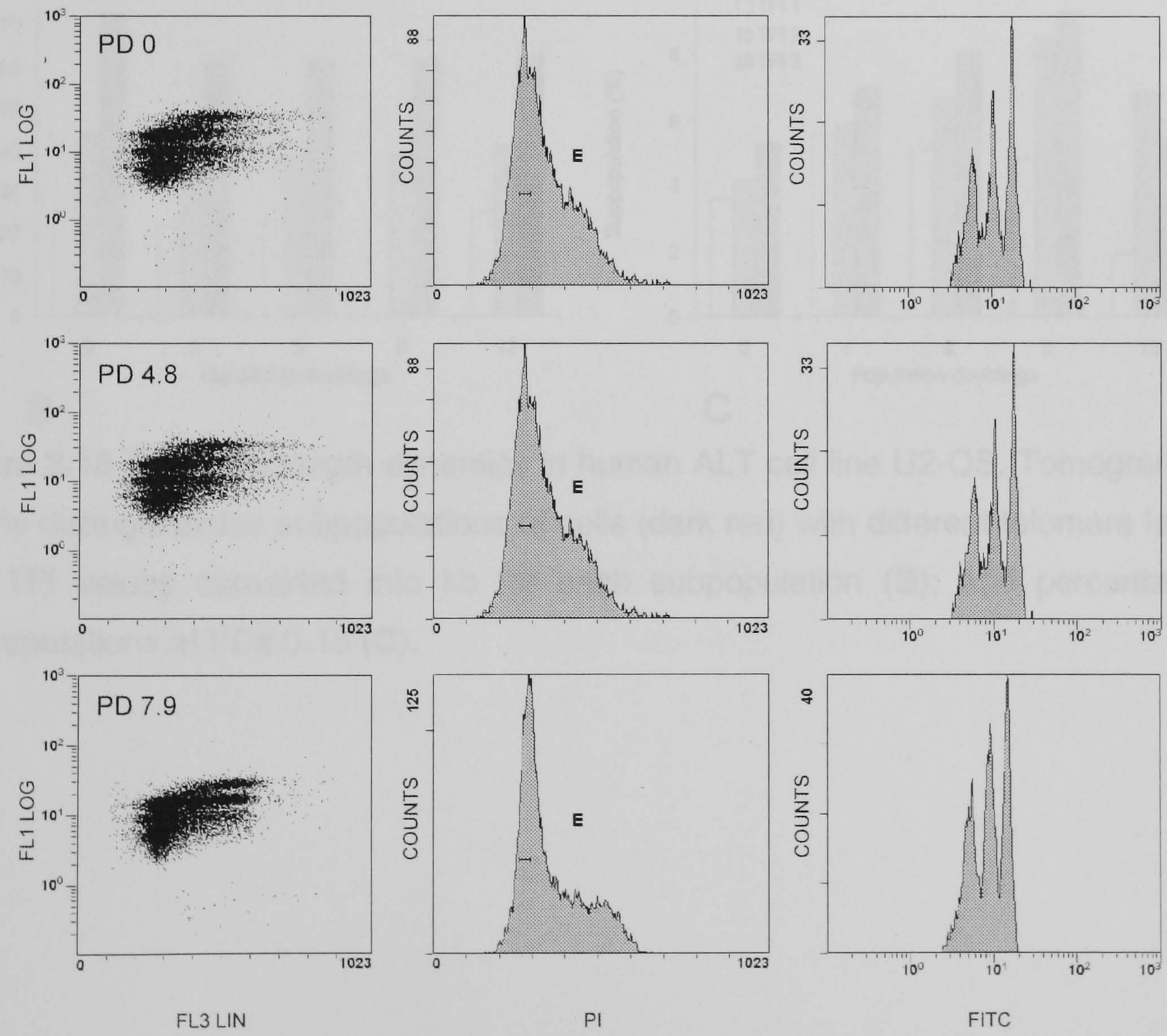

Figure 3.17 Flow-FISH profiles of human ALT cell lines U2-OS. Note the presence of three subpopulations (dot plot and FITC channel) of cells with average telomere lengths of 23.7, 39.8 and 64.3 kb. PD: population doubling

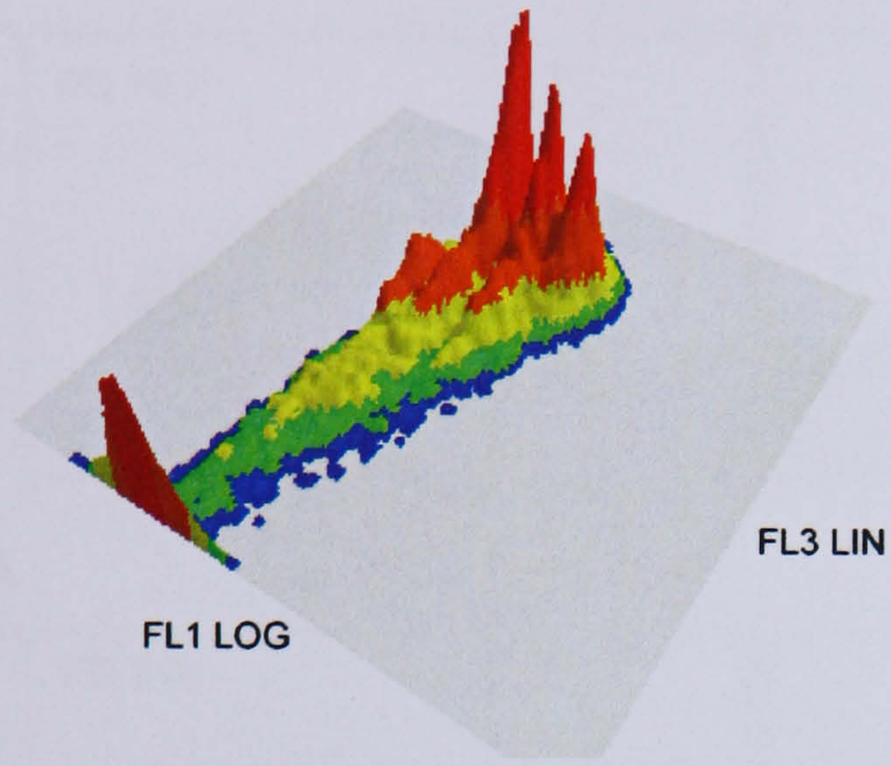

A

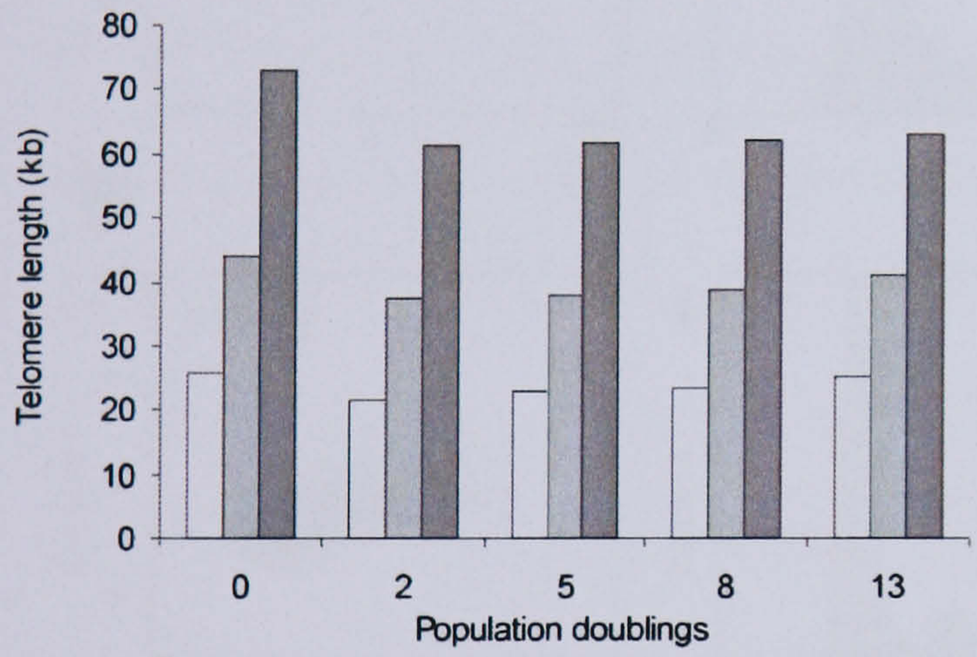

B

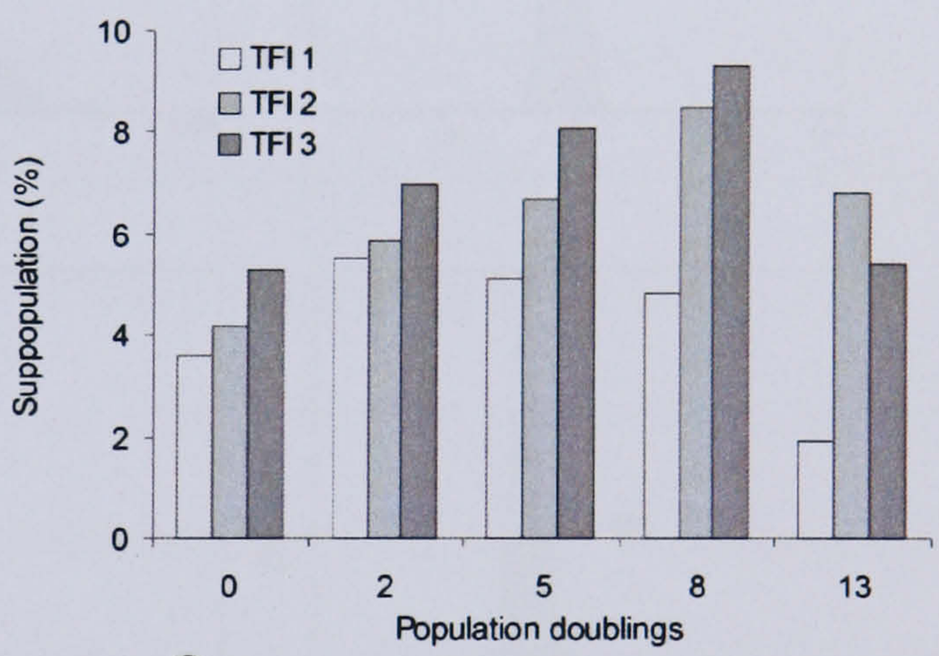

C

Figure 3.18 Telomere length dynamics in human ALT cell line U2-OS. Tomogram with clearly distinguishable subpopulations of cells (dark red) with different telomere lengths (**A**); TFI values converted into kb for each subpopulation (**B**); and percentage of subpopulations at PDs 0-13 (**C**).

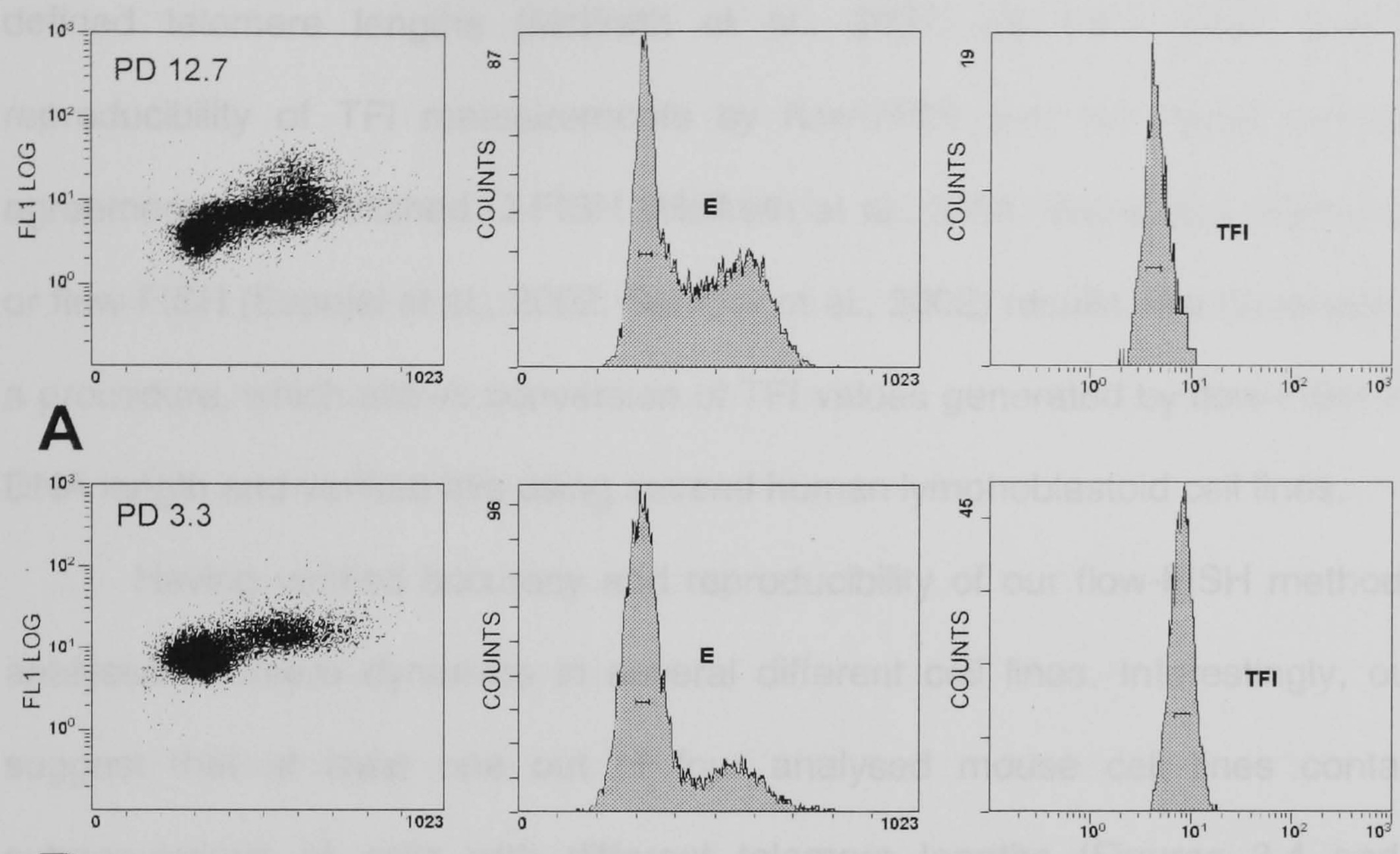

Figure 3.19 Flow-FISH profiles of human ALT cell lines: WI-38 VA13/2RA (**A**), SK LU1 (**B**) and G-292 (**C**). One single population was distinguished on FL3 vs. FL1 dot plot and in the FL1 (FITC) histogram.

3.3 Discussion

The initial aim of this study was to set up the flow-FISH method in our laboratory. Using a pair of mouse lymphoma cell lines LY-R and LY-S which have well defined telomere lengths (McIlrath et al., 2001) we have been able to show reproducibility of TFI measurements by flow-FISH and our results were in good agreement with published Q-FISH (McIlrath et al., 2001; Wong and Slijepcevic, 2004) or flow-FISH (Espejel et al., 2002; Samper et al., 2002) results. We have also designed a procedure, which allows conversion of TFI values generated by flow-FISH into kbs of DNA length and verified this using several human lymphoblastoid cell lines.

Having verified accuracy and reproducibility of our flow-FISH method we then analysed telomere dynamics in several different cell lines. Interestingly, our results suggest that at least one out of four analysed mouse cell lines contained two subpopulations of cells with different telomere lengths (Figures 3.4 and 3.7). In addition, two subpopulations of cells with different telomere lengths were identified in 1 out of 18 analysed human non-ALT cell lines. Finally, we observed multiple subpopulations of cells with different telomere lengths in 1 out of 4 analysed human ALT cell lines. Differences in telomere lengths between subpopulations of cells were significant in all cases and we name this phenomenon TELEFLUCS (TElomere LEngth FLUtuation in Cell Subpopulations). It is possible that TELEFLUCS could be more widespread in mouse cell lines as shown by the observations of two distinct but not clearly separated peaks representing telomere fluorescence in two mouse ES cell lines (Figure 3.12). To clearly show that these peaks are due to the existence of two subpopulations of cells with different telomere lengths further improvements in flow-FISH methodology are required. One potential improvement of interest is multicolour flow-FISH, which allows simultaneous detection of telomeres and subpopulations of cells carrying specific markers that can be detected by appropriate antibodies (Baerlocher and Lansdorp, 2003).

It is also interesting that the only TELEFLUCS positive human non-ALT cell line had unusually long telomeres (Figure 3.13). This suggests that cells with long telomeres may be potentially more susceptible to TELEFLUCS than cells with short telomeres. In line with this possibility, we observed only a single cell population with uniform telomere length in the mouse cell line, LY-S, with short telomeres, which are comparable in length to human telomeres, whereas mouse cells with expected average telomere length were either TELEFLUCS positive, or suspected to be TELEFLUCS positive as shown by the observation of two distinct but not clearly separated peaks on the FL channel representing telomere fluorescence in two mouse ES cell lines (Figure 3.12). Also, human cells with expected average telomere length completely lacked TELEFLUCS, whereas 1 out of 4 analysed human ALT cell lines, regularly associated with long telomeres, showed multiple subpopulations of cells with different telomere lengths (see above). It is now of interest to analyse larger number of ALT cell lines by flow-FISH and determine the extent of TELEFLUCS in these cell lines. The use of flow-FISH could also enable more precise analysis of telomere dynamics in ALT positive human cell lines and help elucidating mechanisms underlying ALT.

It is noteworthy that TELEFLUCS can reliably be detected only by flow-FISH. For example, analysis of telomere restriction fragments by Southern hybridisation is frequently non-informative in mouse cells. In human cells Southern hybridisation cannot identify TELEFLUCS unambiguously. For example, Southern blot analysis in the only TELEFLUCS positive human cell line revealed that the bulk of telomeric signal was concentrated in the narrow smear around 21 kb (Figure. 4.13 B). However, this may also mean that this bulk of telomeric DNA originates from chromosomes with exceptionally long telomeres not necessarily from different subpopulations of cells. Similarly, TELEFLUCS cannot be always accurately detected by Q-FISH because this technique typically relies on the information from 15-20 cells. However, we analysed LY-R and GM14622 cells by Q-FISH and confirmed the presence of cell subpopulations with different telomere lengths (Tables 3.1 and 3.2). This was possible

because two subpopulations of cells with different telomere lengths were approximately equal numerically in LY-R and GM14622 cell lines (see above). However, if one subpopulation is much smaller than the other then Q-FISH becomes statistically unreliable because of low numbers of cells that are typically analysed by this technique. Analysing large numbers of cells by Q-FISH is not practical. In contrast, flow-FISH analyses large numbers of cells (thousands), provides information on proportions of cells with different telomere lengths and as a result it is statistically much more reliable.

Mechanisms of TELEFLUCS are not known. Sudden appearance of new subpopulations of cells within the LY-R cell line with shorter telomeres in comparison with the original population of cells suggest dramatic loss of telomeric DNA. Dramatic loss of telomeric DNA termed TRD (telomere rapid deletion) has been described in yeast (Li and Lustig, 1996) and it was proposed that a similar mechanism exists in human and mouse cells (Lustig, 2003). In line with this possibility recent studies indicate that a more dramatic loss of telomeric DNA could occur through the formation of extra-chromosomal telomeric circles (Cesare and Griffith, 2004; Wang et al., 2004). It is therefore possible that subpopulations of cells with short telomeres in the LY-R cell line may have arisen as a result of these or similar mechanisms. However, TELEFLUCS reflects not only a dramatic loss of telomeric DNA but also its dramatic gain. For example, flow-FISH analysis of the human non-ALT cell line, GM14622, showed two subpopulations of cells, one with telomere length typical of most human cell lines and the other subpopulation with unusually long telomeres (Figure 3.13). It has been previously shown that individual telomeres in ALT cells can rapidly shorten and elongate (Murnane et al., 1994). This is consistent with the role of telomere-telomere recombination, which has been shown to occur in GM847 cells (Dunham et al., 2000), as the principal mechanism of ALT telomere maintenance as recombination/copy switching has the potential to generate such telomere length dynamics. Also, a human ALT cell line, U2-OS, showed multiple subpopulations of cells

with different telomere lengths (Figure 3.17) and according to our estimate the subpopulation with the longest telomeres had an average telomere length of 64 kb. Therefore, significant gains of telomeric DNA associated with TELEFLUCS may occur by both ALT and non-ALT related mechanisms. Future studies are now required to examine mechanisms of TELEFLUCS.

Based on the above results, as well as published results, we would like to propose that flow-FISH should be used as a method of choice for the estimate of average telomere length when human blood samples are used as a source of cells for telomere length measurement. The arguments for this proposal are summarized in Table 3.3, which also contains description of advantages and disadvantages of each technique used for this purpose. While some other techniques provide more sensitive assessments of telomere length in individual chromosomes (Q-FISH, STELA) or have better resolutions (quantitative PCR, HPA) there is no technique which is (**i**) better in detecting subpopulations of cells with different telomere lengths or (**ii**) faster than flow-FISH (see above). While Q-FISH and Southern blot can detect subpopulations of cells with different telomere lengths in some cases, the information provided by these two techniques is statistically far less reliable than that provided by flow-FISH (see above). The importance of using flow-FISH when measuring telomere length in human blood samples is supported by following arguments. Peripheral blood is a mixture of different cell types among which lymphocytes comprise the largest percentage of cells utilized for measurement by any technique described in Table 3.3. Peripheral blood lymphocytes are not homogeneous population of cells in terms of telomere length (Rufer et al., 1998; 1999; Brummendorf et al., 2000; Batliwalla et al., 2000; Baerlocher and Lansdorp, 2003) and a technique that can make distinction between these subpopulations can provide qualitatively highly relevant information. For example, measurement of telomere length in human blood samples is frequently used to make important clinical predictions.

Table 3.3 Comparative assessment of the principal methods employed in telomere length measurements.

	Flow-FISH (Rufer et al., 1998 and this study)	**Southern blot** (Gan et al., 2001 and this study)	**Q-FISH** (Slijepcevic, 2001 and this study)	**Telomere PCR** (Förstemann et al, 2000)	**HPA** (Freulet-Marriere et al., 2004)	**STELA** (Baird et al., 2003)
Number of starting cells	intermediate	large	intermediate	small	small	small
Sensitivity (detect small changes in telomere length)	intermediate	low	high	high	intermediate	high
Detect individual telomeres	no	no	yes	yes	no	yes
Signal includes 3' overhang	yes	yes	yes	yes	yes	no
Lower telomere length detection limit	> 200 bp	> 500 bp	> 200 bp	50 bp	54 bp	> 406 bp
Main advantage	detection of sub-populations of cells with different telomere lengths	measurement of long telomere lengths when pulse field gel electrophoresis is used	more precise estimate of telomere length from individual chromosomes	allows high throughput screening	allows high throughput screening without any DNA purification step	accurate estimate of telomere length from an individual chromosome
Main disadvantage	high cost of cytometer and maintenance	includes variable amount of subtelomeric repeat variants	only a small data set can be produced of cells that are still proliferating	requires a marker gene close to subtelomeric region	use of captor-coated plates	measures telomere length only up to 20 kbp

Cawthon et al. (2003) discovered that people over the age of 60 with shorter telomeres in peripheral blood cells have higher mortality rates than people with longer telomeres from the same age group. It is almost certain that this analysis may have been refined had flow-FISH been used instead of quantitative PCR analysis i.e. flow-FISH combined with antibodies against different lymphocyte subpopulations (there is no limit here in terms of the number of subpopulations) would generate a profile of telomere lengths in cell subpopulations from each sample which potentially could be a better prognostic indicator than a single value of average telomere length from a mixture of cell subpopulations. In addition, blood cells are ideal for use in flow-FISH as no significant preparatory efforts are required and a chosen subpopulation(s) of lymphocytes can be selected to serve as internal control(s) i.e. subpopulation with shortest or longest telomeres. The availability of appropriate internal controls is crucial for any telomere length measurement technique and no method other than flow-FISH has better flexibility or adaptability for this purpose. The only disadvantage of flow-FISH is that relatively expensive equipment is required but it is likely that any major laboratory will have this equipment.

In conclusion, we show here that at least 1 out of 4 mouse cell lines, 1 out of 18 human non-ALT cell lines and 1 out of 4 human ALT cell lines exhibit subpopulations of cells with different telomere lengths. These results together with points discussed above underscore the importance of flow-FISH in telomere length analysis.

3.4 Summary

Telomeres are specialized nucleoprotein structures at chromosome ends that undergo dynamic changes after each cell cycle. Understanding the mechanisms of telomere dynamics is critically dependent upon the ability to accurately measure telomere length in a cell population of interest. Techniques such as Southern hybridisation, which measures average telomere length, and quantitative fluorescence

in situ hybridisation (Q-FISH), which can estimate telomere length in individual chromosomes, are limited in their capacity to determine the distribution of cells with different telomere lengths in a given cell population. We employed flow-FISH to ask a question if mouse and human cell lines exhibit subpopulations of cells with different telomere lengths.

Our analysis revealed that at least one out of four analysed mouse cell lines showed multiple subpopulations of cells with different telomere lengths. Differences in telomere length between subpopulations of cells were significant and we term this phenomenon TELEFLUCS (TElomere LEngth FLUctuations in Cell Subpopulations). TELEFLUCS was also observed in 1 out of 18 analysed human non-ALT cell lines and in 1 out of 4 analysed human ALT cell lines. The existence of cell subpopulations with different telomere lengths was confirmed by Q-FISH. These results underscore the importance of flow-FISH in telomere length analysis.

CHAPTER 4

ACCELERATED TELOMERE SHORTENING AND TELOMERE DYSFUNCTION IN CELLS WITH DEFECTIVE DNA DAMAGE RESPONSE

4.1 Introduction

Results presented in the previous chapter indicate that we can use flow-FISH to reliably measure average telomere length in human and mouse cell lines. The main advantage of flow-FISH over other common methods for telomere length measurement, such as Southern blot and Q-FISH, includes the ability to identify subpopulations of cells with different telomere lengths. In addition, flow-FISH is a much faster and less time-consuming method than Southern blot and Q-FISH and it is ideal for analysing large number of samples in a short period of time. We have also proposed that flow-FISH should be the method of choice for determining the average telomere length in human lymphocytes, especially in combination with immunological detection of lymphocyte subpopulations (multi-colour flow-FISH) (Rufer et al., 1998; Baerlocher et al., 2003).

However, flow-FISH has not been used to analyse telomere length in non-hematopoietic cells such as cell lines of fibroblast or of epithelial origin, which are more common in many laboratories than lymphocytes. Potential problems with applying flow-FISH on fibroblast or epithelial cells include auto-fluorescence. This particularly applies to primary cells such as human fibroblasts which senesce in culture i.e. senescent cells show increased auto-fluorescence intensities (personal observation). Our preliminary results on telomere length measurements by flow-FISH in 11 different human fibroblast cell lines indicate that flow-FISH can work in these cells as well (see previous chapter). However, it is not known if flow-FISH is sensitive enough to detect telomere shortening in human fibroblast/epithelial cell lines during replicative senescence. To test for this possibility we used 12 human primary fibroblast cell lines, cultured them for 20-40 PDs and measured telomere length by flow-FISH at multiple intervals during this period. As a control in this experiment we used telomere length measurement by Southern blot analysis. To the best of our knowledge this is the first successful attempt (see below) to determine the rate of telomere shortening during replicative senescence of human fibroblasts by flow-FISH.

Primary fibroblast cell lines selected for this study reflect our interest in the role of telomeres in DNA damage response. Apart from three cell lines established from normal individuals, all other cell lines have been established from patients with genetic defects that confer sensitivity to ionising radiation (IR), i.e. these defects cause altered DNA damage responses (for the list of cell lines see Table 2.1). Previous studies including our own have shown that short telomeres correlate with increased sensitivity to IR in lymphocytes from breast, head and neck, kidney, bladder and lung cancer patients, as well as in mice lacking *mTERC*, a gene encoding the RNA component of telomerase (Goytisolo et al., 2000; Wong et al., 2000; McIlrath et al., 2001; Wu et al., 2003). Another striking example of the correlation between radiosensitivity and short telomeres are the LY-R and LY-S cell lines described in the previous chapter. LY-S

cells have exceptionally short telomeres and are more sensitive to IR than parental LY-R cells (Figures 3.8 and 3.9).

Alterations in telomere maintenance have been observed in several human diseases characterized by defects in DNA damage responses that confer either a high sensitivity to IR e.g. ataxia telangiectasia (AT) (Metcalfe et al., 1996; Smilenov et al., 1997; Pandita and Dhar, 2000; Hande et al., 2001; Tchirkov and Lansdorp, 2003) and Nijmegen breakage syndrome (NBS) (Ranganathan et al., 2001) or a minor sensitivity to IR e.g. Fanconi anemia (FA) (Metcalfe et al., 1996; Adelfalk et al., 2001). Furthermore, proteins involved in the repair of DNA double strand breaks (DSBs), Ku and DNA-PKcs, are located at telomeres and their deficiencies cause both telomere dysfunction and IR sensitivity (Samper et al., 2000; Goytisolo et al., 2001). Taken together above observations argue that mechanisms involved in telomere maintenance may be linked with mechanisms that confer sensitivity to IR (Slijepcevic, 2004).

Although the primary aim of this study was to test whether flow-FISH can be used for measuring rates of telomere shortening in human primary fibroblasts during replicative senescence, we reasoned that if this approach is successful we can then test whether the observed link between telomere maintenance and DNA damage response exist in the above cell lines. We also examined telomere maintenance in mouse embryonic stem (ES) cells deficient in *BRCA1* and human lymphoblastoid cell lines established from carriers of *BRCA1* and *BRCA2* mutations (Table 2.2). BRCA1 participates in the repair of DNA double strand breaks (DSBs) through homologous recombination (see Chapter 1) and lack of functional BRCA1 causes sensitivity to IR (Abott et al., 1999; Foray et al., 1999). Also BRCA2 is involved in homologous repair of DSBs (Yang et al., 2002). We compared telomere maintenance between mouse ES cells in which both copies of *BRCA1* were disrupted by gene targeting (Snouwaert et al., 1999) and matching $BRCA1^{+/+}$ ES cells and telomere length dynamics in lymphoblastoid cells heterozygous for *BRCA1* and *BRCA2* mutations and their corresponding controls.

4.2 Results

4.2.1 Telomere length analysis by flow-FISH in human primary fibroblast cell lines

Having verified the accuracy of flow-FISH measurements in several different human and mouse cell lines (see previous chapter) we wanted to examine whether flow-FISH can be used to measure the rates of telomere shortening in primary human fibroblasts during replicative senescence. The panel of cell lines used in this study is shown in Table 2.1. Our panel included cell lines from nine patients with different DNA damage response defects and from three normal individuals (Table 2.1). We used primary cell lines from patients with AT, NBS, FA, Xeroderma pigmentosum (XP), Ligase IV syndrome, a patient with defective Ligase I, a patient with an unknown mutation (2BN) and a patient with an Artemis defect. As a result of these defects all patients were clinically sensitive to IR (for references see Table 2.1). However, in one case sensitivity to IR was absent *in vitro* and these cells, isolated from a FA patient, showed sensitivity to mitomycin C an alkylating agent which induces interstrand and/or intrastrand DNA crosslinks that inhibit DNA synthesis. The XP patient from complementation group C (XP-C) was also sensitive to IR suggesting that this patient may have an additional mutation conferring IR sensitivity i.e. XP patients are only sensitive to UV radiation but not to IR (Rogers et al., 2000).

Telomere maintenance was not examined before in *ligase I* deficient cells or in cells defective in Artemis, a protein involved in DSB repair (Jeggo and O'Neill, 2002; Lees-Miller and Meek, 2003). Telomere maintenance was not examined before in cells from the above XP-C patient. Also, telomere maintenance was not examined before in cells from an immuno-deficient patient characterised by impaired DSB repair and extreme IR sensitivity (cell line 2BN, Table 2.1). All known DSB repair components are normal in 2BN cells suggesting that an additional factor, defective in these cells, may be required for DSB repair (Dai et al., 2003).

Previous results indicated that cells sensitive to IR in many cases also showed alterations in telomere maintenance (see above). Most cell lines were grown for between 20 and 40 PDs and telomere length was measured at multiple points during the period of cell culture by flow-FISH but also by classical Southern hybridisation.

Our preliminary experiments with fibroblast cell lines (see previous chapter) indicated higher levels of FITC fluorescence intensity in non-hybridised pre-senescent cells (results not shown). These high fluorescence intensity values are probably due to the presence of cytoplasmic and nuclear bodies, specific for fibroblasts, which are highly auto-fluorescent. The same phenomenon is observed when immunocytochemistry-based techniques are applied on fibroblasts (personal observation). Therefore, the high level of auto-fluorescence could be the major problem for using flow-FISH in senescing fibroblast cells and it does not occur, for example, in cells of hematopoietic origin such as lymphocytes or lymphoblastoid cell lines. We noticed that auto-fluorescence in fibroblasts increases with the cell passage number (see below).

To avoid the problem of auto-fluorescence our flow-FISH method adapted for fibroblasts included subtracting fluorescence intensity values due to FITC (fluorochrome used to detect telomeres in our flow-FISH set-up) observed in non-hybridised control cells from telomere fluorescence intensity (TFI) values observed in cells hybridised with the telomeric PNA probe. Results of our analysis are presented in Figure 4.1 (please note that an example of flow-FISH profile in fibroblast cell lines can be seen in Figure 3.16). The portions of bars in grey represent TFI in non-hybridised cells (Figure 4.1). Interestingly, particularly high fluorescence intensity values in non-hybridised cells were measured when cells reached a pre-senescent state in almost all DNA damage response defective cell lines in contrast to control lines. We also noticed, based on flow cytometry parameters, that pre-senescent cells had a tendency to stick to each other more frequently than younger cells and this contributed to the reduction of cells analysable by flow-FISH in higher passage cell samples. In parallel to flow-

FISH we have also performed Southern blot analysis (see below) for which high numbers of cells were required. Given all factors that contributed to the reduction of cells available for analysis by flow-FISH we measured TFI values only at 3-5 time points during the *in vitro* culture period (several months) in most cell lines (Figure 4.1).

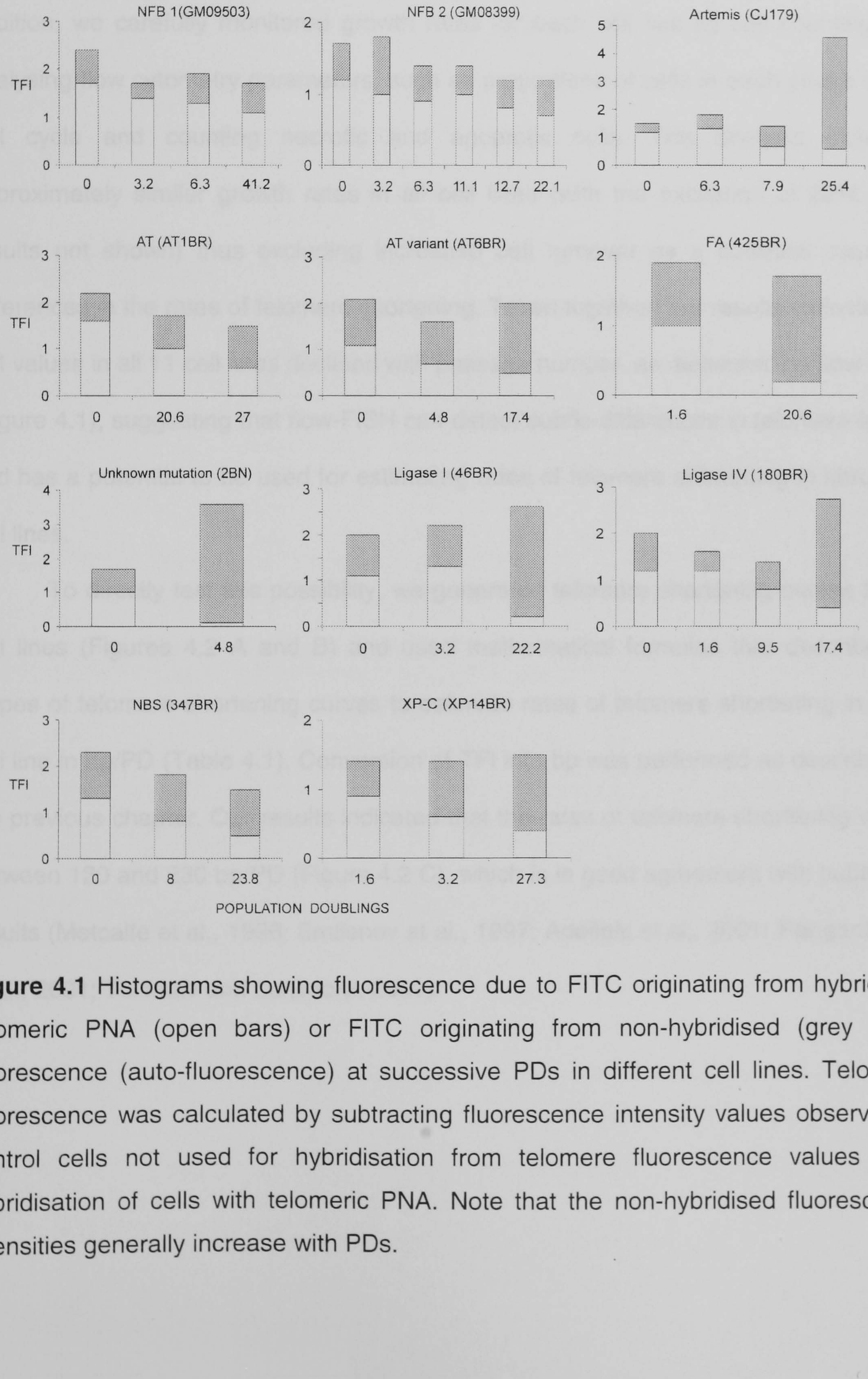

Figure 4.1 Histograms showing fluorescence due to FITC originating from hybridised telomeric PNA (open bars) or FITC originating from non-hybridised (grey bars) fluorescence (auto-fluorescence) at successive PDs in different cell lines. Telomere fluorescence was calculated by subtracting fluorescence intensity values observed in control cells not used for hybridisation from telomere fluorescence values after hybridisation of cells with telomeric PNA. Note that the non-hybridised fluorescence intensities generally increase with PDs.

However, in two cell lines we were able to measure telomere length by flow-FISH on two occasions only (Figure 4.1). The level of apoptotic cells was low in all cell lines as indicated by flow cytometry parameters (data not shown) suggesting that telomere shortening observed, results from normal cell proliferation and not apoptosis. In addition, we carefully monitored growth rates for each cell line by cell counting and analysing flow cytometry parameters, such as proportions of cells in each phase of the cell cycle and counting necrotic and apoptotic cells. This analysis indicated approximately similar growth rates in all cell lines (with the exception of 2BN cells; results not shown) thus excluding increased cell turnover as a potential cause of differences in the rates of telomere shortening. Taken together, our results indicate that TFI values in all 11 cell lines declined with passage number, as measured by flow-FISH (Figure 4.1), suggesting that flow-FISH can detect subtle differences in telomere length and has a potential to be used for estimating rates of telomere shortening in fibroblast cell lines.

To directly test this possibility, we generated telomere shortening curves for all cell lines (Figures 4.2 A and B) and used mathematical formulas that describe the slopes of telomere shortening curves to estimate rates of telomere shortening in each cell line in bp/PD (Table 4.1). Conversion of TFI into bp was performed as described in the previous chapter. Our results indicated that the rates of telomere shortening varied between 120 and 230 bp/PD (Figure 4.2 C), which is in good agreement with published results (Metcalfe et al., 1996; Smilenov et al., 1997; Adelfalk et al., 2001; Ranganathan et al., 2001; Tchirkov and Lansdorp, 2003).

Table 4.1 Calculation of telomere shortening in bp/PD by use of flow-FISH and Southern blot hybridisation methods. Data from 2BN obtained by flow-FISH was excluded from the analysis because the telomere shortening rate was unusually high.

		flow-FISH				Southern hybridisation		
Phenotype	Cell line	PD	TFI	bp	bp/PD	PD	TRF (bp)	bp/PD
normal (NFB 1)	GM09503	0	1.7	9581	60.1	0	9.9	89.7
		3.2	1.4	8342		20.5	9.0	
		6.3	1.3	7029		37.9	6.5	
		41.2	1.1	7103		-	-	
normal (NFB 2)	GM08399	0	1.2	7516	93.4	0	10.1	97.7
		3.2	1.0	6690		7.9	7.5	
		6.3	0.9	6277		17.4	8.4	
		11.1	1.0	6690		-	-	
		12.7	0.8	5864		-	-	
		22.1	0.7	5451		-	-	
normal (NFB 3)	GM04505	-	-	-	-	0	6.6	34.5
		-	-	-		6.3	6.3	
		-	-	-		17.4	6.0	
Artemis	CJ179	0	1.6	9168	162.6	0,0	7.7	113.1
		6.3	1.3	7929		7.9	5.8	
		7.9	0.7	5451		22.1	5.2	
		25.4	0.6	5038		-	-	
AT	AT1BR	0	1.4	8342	122.4	0	10.2	177.9
		20.6	1.0	6690		14.2	5.9	
		27.0	0.6	5038		25.3	5.7	
AT variant	AT6BR	0	1.1	7103	142.4	0,0	8.1	182.8
		17.4	0.5	4625		6.3	7.0	
		-	-	-		12.6	5.7	
		-	-	-		14.2	5.5	
FA	425BR	1.6	1.0	6690	160.4	0	7.8	147.7
		20.6	0.2	3386		7.9	6.5	
		-	-	-		12.6	5.9	
		-	-	-		14.2	5.7	
Unknown mutation	2BN	0	1.0	6690	774.4	0	6.2	142.4
		4.8	0.1	2973		1.6	5.5	
		-	-	-		3.2	5.4	
		-	-	-		6.3	5.3	
DNA ligase I	46BR	3.2	1.3	7929	204.6	0	7.2	120.8
		22.2	0.2	3386		12.6	6.6	
		-	-	-		17.4	5.1	
DNA ligase IV	180BR	0	1.2	7516	237.4	0	7.1	180.8
		9.5	0.8	5864		7.9	5.6	
		17.4	0.2	3386		11.1	5.1	
NBS	347BR	0	1.3	7929	138.8	0	8.3	145.6
		8.0	0.8	5864		9.5	6.9	
		23.8	0.5	4625		15.8	6.0	
XP-C	XP14BR	0	0.9	6277	130.7	0	5.7	51.7
		3.2	0.6	5038		6.3	4.9	
		15.8	0.4	4212		17.4	4.8	

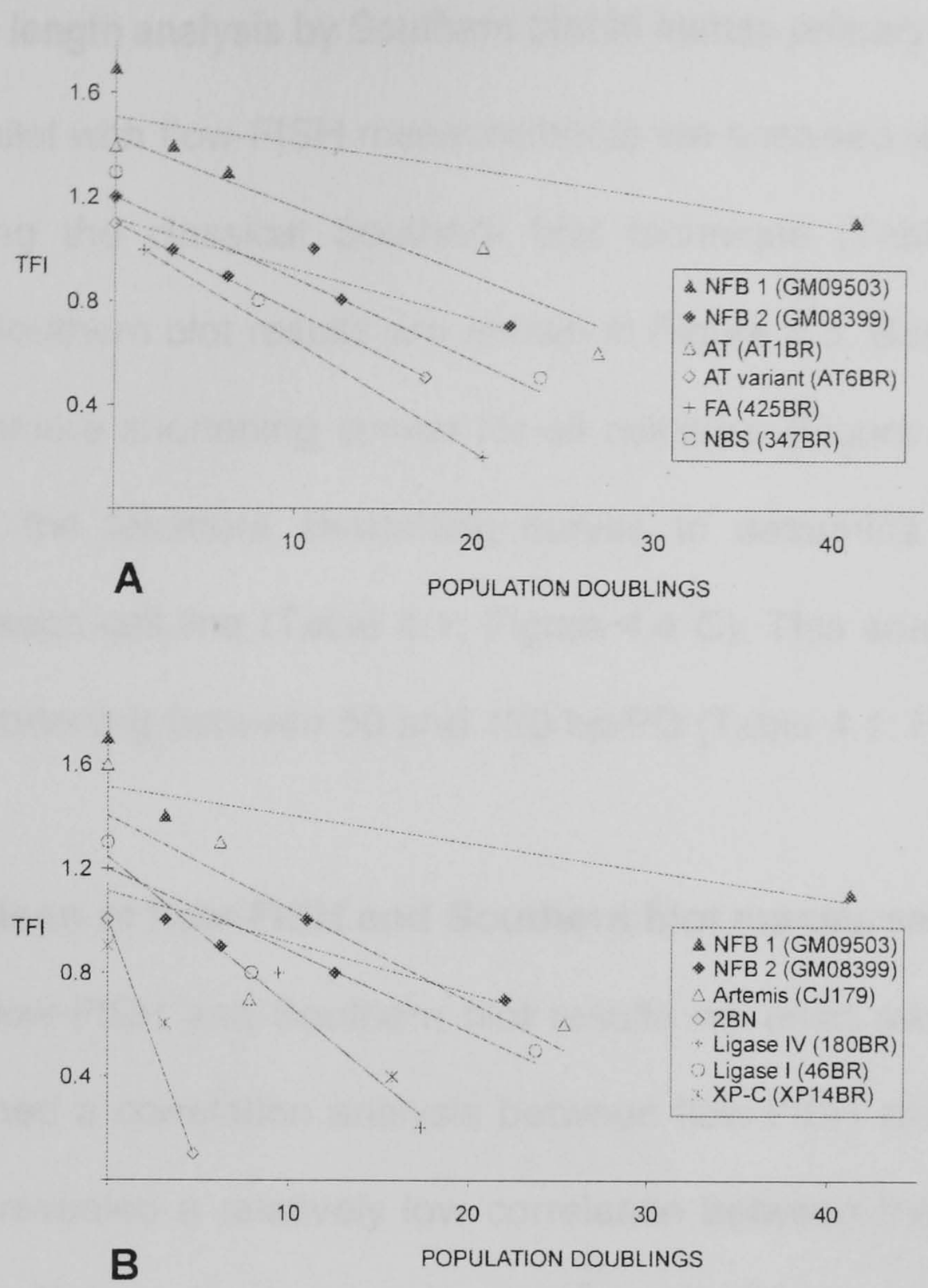

Figure 4.2 A and **B**. Telomere shortening curves constructed on the basis of flow-FISH results in human primary fibroblast cell lines presented in Figure 4.1 and Table 4.1. Curves are presented in two separate panels to avoid overlaps, which may create difficulties in identifying points used for curve fitting. **C**. Rates of telomere shortening in primary human fibroblasts in base pairs (bp)/PD as determined by flow-FISH. Telomere shortening for cell lines 425BR and 2BN were based on two measuring points only, all the others on minimum of 3 points. Zero point PD represents the first point at which we measured telomere length in the above cell lines since we received them. Real PD numbers can be obtained by adding PD values indicated in Table 2.1.

4.2.2 Telomere length analysis by Southern blot in human primary fibroblast cell lines

In parallel with flow-FISH measurements we analysed telomere length in above cell lines using the classical Southern blot technique (Table 4.1). Representative examples of Southern blot results are shown in Figure 4.3. Based on these results we generated telomere shortening curves for all cell lines (Figure 4.4 A and B) and used the slopes of the telomere shortening curves to determine the rates of telomere shortening in each cell line (Table 4.1; Figure 4.4 C). This analysis revealed the rates of telomere shortening between 50 and 180 bp/PD (Table 4.1; Figure 4.4 C).

4.2.3 Comparison of flow-FISH and Southern blot measurements

To compare flow-FISH and Southern blot results we used two approaches. First, we simply performed a correlation analysis between flow-FISH and Southern blot results. This analysis revealed a relatively low correlation between these two methods in the case of above fibroblast cell lines used (R^2=0.52) (Figure 4.5). However, there are some important differences between the methods that may not justify direct comparisons between them. For example, flow-FISH quantifies exclusively telomeric TTAGGG sequences whereas Southern hybridisation may also take account of telomeric sequences present in subtelomeric chromosome regions (Nakamura et al., 1999; Freulet-Marriere et al., 2004). Individuals that have the same mean length of terminal hexamer repeat array may nevertheless have very different mean telomere/terminal restriction fragment (TRF) lengths, due to restriction site polymorphisms and/or length polymorphisms in the subtelomeric regions that determine the length of the subtelomeric portions of the TRF. Early studies showed that the mean length of this subtelomeric portion of the TRFs in unrelated individuals ranged from 2.5 to 6 kb (Levy et al., 1992).

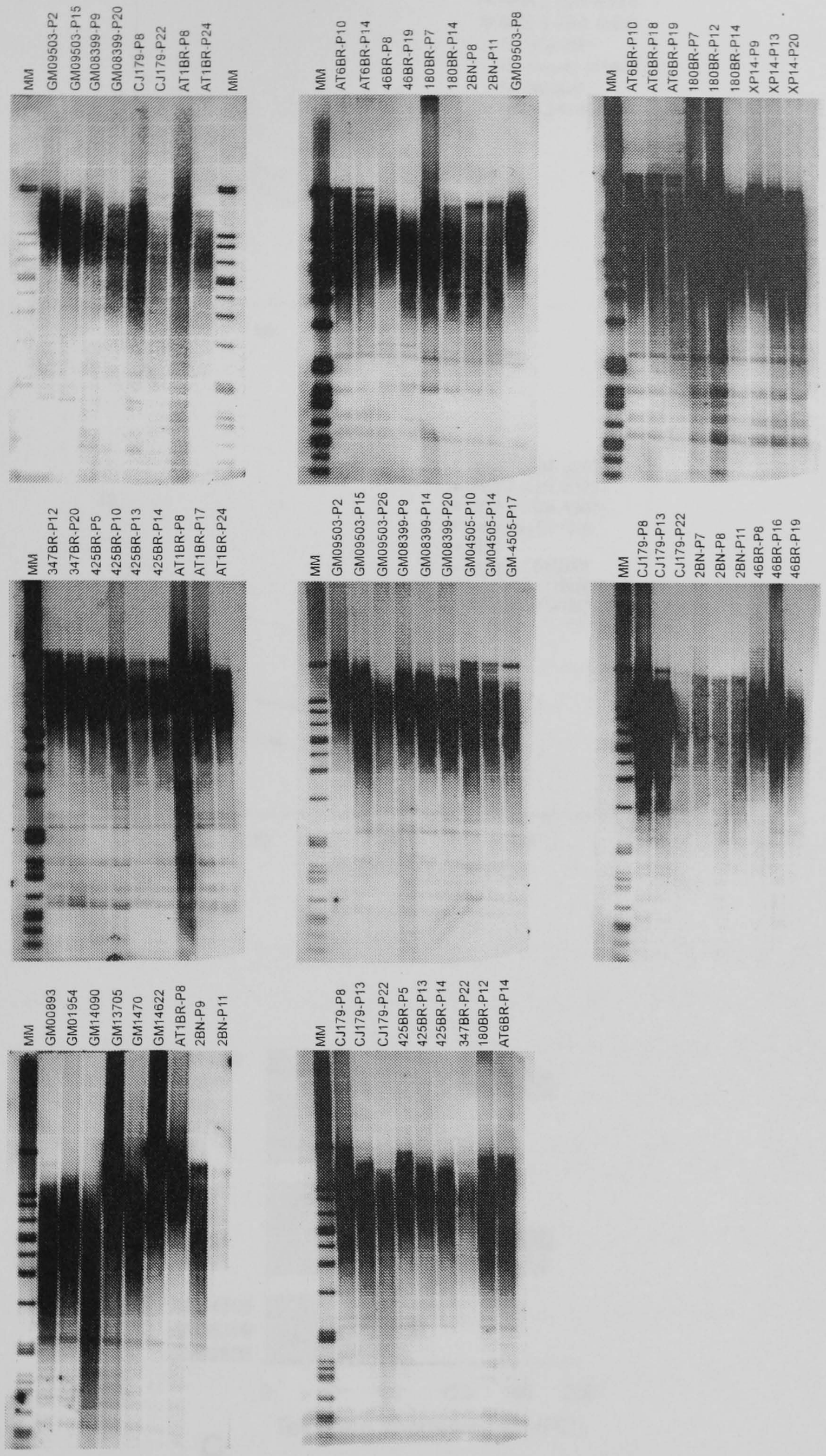

Figure 4.3 Representative examples of Southern blot-based telomere length measurements in human primary fibroblast cell lines. MM: Molecular weight marker, P: passage number. The conversion of passages into PDs is described in Materials and Methods.

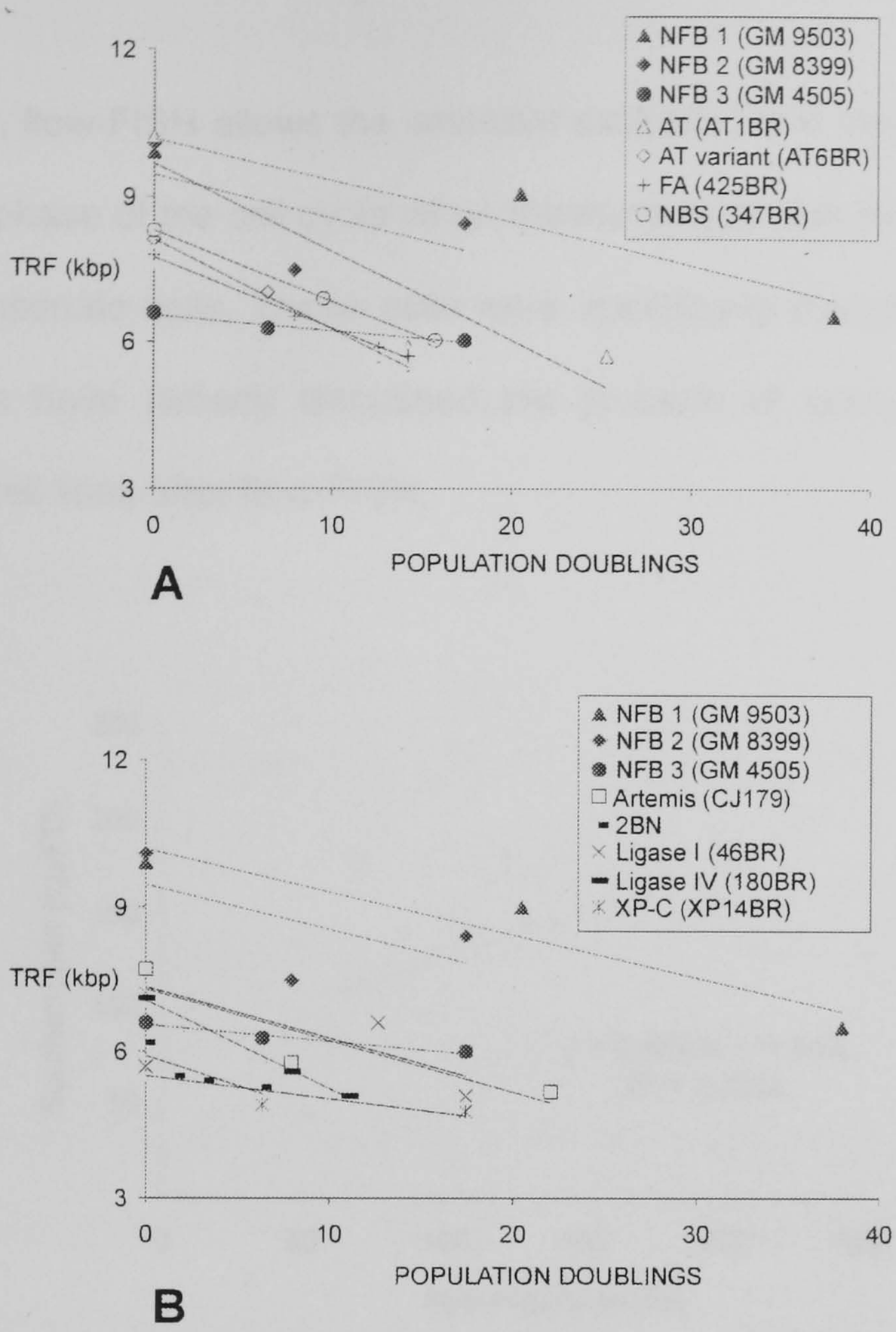

Figure 4.4 A and **B**. Telomere shortening curves based on Southern hybridisation results in human primary fibroblast cell lines presented in Figure 4.3 and Table 4.1. Two separate panels are used to avoid significant curve overlaps. **C**. Rates of telomere shortening in primary human cell lines in base pairs (bp)/PD as determined by Southern blot analysis.

In addition, flow-FISH allows the selective exclusion of a specific cell population during the G_0/G_1 phase of the cell cycle when measurements are performed, i.e. polyploid and apoptotic/necrotic cells. These cells were specifically excluded in flow-FISH analysis. Finally, we have already discussed the problem of auto-fluorescence observed in fibroblast cell lines after flow-FISH.

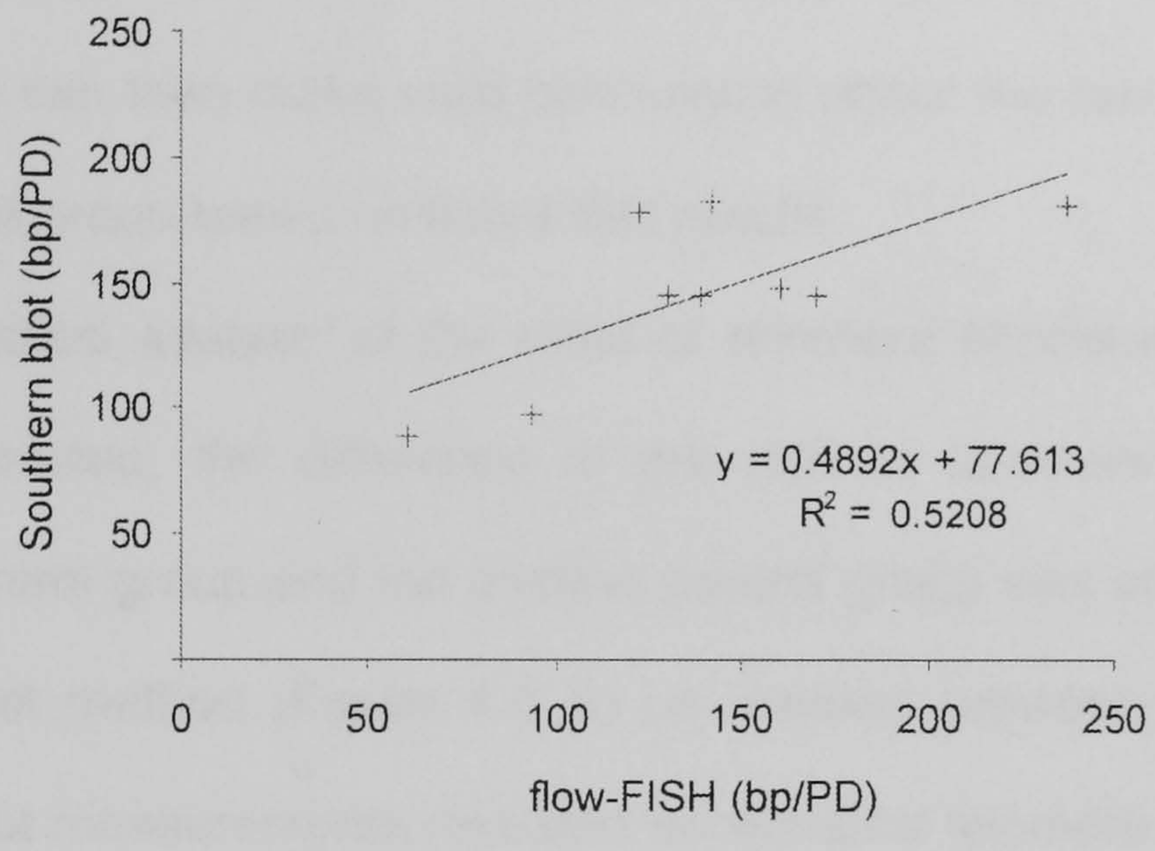

Figure 4.5 Comparison of telomere shortening rates (bp/PD) obtained by flow-FISH and Southern blot methods. All cell lines included from Table 2.1 were used except 2BN, XP14BR, and GM04505. The rate of telomere shortening in the 2BN cell line was unusually high. The flow-FISH and Southern blot results of telomere length measurement for the XP14BR cell line were apparently different. The GM04505 cell line was not analysed by flow-FISH.

Given the differences between the two methods when fibroblasts are used we decided to take an alternative approach to test if flow-FISH can detect biologically relevant differences between cell lines that can be detected by Southern blot. We divided our cell lines into three groups, namely the negative control group - cell lines from normal individuals, the positive control group - four cell lines from AT, NBS and FA patients shown earlier to have accelerated telomere shortening (Metcalfe et al., 1996; Smilenov et al., 1997; Adelfalk et al., 2001; Hande et al., 2001; Ranganathan et

al., 2001; Tchirkov and Lansdorp, 2003) and the novel cell group - the five cell lines in which the rate of telomere shortening was not previously examined. The reasoning behind this approach is that if flow-FISH can reproduce differences between the negative control group and the positive control group that are now well documented largely based on Southern blot measurements (Metcalfe et al., 1996; Smilenov et al., 1997; Adelfalk et al., 2001; Hande et al., 2001; Ranganathan et al., 2001; Tchirkov and Lansdorp, 2003) then we can argue that this method may be as good as Southern blot for calculating the rates of telomere shortening in primary fibroblast cell lines. If this is the case we can then make valid conclusions about the rate of telomere shortening in the novel cell group based on flow-FISH results.

Statistical analysis of the rates of telomere shortening/PD is shown in Figure 4.6. As expected, the difference in the rate of telomere shortening between the negative control group and the positive control group was statistically significant using Southern blot method (Figure 4.6 B) i.e. several previous studies largely based on Southern blot measurements revealed accelerated telomere shortening in AT, FA and NBS patients in comparison with control individuals (Metcalfe et al., 1996; Smilenov et al., 1997; Adelfalk et al., 2001; Hande et al., 2001; Ranganathan et al., 2001; Tchirkov and Lansdorp, 2003). Interestingly, we also observed a statistically significant difference in the rates of telomere shortening between the negative and the positive control groups using flow-FISH (Figure 4.6 A) suggesting that in spite of a relatively low correlation between Southern blot and flow-FISH results, when compared directly against each other, flow-FISH can detect biologically relevant differences between the cell lines.

We then compared the rates of telomere shortening in the novel cell group using both methods. The rate of telomere shortening in the novel cell group was statistically significantly higher in comparison to the negative control group using the Southern blot method (Figure 4.6 B) in spite of the normal rate of telomere shortening in XP14BR cells (Figure 4.4 C). Similarly, comparison of the rates of telomere

shortening between the negative control cell group and the novel cell group using flow-FISH revealed statistically significant differences (Figure 4.6 A). Therefore, this reinforces the view that flow-FISH can detect differences between the cell lines that are also detectable by Southern blot.

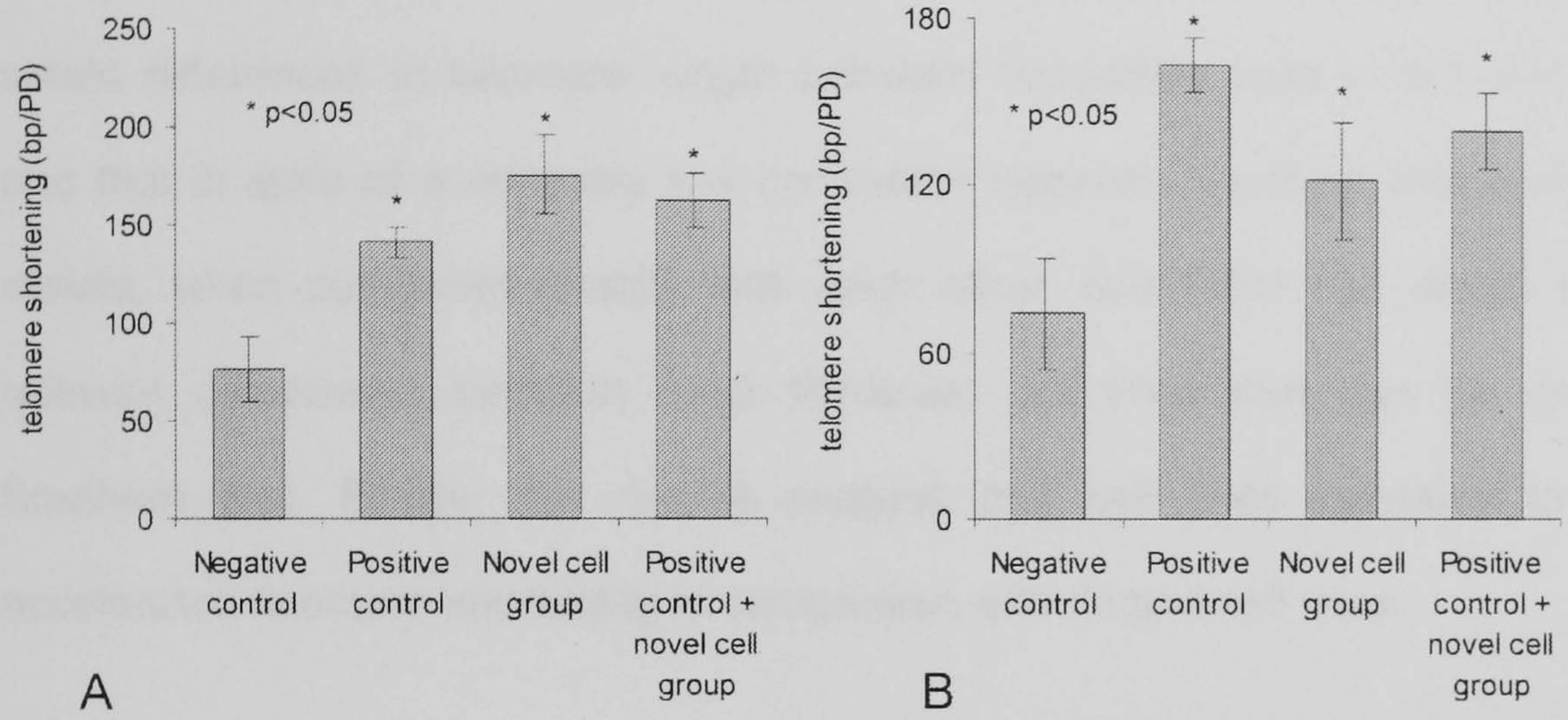

Figure 4.6 Statistical analysis (two-way t-test) of telomere shortening rates in bp / PD in the negative control group (GM09503, GM08399 and GM04505), the positive control group (AT1BR, AT6BR, 347BR and 425BR) and the novel cell group (46BR, CJ179, 2BN, XP14BR and 180BR) as determined by flow-FISH (**A**) and Southern blot (**B**). Note that telomere shortening rates were taken from Figures 4.2 C and 4.4 C. * Significantly higher than negative control ($p<0.05$ t-test).

However, it is important to stress that discrepancies observed between Southern blot and flow-FISH measurements require further clarification perhaps by using alternative methods such as Q-FISH. For example, although in most cases the rates of telomere shortening were higher in radiosensitive cell lines than in normal cell lines as revealed by both methods we found one clear difference. In the case of XP14BR cells the rate of telomere shortening as measured by Southern blot was within the normal range whereas the rate measured by flow-FISH was within the range of the positive control group (Figures 4.2 C and 4.4 C). We also would like to point out that in

contrast to a previous study which indicated normal telomere length in *ligase IV* deficient 180BR cells, when compared with fibroblasts from an age matched normal individual as measured by Southern blot (d'Adda di Fagagna et al., 2001), our results indicate accelerated telomere shortening in this cell line *in vitro* (Figures 4.2 C and 4.4 C).

Taken together our results suggest that flow-FISH is sensitive enough to detect subtle differences in telomere length between fibroblasts cells in different passages and that in spite of a relatively low correlation between Southern blot and flow-FISH results, when compared directly with each other, flow-FISH can detect biologically relevant differences between most fibroblast cell lines that can be detected by Southern blot. Finally, our results suggest that cell lines sensitive to IR show accelerated telomere shortening in comparison with control cell lines.

4.2.4 Analysis of telomere function in radiosensitive human cell lines

Accelerated telomere shortening is a predisposing factor for premature loss of telomere capping function, which may lead to appearance of chromatin bridges in anaphase cells. Therefore, one way to verify that telomere length measurements in above cell lines were accurate would be to measure frequencies of anaphase bridges i.e. cells with higher rates of telomere shortening are expected to show higher frequencies of anaphase bridges than cells with lower rates of telomere shortening. To achieve this we decided to monitor frequencies of anaphase bridges in pre-senescent cells in at least two different passages between PDs 20 and 30 i.e. it is more likely that anaphase bridges will be detected in pre-senescent cells than in cells in early passages. For this we treated cells with cytochalasin B. Cytochalasin B inhibits cytokinesis and two nuclei remain preserved in a single cytoplasm after this treatment, which should make it easy to detect chromatin bridges arising as a result of inability of sister chromatids to separate in anaphase. However, contrary to our expectation this assay did not allow us to detect anaphase bridges clearly (Figure 4.7 A). We then used

a classical anaphase bridge assay without cytochalasin B treatment (Figure 4.7 B). Frequencies of anaphase bridges were low in all cell lines but nevertheless some differences were observed between radiosensitive and normal cell lines (Figure 4.8 A). The 2BN cell line showed a low mitotic index and complete lack of anaphase cells and as a result was excluded from the analysis. Statistical analysis revealed significantly higher frequencies of anaphase bridges in cells from the positive control group in comparison to cells from the negative control group (Figure 4.8 B). This is in line with previous studies reporting an increased incidence of telomeric fusions in cells from AT and FA patients (Metcalfe et al., 1996; Callen et al., 2002). Frequencies of anaphase bridges were also significantly higher in cell lines from the novel cell group in comparison to cell lines from the negative control group (Figure 4.8 B).

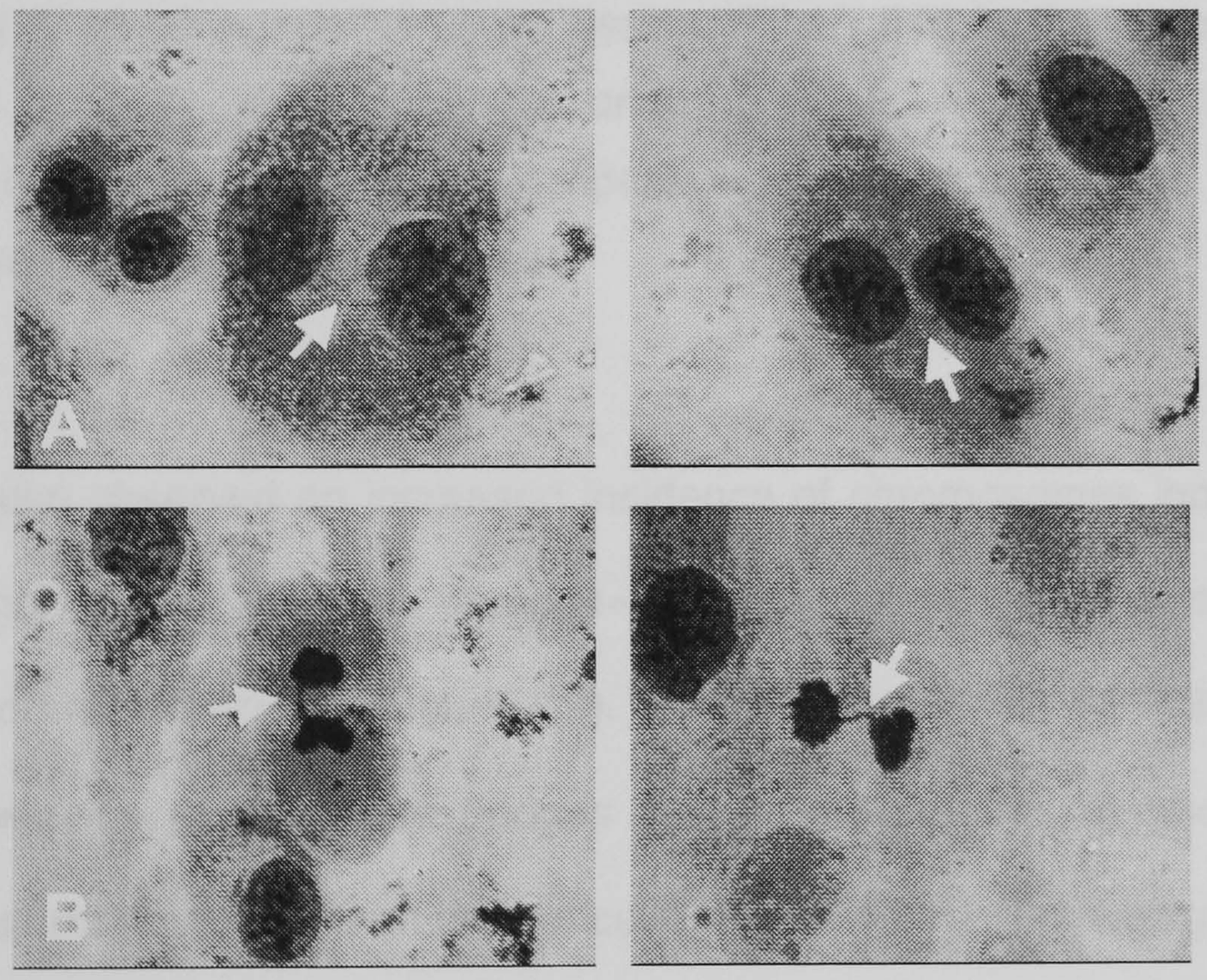

Figure 4.7 (**A**) Chromatin bridges detected in cytochalasin B treated bi-nucleated cells. In most cases these chromatin bridges were difficult to identify i.e. two observers could not agree whether these events were really chromatin bridges or artefacts caused by staining. (**B**) Anaphase bridges in human fibroblasts. In contrast to above chromatin bridges in bi-nucleated cells anaphase bridges were unambiguously identifiable.

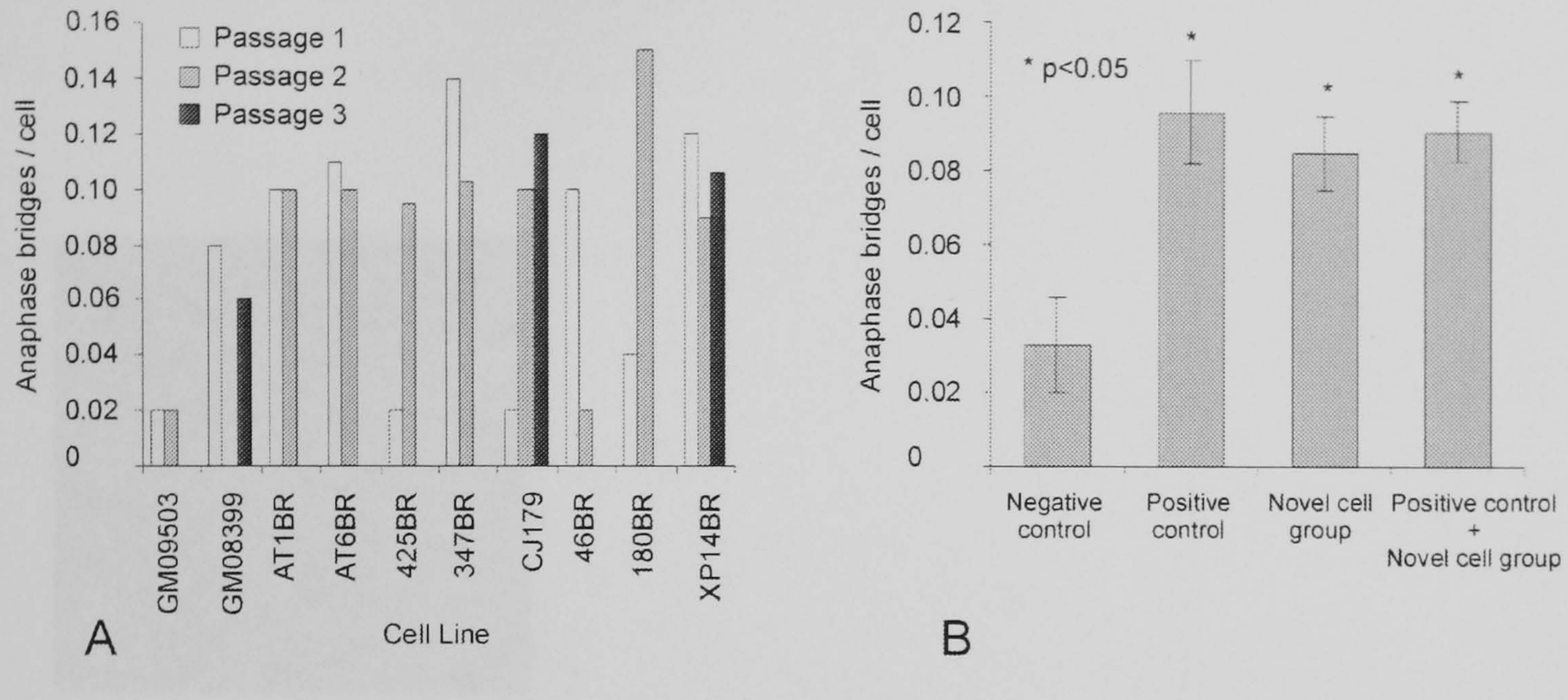

Figure 4.8 (**A**). Analysis of anaphase bridges in 10 human fibroblast cell lines at 2-3 different passages between PDs 20 and 30. For this purpose all cell lines have been synchronized to have similar PD numbers. In the case of some cell lines bars representing a passage number are missing. When this is the case that particular sample was not suitable for anaphase bridge analysis. A minimum of 50 anaphase cells / point were analysed (**B**). Comparison of anaphase bridge frequencies in radiosensitive fibroblasts. (*p<0.5, t-test)

We also observed an increased incidence of chromosomes lacking detectable telomeric signals in all the DNA damage response deficient cells in comparison with cells from normal individuals (Figure 4.9). It is noteworthy that XP14BR cells showed higher frequencies of anaphase bridges (Figure 4.8 A) and chromosomes lacking detectable telomeric signals than normal cells (Figure 4.9 B) suggesting that the normal rate of telomere shortening observed in these cells by Southern blot analysis is not a good predictor of telomere function. However, metaphase end-to-end chromosome fusions were absent or rare in all cell lines (data not shown) and in contrast to earlier studies (Metcalfe et al., 1996; Callen et al., 2002), metaphase fusion events were not consistently observed either in AT or in FA cells. The fact that anaphase bridges were

observed reproducibly in all cell lines and metaphase end-to-end chromosome fusions rarely and irregularly may be explained by differences in the numbers of analysed anaphase cells (50/point) and metaphase cells (25/point).

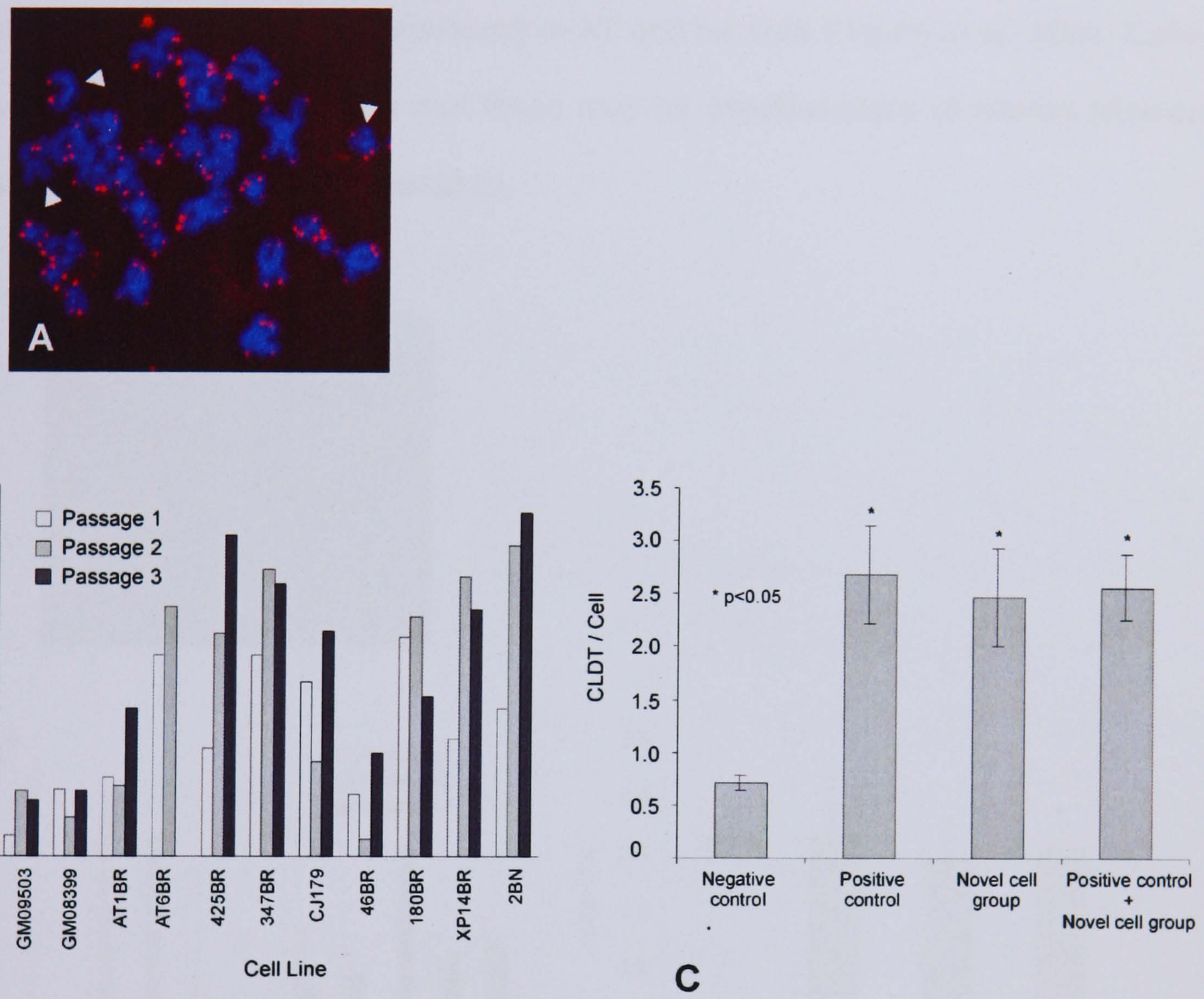

Figure 4.9 (**A**). A metaphase cell hybridised with a telomeric PNA probe labelled with Cy-3 (see Material and Methods). Arrows indicate chromatids lacking signal. (**B**). Frequencies of CLTD (chromatids lacking detectable telomere) / cell in fibroblast cell lines as observed in 2-3 different passages between PDs 20 and 30 (i.e. presenescent cells). Missing bars indicate samples not suitable for analysis. (**C**). Comparison of chromatids lacking detectable telomere (CLDT) frequencies in human fibroblast cell lines. All bars represent the mean number of CLDT in a metaphase while the error bars represent the standard error of the mean (SEM). (*p<0.5, t-test)

We have also observed another unusual cytological phenomenon in radiosensitive cell lines: split telomeric signals. Examples of these split telomeric signals are shown in Figure 4.10 A. Frequencies of split telomeric signals were significantly higher in radiosensitive cell lines in comparison to control cell lines (Figure 4.10 B and C). Split telomeric signals are remarkably similar to extra-chromosomal telomeric fragments observed previously in AT and FA cells (Hande et al., 2001; Callen et al., 2002) and we speculate that these may be manifestations of altered telomere metabolism (for details see discussion).

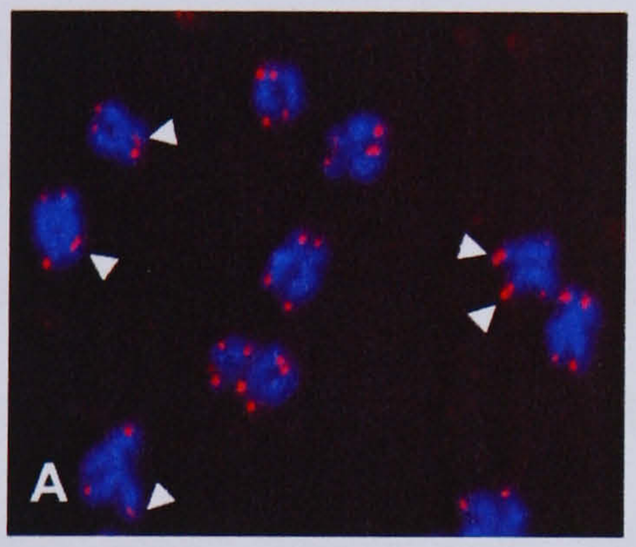

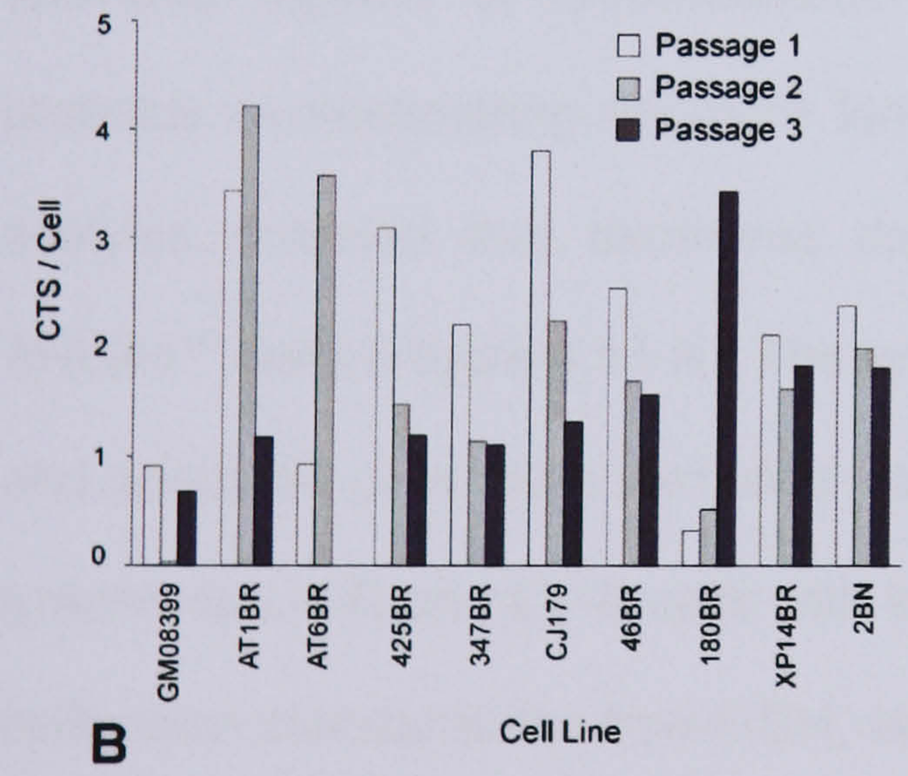

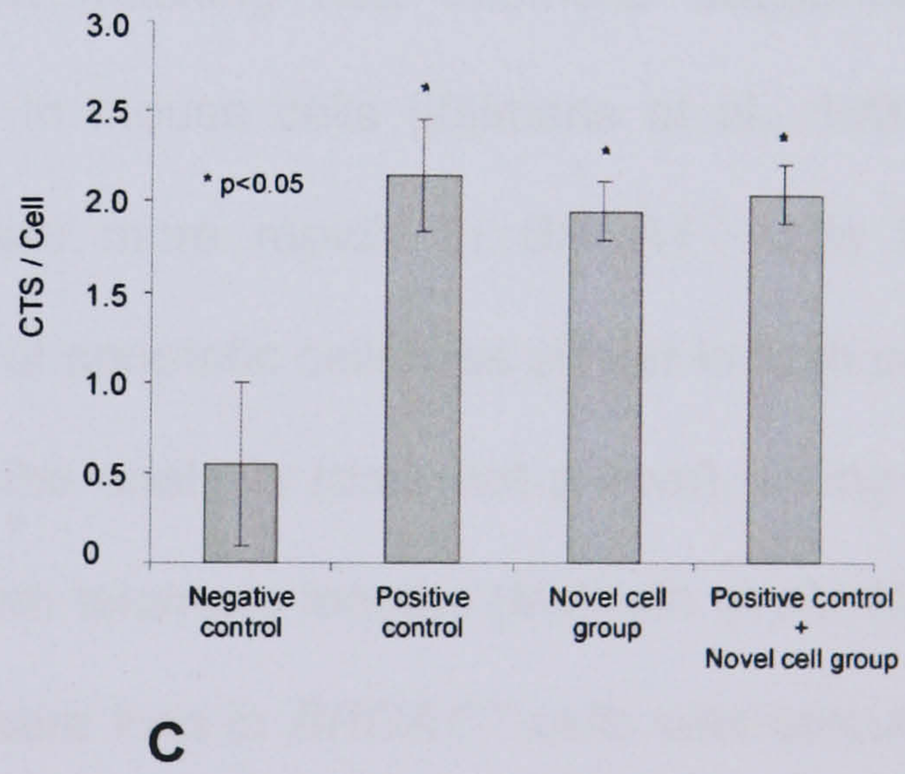

Figure 4.10 (**A**). A representative example of split telomeric signals (arrows) in chromosomes originating from a human fibroblast cell. (**B**). Chromatids with telomeric split (CTS) per cell in pre-senescent cells in 2-3 different passages between PDs 20 and 30. Missing bars indicate samples not suitable for analysis. (**C**). Comparison of CTS/cell frequencies in human fibroblast cell lines. All bars represent the mean number of CTS in a metaphase while the error bars represent the standard error of the mean (SEM). (*p<0.5, t-test)

Taken together these results suggest that radiosensitive pre-senescent cells show altered telomere maintenance in comparison with control pre-senescent cells and it is likely that the observed accelerated telomere shortening in these cell lines as identified by flow-FISH and Southern blot is not an artefact.

4.2.5 Telomere maintenance in mouse *BRCA1* deficient cells

To examine the association between radiosensitivity and telomere maintenance in non-human cells, mouse embryonic stem (ES) cells were used in which both copies of *BRCA1* were disrupted by gene targeting (Snouwaert et al., 1999). *BRCA1* deficiency confers genomic instability and sensitivity to IR (Abbott et al., 1999; Foray et al., 1999). Mouse *BRCA1*$^{-/-}$ ES cells as well as *BRCA1*$^{+/+}$ ES cells, were grown for ~ 25 PDs and their telomere lengths measured after each 3 PDs by flow-FISH. Southern blot cannot accurately estimate telomere length in mouse cells because this technique probably takes account of degenerate telomere-like sequences present in sub-telomeric regions of chromosomes thus masking real telomeric sequences and probably overestimating telomere length in mouse cells (Zijlmans et al., 1997). Our analysis revealed that telomeres degrade more rapidly in *BRCA1*$^{-/-}$ cells than in *BRCA1*$^{+/+}$ cells (Figure 4.11 A). The level of apoptotic cells was similar in both cell lines and apoptotic cells were excluded from the analysis (data not shown). Using mouse lymphoma LY-R and LY-S cells with known telomere lengths (McIlrath et al., 2001) as calibration standards for flow-FISH, telomere loss in *BRCA1*$^{+/+}$ cells was calculated to be ~ 580 base pairs (bp) / PD. Telomere loss in *BRCA1*$^{-/-}$ cells was more pronounced and on average these cells were loosing ~ 1,000 bp / PD. Observation of telomere shortening in *BRCA1*$^{+/+}$ cells was somewhat surprising because mouse cells with normal telomerase activity are not expected to lose telomeric sequences. However, it is important to stress that *BRCA1* proficient mouse embryonic stem cells used here might not be entirely normal i.e. this cell line has a mutation in the *HPRT* gene (Snouwaert et al., 1999) which could contribute to this phenotype. Also, our estimate of the rate of

telomere shortening in the above two mouse cell lines is unusually high in comparison with estimated rates of telomere shortening in human cell lines (see above). One possibility is that these cells were under physiological stress and we did observe changes in cell shape consistent with this possibility. ES cells require special media and supplements and the physiological stress could have been caused by our serum replacement (Knockout SR, Gibco) used instead of the standard foetal calf serum (see Materials and Methods). Another observation in line with a high level of physiological stress in these cells is increased levels of DSBs as detected with DSB-specific antibody (see below). Finally, in contrast to mouse ES cells the average telomere length was stable in human lymphoblastoid cells heterozygous for *BRCA1* and *BRCA2* mutations (Figure 4.11 B) suggesting further potential presence of physiological stress in mouse ES cells.

Next, we examined chromosome abnormalities in *BRCA1*$^{-/-}$ and *BRCA1*$^{+/+}$ cells. We observed end-to-end chromosome fusions and chromosomes lacking detectable telomeric signals in *BRCA1*$^{-/-}$ cells, whereas these events, indicative of telomere dysfunction, were absent in *BRCA1*$^{+/+}$ cells (Figure 4.12). Chromosome ends that lack a FISH signal preferentially participate in end-to-end fusions, providing a direct evidence for the link between short telomeres and end-to-end chromosome fusions (Hemann et al., 2001). Approximately 50% fusion events involved telomeric sequences at the fusion points. In addition, we observed elevated frequencies of extra-chromosomal telomeric fragments (ECTFs) in the form of double minute chromosomes in late passage *BRCA1*$^{-/-}$ cells in comparison with control *BRCA1*$^{+/+}$ cells (Figure 4.12 B and C). These ECTFs could reflect a mechanism responsible for generating split telomeric signals observed in human fibroblast cell lines sensitive to IR (see above). Therefore, our cytogenetic analysis indicates that accelerated telomere shortening in *BRCA1*$^{-/-}$ cells causes mild telomere dysfunction whereas telomeres remain functional in spite of their shortening in *BRCA1*$^{+/+}$ cells.

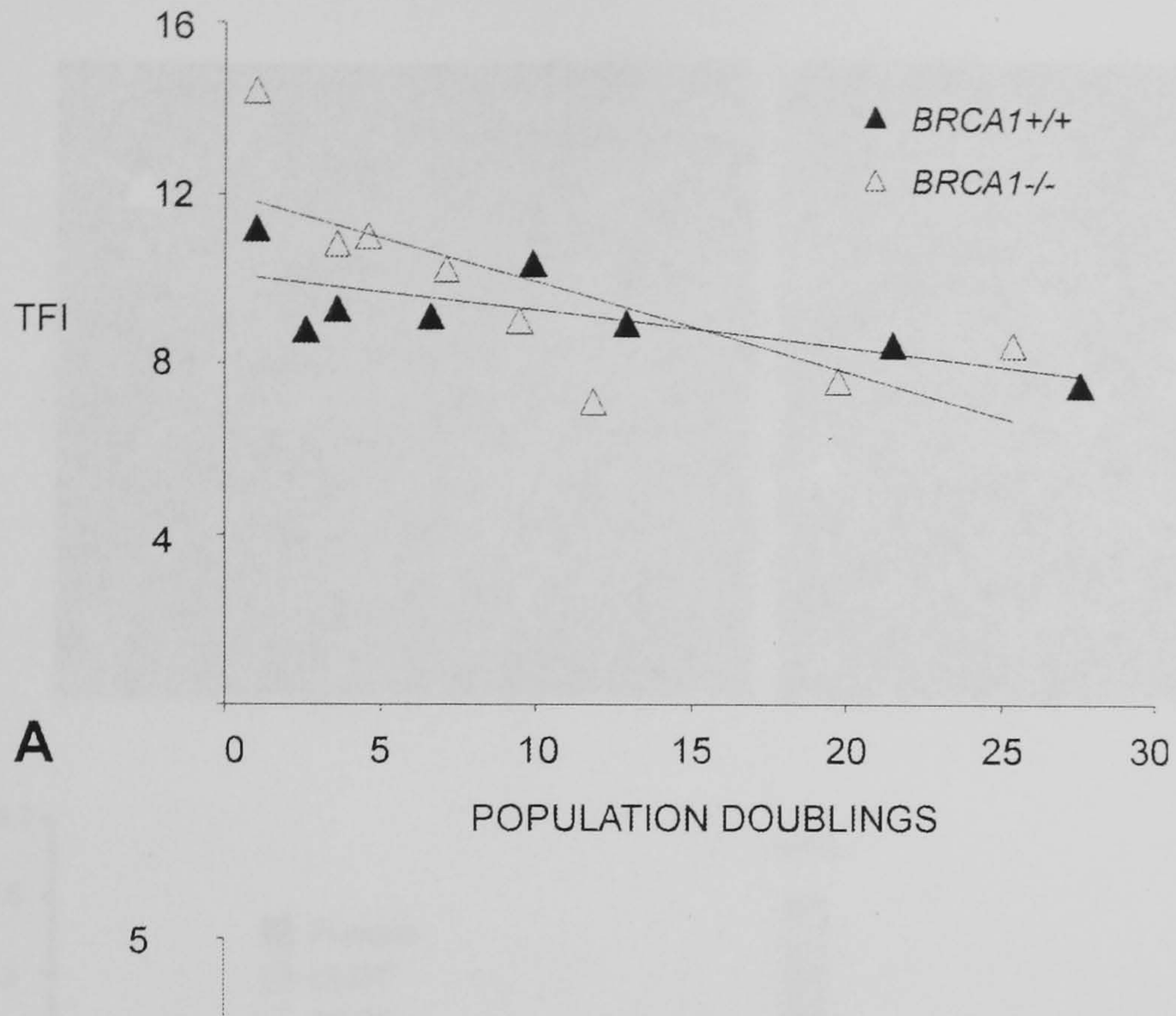

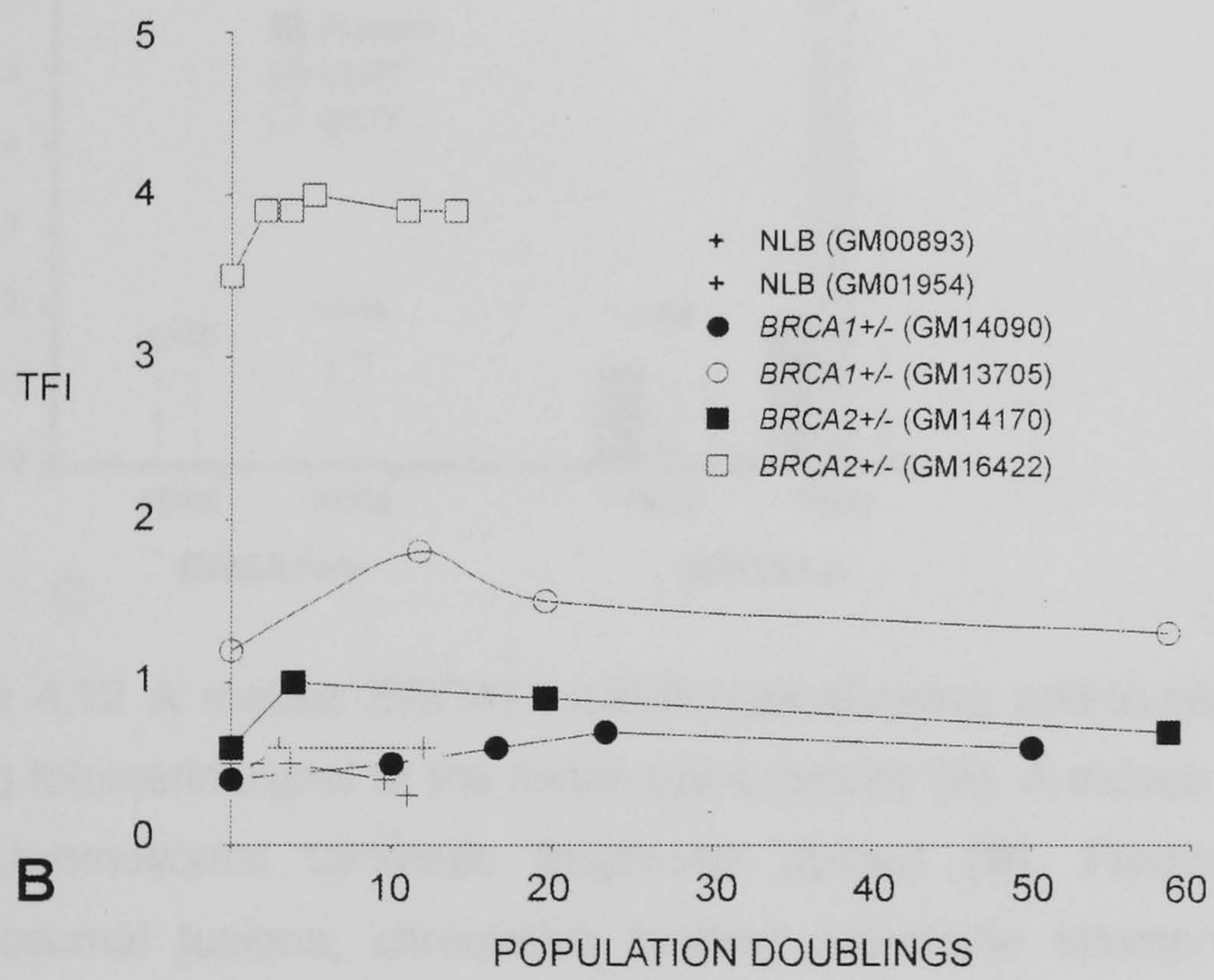

Figure 4.11 (**A**). Telomere length analysis by flow-FISH in mouse *BRCA1*$^{+/+}$ and *BRCA1*$^{-/-}$ embryonic stem cells. *BRCA1*$^{+/+}$ cells were obtained at PD 35 and *BRCA1*$^{-/-}$ cells at PD 23. (**B**). Telomere length analysis by flow-FISH in human lymphoblastoid cell lines established from carriers of *BRCA1*$^{+/-}$ and *BRCA2*$^{+/-}$ mutations as well as in lymphoblastoid cell lines from normal individuals (NLB).

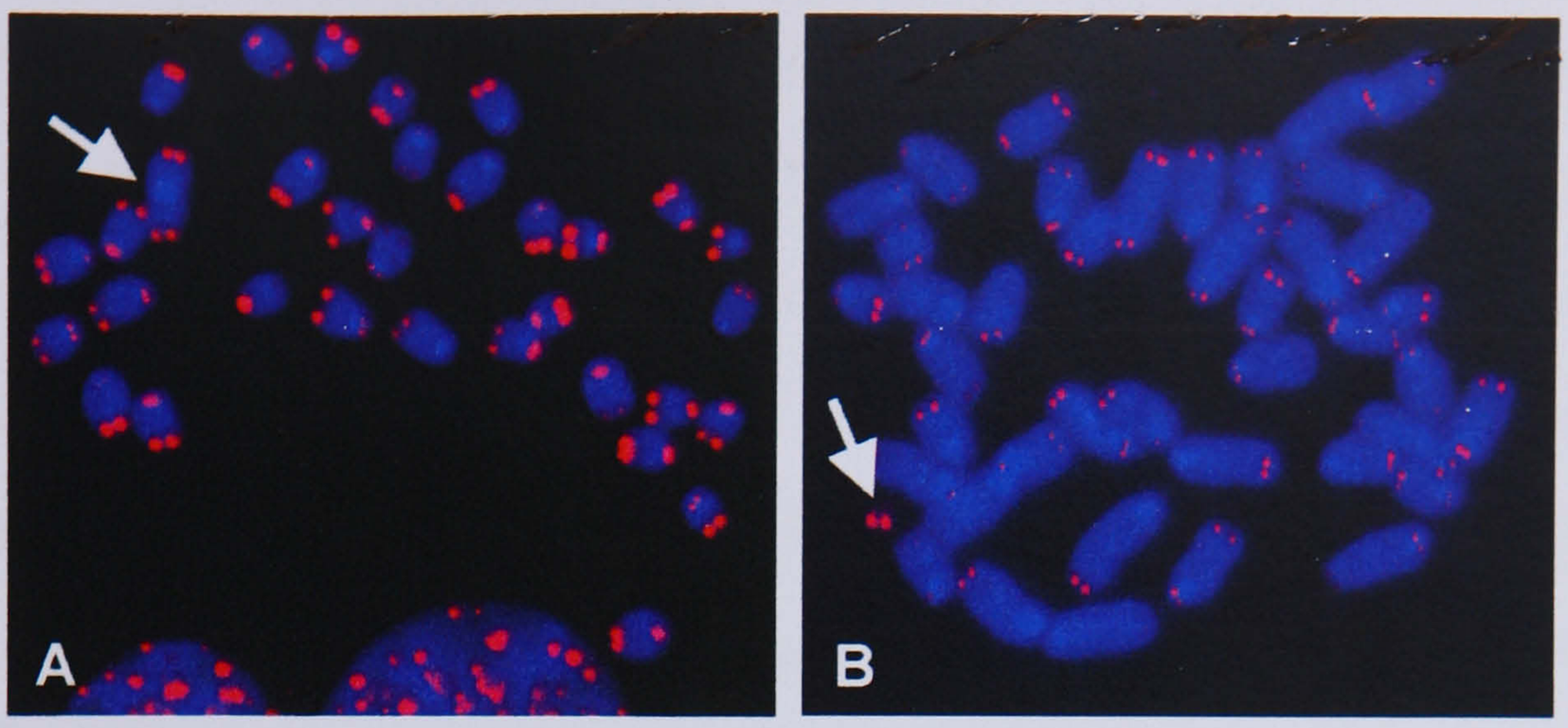

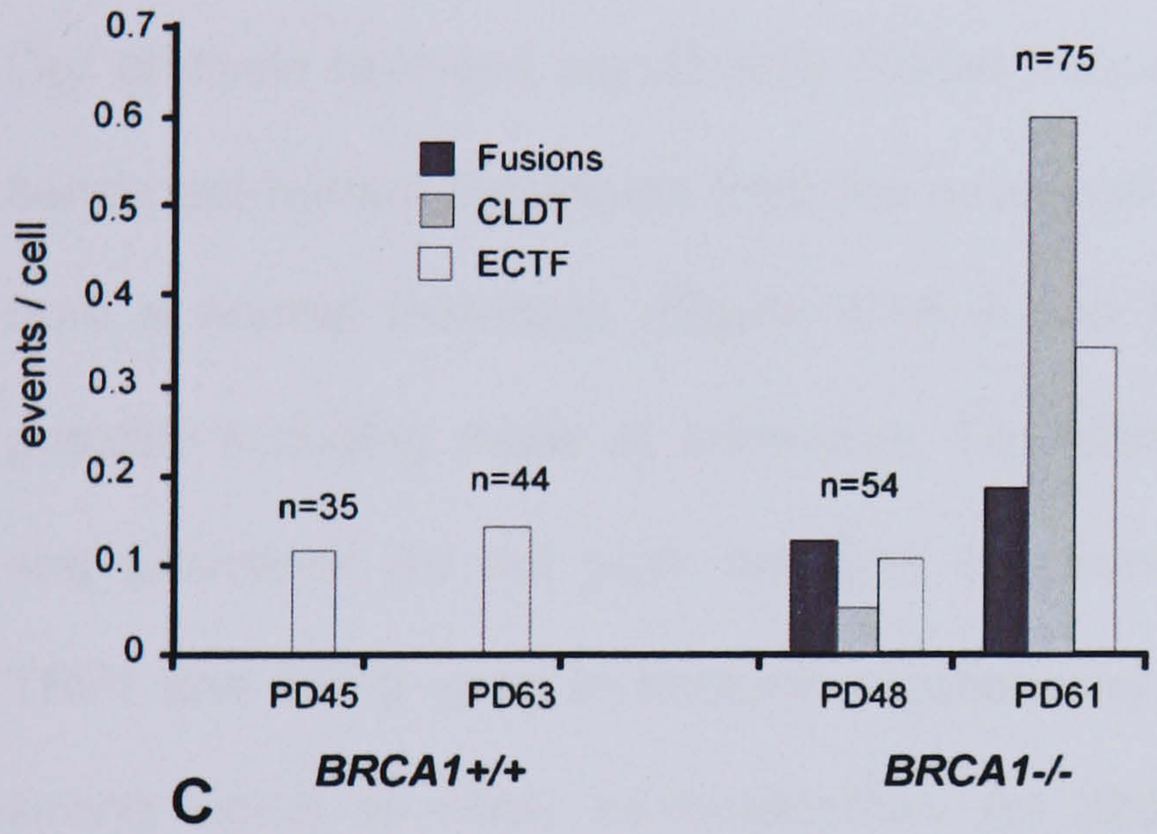

Figure 4.12 A mouse *BRCA1*$^{-/-}$ mitotic cell showing end-to-end chromosome fusion lacking telomeric signal at the fusion point (arrow) (**A**). A mouse *BRCA1*$^{-/-}$ cell showing extra-chromosomal telomeric fragments (arrow) (**B**). Frequencies of end-to-end chromosomal fusions, chromatids lacking detectable telomere (CLDT) and extra-chromosomal telomeric fragments (ECTF) in mouse *BRCA1*$^{+/+}$ and *BRCA1*$^{-/-}$ cells (**C**).

4.2.6 DNA damage foci

It has recently become possible to identify sites of DNA DSBs in mammalian cells by using antibodies against γ-H2AX. Unphosphorylated H2AX is interspersed in chromatin throughout the genome, and following DNA damage one of the earliest events is the phosphorylation of Ser139 of H2AX in large DNA domains encompassing a million base pairs. γ-H2AX forms discrete foci within 10 minutes of DNA DSBs induction with BRCA1 detectable in these foci (Fernandez-Capetillo et al., 2004). In

human senescent cells or cells with dysfunctional telomeres γ-H2AX co-localizes with telomeres suggesting that dysfunctional telomeres behave as DSBs (d'Adda di Fagagna et al., 2003; Takai et al., 2003). We have used an antibody against γ-H2AX in our panel of novel human fibroblast cell lines sensitive to IR and in mouse ES cells (Figure 4.13). Human fibroblasts used for this purpose were in similar passages i.e. PDs 20-30 (pre-senescent) and mouse ES cells were in matching passages. We detected up to 5 positive foci per cell in fibroblasts cultures (Figure 4.13 A) whereas mouse embryonic stem cells showed a much higher number of foci positive for γ-H2AX (Figure 4.13 B and 4.14 C) indicating that these cells were under physiological stress. Our analysis revealed significantly higher frequencies of γ-H2AX positive foci in pre-senescent human fibroblasts from the novel cell group in comparison with the cell line from a normal individual (Figure 4.14 A and B) indicating a higher level of DSBs possibly including those at telomeres. Our attempt to detect simultaneously γ-H2AX and telomeres did not work because commercially available antibodies specific for TRF1 and TRF2 used in immunocytochemistry experiments did not yield sufficiently strong signal to allow co-localization. An alternative for this is an immuno-FISH technique (immunocytochemistry combined with FISH). We have been able to use immuno-FISH only recently (for details see Chapter 5) but immuno-FISH analysis of human fibroblast was not sufficiently complete to be included in this thesis. High frequencies of γ-H2AX positive foci in both human radiosensitive fibroblast cell lines from the novel cell group and mouse *BRCA1* deficient cells indicate that the level of spontaneous DNA damage is higher in these cells than in normal control cells.

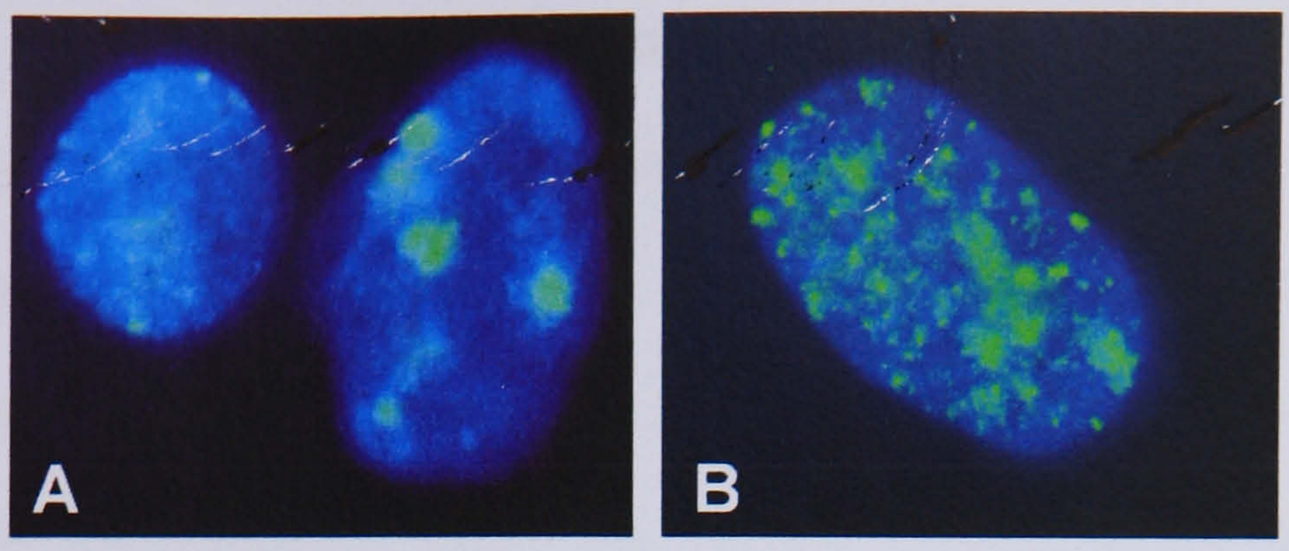

Figure 4.13 Representative examples of nuclei stained with γ-H2AX antibody (FITC) and counterstained with DAPI in a radiosensitive fibroblast cell line (**A**) and in a *BRCA1* deficient mouse embryonic stem cell (**B**). The type of intense nuclear staining with γ-H2AX antibody shown in panel B can rarely be found in radiosensitive fibroblasts.

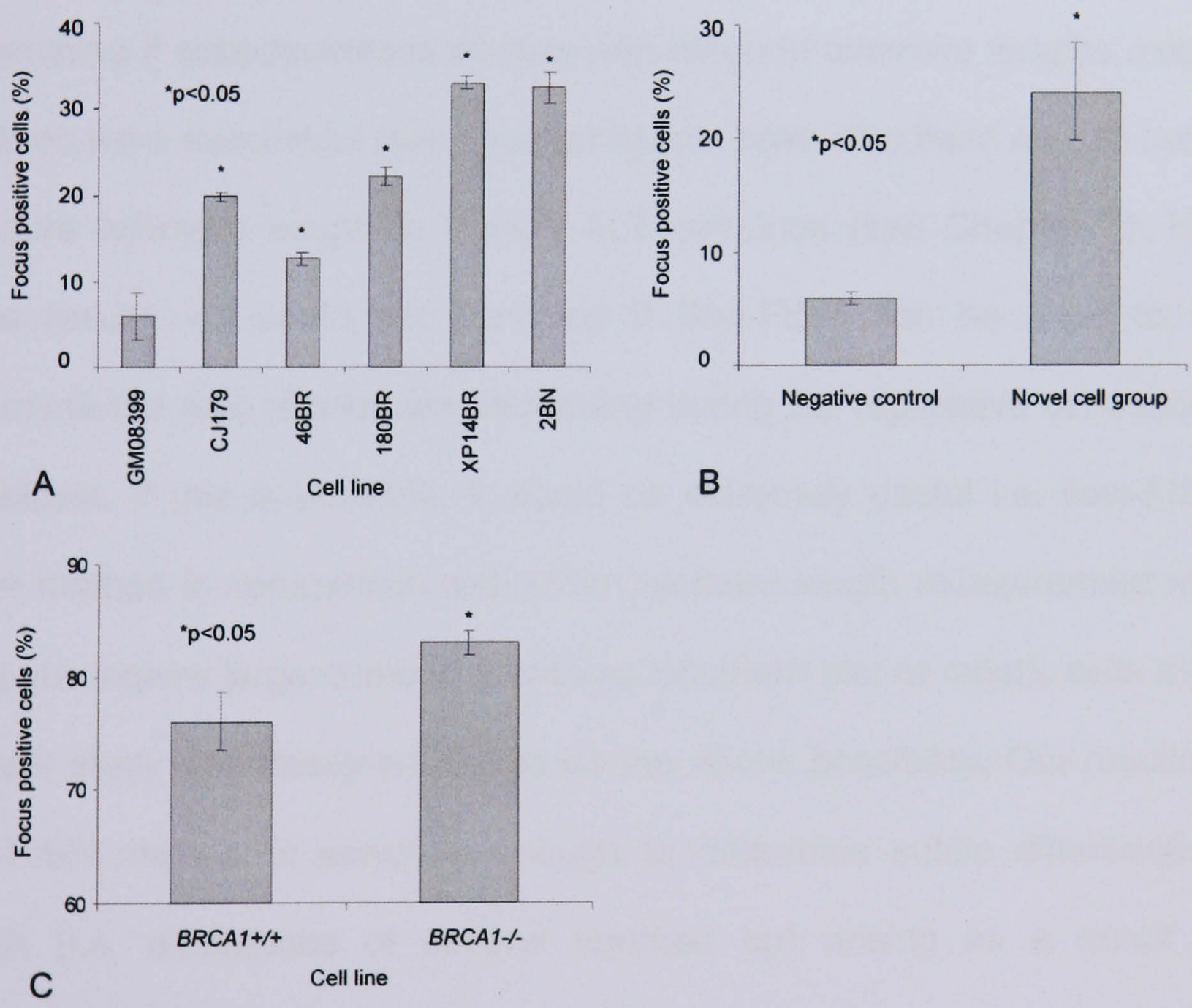

Figure 4.14 Percentages of radiosensitive fibroblasts positive for γ-H2AX staining (i.e. a cell with at least one focus was considered positive) (**A**) and statistical analysis (**B**). Percentages of γ-H2AX positive cells in mouse embryonic stem cells (**C**). (*p<0.5, t-test)

4.3 Discussion

4.3.1 Use of flow-FISH to measure telomere length in human fibroblasts

So far, flow-FISH has been used to measure telomere fluorescence intensity, which is proportional to telomere length, mainly in human peripheral blood lymphocytes (Martens et al., 2002; Brummendorf et al., 2002; Baerlocher and Lansdorp, 2003) or other cells of hematopoietic origin i.e. human lymphoblastoid cell lines or mouse lymphoma cell lines (Scheding et al., 2003; Van Ziffle et al., 2003; Rigolin et al., 2004; and see Chapter 3). Cells of hematopoietic origin are particularly suitable for flow-cytometry analysis because of their intrinsic properties including cell shape, natural separation from other cells and low auto-fluorescence values. Our preliminary attempts to measure telomere length in human fibroblast cell lines with the purpose of determining if subpopulations of cells with different telomere lengths exist within these cell lines were successful (see Chapter 3). We have also been able to use flow-FISH to measure telomere length in human ALT cell lines (see Chapter 3). However, from these results we could not conclude if flow-FISH can be used to, for example, determine the rate of telomere shortening during the replicative senescence of human fibroblasts. If this is possible, it would be extremely useful i.e. flow-FISH is a much faster method in comparison with other telomere length measurement methods and it does not require large number of cells as Southern blot or mitotic cells as Q-FISH. The present study was designed to test for the above possibility. Our results suggest that flow-FISH method is sensitive enough to determine subtle differences in telomere length (i.e. differences of several hundred bp) arising as a result of replicative senescence in human fibroblasts. Moreover, our results suggest that flow-FISH can detect biologically relevant differences in the rates of telomere shortening between different fibroblast cell lines. For example, we observed accelerated telomere shortening in AT, NBS and FA cell lines in comparison with normal cell lines by flow-FISH. This is in line with published results (Metcalfe et al., 1996; Smilenov et al., 1997; Hande et al., 2001; Ranganathan et al., 2001; Tchirkov and Lansdorp, 2003) and we

have also confirmed this using Southern blot analysis. Furthermore, similar results were obtained with Southern blot and flow-FISH in the novel cell group in which telomere length was not measured before.

However, direct comparison between flow-FISH and Southern blot results revealed a relatively low correlation between these two techniques. We have already provided arguments for the possibility that these two techniques may differ in the sense, which DNA sequences are measured (i.e. discrepancy between telomeric and sub-telomeric sequences in the case of Southern blot) or which cells are taken into account for measurements (specific exclusion of some cells in flow-FISH) (see above). However, we cannot rule out the possibility that our method for telomere length measurement by flow-FISH in human fibroblast requires further optimisation to improve its correlation with Southern blot. Usually, a good correlation exists between Southern blot and flow-FISH when using human lymphocytes (Rufer et al., 1998). Similarly we obtained a good correlation between telomere length measurement by Southern blot and flow-FISH in a group of six human lymphoblastoid cell lines (see Chapter 3). One way to further optimise our method would be to treat fibroblasts with detergents, which will specifically remove the cytoplasm. Auto-fluorescence seems to be generated by the fibroblast cytoplasm to a larger degree than by the nucleus and stripping the cytoplasm from the cell could eliminate the problem of auto-fluorescence mentioned above (see Figure 4.1). We believe that further optimisation steps will improve the resolution of flow-FISH and make it suitable for telomere analysis in all cell types.

4.3.2 Accelerated telomere shortening in radiosensitive cell lines

We have shown previously, using peripheral blood lymphocytes from a group of 29 breast cancer patients, that there is a correlation between chromosomal radiosensitivity and short telomeres (McIlrath et al., 2001). This observation was recently confirmed by an American study in which lymphocytes from a much larger group of head & neck, lung, bladder and kidney cancer patients and equal number of

healthy individuals were used (Wu et al., 2003). This study revealed a significant negative correlation between telomere maintenance and radiosensitivity i.e. the shorter the telomeres the higher the radiosensitivity. In line with these results it was demonstrated that senescent human fibroblasts with short telomeres are significantly more radiosensitive than the same fibroblast with long telomeres (Rubio et al., 2002).

Taken together above results argue that the mechanisms conferring sensitivity to IR may be linked with telomere maintenance mechanisms and this prompted us to investigate telomere length in cell lines known to be sensitive to IR. Our telomere length analysis by flow-FISH and Southern hybridisation demonstrated that radiosensitive cells generally show higher rates of telomere shortening than cell lines from apparently normal individuals. Our measurements are in agreement with previously published studies, which revealed accelerated rates of telomere shortening in AT, NBS and FA patients (Metcalfe et al., 1996; Ranganathan et al., 2001; Adelfalk et al., 2001). Furthermore, our results indicate accelerated telomere shortening in cells defective in ligase I, ligase IV, Artemis and two more defects that have not been examined before. We have also examined telomere shortening rates in mouse ES cells deficient in *BRCA1* by flow-FISH and found that although telomeres were, on average, initially longer in *BRCA1*$^{-/-}$ cells, they degraded more rapidly than telomeres in *BRCA1*$^{+/+}$ cells (Figure 4.11). We found approximately a two-fold difference in the rate of telomere shortening between radiosensitive mouse *BRCA1* deficient cells and matching control cells.

In all cases accelerated telomere shortening was accompanied by signs of telomere dysfunction including anaphase bridges (human fibroblasts), end-to-end chromosome fusions (mouse ES cells), increased incidence of chromatids lacking telomeric signals and increased incidence of split telomeric signal (human fibroblasts) or extra-telomeric signal (mouse ES cells). We believe that the split telomeric signal may reflect detachment of a broken telomeric fragment from a chromosome. This possibility is supported by several lines of evidence. First, in all cases we observed an

actual physical separation of two telomeric signals on a single chromatid leading to at least 5 telomeric signals/chromosome instead of expected 4 (see Figure 4.10 A). This suggests that a DSB occurred within the telomeric sequence. In line with this possibility the size of two split signals on a single chromatid was usually equivalent to the size of a single signal at its sister chromatid (see Figure 4.10 A). Sister chromatids are exact replicas of each other and they should have the telomeres of exactly the same size. Secondly, the fact that we observed increased incidence of split telomeric signal in cells with increased incidence of γ-H2AX stained foci (marker of DSBs) (Figure 4.14 A) suggests that some DSBs detected by γ-H2AX staining may occur at telomeres. This possibility can be tested by measuring co-localization of γ-H2AX with telomeres and these experiments will be carried out in the near future in our laboratory. Thirdly, split telomeric signals could be cytological manifestation of a recently discovered mechanism of extra-chromosomal telomeric circle formation (Cesare and Griffith, 2004; Wang et al., 2004). Since the incidence of split telomeric signal is significantly elevated in cells with accelerated telomere shortening it is possible that split telomeric signals could contribute to telomere shortening i.e. a detached signal will be lost in the next cell division.

The mechanisms that cause accelerated telomere shortening in radiosensitive cell lines are not known and further research is required to identify these mechanisms. The range of cell lines in our panel and the inclusion of defects in proteins that are not known to be located at telomeres (e.g. Artemis, DNA ligase IV), suggests that telomere shortening may be a consequence of defective DNA repair rather than a dual function of all the defective proteins. However, other mechanisms not directly related to DNA repair defects could also operate. The reduction of telomere length could be a consequence of breakage near or within the telomeres where the chromosome end associations are not resolved while chromosomes move in opposite directions. Extra-chromosomal telomeric DNA was indeed detected in fibroblasts from AT patients and

may represent fragmented telomeres or by-products of defective replication of telomeric DNA (Hande et al., 2001). As indicated above it was recently demonstrated that t-loop deletion by homologous recombination might contribute to extra-chromosomal telomeric fragments (Wang et al., 2004). These fragments were also observed in human ALT cell lines GM847 and WI-38 VA13 (Cesare and Griffith, 2004). We were able to detect higher incidence of extra-chromosomal telomeric fragments in late passage *BRCA1* deficient mouse cells in comparison with control cells (see above). These extra chromosomal telomeric fragments in mouse cells had a form of double minute chromosomes and were similar to those recently reported in cells from *ERCC1/XPF* deficient mice (Zhu et al., 2003). This suggests that *BRCA1* might play a similar role at telomeres as ERCC1/XPF in repressing the formation of extra chromosomal telomeric fragments.

Another phenomenon that could be responsible for the accelerated telomere shortening in radiosensitive cells is oxidative stress. Since telomeres are highly sensitive to oxidative stress (von Zglinicki, 2002) it is possible that accelerated telomere shortening observed here could be caused by abnormalities in oxidative metabolism in the above cell lines i.e. a large proportion of IR induced damage arises via oxidative damage. The primary cause of accelerated telomere shortening in *ATM* deficient cells is oxidative stress (Tchirkov and Lansdorp, 2003).

At the end we would like to mention a discrepancy between our results for the *ligase IV* deficient cell line 180BR and earlier results. d'Adda di Fagagna et al. (2001) found no difference in telomere length between this cell line and an age matched control cell line but no rate of telomere shortening for this cell line was determined. This result was interpreted to mean that ligase IV defect does not affect telomere length. However, our results revealed accelerated telomere shortening *in vitro* in this cell line (Figures 4.2 C and 4.4 C). To exclude the possibility that our results are due to artefacts we have recently obtained a cell line from another *ligase IV*$^{-/-}$ patient (411BR) and compared the rate of telomere shortening in this cell line with that of a cell line

established from a heterozygous parent of the 411BR patient. We have been able to show accelerated telomere shortening in 411BR cells in comparison with its heterozygotic counterparts (Slijepcevic, unpublished results).

In conclusion, our findings suggest that multiple genetic defects that confer radiosensitivity and /or genomic instability also confer telomere shortening. It is worth noting that the converse is not necessarily true, e.g. telomerase deficient mice show an increase in genomic instability at later generations but not at early generations although their rate of telomere shortening is essentially the same (Goytisolo et al., 2000).

4.4 Summary

Telomere maintenance was examined in 9 primary fibroblast cell lines with different genetic defects that confer sensitivity to IR. These included cell lines derived from patients with ataxia telangiectasia, Nijmegen breakage syndrome, Fanconi anemia, defective Artemis, DNA ligase I and DNA ligase IV, an immunodeficient patient with a defect in DNA double strand break repair and a patient diagnosed with xeroderma pigmentosum who, in addition, showed severe clinical sensitivity to ionising radiation. The results from this study, based on flow-FISH and Southern hybridisation measurements, revealed an accelerated rate of telomere shortening in most cell lines derived from the above patients in comparison with cell lines from normal individuals. This accelerated telomere shortening was accompanied by the formation of chromatin bridges in anaphase cells, indicative of the early loss of telomere capping function. Telomere maintenance was also analysed in mouse embryonic stem cells deficient in *BRCA1*, another defect conferring radiosensitivity. Similarly, these cells showed accelerated telomere shortening and mild telomere dysfunction in comparison to control cells. These results suggest that mechanisms that confer sensitivity to IR may be linked with mechanisms that cause telomere dysfunction.

CHAPTER 5

ASSESSMENTS OF BRCA1 ROLE IN TELOMERE MAINTENANCE IN MAMMARY EPITHELIAL CELLS AND TELOMERE FUNCTION IN ALT CELLS

5.1 Introduction

Results presented in the previous chapter indicate that *BRCA1* deficient cells may have a telomere dysfunction phenotype. *BRCA1* deficiency is known to induce genomic instability and sensitivity to ionising radiation (IR) (Abbott et al., 1999; Foray et al., 1999). Similarly, a number of defects that confer sensitivity to IR appear to be associated with accelerated telomere shortening (see previous chapter). These results together with a number of published studies (Metcalfe et al., 1996; Pandita and Dhar, 2000; Adelfalk et al., 2001; Hande et al., 2001; Ranganathan et al., 2001; Tchirkov and Lansdorp, 2003) argue that defective DNA damage responses are frequently accompanied by some form of telomere dysfunction. In this chapter we will explore further a potential involvement of *BRCA1* in telomere maintenance and also examine the status of telomere function in ALT positive cell lines.

When telomeres become dysfunctional, either through the loss of telomeric sequences due to cell senescence or inactivation of key telomere binding proteins, this induces cellular DNA damage response similar to that activated after induction of DNA double strand breaks (DSBs) (d'Adda di Fagagna et al., 2003; Takai et al., 2003). It has been known for several years that key proteins involved in DSB repair e.g. Ku70/Ku86 and DNA-PKcs are involved in telomere maintenance (Bailey et al., 1999; Samper et al., 2000; Goytisolo et al., 2001; Bailey et al., 2004). For example, the absence of Ku70 or Ku86 promotes chromosome end-to-end fusion as a mechanism to repair dysfunctional telomeres. In the absence of chromosome fusions, dysfunctional telomeres may be recognised as DSBs (Espejel et al., 2002).

Several examples of genetic mutations that cause chromosome instability and telomere dysfunction, not necessarily through defective DSB repair, have been documented. For example, chromosome instability and telomere dysfunction can be induced by mutations in specific genes that cause cancer-predisposition syndromes, including Fanconi anemia (FA), Nijmegen breakage syndrome (NBS) and ataxia telangiectasia (AT) (Metcalfe et al., 1996; Pandita and Dhar, 2000; Adelfalk et al., 2001; Hande et al., 2001; Ranganathan et al., 2001; Tchirkov and Lansdorp, 2003). Our results point to the possibility that *BRCA1* deficiency may cause accelerated telomere shortening and also telomere dysfunction (see Chapter 4). This opens an interesting possibility that two tumour suppressor mechanisms (i.e. *BRCA1* is a tumour suppressor gene and functional telomeres constitute a powerful tumour suppressor mechanism) could actually converge to accelerate appearance of a malignant phenotype.

BRCA1$^{-/-}$ cells are hypersensitive to IR (Shen et al., 1998; Foray et al., 1999) suggesting its role in DNA repair. Indeed, cells lacking *BRCA1* are particularly deficient in transcription-coupled repair whereby DNA repair is linked to the transcriptional machinery such that the transcribed strand is preferentially repaired. Cells lacking

BRCA1 are also deficient in homology-directed DNA repair, which uses the homologous sister chromatid as the repair template (Gowen et al., 1998; Abbott et al.. 1999). The role of *BRCA1* in DNA damage repair is further suggested by its association with other proteins involved in DNA repair including ATM, 53BP1, MDC1, RAD51, and the MRE11-RAD50-NBS1 (MRN) complex (reviewed in Deng and Brodie, 2000; Deng and Wang, 2003). In ALT (alternative lengthening of telomeres) cells, the MRN complex is localised with APB (ALT associated PML) bodies during late S-G_2 phase, suggesting its involvement in telomere length maintenance (Grobelny et al., 2000; Wu et al., 2000). Given that the MRN complex is known to associate with BRCA1 and with telomeres and telomere binding proteins, Herbert et al. (2001) suggested that BRCA1 might also play a role in telomere structure and function. Indeed, BRCA1 has been found to associate with APB bodies in tumour cells, which maintain telomeres by the ALT pathway (Wu et al., 2003), and thus with telomeres. APBs are nuclear subdomains that recruit and locally accumulate a large number of proteins, many of which are key regulators of various processes. They contain PML, telomeric DNA, and the telomere-binding proteins TRF1 and TRF2. NBS1 foci co-localise with the APBs during late S to G_2 phase in ALT cells (Wu et al., 2000). PML bodies themselves recruit a variety of other proteins, including Sp100, SUMO-1, Daxx, pRB, p53, and BLM, suggesting roles in DNA replication and repair, cell cycle control, RNA transport and apoptosis (Seeler and Dejean, 1999; Ruggero et al., 2000). The fact that BRCA1 participates in the ALT pathway is consistent with its role in homology-directed DNA repair.

The recruitment of the DNA damage signalling and repair proteins to sites of genomic damage constitutes a primary event triggered by DNA damage. The association of BRCA1 with the MRN complex is critical for this DNA damage response (Wu et al., 2003). Many components of the DNA damage response, including BRCA1, RAD51, and the MRN complex form foci that co-localise with phosphorylated histone H2AX (γ-H2AX) (Paull et al., 2000). These nuclear domains are thought to contain

hundreds to thousands of molecules that accumulate in the vicinity of a DSB. The formation of γ-H2AX foci is a very early event after induction of DSBs and has been proposed to function in recruiting downstream DNA repair factors, including BRCA1, to DNA damage sites (Paull et al., 2000). BRCA1 is thus an early migrant to sites of H2AX phosphorylation (Paull et al., 2000), consistent with a role in the events that follow at the site of breakage. BRCA1 and γ-H2AX detect double strand breaks (Paull et al., 2000; Celeste et al., 2003) and this may thus include breaks at telomeres.

The present study was undertaken to determine the significance of BRCA1 in telomere maintenance in mammary epithelial cells using RNAi and immunocytochemistry. We have also applied immunocytochemistry methods to assess telomere function and BRCA1 co-localisation with DNA damage foci in ALT positive cells.

5.2 Results

5.2.1 Assessment of BRCA1 role in telomere maintenance using mammary epithelial cells

5.2.1.1 siRNA depletion of BRCA1 in mammary epithelial cells

To assess whether BRCA1 plays a role in telomere maintenance we used a siRNA approach. The ability of a siRNA oligonucleotide specific for *BRCA1* (see Materials and Methods) to knockdown BRCA1 protein expression was tested in the breast epithelial cell line MCF10A and breast carcinoma cell line MCF7. MCF10A cells express lower levels of BRCA1 mRNA in comparison with MCF7 cells (Gudas et al., 1996; Blagosklonny et al., 1999). We also planned to include in this analysis the Bre-80 cell line, which is a normal breast epithelial cell line immortalized by ectopic expression of hTERT (Huschtscha et al., 1998). However, this cell line showed a high percentage of anaphase bridges, slow growth and expression of truncated BRCA1 (deletion of exon 11) as revealed by Western blotting (not shown) and therefore was excluded from the analysis.

BRCA1 is a molecule located in nuclear foci of all cell types, as was confirmed by Wilson et al. (1999), and despite the cell cycle dependence of BRCA1 mRNA expression, BRCA1 protein level does not change during the cell cycle (Aprelikova et al., 1996). Following a single transfection with siRNA-BRCA1 (for details of sequence see Material and Methods), BRCA1 protein levels, as assessed by immunocytochemistry (Figure 5.1 A), had fallen dramatically (up to 70%) by 24 h after transfection in MCF10A cells and remained at this level in most cells for at least further 4 days (Figure 5.1 B). From day 6 onwards, a slow and non-uniform return to levels of expression before transfection with siRNA oligonucleotides was observed (Figure 5.1 B). This time course is consistent with published reports for knock down of the *BRCA1* gene (Bruun et al., 2003; Xiong et al., 2003). Inhibition of BRCA1 expression in MCF7 cells was less efficient than in MCF10A cells but nevertheless we observed a significant reduction in frequencies of nuclei stained with BRCA1 antibodies in comparison with control cells (Figure 5.1 C). There are two possible explanations for this. MCF7 cells show an unusual growth pattern with cells growing in two layers and this could affect efficiency of transfection. Alternatively, MCF7 cells express constitutively higher levels of BRCA1 levels compared with MCF10A cells (Blagosklonny et al., 1999) and this could be responsible for the observed difference.

The mRNA expression of BRCA1 was also evaluated by semi-quantitative RT-PCR assays (Figure 5.2). A profile of temporary decrease in BRCA1 expression similar to that observed by immunofluorescence analysis was seen in MCF10A (Figure 5.2 A and B) and to a lesser extent in MCF7 cells (Figure 5.2 C and D). Although an earlier study indicated that MCF7 cells express a higher amount of BRCA1 mRNA than MCF10A cells (Blagosklonny et al., 1999) we could not see differences in BRCA1 mRNA expression levels between the two cell lines. The RT-PCR results were corroborated by Western blot analyses, which clearly indicated reduced levels of BRCA1 expression following transfection with siRNA (Figures 5.3 and 5.4).

Interestingly, it was revealed in a previous study that an exogenous BRCA1 gene strongly inhibited telomerase enzyme activity in human prostate and breast cancer cell lines (Xiong et al., 2003). It was also shown in co-transfection experiments that a wtBRCA1 plasmid inhibited hTERT gene expression in human ovarian cancer (Zhou and Liu, 2003). Therefore, we decided to analyse hTERT expression in both MCF cell lines during BRCA1 depletion. However, no increase of hTERT gene by RT-PCR (Figure 5.2) and protein expression by Western blotting (Figures 5.3 and 5.4) was observed in either MCF cell lines.

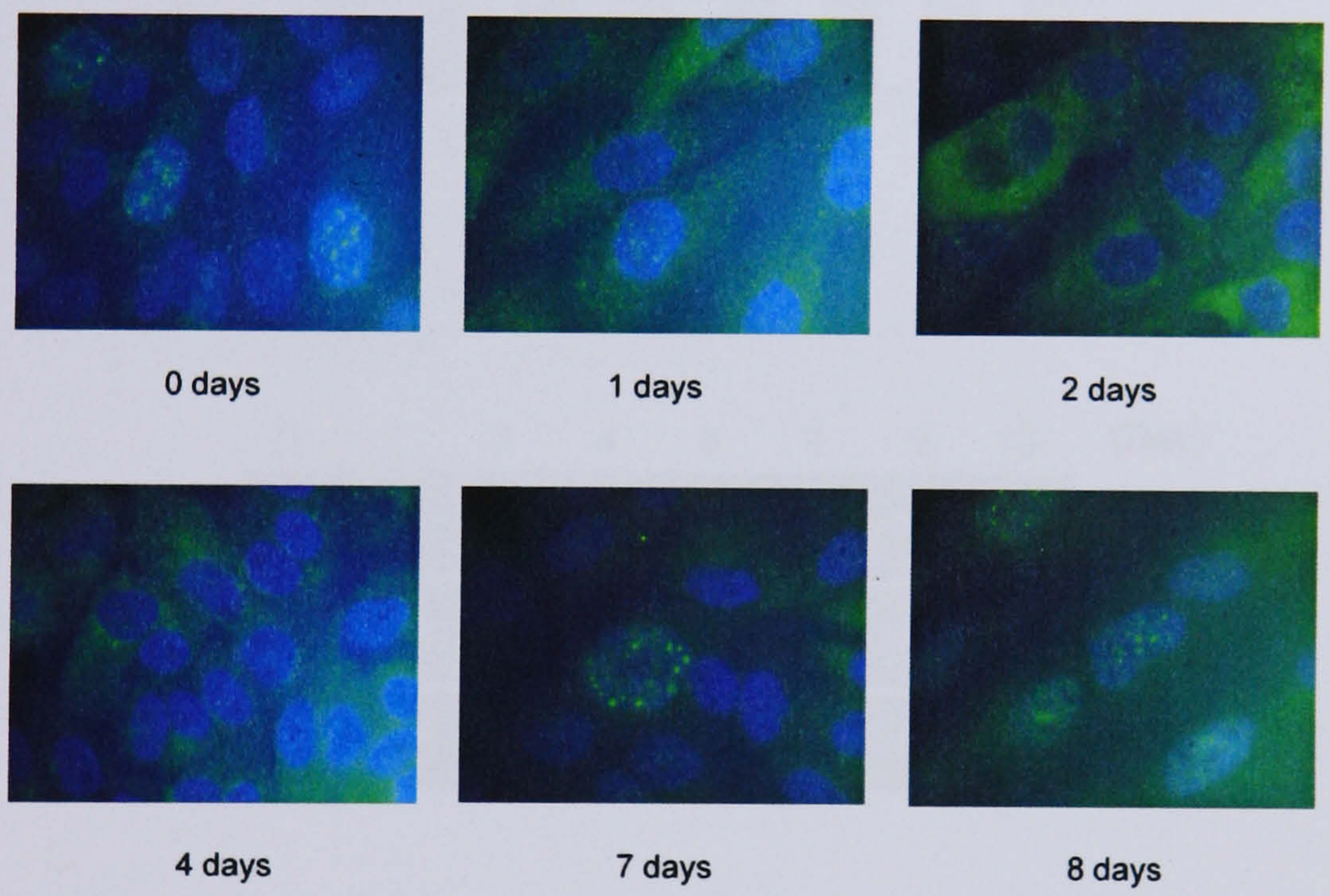

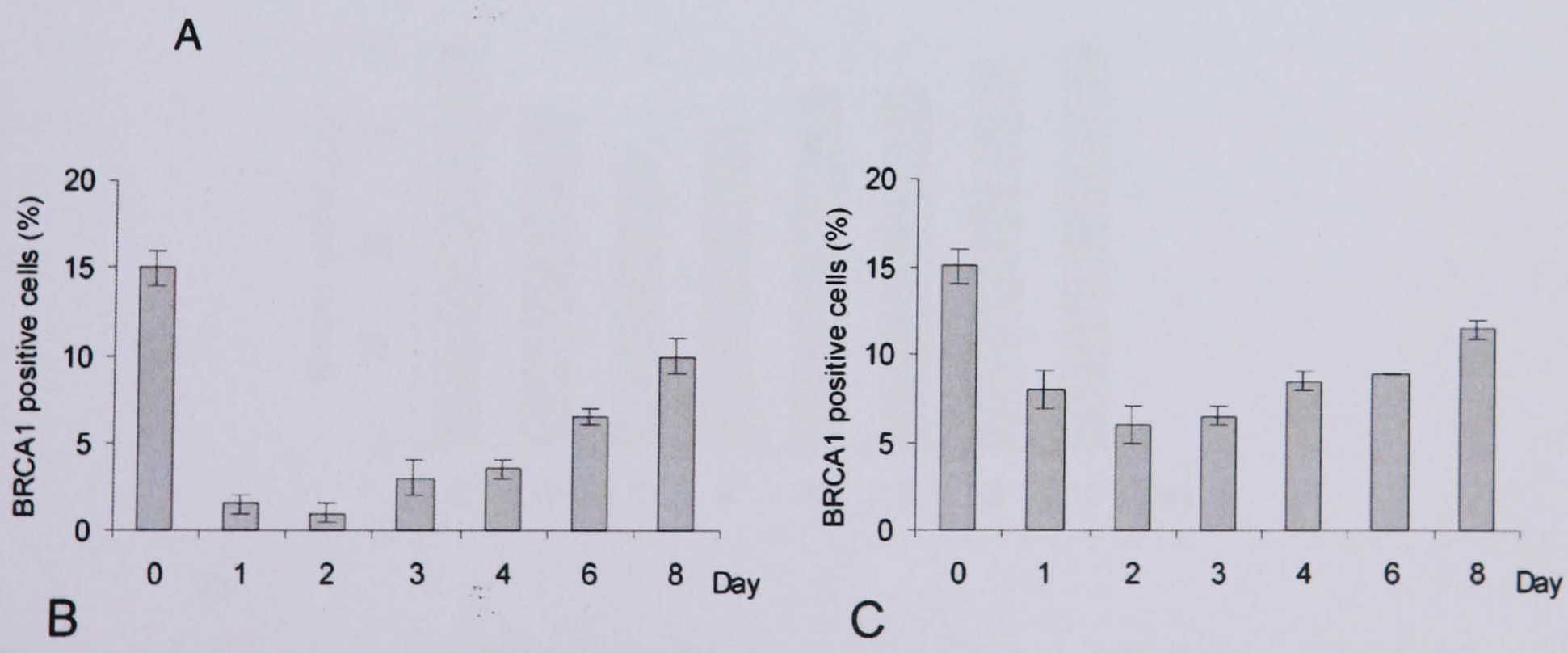

Figure 5.1 Immunofluorescence detection of BRCA1 in MCF10A cell cultures before and after BRCA1-siRNA transfection (**A**). Histograms showing frequencies of BRCA1 positive cells (100 cells counted) during BRCA1 depletion by siRNAs in MCF10A cells (**B**) and in MCF7 cells (**C**).

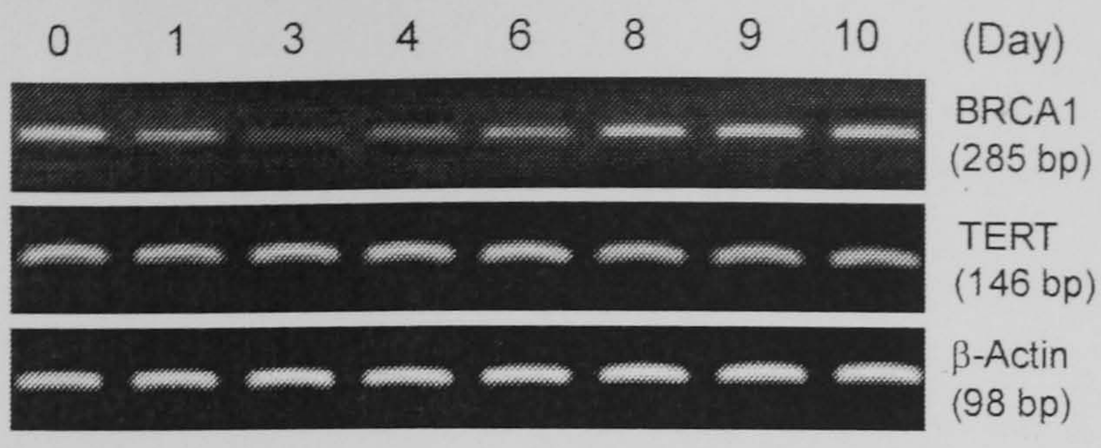

A

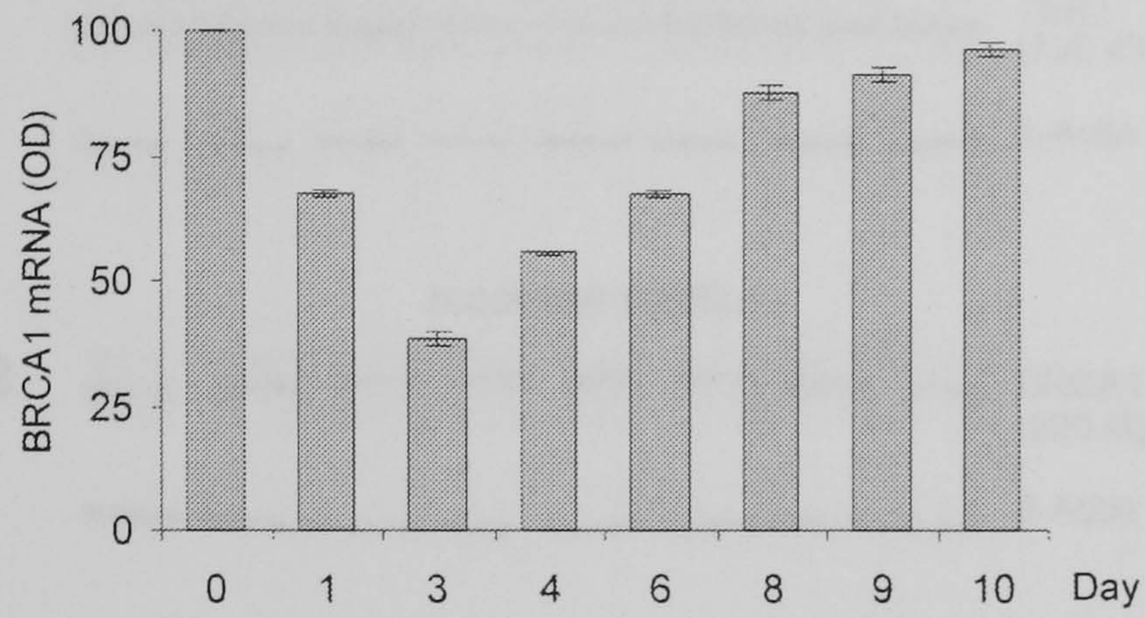

B

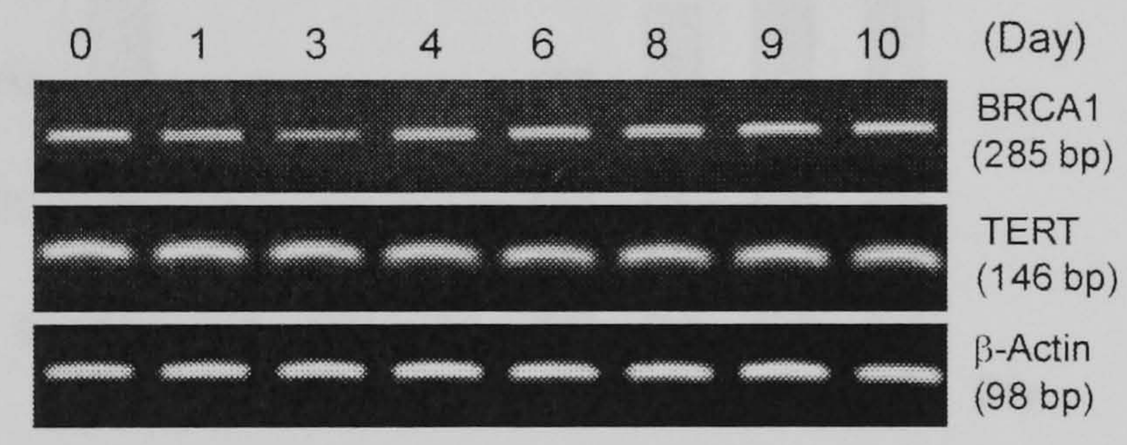

C

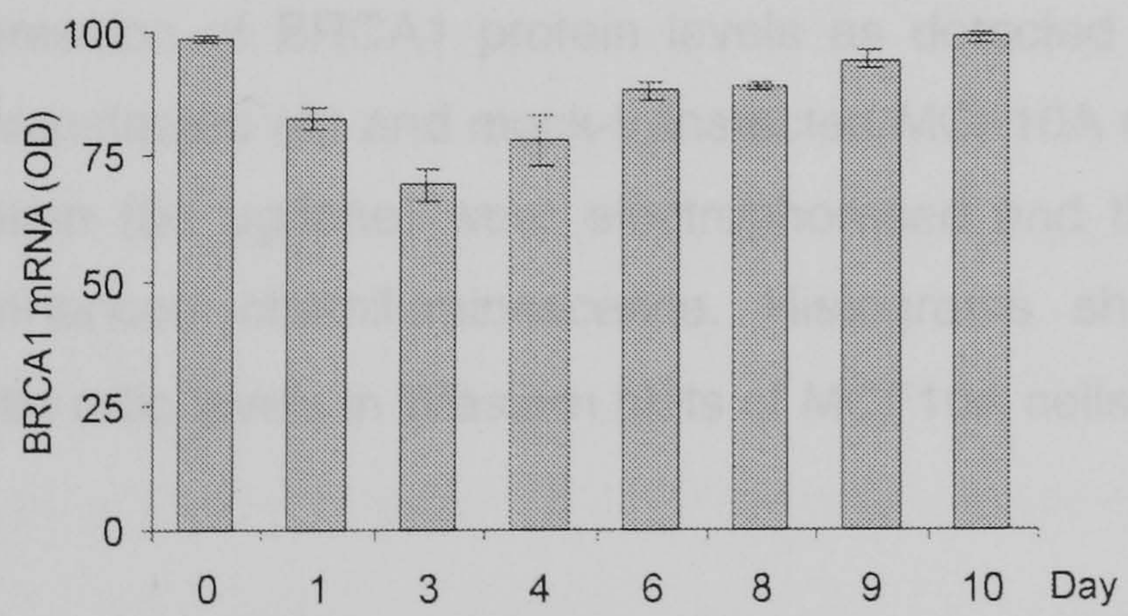

D

Figure 5.2 Expression of BRCA1 mRNAs as detected by RT-PCR in MCF10A cells (**A**) and in MCF7 cells (**C**). Subconfluent proliferating cultures were harvested for RNA isolation and semi-quantitative RT-PCR assays using primer sets shown in Table 2.4. Each amplified cDNA band was quantified by densitometry and expressed relative to β-actin as a control in MCF10A (**B**) and MCF7 cells (**D**)

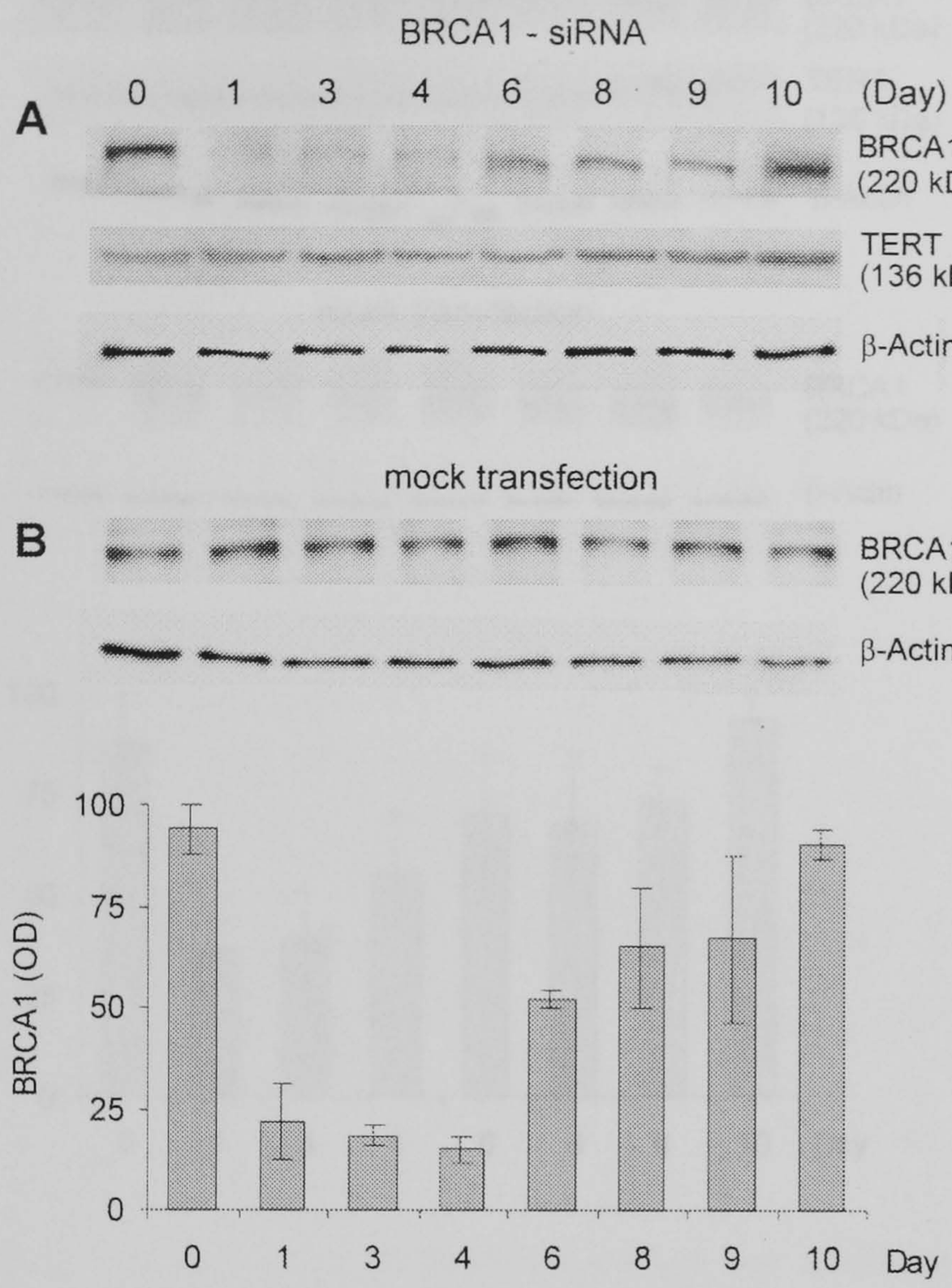

Figure 5.3 Expression of BRCA1 protein levels as detected by Western blotting in BRCA1-siRNA transfected (**A**) and mock-transfected MCF10A cells (**B**). Equal aliquots of total cell protein (50 µg/lane) were electrophoresed and the protein bands were detected by enhanced chemiluminescence. Histograms showing BRCA1 protein expression/β-actin ratio levels in Western blots of MCF10A cells (**C**).

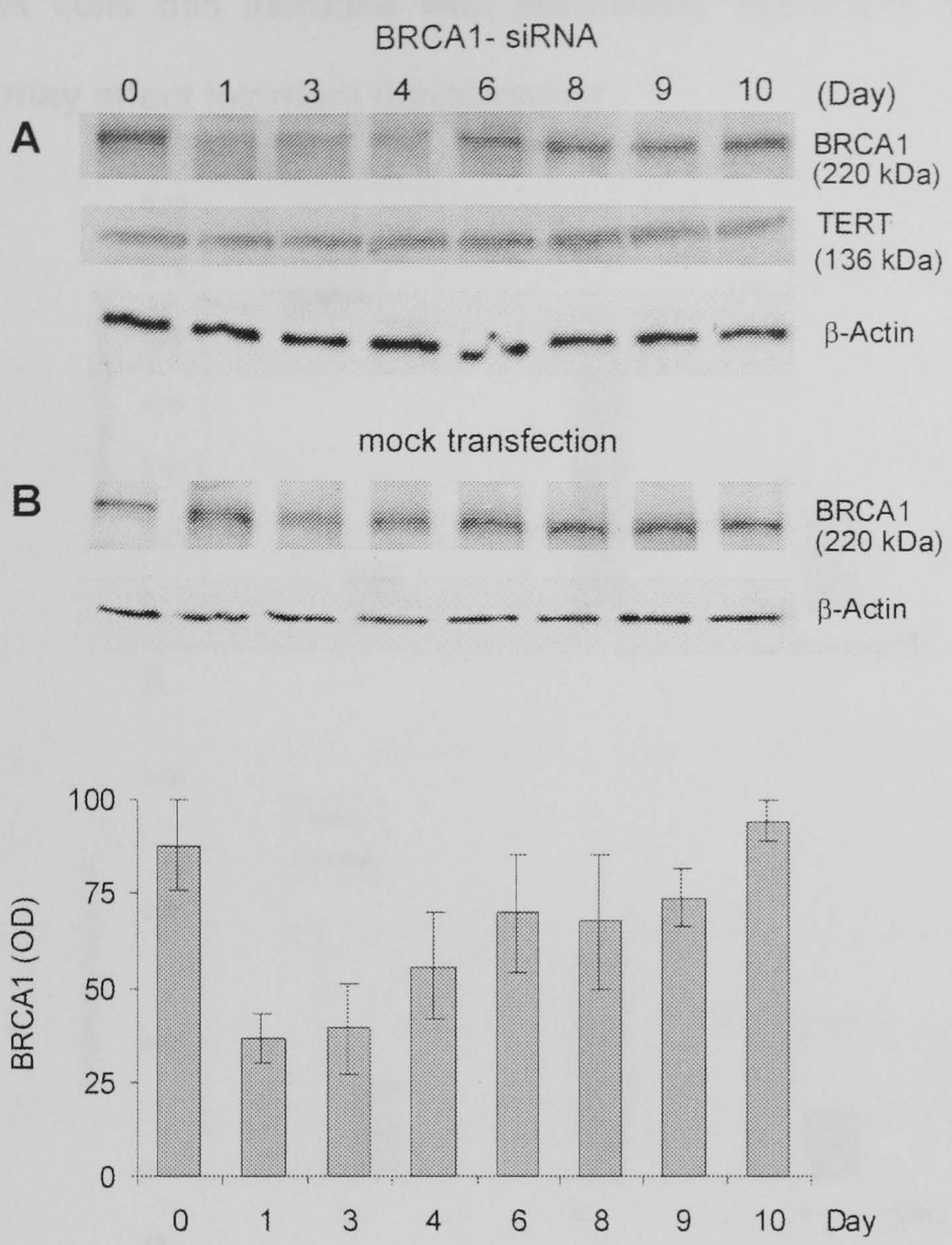

Figure 5.4 Expression of BRCA1 protein levels as detected by Western blotting in BRCA1-siRNA transfected (**A**) and mock-transfected MCF7 cells (**B**). Equal aliquots of total cell protein (50 µg/lane) were electrophoresed and the protein bands were detected by enhanced chemiluminescence. Histograms showing BRCA1 protein expression/β-actin ratio levels in Western blots of MCF7 cells (**C**).

5.2.1.2 The effect of BRCA1 depletion on telomere maintenance

To assess the effect of BRCA1 depletion on telomere maintenance, we analysed telomere function in MCF10A and MCF7 cells by scoring chromatin bridges in anaphase cells. The presence of anaphase bridges in cells is usually a sign of telomere dysfunction (see Chapter 4). The overall levels of anaphase bridge frequencies were low in both cell lines but nevertheless a slight increase was detected during partial

depletion of BRCA1 in comparison with mock-transfected cells (Figure 5.5). In the case of MCF10A cells this increase was statistically significant suggesting that BRCA1 deficiency may affect telomere maintenance.

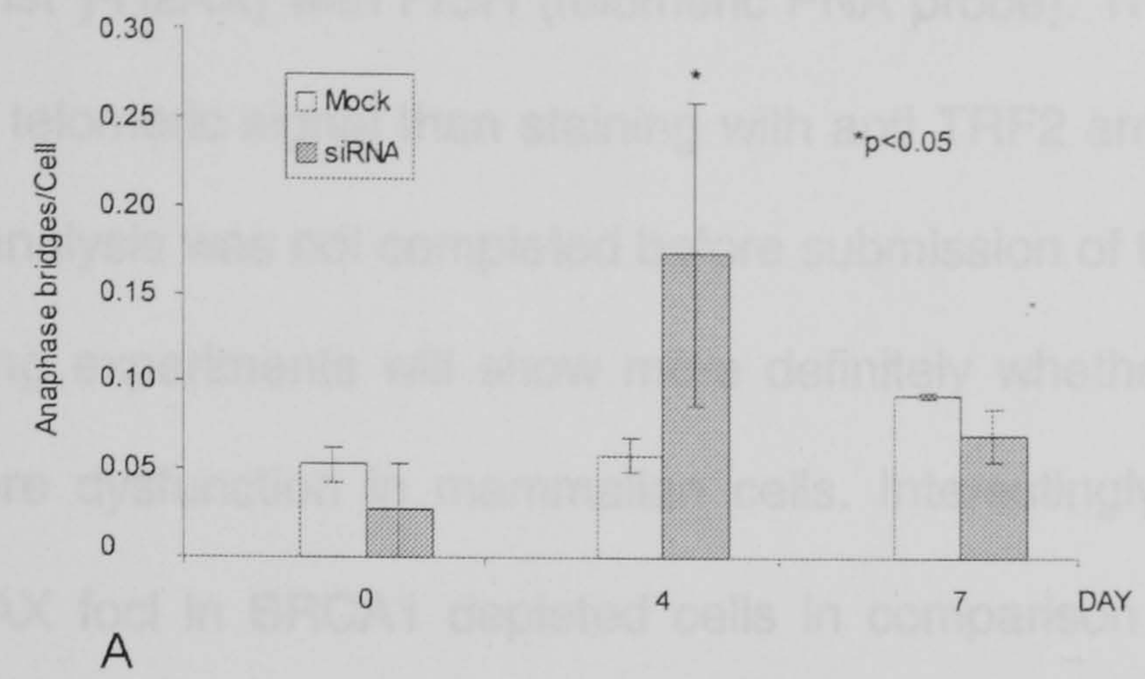

A

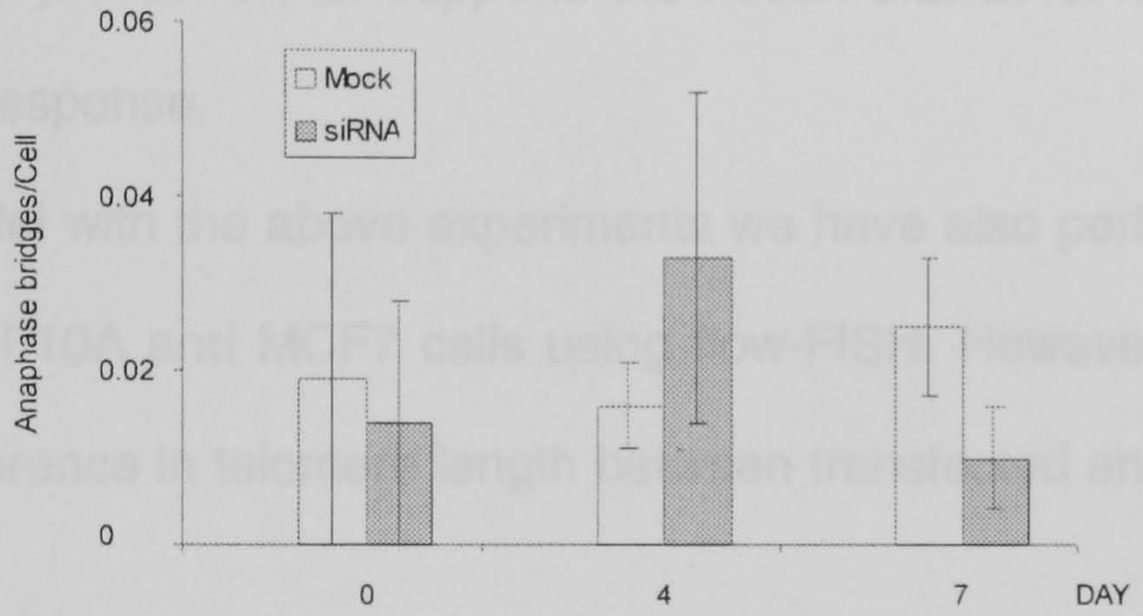

B

Figure 5.5 Effect of transient BRCA1 depletion on anaphase bridge formation in MCF10A (**A**) and MCF7 cells (**B**). (*p<0.05, t-test)

To test this possibility more stringently we performed experiments to detect the DNA damage sensor, γ-H2AX, at telomeres in MCF10A and MCF7 cells. The presence of γ-H2AX at telomeres is consistent with telomere dysfunction. We started this analysis by combining antibodies against γ-H2AX with antibodies against either TRF1 or TRF2. The antibody specific for TRF1 (C-19, Santa Cruz, USA) did not generate any signal. An antibody specific for TRF2 (N-20, Santa Cruz, USA) produced some signal but this was not sufficient to identify efficiently co-localisation of γ-H2AX with telomeres. Telomere length measurements revealed extremely short telomeres in both cell lines (see below) a possibility consistent with weak TRF2 signals due to short telomeres. We

then performed FISH analysis of telomeres in interphase MCF10A and MCF7 cells and found that these are clearly visible under the fluorescence microscope (Figure 5.6). Therefore, we applied immuno-FISH, a technique combining immunofluorescence (antibody against γ-H2AX) with FISH (telomeric PNA probe). This approach generated much stronger telomeric signal than staining with anti TRF2 antibodies (Figure 5.6 A). However, the analysis was not completed before submission of this thesis and we hope that our ongoing experiments will show more definitely whether depletion of BRCA1 causes telomere dysfunction in mammalian cells. Interestingly, we observed higher levels of γ-H2AX foci in BRCA1 depleted cells in comparison with mock-transfected cells (Figure 5.7). This further supports the notion that BRCA1 is involved in cellular DNA damage response.

In parallel with the above experiments we have also performed telomere length analysis in MCF10A and MCF7 cells using flow-FISH. However, this analysis did not reveal any difference in telomere length between transfected and non-transfected cells (Figure 5.8).

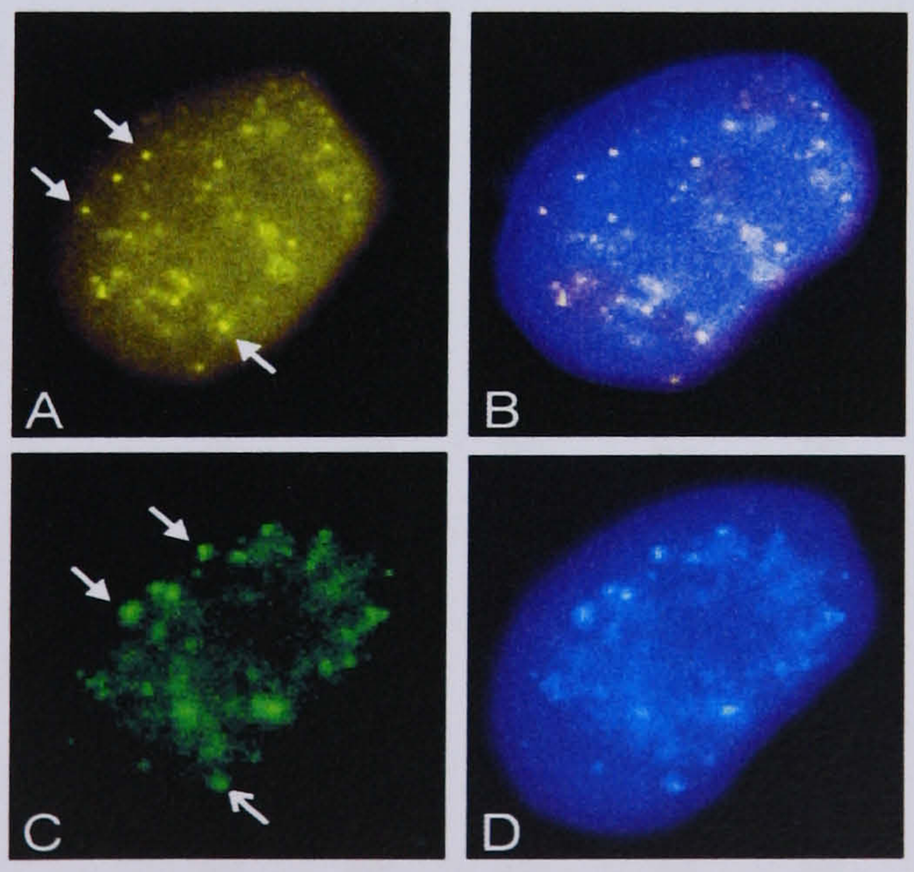

Figure 5.6 A representative example showing telomeres (yellow) (**A**) co-localised with γ-H2AX proteins (green) (**C**) in a MCF10A nuclei by using a combined immunofluorescence with FISH technique counterstained with DAPI (**B** and **D**).

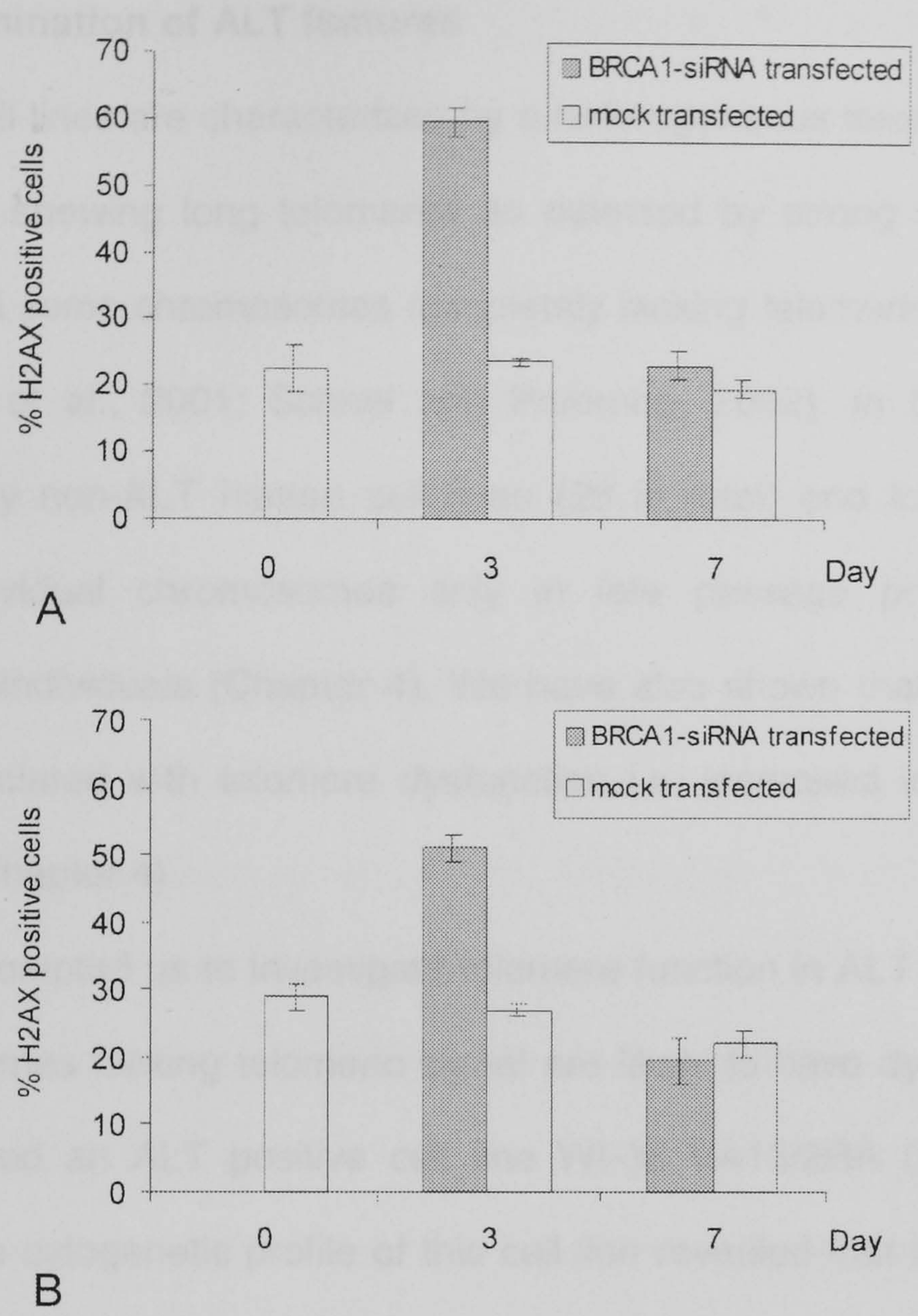

Figure 5.7 Histograms showing γ-H2AX positive cells in *BRCA1* depleted and mock-transfected MCF10A cells (**A**) and MCF7 cells (**B**).

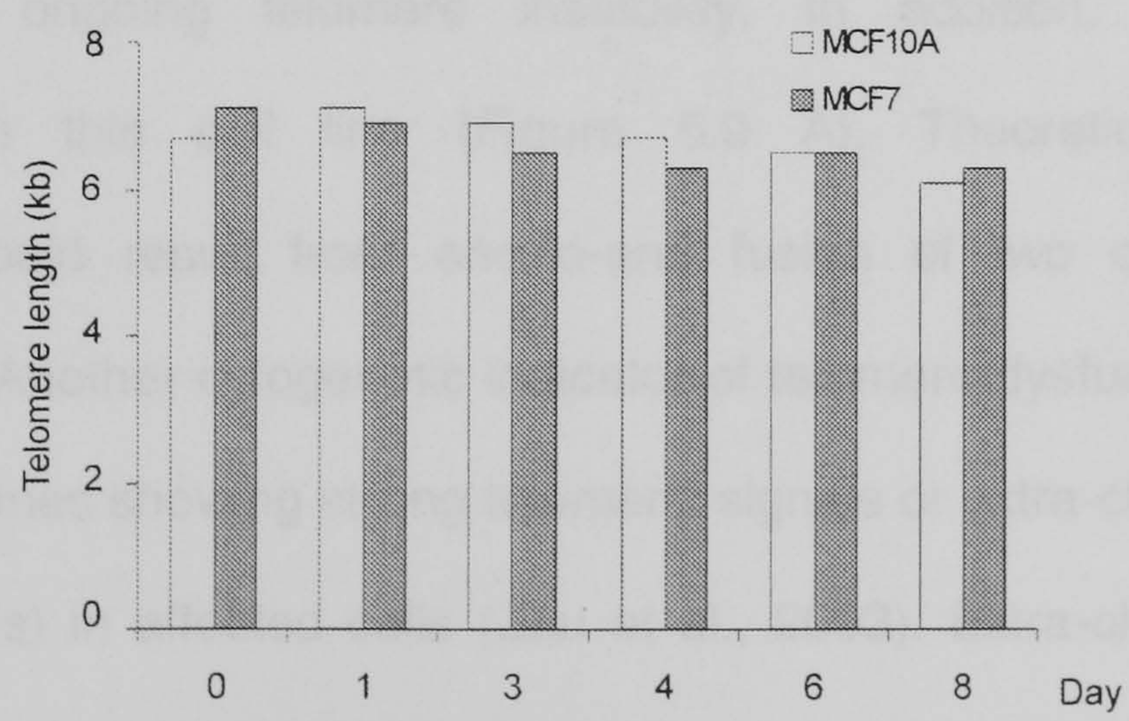

Figure 5.8 Telomere length analysis by flow-FISH in MCF cell lines.

5.2.2 Assessment of telomere function in human ALT cell lines

5.2.2.1 Determination of ALT features

ALT cell lines are characterized by a heterogeneous telomere length with some chromosomes showing long telomeres as detected by strong telomere fluorescence after FISH and some chromosomes completely lacking telomeric signal (Cerone et al., 2001; Scheel et al., 2001; Scheel and Poremba, 2002). In this study, so far, we analysed many non-ALT human cell lines (28 in total) and found lack of telomeric signal in individual chromosomes only in late passage primary fibroblast from radiosensitive individuals (Chapter 4). We have also shown that this lack of telomeric signal is associated with telomere dysfunction i.e. increased incidence of anaphase bridges (see Chapter 4).

This prompted us to investigate telomere function in ALT cells i.e. we reasoned that chromosomes lacking telomeric signal are likely to have dysfunctional telomeres. Initially we used an ALT positive cell line WI-38 VA13/2RA (Henson et al., 2002). Analysis of the cytogenetic profile of this cell line revealed that approximately 10 % of chromosomes lacked telomeric signal (Figure 5.9 A). We also noticed the presence of end-to-end chromosome fusions, with telomeric FISH signal present at the point of fusion, in approximately one third of WI-38 VA13/2RA cells (not shown) a possibility consistent with ongoing telomere instability. In addition, we found dicentric chromosomes in this cell line (Figure 5.9 A). Theoretically these dicentric chromosomes could result from end-to-end fusion of two chromosomes lacking telomeric signal. Another cytogenetic indicator of telomere dysfunction is the presence of mini chromosomes showing strong telomeric signals or extra-chromosomal telomeric fragments (ECTFs) in affected cells (Zhu et al., 2003). Extra-chromosomal telomeric DNA circles were observed in ALT cells by electron microscopy and confirmed by two dimensional pulsed-field gel electrophoresis (Cesare and Griffith, 2004). T-loop deletion by homologous recombination might contribute to ECTFs (Wang et al., 2004).

We found a large number of these indicators of telomere dysfunction in WI-38 VA13/2RA cells (Figure 5.9 A, Table 5.1). Therefore, analysis of cytogenetic profile of the WI-38 VA13/2RA cell line revealed the presence of cytological indicators of telomere dysfunction.

This prompted us to analyse more ALT positive cell lines by cytogenetic methods. For this purpose we used another lung adenocarcinoma cell line, SK-LU1 (Figure 5.9 B) and two osteosarcoma cell lines, U2-OS and G-292 (Figure 5.9 C and D), previously shown to be ALT positive (Henson et al., 2002). Similarly to WI-38 VA13/2RA cells, we found strong evidence of telomere dysfunction in these cell lines as summarized in Table 5.1. Collectively, these results argue that ALT positive cell lines show cytological evidence of telomere dysfunction. Examination of immortalized non-ALT human cell lines (e.g. six human lymphoblastoid cell lines described in Chapter 3) indicated complete lack of above indicators of genomic instability.

Table 5.1 Percentages of cells with at least one chromosome fusion or dicentric chromosome, and with at least one extra-chromosomal fragment (ECTF) in four different ALT cell lines.

Cell Line	Chromosome fusions	Dicentric chromosomes	ECTF
WI-38 VA13/2RA	29.4	17.6	70
SK-LU1	37.5	0	71
U2-OS	21.5	7	100
G-292	67	20	100

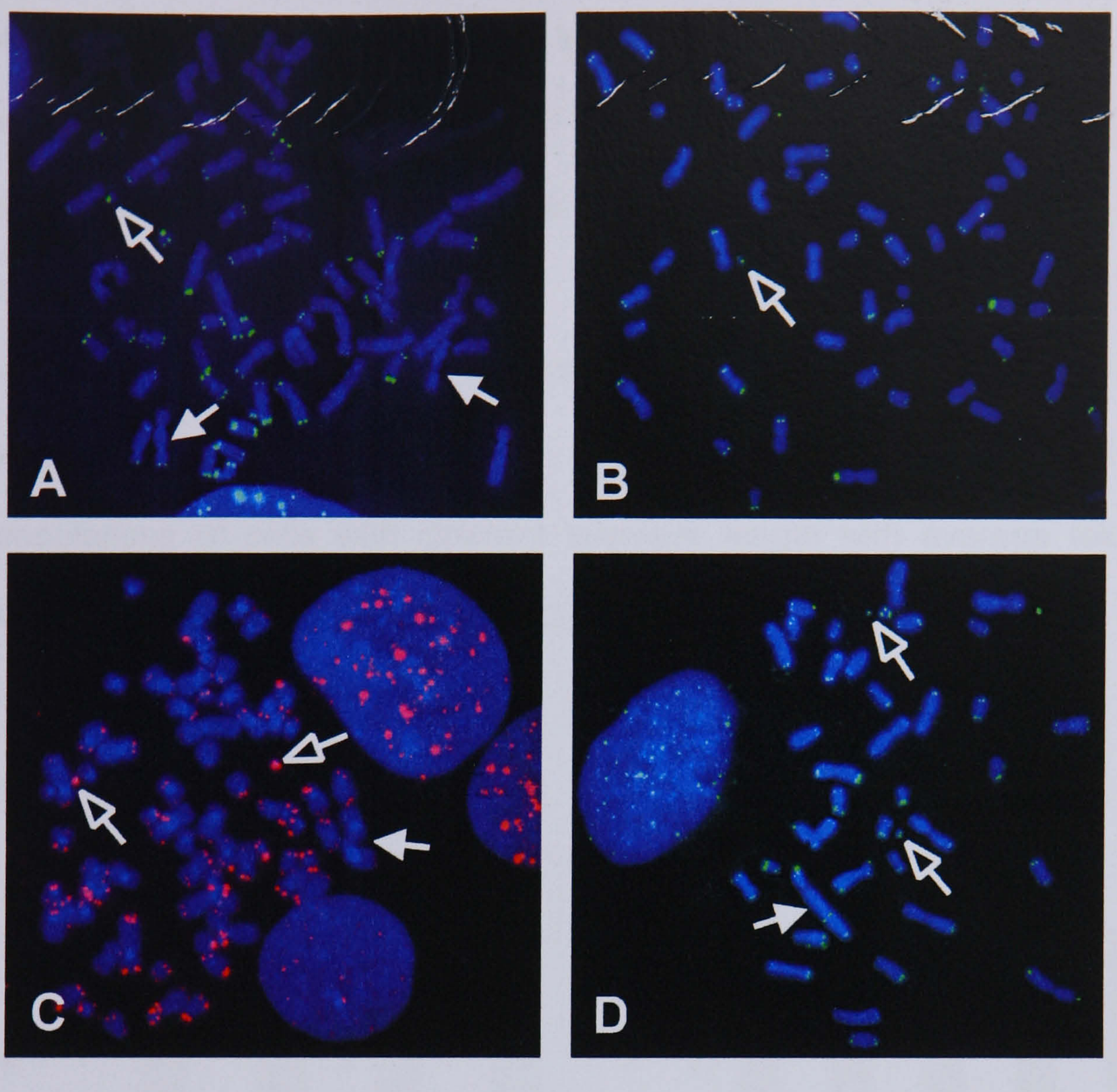

Figure 5.9 Representative examples of metaphases in ALT cells. Chromosomes showing lack of telomeric signal or heterogeneous telomere lengths. Closed arrows indicate either chromosome fusions or dicentric chromosomes and open arrows indicate extra-chromosomal telomeric fragments (ECTFs) in WI-38 VA13/2RA (**A**), SK-LU1 (**B**), U2-OS (**C**), and in G-292 (**D**) cells.

5.2.2.2 Telomere length analyses by flow-FISH in ALT cells

We also evaluated telomere length of ALT cells over time by flow-FISH. As expected, ALT cell telomeres were characterised by a much longer average size than the telomeres of non-ALT cells (Figure 5.10). The telomere length distribution in ALT cells was found to be dynamic, with frequent fluctuations in telomere size i.e. a pattern of erosion and rapid increase in length of telomeric DNA tracts was observed (Figure 5.10). This finding is compatible with recent demonstration of rapid losses and

increases in telomere length of ALT cell lines via recombination (Cesare and Griffith, 2004; Wang et al., 2004). Telomere length in the WI-38 VA13/2RA cell line varied between 17.6 and 31.9 kb (Figure 5.10 B) while in the parental cell line (non ALT WI38 fibroblast cell line) telomere length was on average shorter (13.8 kb) and stable during approximately 5 PDs (Figure 5.10 A). Telomere length in the other ALT cells varied between 21.6 and 33.1 kb in SK-LU1 cells (Figure 5.10 C), and between 15.8 and 21.6 in G-292 (Figures 5.10 D). As shown in Chapter 3, the U2-OS cell line contained 3 subpopulations of cells with different telomere length with average telomere length values 23.7, 39.8 and 64.3 kb (Figure 3.18 B).

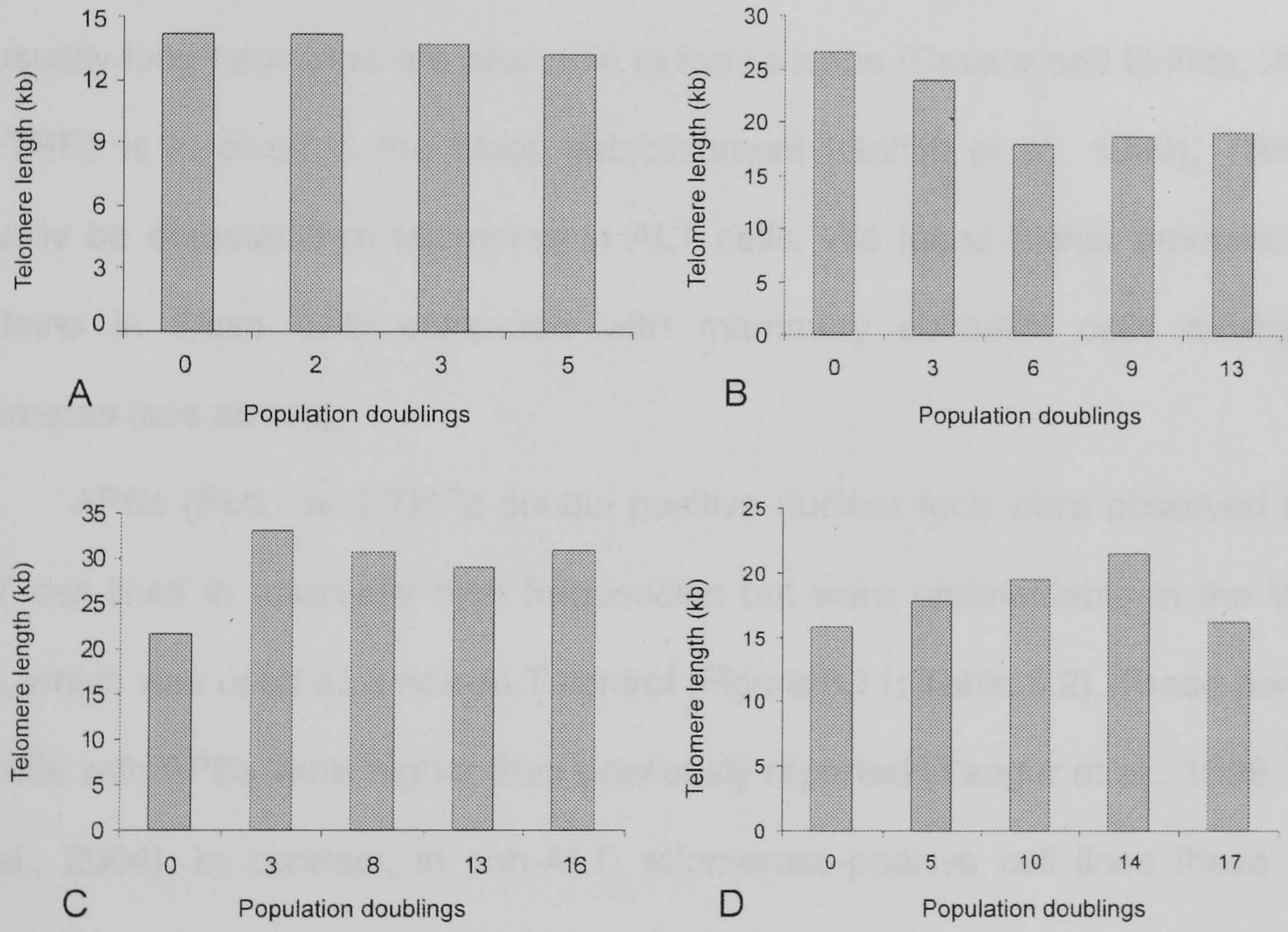

Figure 5.10 Telomere length dynamics as measured by flow-FISH in the WI-38 non-ALT cell line (**A**) and in three different ALT cell lines: WI-38 VA13/2RA (**B**); SK-LU1 (**C**); and G-292 (**D**).

5.2.2.3 Immunocytochemical analysis in ALT cells

5.2.2.3.1 Detection of APBs in ALT cell lines

Since above results indicate telomere dysfunction at the chromosome level, this prompted us to investigate whether ALT cell lines will show telomere dysfunction by immunocytochemistry methods. We first performed immunocytochemistry experiments to detect APBs, ALT associated PML bodies which represent markers of ALT. APBs are defined by the co-localisation of PML with TRF1/TRF2 proteins and/or telomeric DNA in ALT cells (Yeager et al., 1999) and are specific for ALT cells that maintain telomeres by recombination. The Santa Cruz antibody against TRF2 gave the best results and was used in subsequent co-localisation experiments. ALT cells with unusually long telomeres are also able to form t-loops (Cesare and Griffith, 2004) and, as TRF2 is involved in the t-loop establishment (Griffith et al., 1999), TRF2 should equally be detectable at telomeres in ALT cells. We found higher amounts of TRF2 proteins in these cells compared with mammary epithelial cells having shorter telomeres (see above).

APBs (PML- and TRF2 double positive nuclear foci) were observed in all four ALT cell lines in unusually high frequencies but were undetectable in the WI-38 cell line, which was used as a non-ALT control (Figure 5.11; Table 5.2). These percentages of cells with APBs were higher then previously reported (Yeager et al., 1999; Nabetani et al., 2004). In contrast, in non-ALT, telomerase-positive cell lines these telomeric proteins and the PML nuclear bodies occupy distinct and separate subnuclear domains (Yeager et al., 1999; Grobelny et al., 2000; Nabetani et al., 2004). The WI-38 VA13/2RA and the U2-OS cells contained smaller nuclear aggregates than the other 2 ALT lines and we are currently investigating reasons for this.

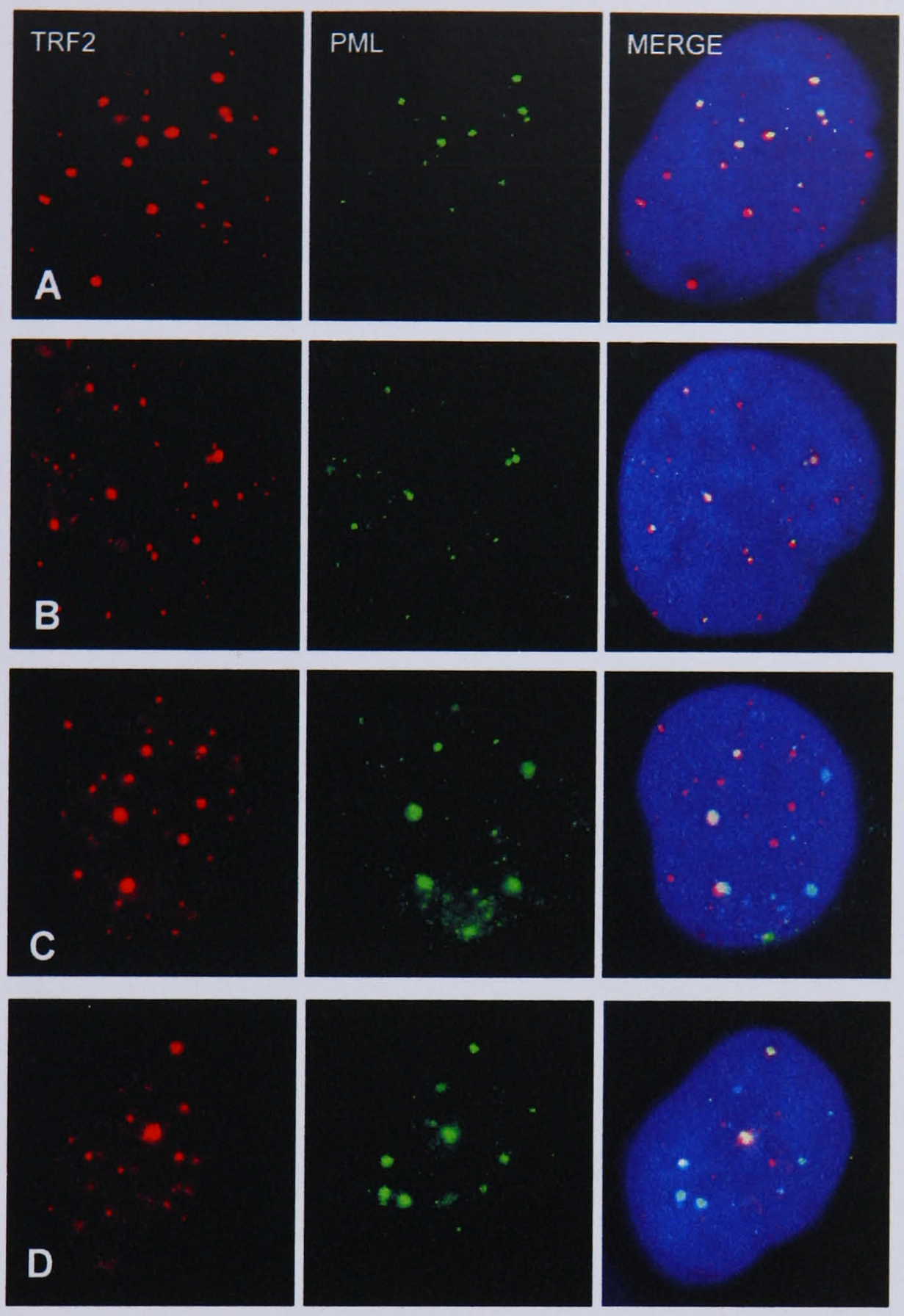

Figure 5.11 Detection of APBs by immunofluorescence in ALT cell lines. PML co-localises with TRF2 in the cell line WI-38 VA13/2RA (**A**), SK-LU1 (**B**), US-OS (**C**) and G-292 (**D**). Interphase cells were permeabilised and stained with anti-PML (green) and anti-TRF2 (red) antibodies. Nuclei were counterstained with DAPI.

Table 5.2 Percentages of interphase cells positive for staining with PML, BRCA1, and γ-H2AX antibodies and co-localisation of these with TRF2 antibodies in four ALT cell lines and a control non-ALT cell line. The cell was considered positive for staining with a particular antibody if at least one fluorescence focus per nucleus was observed. (*) Note that WI-38 parental cells had much smaller number of γ-H2AX and BRCA1 foci per nucleus as compared with four ALT cell lines.

Cell line	PML(+)	APB(+)	γ-H2AX(+)	γ-H2AX(+)TRF2(+)	BRCA1(+)	BRCA1(+)/TRF2(+)
ALT cell line						
WI-38 VA13/2RA	99	89	39	32	45	26
SK-LU1	92	81	71	67	43	41
U2-OS	99	92	48	44	19	14
G-292	94	79	64	57	28	22
non-ALT cell line						
WI-38 (parental line of WI-38 VA13/2RA)	98	0	38(*)	0	12(*)	0

5.2.2.3.2 Telomerase activity in ALT cells

The absence of telomerase activity from ALT cells correlates with lack of expression of hTERT and sometimes hTR (Bryan et al., 1997; Henson et al., 2002). We evaluated all four ALT cell lines for hTERT expression and two ALT cell lines for telomerase activity. Surprisingly, however, RT-PCR detected hTERT mRNAs in U2-OS cell line (Figure 5.12 A) in contrast to a previous report (Scheel et al., 2001). Also, RTQ-TRAP assays revealed high telomerase activity levels in early passages of the U2-OS and WI-38 VA13/2RA cell lines (Figure 5.12 B). Equally Saos-2, another ALT cell line (Henson et al., 2002), showed telomerase activity (Scheel et al., 2001; Scheel and Poremba, 2002) suggesting that ALT cell lines do not necessarily lack this enzyme activity.

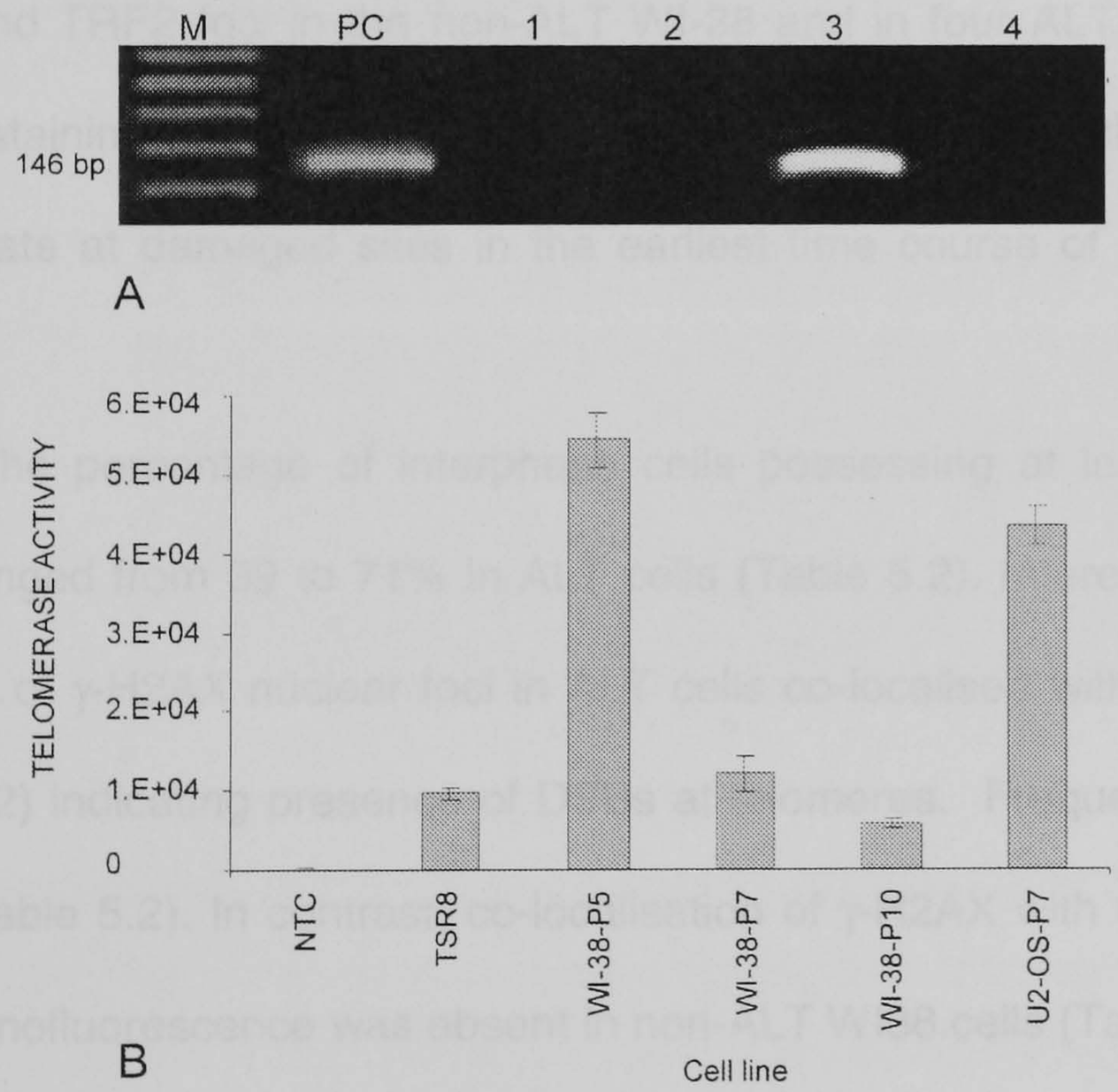

Figure 5.12 Detection of hTERT mRNA expression in ALT cell lines. 1: WI-38 VA12/2RA; 2: SK-LU1; 3: U2-OS; 4: G-292. M: molecular weight marker, PC: human mammary epithelial Bre-80 cells as a positive control (**A**). Telomerase activity levels during early passages in WI-38 VA13/2RA and in U2-OS cell lines as detected by RTQ-TRAP (**B**). NTC: negative control; TSR8 oligonucleotide template: positive control.

5.2.2.3.3 Association of BRCA1 with telomeres in ALT cells

Next, we examined the co-localisation of endogenous BRCA1 with TRF2 in the non-ALT WI-38 cells and in four ALT cell lines by fluorescent immunostaining using mouse anti-BRCA1 antibody. The analysis of a two-colour fluorescence immunostaining demonstrated that BRCA1 foci were overlaid with nuclear dots of TRF2 (Figure 5.13) in ALT cells but not in the non-ALT WI-38 cells. These results indicate that BRCA1 proteins co-localise with TRF2 and telomeres in ALT cell lines. Frequencies of co-localised spots ranged from 14 to 41 % in ALT cell lines (Table 5.2).

5.2.2.3.4 Association of γ-H2AX with telomeres of ALT cells

We next examined the co-localisation of endogenous phosphorylated histone H2AX and TRF2 foci in the non-ALT WI-38 and in four ALT cell lines by fluorescent immunostaining using mouse anti-γ-H2AX. γ-H2AX is one of the molecular signals that accumulate at damaged sites in the earliest time course of DSB repair (Paull et al., 2000).

The percentage of interphase cells possessing at least one γ-H2AX nuclear focus ranged from 39 to 71% in ALT cells (Table 5.2). Interestingly, it was found that fractions of γ-H2AX nuclear foci in ALT cells co-localised with TRF2 (Figure 5.14 and Table 5.2) indicating presence of DSBs at telomeres. Frequencies ranged from 32 to 67 % (Table 5.2). In contrast, co-localisation of γ-H2AX with telomeres as determined by immunofluorescence was absent in non-ALT WI38 cells (Table 5.2).

γ-H2AX also associated with PML bodies in ALT cells (Figure 5.15). The PML bodies co-localised with γ-H2AX are probably APBs, thus corroborating results from recently published studies (Nabetani et al., 2004) that γ-H2AX is a constitutive component of APBs in ALT cells.

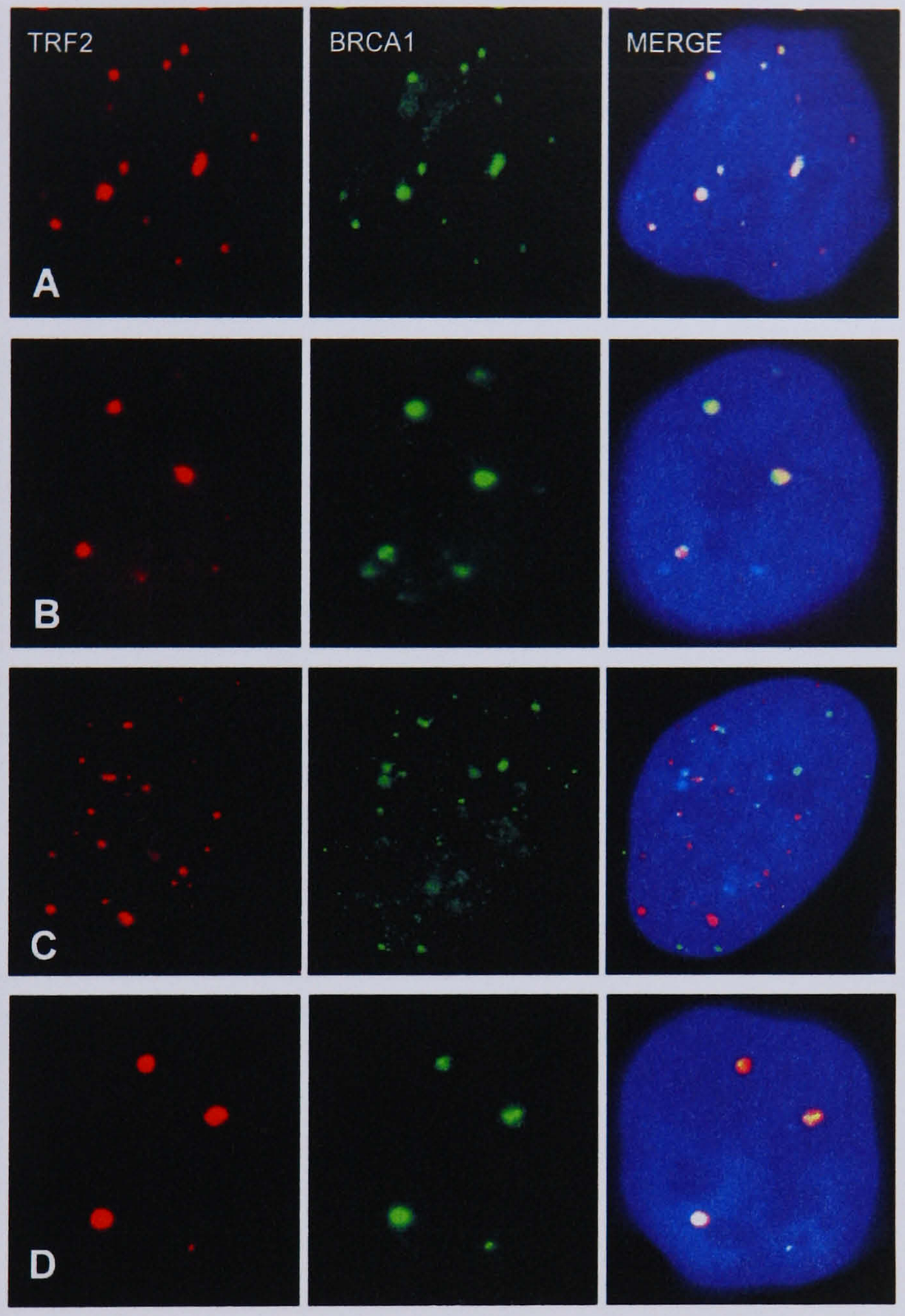

Figure 5.13 Detection of BRCA1 by immunofluorescence in ALT-positive cell lines. The visible BRCA1 foci are likely to represent aggregates of hundreds or more molecules. BRCA1 co-localises with TRF2 in the cell line WI-38 VA13/2RA (**A**), SK-LU1 (**B**). US-OS (**C**) and G-292 (**D**). Interphase cells were permeabilised and stained with anti-BRCA1 (green) and anti-TRF2 (red) antibodies. Nuclei were counterstained with DAPI.

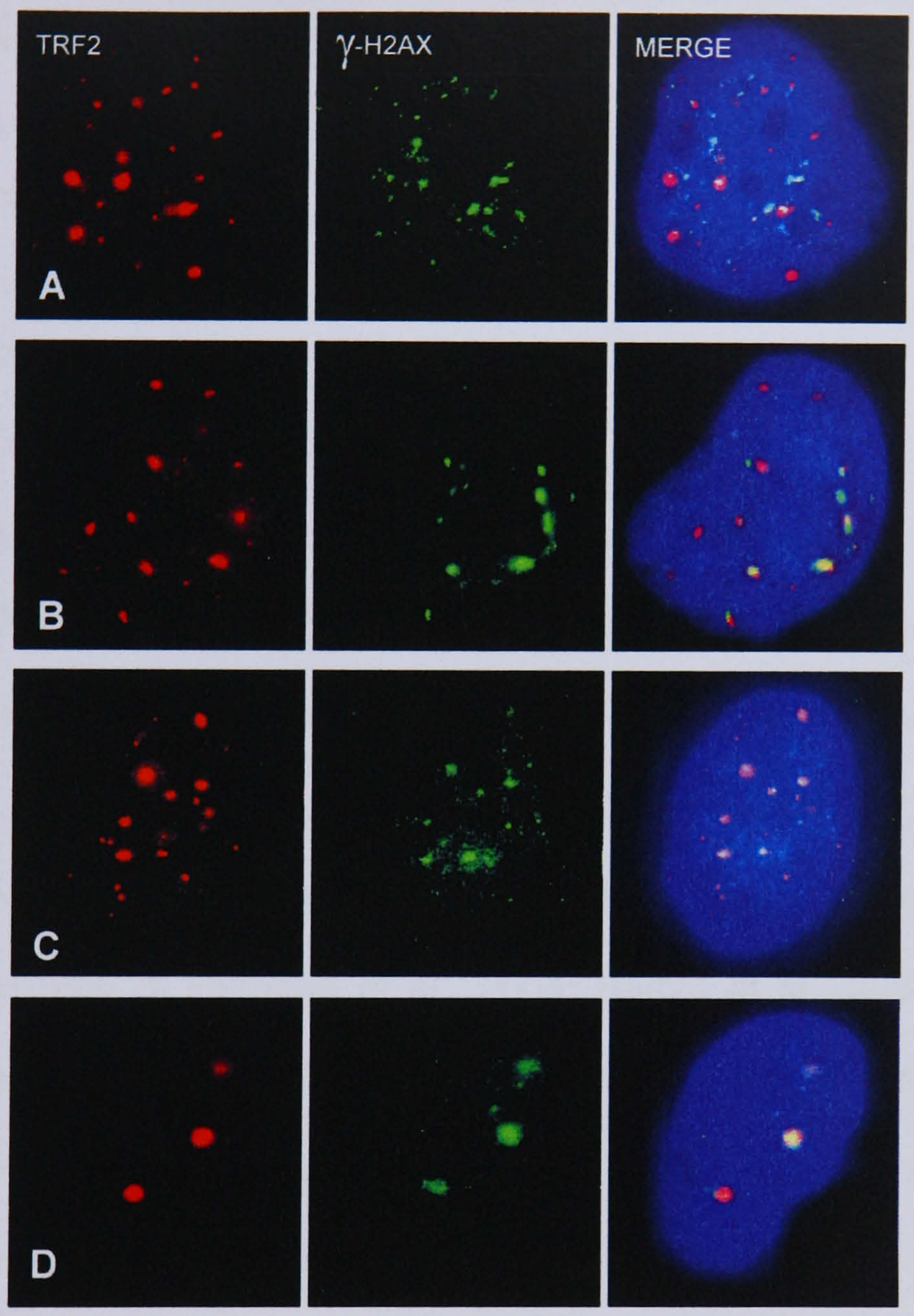

Figure 5.14 Detection of γ-H2AX by immunofluorescence in ALT cell lines. γ-H2AX co-localises with TRF2 in the cell line WI-38 VA13/2RA (**A**), SK-LU1 (**B**), US-OS (**C**) and G-292 (**D**). Interphase cells were permeabilised and stained with anti-γ-H2AX (green) and anti-TRF2 (red) antibodies. Nuclei were counterstained with DAPI.

Figure 5.15 A representative example of PML (green) co-localisation with γ-H2AX (red) in a SK-LU1 nuclei.

5.3 Discussion

5.3.1 BRCA1 and telomere maintenance

Telomere dysfunction induces a DNA damage response in mammalian cells. The MRE11-RAD50-NBS1 (MRN) complex, which is implicated in DNA DSB repair, was found to interact with TRF2 and to localise at telomeres (Zhu et al., 2000). Other DNA damage response factors, such as γ-H2AX, 53BP1, RAD17, RAD51D, and ATM were discovered to become associated with dysfunctional, uncapped telomeres (Takai et al., 2003; d'Adda di Fagagna et al., 2004; Herbig et al., 2004; Tarsounas et al., 2004). It was also reported that BRCA1 interacts and co-localises with the MRN complex following DNA damage (Zhong et al., 1999; Wang et al., 2000; Wu et al., 2003) suggesting that BRCA1 could also associate with telomeres.

Support for the notion that the *BRCA1* gene suppresses genome instability comes from several sources. Embryonic tissue lacking wild type *BRCA1* revealed IR hypersensitivity, consistent with a defect in DSB repair (Sharan et al., 1997; Deng et al., 2000). *BRCA1* homozygous mutant mouse embryo fibroblasts undergo spontaneous chromosome breakage accompanied by checkpoint-mediated growth arrest (Deng et al., 2000). Alterations in the *BRCA1* gene affect multiple pathways including DNA repair through homologous recombination, transcription coupled repair, chromatin remodelling, centrosome duplication, apoptosis and cell cycle checkpoint

control (reviewed in Venkitaraman, 2002). Accelerated shortening of telomeres in *BRCA1* deficient mouse embryonic stem cells was demonstrated in Chapter 4, indicating that lack of *BRCA1* may affect telomere function. Consistent with this possibility mouse cells with targeted truncation in exon 11 of *BRCA1* showed dicentric chromosomes (Xu et al., 1999; Weaver et al., 2002) some of which may result from end-to-end chromosome fusions, which represent signatures of telomere dysfunction. The most recent study revealed dramatically elevated levels of end-to-end chromosome fusions in *BRCA1*$^{-/-}$*p53*$^{-/-}$ mouse T-cells in comparison with cells from *p53*$^{-/-}$ mice (McPherson et al., 2004). A recently demonstrated ability of BRCA1 to suppress telomerase may contribute to its tumour suppressor activity (Xiong et al., 2003).

By depleting BRCA1 in two MCF cell lines, we wished to assess its effect on telomere maintenance. This part of our research is still in progress but initial results show that a transient decrease in BRCA1, as was determined by three independent techniques, immunofluorescence, RT-PCR and Western blotting, causes accumulation of DNA damage. Elevated levels of DNA damage were demonstrated by an increase in histone H2AX phosphorylation (γ-H2AX) indices. We have also observed moderate telomere dysfunction levels in MCF10A cells possessing significantly higher levels of anaphase bridges than control mock-transfected cells. Telomere length was not affected during depletion of BRCA1 mRNA, possibly because lower levels of BRCA1 protein lasted only 2-4 days. These results are consistent with the fact that *BRCA1* deficient cells suffer from both DSB repair and chromosomal instability (Wang et al., 2001).

Human telomerase reverse transcriptase (hTERT), the catalytic subunit of human telomerase, is responsible for the synthesis and maintenance of the telomeric repeats at the ends of human chromosomes. Previous studies have shown that c-Myc stimulates hTERT transcription through the binding sites located on the hTERT

promoter (Zhou and Liu, 2003). Recently, evidence has been provided that BRCA1 protein binds to the c-Myc protein, turns off the transcription of hTERT, and prevents incidental cellular immortalisation (Li et al., 2002; Zhou and Liu, 2003; Xiong et al., 2003). Xiong et al (2003) demonstrated that an exogenous *BRCA1* gene strongly inhibited telomerase enzyme activity in human prostate and breast cancer cell lines. It was also shown in co-transfection experiments that a wtBRCA1 plasmid inhibited hTERT gene expression in human ovarian cancer (Zhou and Liu, 2003). Therefore, we expected to observe changes in hTERT expression in both MCF cell lines during transient BRCA1 mRNA depletion. Surprisingly, however, no changes in hTERT expression were observed by RT-PCR and Western blotting. One possible explanation could be that the depletion of BRCA1 protein lasted too short to affect expression of hTERT in our cell lines. Alternatively, different cell lines may use different mechanisms of regulating hTERT i.e. we used genetically highly abnormal cell lines, which may show differences in either genetic content or gene expression in comparison with lines used in the study by Xiong et al. (2003).

5.3.2 Analysis of telomere function in ALT cell lines

One of the research aims in our laboratory is to identify the extent to which dysfunctional telomeres contribute to genomic instability. For this reason we decided to analyse telomere function in human ALT cell lines. As mentioned earlier these cell lines show highly heterogeneous telomeres with many chromosomes lacking telomeric signals as detected by PNA-FISH (Cerone et al., 2001; Scheel et al., 2001; Scheel and Poremba, 2002). Telomere function in ALT cells can be assessed by a novel method based on immunnocytochemical co-localisation of DSBs and telomeres (d'Adda di Fagagna et al., 2003; Takai et al., 2003). Using this method we assessed telomere function in four human ALT cell lines. In addition we assessed telomere function in ALT cells based on cytogenetic parameters i.e. cytologically apparent indicator of telomere

dysfunction such as dicentric chromosomes, end-to-end chromosome fusions and small telomere positive extrachromosomal fragments. Both methods revealed clear telomere dysfunction in ALT cell lines.

Like BRCA1, histone H2AX is a target for ATM- or ATR-mediated phosphorylation and participates in transmission of the DNA damage signal to downstream molecules such as Chk1 and Chk2 (Motoyama and Naka, 2004). The molecular mechanism of the sensing of DNA damage, however, is still not clearly defined. Although phosphorylation of histone H2AX, γ-H2AX, is dispensable for the initial recognition of DNA damage, γ-H2AX is essential for the recruitment of BRCA1 and other DNA-repair and damage-response factors like 53BP1, MDC1, and the MRN complex to the site of DNA damage (Fernandez-Capetillo et al., 2002; Stewart et al., 2003). The appearance of γ-H2AX foci before these repair factors, and the dependence of all these foci on the prior phosphorylation of H2AX, suggests that phosphorylation of H2AX and focus formation is a necessary first step in the organisation of repair factor foci (Paull et al., 2000). Sites of DNA damage are marked within minutes by the phosphorylation of H2AX, which spreads over a region spanning thousands of bases around the lesion, suggesting that chromatin remodelling may occur to facilitate access of the repair machinery. As phosphorylation of H2AX is specific to DSBs (Bassing et al., 2002), this very likely indicates a high level of DSBs present in the cell all the time, which was especially observed in mouse ES cells (see Chapter 4). It is not yet clear whether these foci represent many DSBs being made with a high turnover of repair, or whether there are relatively few DSBs that persist in the cells for a longer time without being repaired. Interestingly, H2AX deficiency causes a dramatic decrease in BRCA1 focus formation after IR (Bassing et al., 2002).

We observed co-localisation of γ-H2AX with the telomere binding protein TRF2 in all four ALT cell lines analysed. In each of the four analysed ALT cell lines we found approximately 50% of cells positive for γ-H2AX foci, of which nearly all showed at least

one γ-H2AX focus co-localising with TRF2, demonstrating DNA repair response at telomeres i.e. the presence of DSBs at telomeres. This clearly suggests that telomeres in ALT cell lines are dysfunctional. To check whether this telomere dysfunction has any effect on cell survival we are currently irradiating ALT cell lines and monitoring their survival rates after IR relative to the non-ALT WI38 cell line. We are also further examining the unexpected detection of telomerase activity (at least in early passages) in ALT cell lines. However, it has been shown that telomerase and ALT can co-exist in the same cell line (Cerone et al., 2001) and that some ALT cell lines have detectable telomerase activity (Scheel et al., 2001; Scheel and Poremba, 2002).

One of the features of ALT is an accumulation of ALT associated PML bodies (APBs) (Yeager et al., 1999), which consist of DNA repair proteins that specifically coalesce, presumably, at telomeres (as judged by co-localisation in immunofluorescence experiments with telomeric DNA and the foci of TRF proteins). Proteins found associated with APBs include BRCA1, NBS1, RAD51, BLM, and others. These foci of repair proteins are generally considered to be hallmarks of active complexes, and possibly of active recombination at telomere ends. It was also demonstrated by incorporation of BrdU into the nucleus that DNA synthesis occurs at APBs (Grobelny et al., 2000; Nabetani et al., 2004), indicating a role for APBs in telomere elongation. In line with above results we found high percentages of APBs in all four ALT cell lines analysed. However, these percentages were much higher then previously reported by Yeager et al (1999) and Nabetani et al (2004). Yeager et al. (1999) detected APBs in only a subset (~5%) of interphase nuclei. Their lower percentages of cells with APBs can be explained by using paraffin embedded tissues and the antigen retrieval method, which suffers, depending on the antibody used, from a lower detection resolution (personal observation).

Similarly to the study by Wu et al. (2003) we found that BRCA1 co-localises with telomeric protein TRF2 in all ALT cell lines. On average, 20% of cells in all four ALT

cell lines showed co-localisation of BRCA1 with TRF2 (Table 5.2). This, however, does not implicitly suggest that BRCA1 targets telomeric DNA since BRCA1 associates also with APBs, specifically during late S-G_2 phase of the cell cycle phase (Wu et al., 2003), which contains TRF2 proteins. The focal location of BRCA1 in nuclear dots reflects possibly only a fraction of the cellular pool, perhaps that which is bound to particular nuclear structures. Nevertheless, we observed higher percentages of cells positive for BRCA1 in ALT cell lines compared to human non-ALT fibroblast cell lines. These results, therefore, are inconsistent with suggestions that long telomeres may provide a protective effect against genomic insults. Also mouse scid (severe combined immunodeficiency) cells have elongated telomeres and yet show telomere dysfunction (Slijepcevic et al., 1997; Bailey et al., 1999; Hande et al., 1999) suggesting that longer telomeres do not necessarily provide protection to chromosome ends. A similar conclusion was also drawn by a study on mouse leukaemia cells (Finnon et al., 2001).

In conclusion, results presented in this chapter indicate clear telomere dysfunction in ALT cells and point to the possibility that BRCA1 could also affect telomere maintenance. Future work is required to conclusively demonstrate the role of BRCA1 at telomeres and such experiments are currently under way in our laboratory.

5.4 Summary

We examined the role of BRCA1 in telomere maintenance in two mammary epithelial MCF cell lines. BRCA1 was transiently depleted for 1-5 days to assess its effect on telomere function. This work is still in progress but preliminary results show that a transient decrease in BRCA1, as was determined by three independent techniques, immunofluorescence, RT-PCR and Western blotting, increased the number of histone H2AX phosphorylation (γ-H2AX), indicating elevated levels of DNA damage repair. Moderate telomere dysfunction may also be seen in MCF10A cells possessing slightly more anaphase bridges. Telomere length was not affected during depletion of

BRCA1 mRNA, possibly because lower levels of BRCA1 protein lasted only for a few days. These results are consistent with the fact that BRCA1 deficient cells suffer from both DSB repair and chromosomal instability.

We also assessed telomere function in four human ALT positive cell lines. Using cytogenetic and immunocytochemistry methods we observed telomere dysfunction in ALT positive cell lines. We observed unexpectedly high frequencies of APBs in ALT cells. Not only BRCA1, also γ-H2AX was used as a novel marker in detecting telomere dysfunction. We demonstrated that these early DNA damage response factors associate at telomeres in ALT cells. We are still investigating whether BRCA1 at telomeres aid in maintaining telomere end protection and in the repair of double strand breaks.

CHAPTER 6

TELOMERASE ACTIVITY AND ALTERNATIVE SPLICING OF THE TELOMERASE REVERSE TRANSCRIPTASE (hTERT) TRANSCRIPT IN BRAIN TUMOURS

6.1 Introduction

In the previous chapters we have shown that fibroblasts with defects in DNA damage response and human ALT cells show dysfunctional telomeres. We argued that these phenotypes, at least in the case of human fibroblast cell lines defective in DNA damage response, may be the consequence of radiosensitivity. Cells that are radiosensitive usually show chromosomal instability. A typical example is cells from ataxia telangiectasia (AT) patients, which display a high degree of spontaneous or induced chromosomal instability (Metcalfe et al., 1996; Pandita and Dhar, 2000; Hande et al., 2001; Tchirkov and Lansdorp, 2003). It is likely that dysfunctional telomeres contribute to chromosomal instability in AT cells (e.g. Hande et al., 2001).

Brain tumours exhibit considerable chromosomal instability (El-Zein et al., 1999; Hui et al., 2001; Sawyer et al., 2003). Given that chromosomal instability is usually a consequence of altered DNA damage response (see above) this suggests that alterations in DNA damage response mechanisms, some of which may involve

telomeres, could be responsible for tumorigenesis in brain cells. The presence of dicentric chromosomes in telomerase negative meningiomas (Carroll et al.. 1999; Sawyer et al., 2003), for example, could indicate abnormal telomere function.

There is relatively little information about the role of telomeres/telomerase in brain tumorigenesis and in this chapter we were interested to assess telomerase activity in brain tumours, particularly in meningiomas. Previous studies of meningiomas showed contradicting results with regard to telomerase activity as revealed by the classical telomere repeat amplification protocol (TRAP) (DeMasters et al., 1997; Hiraga et al., 1998; Langford et al., 1997; Sano et al., 1998; Carroll et al., 1999; Falchetti et al., 1999; Simon et al., 2000; Boldrini et al., 2003). However, when we started this study expression levels of the telomerase components in meningiomas and in other brain tumours were not known. We reasoned that by employing RT-PCR we would be able to monitor expression levels of telomerase components in brain tumours and thus resolve above contradicting reports. This is particularly important because the presence or absence of telomerase in meningiomas and other brain tumours may be used to predict the clinical outcome (Boldrini et al., 2003). In addition, the mRNA splicing variants of the telomerase reverse transcriptase component (hTERT) inhibit telomerase (see below) and this could explain the absence of telomerase activity not only in meningiomas but also in other brain tumours. Therefore, we analysed the role of hTERT mRNA and their splice variants in telomerase positive and negative brain tumours.

Several publications deal with telomere length in brain tumours, more specifically in meningioma (Hiraga et al., 1998; Chen et al., 2000), glioblastoma (Hiraga et al., 1998; Falchetti et al., 2000; Hakin-Smith et al., 2003), oligodendroglial brain tumours (Hiraga et al., 1998; Chong et al., 2000), and in ependymal tumours (Chong et al., 2000). The method of choice for telomere length measurement in brain tumours was Southern hybridisation. The telomere restriction fragment (TRF) length in brain tumours was considered normal if it ranged between 8.5 and 14 kb or abnormally elongated if

longer than 14 kb (Hiraga et al., 1998; Chen et al., 2000; Chong et al., 2000; Hakin-Smith et al., 2003). Chen et al (2000) found that the mean TRF of brain tumours with telomerase activity was significantly shorter than that of the tumours with undetectable telomerase activity. In addition, Hiraga et al. (1998) and Morii et al. (1997) reported that telomerase-negative gliomas had longer telomeres when compared with telomerase-positive gliomas. It seems likely that ALT (alternative lengthening of telomeres) was present in one case of malignant meningioma (case 30) showing no telomerase activity and telomere length greater than 25 kb although this was not specifically mentioned by the authors (Chen et al., 2000). On the other hand, no statistical differences were found between the mean telomere length in telomerase-positive and telomerase-negative tumours (Chong et al., 2000) although a slightly shorter length was observed in telomerase-positive oligodendroglial tumours. In addition, Falchetti et al. (2000) showed that there is no significant difference in telomere length pattern between TRAP-positive and TRAP-negative glioblastoma multiforme (GBM) tumours. Basically, they found normal or elongated telomeres in all samples. They concluded that, because they could not find any difference in TRF pattern between GBM samples with or without telomerase activity as detected by TRAP, all GBM tumours could have telomerase activity, which may not always be detectable by the standard TRAP assay. However, in this study only one restriction enzyme, DpnII, was used for TRF measurement instead of a combination of two enzymes (Hinf1 and Rsa1), which are more commonly used and give better results. Therefore, the conclusion made in this study regarding the lengths of TRFs may not be entirely accurate. In spite of lack of clarity in the above results, the possibility cannot be excluded that ALT mechanisms could operate in brain tumours as shown by the presence of relatively long telomeres in many of them in spite of telomerase absence. ALT has been detected in a variety of human tumours. These include bone and soft tissue sarcomas, carcinomas of the lung, kidney, adrenal gland, breast, and ovary (Mehle et al.. 1996; Bryan et al., 1997). Recently, Hakin-Smith et al. (2003) discovered that some patients had GBM tumours

with the ALT phenotype and that ALT can be considered as a prognostic indicator for patients with these malignant tumours.

A limited number of studies have also been performed on telomerase activity in brain tumours, particularly in meningiomas, which represent a common neoplasm arising from the meninges (Kleihues and Cavenee, 2000) (see section 1.9; Figure 1.5). To date, it is generally accepted that high telomerase activity levels characterise high-grade gliomas (Le et al., 1998; Falchetti et al., 1999; Huang et al., 1999; Harada et al., 2000; Sugita et al., 2000) but the picture for meningiomas is less clear with some tumours shown to be telomerase positive and some telomerase negative. The hypothesis that reactivation of telomerase is required to maintain tumour growth (Kim and Wu, 1997) or may play a critical role in the progression or maintenance of the malignant phenotype (Rhyu, 1995), are in conflict with findings in meningiomas. Several previous studies performed on single specimens of intracranial tumours have reported that telomerase activity is present in the vast majority of malignant brain tumours while enzyme activity could not be detected in benign meningiomas (DeMasters et al., 1996; Hiraga et al., 1998; Sano et al., 1998; Carroll et al., 1999; Falchetti et al., 1999). However, up to 21% of single specimens of benign meningiomas had telomerase activity (Langford et al., 1997; Simon et al., 2000). The difference between intrinsically benign and more aggressive meningioma variants is of great importance: whereas typical meningiomas can frequently be cured by complete resection, atypical and anaplastic meningiomas are characterised by a substantially increased risk of tumour recurrence (Hiraga et al., 1998; Simon et al., 2000), with a clearly documented bad prognosis. Telomerase activity and its hTERT mRNA expression tended to increase as the histological grading of intracranial meningiomas increased, suggesting a role for telomerase reactivation in the progression of these tumours (Boldrini et al., 2003).

These findings prompted us to investigate whether undetectable telomerase activity in meningiomas is also reflected in the absence of hTERT mRNA expression.

Second, intratumoral differences in tumour tissues may have resulted in a false-high proportion of telomerase-negative tumours. Benign meningiomas were therefore evaluated for telomerase activity and telomerase gene expression in multiple specimens of a single tumour.

Third, because hTERT spliced variants are believed to be a limiting factor for the expression of telomerase activity (Kilian et al., 1997; Wick et al., 1999), we examined whether these were limiting components for the expression of telomerase activity in benign meningiomas. We therefore used primers to amplify a sequence located upstream and a sequence within the reverse transcriptase domains A and B', including two potential splice sites (Figure 6.1), to determine hTERT mRNA expression. Hence, we amplified both functional and non-functional spliced variants.

Finally, we investigated the tumour growth rate mainly by use of Ki-67 which is a nuclear protein detected in proliferating cells in all phases of the cell division cycle and is widely used as a proliferation marker.

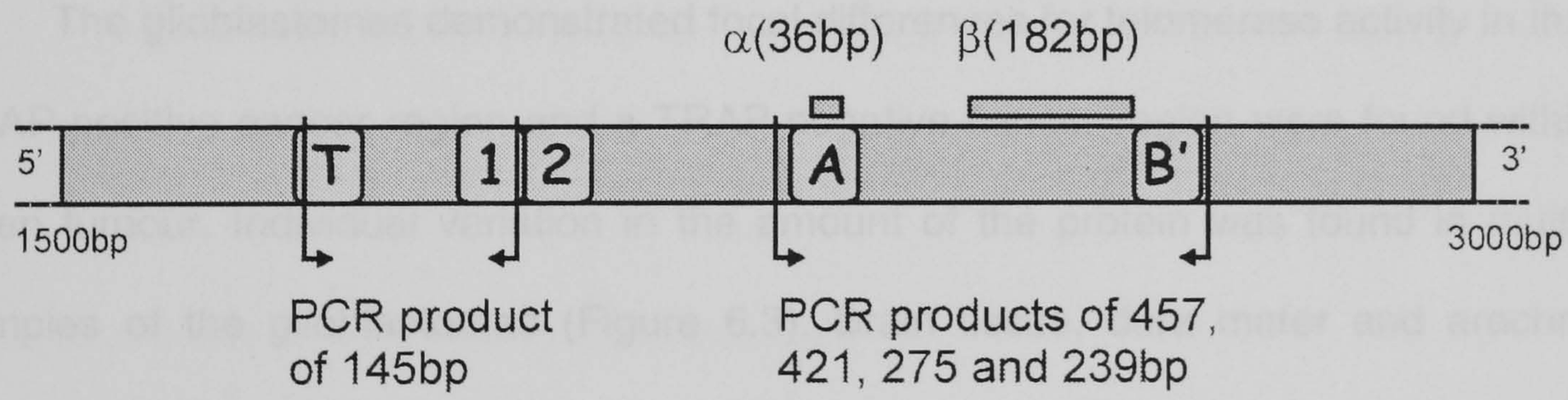

Figure 6.1 Schematic diagram of hTERT mRNA with telomerase-specific T-motif and 1, 2, A and B' conserved reverse transcriptase motifs highlighted. Deletion α which occurs within the A motif (lacking 36 nucleotides at the beginning of exon 6), and deletion β (lacking 182 nucleotides corresponding to exons 7 and 8), situated between motif A and B', of hTERT cause 4 spliced products. First set of PCR primers (hTERT-1784S and hTERT-1928A) amplifies a 145-base region upstream of the reverse transcriptase domain. Second set of PCR primers (hTERT-2164S and hTERT-2620A) amplifies a region within the reverse transcriptase domain, which includes both α and β splices sites.

6.2 Results

6.2.1 Telomerase activity in brain tumour samples

Telomerase activity was examined in 49 specimens of brain tumours from 32 patients (Figure 6.2, Table 6.1). The presence of telomerase activity was tested only once in a previously frozen protein lysate (liquid nitrogen) because a rapid sample degradation occurs after two or more cycles of cell thawing. A total of 7 out of 32 examined tumours (22%) contained detectable telomerase activity. The glioblastomas in lanes 13, 24, 32 and the medulloblastoma in lane 11 expressed high telomerase activity (Figure 6.2). The atypical meningiomas in lanes 17 and 27, and the ependymoma in lane 14 displayed reduced telomerase activity (Figure 6.2). Telomerase activity was undetectable in all (18) benign meningiomas at both 0.7 µl and 2.0 µl protein content per PCR reaction mixture (data not shown). Two of the three locally recurring tumours (case 12, 23, and 27) failed to display telomerase activity (Figure 6.2).

The glioblastomas demonstrated focal differences for telomerase activity in that a TRAP-positive cancer region and a TRAP-negative cancer region were found within a given tumour. Individual variation in the amount of the protein was found in multiple samples of the glioblastomas (Figure 6.3). Brain tissue, dura mater and arachnoid tissue did not reveal telomerase activity (data not shown). Telomerase activity could be assigned to a higher cellular density as a histomorphological feature in histological sections adjacent to telomerase-positive samples.

To rule out false-negative results due to the presence of tissue-specific inhibitors, all extracts with no detectable telomerase activity were re-evaluated. Small amounts of protein extracts of Molt-4 cells with known telomerase activity were mixed with telomerase-negative extracts (1:4) and the TRAP assay was repeated. In all re-evaluated cases, a similar telomerase-specific 6 nt repeat ladder was obtained, indicating that these tissues did not contain telomerase inhibitors (data not shown).

Telomerase activity could not be detected in *in vitro* cultures of some meningiomas and glioblastomas (data not shown). However, *in vitro* telomerase activity is not necessarily synonymous with *in vivo* enzyme activity.

6.2.2 Expression of hTERT in brain tumours

hTERT transcripts were initially detected by RT-PCR using a set of primers (hTERT-1784S and hTERT-1928A) that amplify a region within the T-motif of hTERT mRNA giving a product of 145 bp (Figure 6.1; Figure 6.4A). The 145 bp hTERT cDNA was present in 20 of 32 (63%) intracranial tumours (Table 6.1). Whereas hTERT mRNA was consistently low or absent in meningiomas, brain tumours with telomerase activity exhibited elevated levels (Figure 6.4A; Table 6.1). In 13 cases (40.6 %), detectable hTERT mRNA was demonstrated in the absence of telomerase activity (Table 6.1). Different samples from the same tumour showed individual variation in hTERT mRNA expression, e.g. case 24 (Figure 6.4A; Table 6.1). We were unable to detect hTERT mRNA expression in the confluent cell cultures of meningiomas (cases 5, 7, 9, 17, and 20). hTERT could not be detected in cell cultures, derived from the arachnoid or from the dura mater.

6.2.3 Expression of hTERC in brain tumours

The expression of telomerase RNA component (hTERC) in brain tumours was determined by RT-PCR. Since hTERC transcript of approximately 450 bases is not polyadenylated, first-strand cDNA was reverse transcribed using random hexanucleotides and cDNA fragments were amplified by PCR. PCR bands of the predicted size were generated from all brain tumour specimens (Figure 6.4B) and also from normal brain and meninges (data not shown).

Although we were unable to detect hTERT mRNA expression in the confluent cell cultures of meningiomas, all cultures expressed the hTERC mRNA.

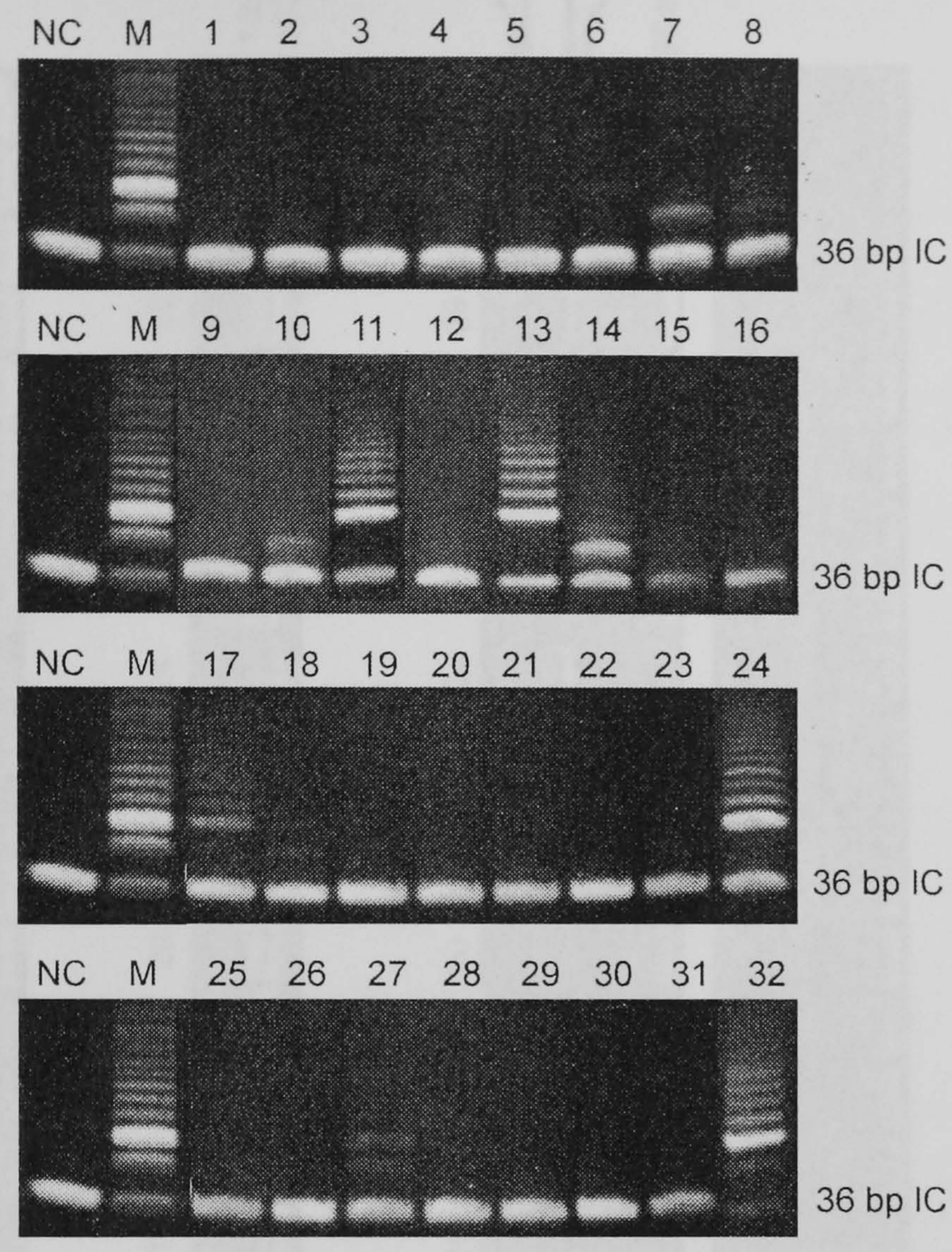

Figure 6.2 Telomerase activity in intracranial tumours, as measured by TRAP assay. The presence of a 6-base incremental ladder is evidence for telomerase activity in a given sample. NC: cDNA was replaced by lysis buffer as negative control. M: Molt-4 positive control. IC: 36 bp internal control.

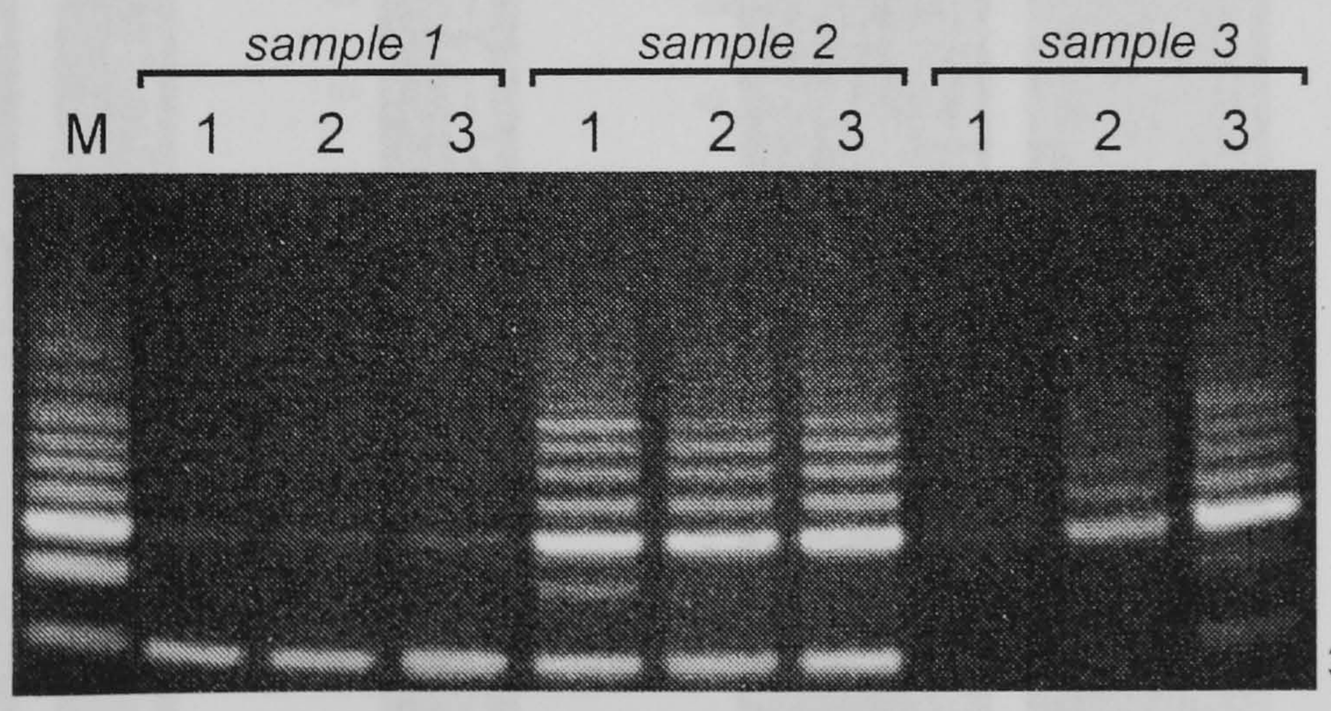

Figure 6.3 Telomerase activity in 3 different samples of a glioblastoma, case 24. PCR cycles were 27, 30 and 33 in lane 1, 2 and 3, respectively. M: Molt-4 with 33 PCR cycles; IC: 36 bp internal control.

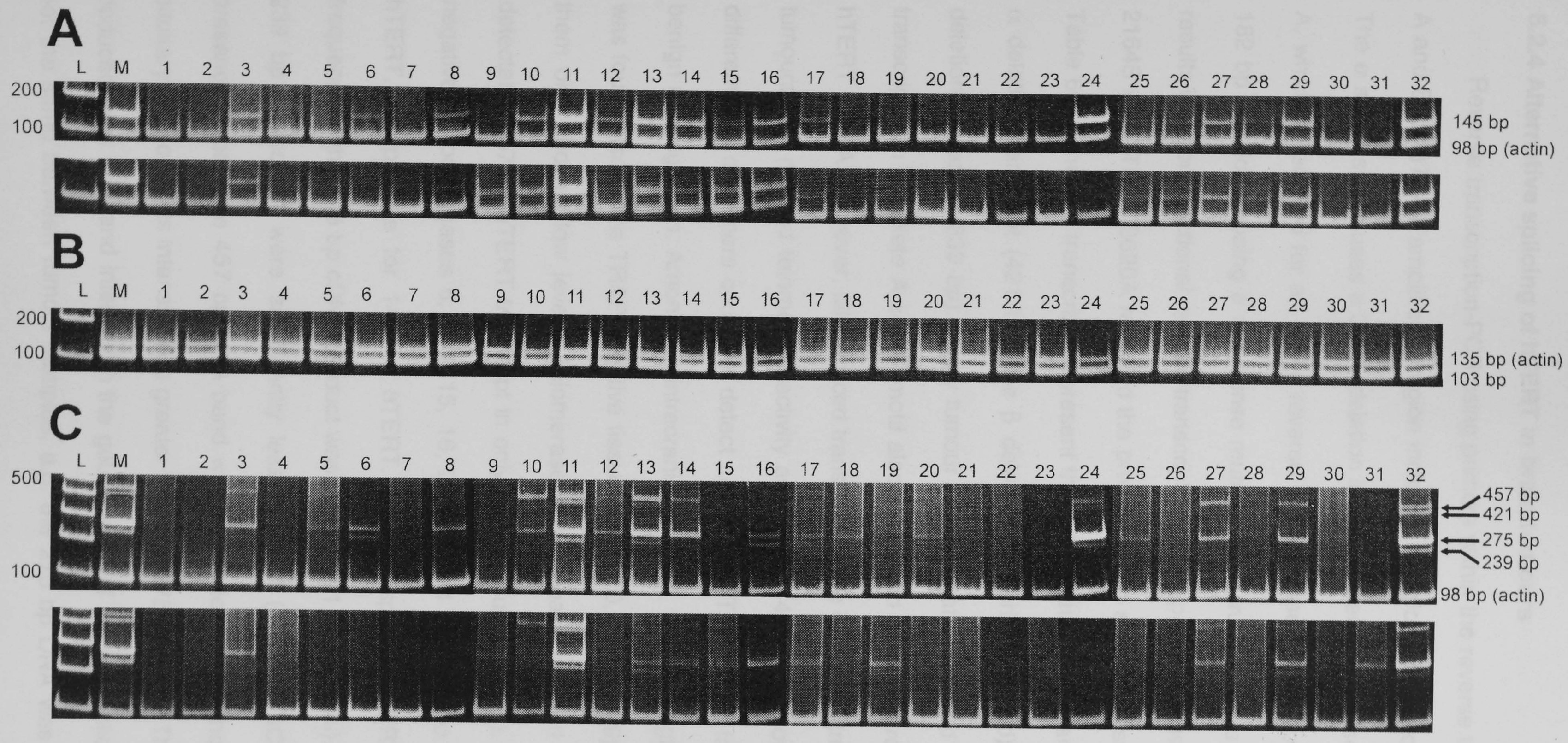

Figure 6.4 RT-PCR detection of hTERT and hTERC in brain tumours. hTERT and alternate splicing of hTERT measured in 2 different samples of each tumour (upper and lower lanes in A and C); (**A**) Expression of hTERT with first set of primers; (**B**) Expression of hTERC. (**C**) Expression of hTERT spliced products with second set of primers. Amplification of β-actin was used to confirm synthesis and integrity of cDNA templates in all samples. L: 100 bp DNA molecular marker; M: Molt-4 positive control.

6.2.4 Alternative splicing of hTERT in brain tumours

Reverse transcription-PCR using primers within the reverse transcriptase domain A and B' of *hTERT* amplified a region including two potential splice sites (Figure 6.1). The α splice site causes a 36 bp deletion in the conserved reverse transcriptase motif A, which is required for an active reverse transcriptase. The β splice site results in a 182 bp deletion causing a non-sense mutation that truncates the protein, which also results in a non-functional reverse transcriptase. PCR performed using primers hTERT-2164S and hTERT-2620A revealed the presence of 4 spliced messages (Figure 6.4C, Table 6.1). These 4 transcripts represent the full-length hTERT transcript (457 bp), the α deletion transcript (421 bp), the β deletion transcript (275 bp), and the α and β deletion transcript (239 bp). Every tumour sample that expressed the 457 bp hTERT transcript with complete A and B' motif also expressed one or more spliced variants of hTERT mRNA. However, all 4 spliced transcripts were detected simultaneously only in tumours with marked telomerase activity and in Molt-4 positive control cells. The two different sets of primers could not detect any of the hTERT PCR fragments in 7 of 18 benign meningiomas. Among the intracranial tumours, the full-length hTERT message was found also in the TRAP-negative tissues (3, 5, 10, 12, and 29), although some of them only showed low levels. Telomerase activity was observed in the absence of detectable 457 bp hTERT transcript in only one tumour (case 17). Eight of 13 TRAP-negative tumours (cases 6, 8, 9, 15, 16, 25, 26, and 28) with no detectable 457 bp hTERT, but positive for 145 bp hTERT, showed spliced hTERT transcripts. The frequency of the 275 bp cDNA product was highest (21 of 32, 66%). The 457, 421 and 239 bp transcripts were significantly less frequent (Figure 6.4C, Table 6.1). The presence of only the 457 bp DNA band was never detected, although in case 10, a pituitary adenoma, its intensity was greater than the 275 bp band. The relative amount, deduced from the band intensity in the gel, of each of the four spliced fragments was not the same between tumour samples, e.g. the 275 bp DNA was relatively more or

less present in comparison with the 457 bp DNA. Analysis of a rapidly growing cell culture from a glioblastoma (U251), not being part of the brain tumours under study, showed all hTERT spliced products *in vitro*.

6.2.5 Immunohistochemical analysis of brain tumour proliferation

Immunohistochemical analysis of tumour proliferation has been accomplished with the Ki-67 monoclonal antibody, which recognizes a nuclear antigen expressed during late G_1, S, G_2 and M phases of the cell cycle. The Ki-67 labelling indices (LI) were determined in randomly chosen areas and calculated as a percentage of the positively stained nuclei over the total number of tumour cell nuclei counted. The mean percentage of proliferating cells in the 32 intracranial tumours is given in Table 6.1. We observed relatively homogenous staining in all samples (Figure 6.5), but in some malignant tumours a heterogeneous distribution was evident. Cases 15, 16 and 23 were excluded because most of the paraffin blocks contained partially or completely oedematous brain tissue. In benign meningiomas, the mean proliferation index was 1.2% (sd=1.0), in atypical meningiomas 3.4% (sd=0.4), and in the remaining malignant brain tumours 13.6% (sd=9.0), revealing a highly significant difference between benign and malignant tumours. The mean proliferation index was 1.9% (sd=1.8) for TRAP-negative tumours, 6.1% (sd=4.7) for low telomerase activity tumours, and 17.5% (sd=10.5) for high telomerase activity tumours. A significant correlation between telomerase activity scores and mean Ki-67 LI was found in intracranial tumours ($y=7.8x-7.1$, $r_p=0.71$ Spearman rank correlation, Figure 6.6), as well as between Ki-67 LI and the degree of the 145 bp hTERT expression ($y=7.7x+2.9$, $r_p=0.74$ Spearman rank correlation, Figure 6.7).

We studied a large array of other proliferation related markers in all samples of brain tumours *in vivo* (tissues embedded in paraffin) as well as *in vitro* (cells grown on thermanox coverslips or fixed and dropped on slides). The rate of ribosome biogenesis is closely related with cell growth and cell cycle progression of the cell. Therefore

AgNORs, which associate with transcriptionally active sites of ribosomal DNA and nucleolin, which regulates the rate of pre-ribosome production were chosen as alternative proliferation markers (Tuteja and Tuteja, 1998; Sirri et al., 2000; Derenzini et al., 2004). They can be considered as markers for protein synthesis and thus the proliferation rate of a given cell. Also of interest is that telomerase RNA accumulates in nucleoli (Filipowicz and Pogacic, 2002). A representative overview of applied proliferation markers is shown in Figure 6.8. Higher percentages of AgNORs and nucleolin dots showed a positive correlation with malignant brain tumours (data not shown). The use of PCNA antibodies proved not to be useful as a proliferation marker in brain tumours (data not shown).

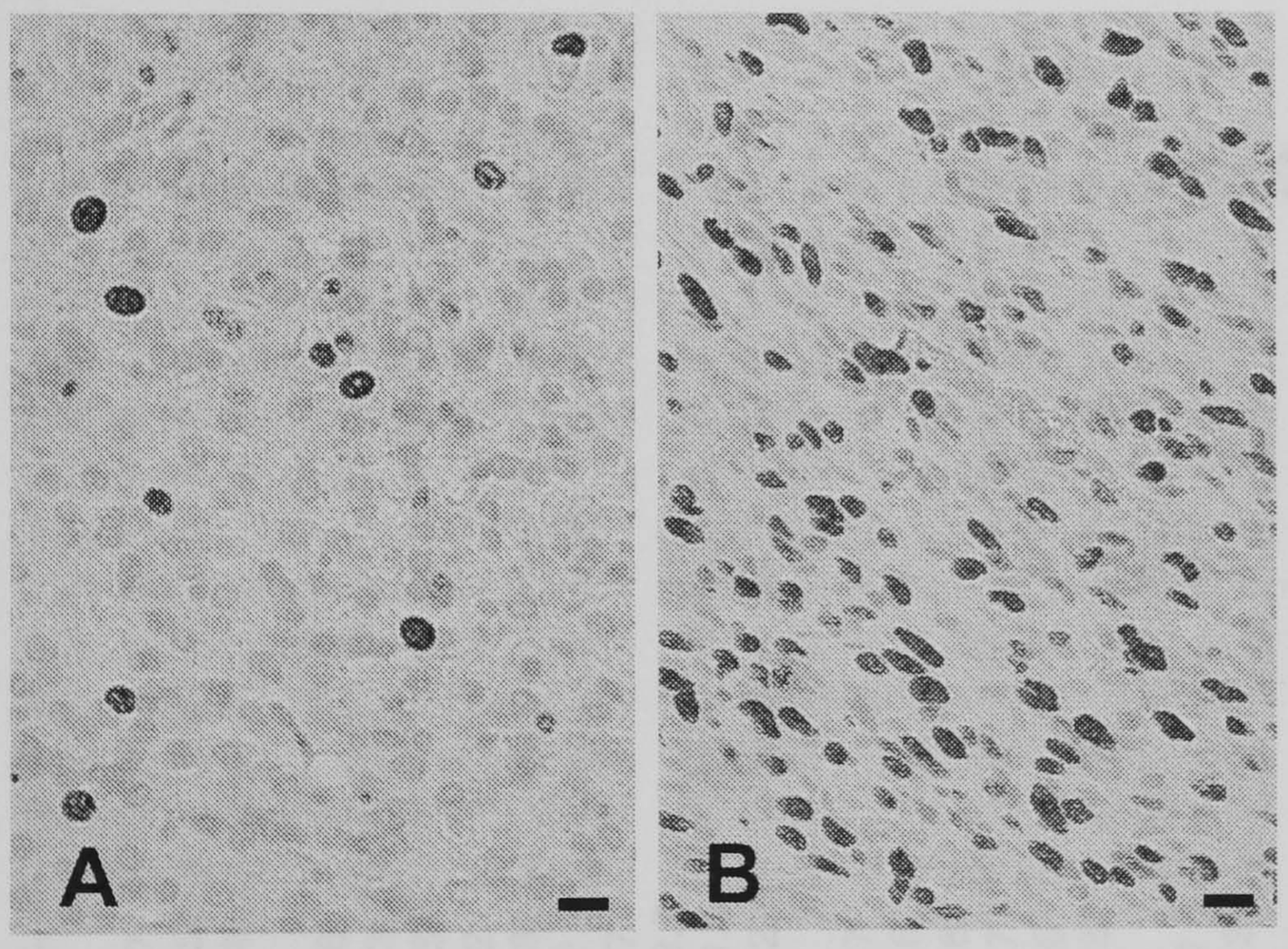

Figure 6.5 Detection of proliferating cells by Ki-67 immunostaining in meningioma (**A**) and in glioblastoma (**B**). Malignant brain tumours, like this glioblastoma in B showed a much higher percentage of proliferating cells than their benign counterparts as meningioma in A.

Table 6.1 Relationship between intracranial tumour type and KI-67 LI, telomerase activity, and telomerase mRNA. [a] All samples were frozen immediately after collection except for *, which were frozen 2-4 h after tumour resection; [b] oedematous brain tissue present in samples from *; [c] – no telomerase activity, + low telomerase activity and ++ high telomerase activity detected in one or two samples; [d] + transcript present and - transcript absent in two different samples. OD: optical density

Case[a] No.	Diagnosis[b]	Ki-67 mean LI (%)	Telomerase[c] activity	hTERT[d] 145bp	hTERT OD	hTERT spliced products[d] 457bp	421bp	275bp	239bp
1	meningothelial meningioma	0	-	-/-	0	-/-	-/-	-/-	-/-
2	meningothelial meningioma	1.7	-	-/-	0	-/-	-/-	-/-	-/-
3*	transitional meningioma	3.5	-/-	+/+	66	+/-	-/-	+/+	-/-
4	transitional meningioma	1.4	-	-/-	0	-/-	-/-	-/-	-/-
5	angiomatous meningioma	2	-	+/-	0	+/-	-/-	+/-	-/-
6	meningothelial meningioma	1.6	-	+/-	35	-/-	-/-	+/-	+/-
7	meningothelial meningiomas	2.3	-	-/-	0	-/-	-/-	-/-	-/-
8	meningiothelial meningioma	1.5	-/-	+/-	34	-/-	-/-	+/-	-/-
9	acoustic schwannoma	2.2	-	-/+	0	-/-	-/-	-/+	-/-
10	pituitary adenoma	1.8	-/-	+/+	53	+/+	-/-	+/-	-/-
11	medulloblastoma	12.1	++/++	+/+	100	+/+	+/+	+/+	+/+
12	astrocytoma	7.7	-/-	+/-	43	+/-	-/-	+/-	-/-
13	glioblastoma multiforme	13.7	++/+	+/+	92	+/+	+/-	+/+	+/+
14*	ependymoma	11.5	+/-	+/+	66	+/-	+/-	+/+	-/-
15*	glioblastoma multiforme*	1.2	-/-	+/+	23	-/-	-/-	-/+	-/-
16*	astrocytoma*	0	-	+/+	50	-/-	-/-	+/+	+/-
17	atypical meningioma	3.7	+/-	+/+	29	-/-	-/-	+/+	+/-
18	meningothelial meningioma	2.6	-/-	-/-	0	-/-	-/-	+/-	-/-
19	meningiothelial meningioma	0.8	-	-/-	0	-/-	-/-	-/+	-/+
20	meningiothelial meningioma	0.7	-	-/-	0	-/-	-/-	+/-	-/-
21	meningiothelial meningioma	0.6	-/-	-/-	0	-/-	-/-	-/-	-/-
22	meningiothelial meningioma	0.8	-	-/-	0	-/-	-/-	-/-	-/-
23*	medulloblastoma*	0	-/-	-/-	0	-/-	-/-	-/-	-/-
24	glioblastoma multiforme	11	++/-	+/-	100	+/-	+/-	+/-	+/-
25	transitional meningioma	0.2	-/-	-/+	0	-/-	-/-	+/-	-/-
26	fibrous meningioma	0	-	+/+	26	-/-	-/-	-/-	-/-
27	atypical meningioma	3.1	+/-	+/+	58	+/+	-/-	+/+	-/-
28	transitional meningioma	1.9	-	+/+	19	-/-	-/-	-/-	-/-
29*	glioblastoma multiforme	6	-	+/+	81	+/+	-/-	+/+	-/+
30	psammomatous meningioma	0.6	-/-	-/-	0	-/-	-/-	-/-	-/-
31	transitional meningioma	0.2	-	-/-	0	-/-	-/-	-/+	-/-
32	glioblastoma multiforme	33.3	++/+	+/+	96	+/+	+/-	+/+	+/+
			7/32 (22%)	20/32 (63%)					

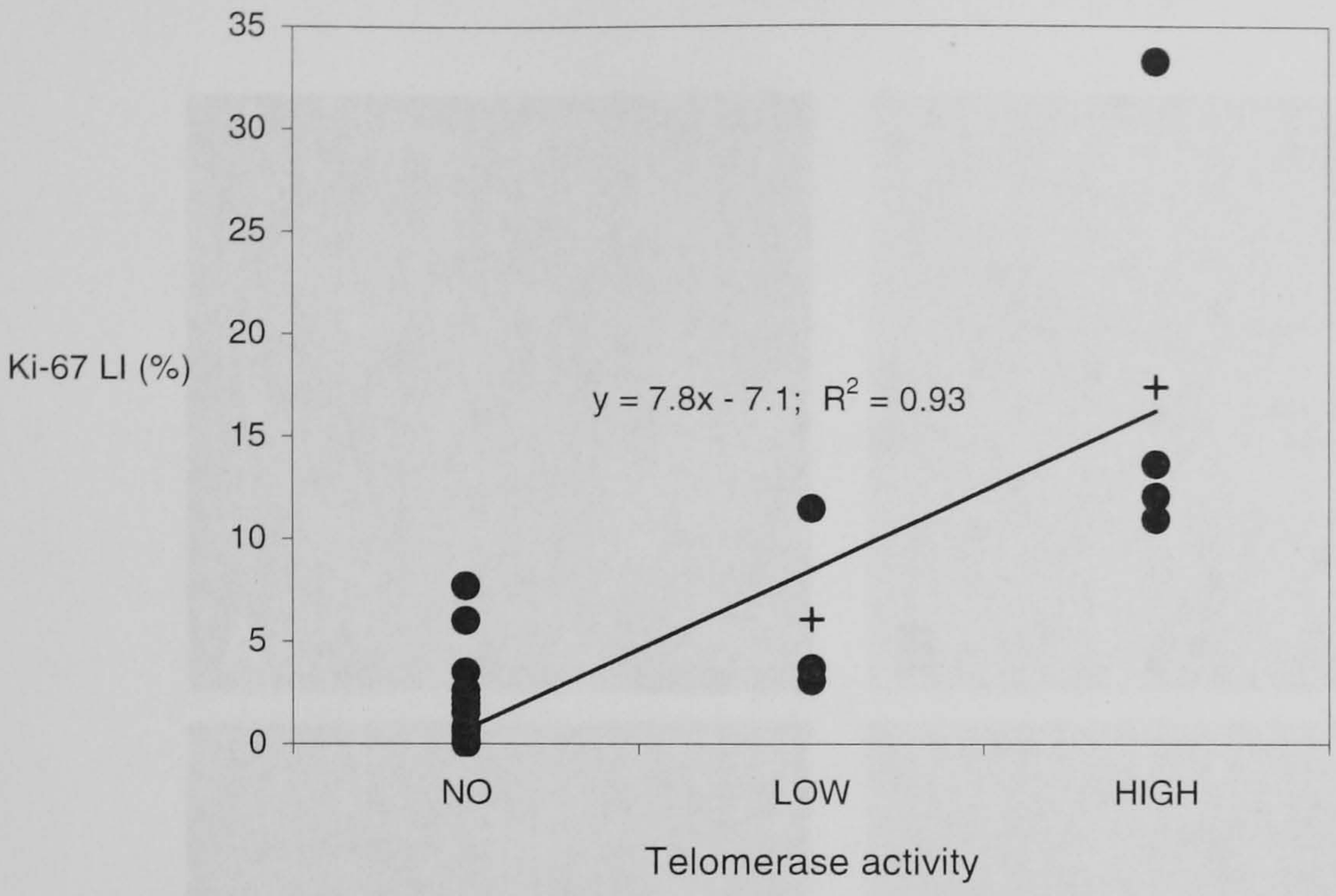

Figure 6.6 Correlation between Ki-67 labelling index (%) and negative, low and high telomerase activity in intracranial tumours as determined by immunohistochemistry and TRAP assay, respectively.

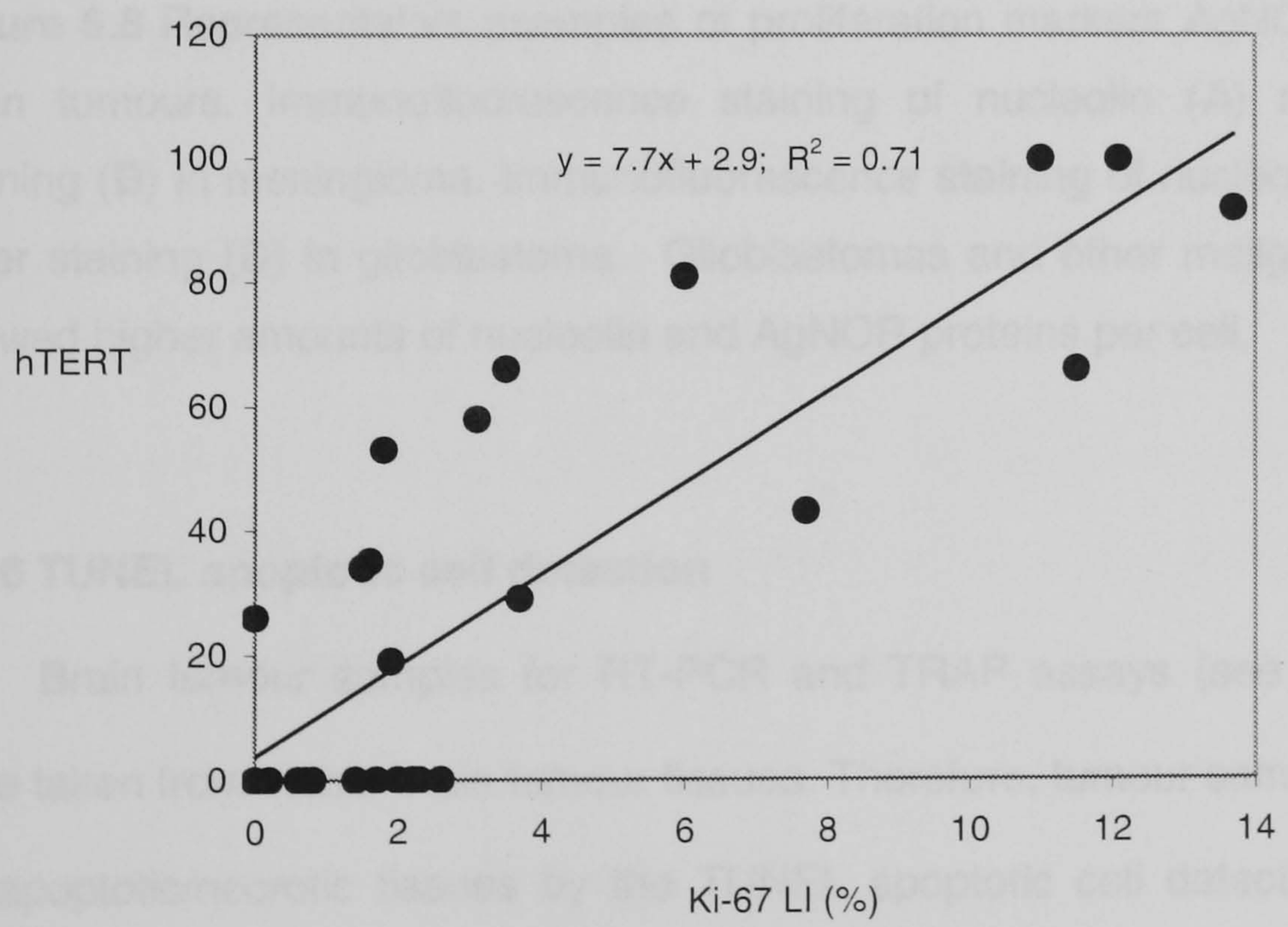

Figure 6.7 Correlation between Ki-67 labelling index (%) and hTERT mRNA expression levels (145 bp hTERT transcripts) in intracranial tumours as determined by immunohistochemistry and RT-PCR, respectively.

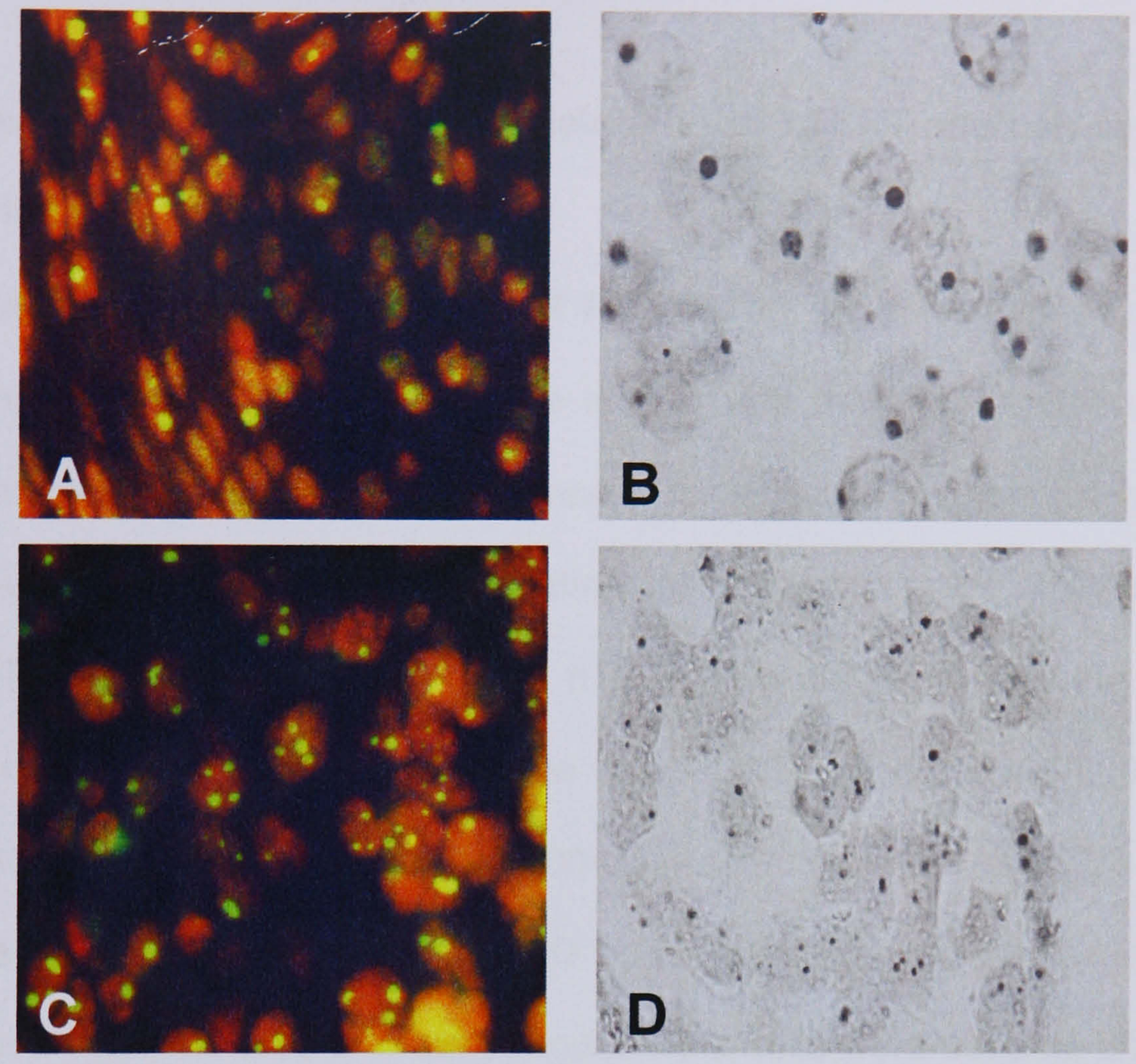

Figure 6.8 Representative examples of proliferation markers AgNOR and nucleolin in brain tumours. Immunofluorescence staining of nucleolin (**A**) and AgNOR silver staining (**B**) in meningioma. Immunofluorescence staining of nucleolin (**C**) and AgNOR silver staining (**D**) in glioblastoma. Glioblastomas and other malignant brain tumours showed higher amounts of nucleolin and AgNOR proteins per cell.

6.2.6 TUNEL apoptotic cell detection

Brain tumour samples for RT-PCR and TRAP assays (see previous sections) were taken from viable brain tumour tissues. Therefore, tumour samples were analysed for apoptotic/necrotic tissues by the TUNEL apoptotic cell detection assay. For the detection of apoptosis only fields of vision containing immunostained nuclei were accepted for the calculation. The apoptotic index (AI) was calculated as a percentage of TUNEL stained nuclei divided by the total number of tumour cell nuclei counted. Regions of apoptotic/necrotic brain tumour tissues were only found in highly malignant

glioblastomas (data not shown) and were discarded for hTERT and telomerase activity analysis.

6.2.7 Double immunocytochemical detection of hTERT and cell cycle-related Ki-67 in brain tumour cells *in vitro*

Brain tumours analysed by hTERT RT-PCR and the TRAP assay demonstrated a correlation between hTERT/telomerase activity with the Ki-67 antigen. However, the level of telomerase activity in brain tumours composed of telomerase-competent cells may depend on the fraction of proliferating cells. Therefore, we assessed the position of hTERT and Ki-67 protein in the cell. hTERT is found throughout the nucleus and is also concentrated in nucleoli (Etheridge et al., 2002; Wong et al., 2002; Yang et al., 2002) and in Cajal bodies (Zhu et al., 2004).

We investigated hTERT and Ki-67 by different immunocytochemical techniques in 21 primary cell cultures of brain tumours. Hela cells were used as a positive control and monocytes and quiescent lymphocytes were used as a negative control. hTERT was detected strongly in Hela cells but was absent in the mononuclear blood cells (Figure 6.9 A-B). Overall, meningiomas showed less hTERT in their nuclei compared with malignant brain tumours (Figure 6.9 C-E). Interestingly, detection of hTERT in the nuclei failed after a week suggesting that hTERT disapears from the nucleus within a few days in cell culture (Figure 6.9 E-F). This could explain the reason why these primary cell cultures were TRAP negative. Similarly, cell culture growth reduction by contact inhibition, as shown by a lower Ki-67 labelling index, revealed also the presence of much less hTERT antigen.

Surprisingly, double staining of hTERT and Ki-67 revealed no positive correlation (Figure 6.10). hTERT antigen is present in proliferating cells *in vitro* but it can also be detected in Ki-67 negative brain tumour cells. This study implies that the hTERT L-20 antigen cannot be used as a proliferation marker in brain tumours *in vitro*.

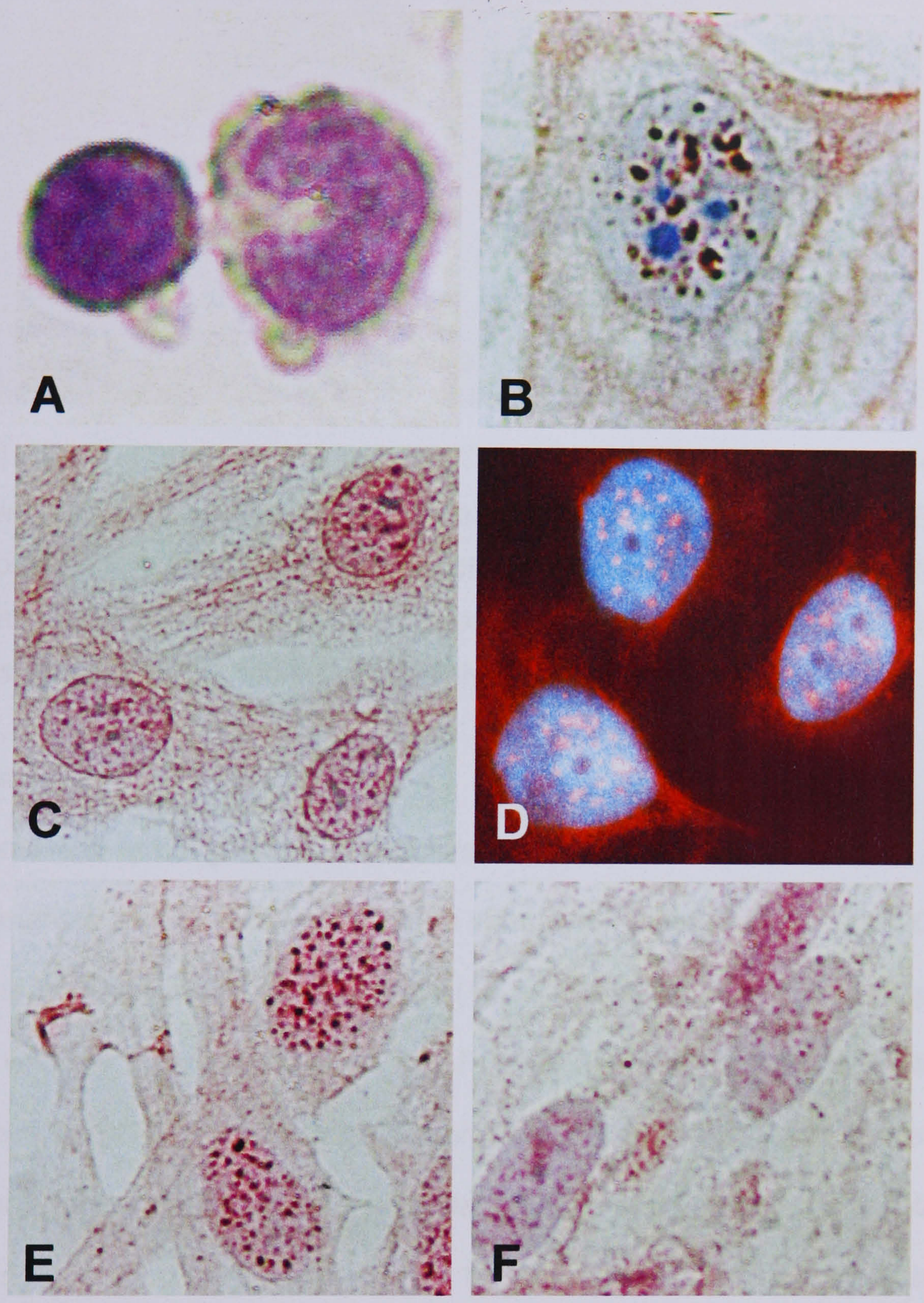

Figure 6.9 Immunocytochemistry of hTERT. Monocytes were used as a negative control (**A**) and Hela cells as a positive control (**B**). hTERT expression in meningioma cells stained with DAB and counterstained with Haematoxylin (**C**); hTERT in meningioma cells stained with Texas Red and counterstained with DAPI (**D**). Glioblastoma cells stained with DAB and counterstained with Haematoxylin (**E**) and after 4 days in culture (**F**).

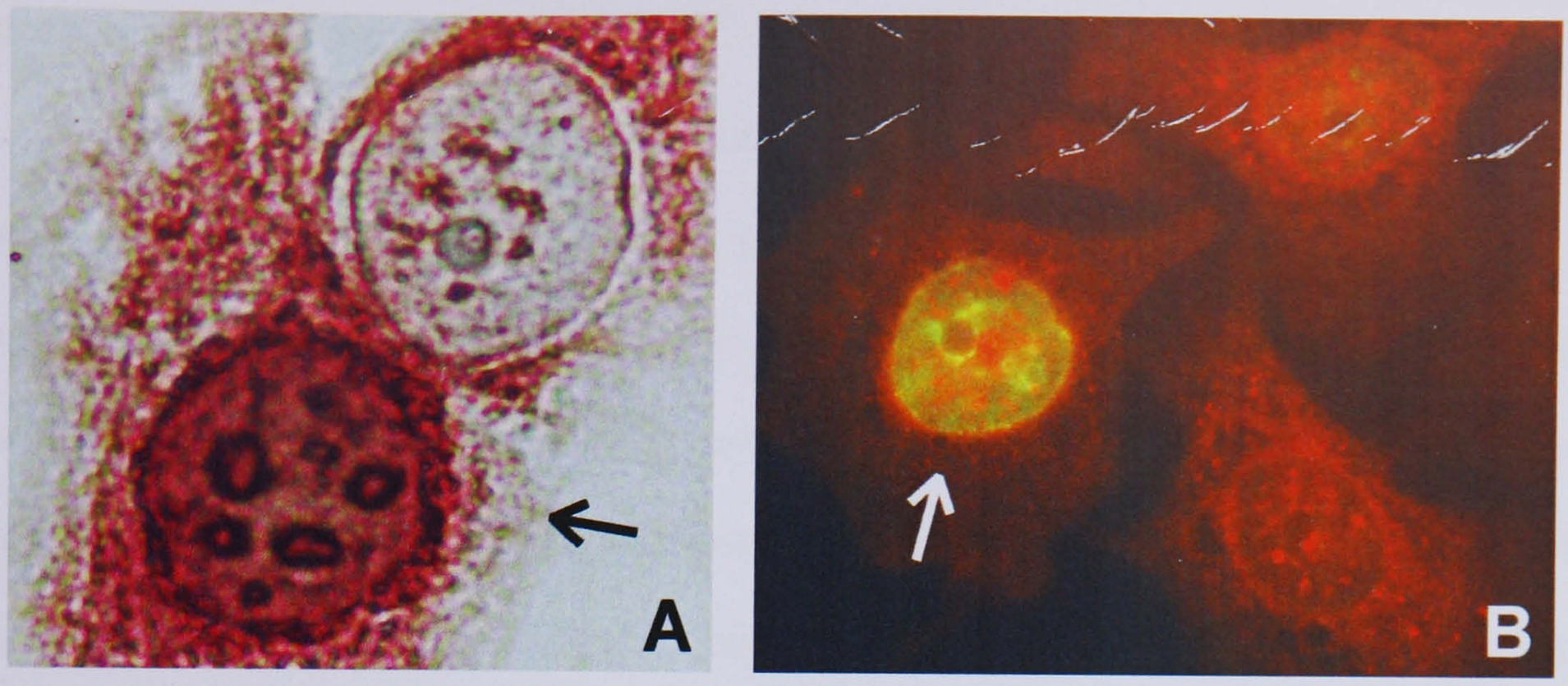

Figure 6.10 Double immunodetection of hTERT and Ki-67 in glioblastoma cells. Cell cultures were grown on thermanox coverslips and stained with anti-TERT L-20 simultaneously either indirectly with a polyclonal anti-Ki-67 (**A**) or directly with a monoclonal anti-Ki-67 (green) (**B**). Arrows point to a nucleus with both hTERT and Ki-67 proteins present. Other nuclei contain only Ki-67 signals.

6.3 Discussion

6.3.1 Telomerase activity in brain tumours

Telomerase activity was undetectable in benign intracranial tumours (20 in total), the majority of which were meningiomas (18 in total) (Table 6.1). It is important to determine whether these results of the TRAP assay are truly negative or positive, since the presence of inhibitors of either the polymerase used in PCR or the telomerase enzyme have been reported to be a potential problem in the analysis of a total protein extract (Wright et al., 1995; Sugino et al., 1997). All meningiomas in our study were attached to the dura and their histological sections, stained with Masson trichrome, mostly showed the presence of connective tissue. Proteins may be present in this connective tissue that inhibit Taq polymerase activity and prevent amplification of telomerase products (Bachor et al., 1999). However, we do not think that telomerase activity in the specimens of meningiomas was suppressed by inhibitors. For example, the amplified 36 bp internal control in each TRAP assay was always present (Figure 6.2) suggesting the absence of PCR inhibitors. In addition, telomerase activity of Molt-4

positive control cells was not inhibited when mixed with the TRAP-negative sample extracts (data not shown).

Although the TRAP assay relies on internal controls to detect PCR inhibitors and spurious telomerase activity, it cannot assess the enzyme inactivation with time. We found that tissue preservation was important for the detection of telomerase activity. Some malignant tumours with a negative or reduced telomerase activity were frozen in liquid nitrogen 2-4 hours after tumour resection. Protein degradation might have occurred in these tissues. We tested this assumption on other tissue samples that had previously been shown to have telomerase activity. We found that telomerase activity was undetectable or showed decreased TRAP products in tissues that had not been frozen immediately (data not shown). Time that elapsed between tumour resection and freezing is apparently important in detecting telomerase enzyme activity. Although telomerase is thought to be detectable even when 100 positive cells are present, small biopsy sizes were excluded because they are far more susceptible to enzyme degradation.

Benign meningiomas, which lacked telomerase activity in multiple regions, showed uniformity of tissue samples in terms of tumour density and cell type. On the other hand, histological sections of malignant tumours invariably consisted of mixtures of tumour cells, necrotic tissues, and remnants of normal brain tissues. It is likely that different regions of glioblastomas may show variation in telomerase activity (Figure 6.3). This finding is supported by *in situ* hybridisation experiments of hTERT, which showed a focal pattern in both TRAP-positive and TRAP-negative glioblastomas (Falchetti et al., 2000). Thus, the classification of a glioblastoma as telomerase-positive, however, seems limited as demonstrated by the markedly intratumoral variation in telomerase activity. This means that a single tumour sample, which was assayed for telomerase activity, can hardly be regarded as representative for a given glioblastoma, limiting the diagnostic value of the telomerase activity assays on glioblastoma cancer biopsies. Intratumoral variations in telomerase activity have also

been documented in high-grade astrocytomas (Kleinschmidt-DeMasters et al., 1998) and in prostate cancer (Wullich et al., 1997). In other studies on telomerase activity, tissue heterogeneity is mostly not taken into account. Histological sections of cases 15, 16 and 23 contained considerable amounts of oedematous brain tissue, which might explain why these malignant tumours were telomerase negative in the specimens used for the TRAP assay.

The absence of telomerase activity suggests that telomerase activity is not an essential prerequisite for meningioma development. Similar observations were made for retinoblastoma (Gupta et al., 1996), renal cell carcinoma (Mehle et al., 1996) and pheochromocytoma (Kubota et al., 1998) as well as for soft tissue tumours (Yan et al., 1999). The absence of telomerase activity in benign meningiomas might correspond to the short telomeres found in these tumours (Chen et al., 2000). Also, the presence of dicentric chromosomes in telomerase negative meningiomas (Carroll et al., 1999; Sawyer et al., 2003), which are absent in glioblastomas (Magnani et al., 1994), might represent abnormal telomere function due to absence of telomerase. Langford et al. (1997) and Simon et al. (2000) observed, however, telomerase activity in five of 30, and in seven of 34 benign meningiomas, respectively. These authors have used the downstream primer CX in the TRAP assay, which can form primer-dimer products and thus lead to false-positive results. We used the alternative downstream primer ACX, which results in a significant reduction of primer-dimer PCR artefact formation (Kim et al., 1994).

6.3.2 Telomerase mRNA expression in brain tumours

The human telomerase catalytic subunit (hTERT) is regarded as the core component of the enzyme telomerase (Wick et al., 1999). *hTERT* expression has been demonstrated in association with telomerase activity, although it may also be present in the absence of telomerase activity (Kyo et al., 1999; Liu et al., 1999; Wu et al., 1999; Yan et al., 1999; Falchetti et al., 2000; Simon et al., 2000; Ulaner et al., 2000). To date,

hTERT regulation in relation to absence or presence of telomerase activity is not fully understood. It is considered to take place at the transcriptional level (Greenberg et al., 1999), post-transcriptional level (Li et al., 1998), or at the post-transcriptional level through alternative splicing (Ulaner et al., 1998; 2000).

In this study, the relative expression of *hTERT* was assessed by densitometric analysis of the PCR products obtained by a duplex PCR protocol that allowed the simultaneous amplification of *hTERT* and the housekeeping gene transcripts. Messenger RNA, encoding the reverse transcriptase of telomerase, was present in 20 of 32 (63%) intracranial tumours, whereas telomerase could be detected in only 7 (22%) intracranial tumours (Figure 6.4; Table 6.1). The detection of hTERT mRNA may be a more sensitive indicator of enzyme activity than TRAP due to its insensitivity to proteases or protein inhibitors. RT-PCR has the added advantage of being far more tolerant in amplifying fragments of partially degraded RNA than the TRAP assay in detecting enzyme activity. This scenario seems plausible in case 29, a glioblastoma which was frozen in liquid nitrogen 2.5 hours after surgery, where hTERT mRNA is expressed in the absence of an expected telomerase activity (Figures 6.2 and 6.4).

Previous studies have shown that the expression of hTERT mRNA correlates with telomerase activity (Kilian et al., 1997; Nakayama et al., 1998; Nakamura et al., 1999; Ulaner et al., 1998; 2000; Chong et al., 2000; Yan et al., 2001; Boldrini et al., 2003) and may be used as an alternative tumour marker (Kyo et al., 1999; Park et al., 1999; Wu et al., 1999). However, hTERT mRNA expression did not coincide perfectly with telomerase activity in cancers of various tissues e.g. glioblastomas (Falchetti et al., 2000), endometrial cancers (Kyo et al., 1999), lymphocytes (Liu et al., 1999), meningiomas (Simon et al., 2000), leiomyomas (Ulaner et al., 2000), skin tumours (Wu et al., 1999) and sarcomas (Yan et al., 1999). Intracranial tumours in our series of samples expressed hTERT independently of the presence or absence of detectable telomerase activity. Thirteen cases were found with hTERT mRNA expression and lacking telomerase activity, but with mostly lower levels of hTERT mRNA expression

than those in TRAP-positive cases. Our results suggest a lack of a strongly positive correlation between hTERT mRNA expression and measurable telomerase activity. Although the extracts used for TRAP assay and RT-PCR were obtained from different portions of the same tumour, these discordances cannot be fully explained by heterogeneity of the tumour cells contained in the specimens or by poor sample preparation for the TRAP assay. Indeed, if telomerase was present in an active or inactive form in the TRAP-negative tumours, a marked expression of hTERT mRNA as in the TRAP-positive tumours would be expected. The lack of telomerase activity in 13 hTERT mRNA-positive meningiomas could indicate that in addition to up-regulation of hTERT expression, further events are required for the expression of functional telomerase, which might lead to proliferation.

To determine whether telomerase activity is regulated at the transcriptional level, the expression of the telomerase RNA component was analysed in telomerase-positive and negative brain tumours. In all brain tumours and normal brain samples examined, the presence of hTERC did not indicate the presence of telomerase activity (Figure 6.4 B). These results are in accordance with recent reports that the presence of telomerase RNA component in the absence of detectable telomerase activity is observed in a number of normal tissues and in some tumours (Feng et al., 1995; Kyo et al., 1999; Wu et al., 1999; Yan et al., 2001).

6.3.3 Alternative hTERT splicing in brain tumours

Like *BRCA1*, which has 4 different splicing variants (Miki et al., 1994), the hTERT transcript has been shown to have at least six alternative splicing sites (four insertion sites and two deletion sites), and variants containing both or either of the deletion sites are present (Kilian et al., 1997; Wick et al., 1999). The α deletion (lacking 36 nucleotides in the beginning of exon 6), the β deletion (lacking 182 nucleotides corresponding to exon 7 and 8) and the α+β deletions (lacking both sites) have been

studied in various tissues relatively frequently (Kilian et al., 1997; Ulaner et al., 1998; 2000; 2001; Wick et al., 1999; Yi et al., 2001) but not in brain tumours. Only the full-length hTERT transcript is considered to be functional in activating telomerase, while the α deletion has been shown to act as an endogenous negative telomerase regulator (Colgin et al., 2000; Yi et al., 2000). The α-form of hTERT inhibits telomerase activities in telomerase-positive cells, which results in telomere shortening and chromosome end-to-end fusions (Colgin et al., 2000). These results suggest a possible role for hTERT splice variants in the regulation of telomerase activity. The function of the remaining splice variants of hTERT is still unclear; it is generally accepted that these cannot play a role in the activation of telomerase, since they lack key reverse transcriptase or C-terminal sequences as a result of open reading frame shifts and premature stop codons (Wick et al., 1999).

Many of the brain tumours in our study had spliced variants of the two conserved hTERT motifs: motif A contained a 36 bp deletion, resulting in the 421 bp band, whereas the 275 bp PCR product contained a 182 bp deletion between motif A and motif B' of telomerase RT protein (Figure 6.1). Certain tumours, cell lines, foetal tissues and normal tissues, show similar spliced variants (Kilian et al., 1997; Brenner et al., 1999; Ulaner et al., 1998; 2000). All four spliced products were detected simultaneously only in samples with marked telomerase activity (Figures 6.2 and 6.4 C). Thirteen hTERT-positive tumours (hTERT full length transcripts and spliced variants) did not express enzyme activity. Alternately spliced hTERT transcripts could account for enzyme inactivity in the absence of hTERT full-length transcripts in some of these tumours (cases 6, 8, 9, 15, 16, 25, 26, and 28) (Figure 6.4 C; Table 6.1).

To explain the absence of telomerase activity in tumours despite absence of telomerase inhibitors and optimal tissue preservation, the existence of an ALT mechanism has been suggested (Bryan et al., 1997; Kim and Wu, 1997; Reddel et al., 1997). Chen et al (2000) found that the mean TRF length of the tumours with telomerase activity was significantly shorter than that of the tumours with undetectable

telomerase activity for each tumour. However, the occurrence of these mechanisms may be ruled out in benign meningiomas because reduced telomere lengths were detected in these tumours (Chen et al., 2000) suggesting that telomere elongation did not occur.

At present, undetectable hTERT mRNA in meningiomas cannot be explained by genetic alterations in hTERT. The *hTERT* gene is located on chromosome 5p and deletions in this region of meningiomas are not reported in literature so far (Sanson and Cornu, 2000; Lusis and Gutmann, 2004; Whittle et al., 2004).

6.3.4 Brain tumour cell proliferation

Telomerase activity was demonstrated in proliferating stem cells and in tissues during embryonic development (Wright et al., 1996; Ulaner and Guidice, 1997; Ulaner et al.,1998). Notably, all telomerase-positive tissues are permanently renewing epithelia or tissues that proliferate in regular cycles. It seems that telomerase activity can be detected also in brain tumours with a high proliferation index. Falchetti et al. (2000) demonstrated that TRAP-positive glioblastomas have a much higher proliferation index than TRAP-negative ones. In our study, benign meningiomas showed no or very low numbers of Ki-67 positive nuclei at the moment of observation, whereas malignant brain tumours with telomerase revealed high Ki-67 LI (Figure 6.5). Apparently, a slowly growing benign meningioma in which most of the cells are quiescent has no or very low levels of telomerase, whereas a rapidly dividing tumour such as a glioblastoma and medulloblastoma has high levels of telomerase. Although the number of TRAP-positive tumours in our series was low, it seems that we found a significant correlation between telomerase activity scores and Ki-67 proliferation index (Figure 6.6). A positive association was also found between Ki-67 proliferation index and the degree of hTERT mRNA expression (Figure 6.7). The correlation that we found between telomerase and *in vivo* cell proliferation is in line with data for lung cancer (Albanell et al., 1997; Fujiwara et al., 2000), melanoma (Miracco et al., 2000),

colorectal adenocarcinomas (Okayasu et al., 1998), and meningiomas (Simon et al., 2000).

6.4 Summary

Telomerase activity was examined in intracranial tumours and compared with gene expression of the two core components of telomerase, the reverse transcriptase subunit (hTERT) and the RNA subunit (hTERC), and proliferative index. We investigated 32 tumours across 3-5 sampled regions (20 meningiomas, 1 acoustic schwannoma, 1 pituitary adenoma, 8 gliomas, and 2 medulloblastomas).

Telomerase activity was demonstrated by the telomeric repeat amplification protocol (TRAP) assay in 7 (22 %) intracranial tumours (4 malignant brain tumours, 2 atypical meningiomas and 1 ependymoma) but could not be detected in the 18 (100 %) benign meningiomas.

hTERT and hTERC mRNA were detected by RT-PCR. hTERT mRNA was present in 20 (63%) intracranial tumours. Whereas hTERT mRNA transcripts were consistently low or absent in meningiomas, malignant brain tumours exhibited elevated hTERT mRNA's. Multiple regions of glioblastomas showed differences in telomerase activity and in the presence of hTERT mRNA.

RT-PCR analysis revealed, for the first time in intracranial tumours, the presence of hTERT mRNA spliced products, corresponding to full-length mRNA as well as spliced mRNA's with critical reverse transcriptase motifs deleted. Only tumours with marked telomerase activity showed all hTERT spliced messages simultaneously. The absence of a positive correlation between telomerase activity and hTERT mRNA could not be attributed to the presence of hTERT spliced variants.

We found a significant correlation between telomerase activity scores and Ki-67 proliferation index. A positive association was also seen between Ki-67 staining and the degree of hTERT mRNA expression. This shows that there seems to be a

relationship between telomerase activity or the degree of hTERT expression and proliferation rate in intracranial tumours.

In summary, multiple specimens of benign meningiomas demonstrated no detectable telomerase activity and expressed no or low levels of hTERT mRNA. hTERT expression may therefore not be a marker for tumour diagnosis as such. Further experiments are needed to clarify whether hTERT splicing is a limiting factor for the expression of telomerase activity in brain tumours. High telomerase activity and hTERT mRNA expression were detected solely in glioblastoma and medulloblastoma, tumours with a high proliferation rate.

CHAPTER 7

GENERAL DISCUSSION AND PROSPECTS FOR FUTURE RESEARCH

In this thesis we assessed the role of telomeres/telomerase in cellular DNA damage response and in benign and malignant brain tumours. Our results revealed some previously unknown aspects of telomere maintenance or telomerase regulation and these are briefly summarized below.

7.1 Telomere length measurement by flow-FISH

To accurately assess telomere function it is frequently necessary to measure telomere length in cells under investigation. As discussed in Chapter 3 several methods are commonly used for telomere length measurements (Table 3.3) and we specifically focused on one of the most recent methods – flow-FISH. The key reason for this is that flow-FISH is much faster than other methods and results can be generated within several hours. In contrast, techniques such as Southern blot or Q-

FISH may require several days to obtain results. By analysing several human and mouse cell lines by flow-FISH we discovered a phenomenon that we termed TELEFLUCS (TElomere LEngth FLUctuations in Cell Subpopulations). Although we observed TELEFLUCS using Q-FISH and Southern blot, these methods are inferior to flow-FISH for detecting cell subpopulations with different telomere lengths within the same sample. For example, Southern blot and Q-FISH can detect TELEFLUCS only if subpopulations of cells with different telomere lengths comprise relatively large percentages of cells in a given sample. In contrast to flow-FISH neither method can provide accurate quantitative assessment of cell subpopulations i.e. the proportion of subpopulation x relatively to subpopulations y or z. In addition, based on our results we proposed that flow-FISH should be a method of choice for assessing the average telomere length in human lymphocytes. A typical sample of peripheral blood contains different subpopulations of lymphocytes and these have different telomere lengths (Rufer et al., 1998; 1999; Batliwalla et al., 2000; Brummendorf et al., 2000; Baerlocher and Lansdorp, 2003). By analysing peripheral blood samples using Southern blot, Q-FISH or quantitative PCR no laboratory was able to show existence of lymphocyte subpopulations with different telomere lengths (Poon et al., 1999; Martens et al., 2000; Terasaki et al., 2002; Wu et al., 2003) and this was only possible to demonstrate by flow-FISH (Rufer et al., 1998; 1999; Batliwalla et al., 2000; Brummendorf et al., 2000; Baerlocher and Lansdorp, 2003). Ability to detect subpopulations of lymphocytes with different telomere lengths is important. For example, the most recent study suggests that the "life-stress" can affect telomere length and that this can be used as a predictor of cell aging and therefore could be a useful indicator of patient general health (Epel et al., 2004). Epel et al. (2004) measured telomere length in peripheral blood lymphocytes by real-time PCR. By using flow-FISH in similar future studies the resolution of average telomere length measurement from any individual will be greatly improved through identifying telomere length in several subpopulations of lymphocytes as detected by

antibodies specific to these lymphocyte subpopulations, a technique known as multi-colour flow-FISH. The use of multi-colour flow-FISH on peripheral blood samples, therefore, may have important prognostic applications.

We have also shown that we can use flow-FISH for telomere length measurements in human fibroblasts. To the best of our knowledge this is the first successful attempt to measure telomere length by flow-FISH in human fibroblasts. However, further improvements in our flow-FISH method are required to optimise telomere length measurements in fibroblasts. For example, we think that stripping fibroblasts from the cytoplasm can result in reduced auto-fluorescence, which is one of the problems associated with telomere length measurements in senescing human fibroblasts.

7.2 Accelerated telomere shortening and telomere dysfunction in DNA damage response defective cells

Accelerated telomere shortening has been conclusively demonstrated in several human syndromes characterized by defective DNA damage responses at cellular and molecular levels. These include ataxia telangiectasia (AT), Nijmegen breakage syndrome (NBS) and Fanconi anemia (FA) (Metcalfe et al., 1996; Pandita and Dhar, 2000; Adelfalk et al., 2001; Hande et al., 2001; Ranganathan et al., 2001; Tchirkov and Lansdorp, 2003). We have previously been able to show association between short telomeres and alterations in DNA damage response as measured by chromosomal radiosensitivity in a group of breast cancer patients (McIlrath et al., 2001) and our results have recently been confirmed in a much larger group of different cancer patients (Wu et al., 2003). Collectively, these results provide an intriguing clue i.e. that alterations in telomere maintenance could constitute a marker of defective DNA damage responses. If correct, this possibility would be enormously useful in, for example, detecting people at risk from cancer i.e. defective DNA damage response is a

cancer predisposing factor (Slijepcevic, 2004). To provide a theoretical framework for understanding these results from the perspective of cancer detection and treatment we have recently proposed that a group of genes in mammalian cells can, if affected. cause dual phenotypes, namely sensitivity to ionising radiation (IR) as one phenotype and telomere dysfunction as the other phenotype and this group of genes is termed TERAGENE (TElomeres and RAdiosensitivity GEne NEtwork) (Slijepcevic, 2004). The current number of genes that cause these phenotypes in mammalian cells stands at 10 and they are summarized in Table 7.1. Therefore, the main implication of the TERAGENE hypothesis is that the two phenotypes, namely cellular/organismal sensitivity to IR and telomere dysfunction are in many cases linked.

Results generated during the course of this project provide additional evidence for the possibility that IR sensitivity and telomere dysfunction may be linked. For example, in addition to being able to confirm accelerated telomere shortening in cells from AT, NBS and FA patients in comparison with cells from apparently normal individuals (Figures 4.2 A and 4.4 A), we have also detected accelerated telomere shortening in a panel of five novel cell lines originating from patients who over-responded to radiation therapy (Figures 4.2 B and 4.4 B). Radiosensitivity of these patients is caused by different genetic defects including defects in ligase I, ligase IV, Artemis, and two less well-defined defects. In the case of one patient (named 2BN) it is likely that a new, as yet unidentified, factor involved in DNA double strand break (DSB) repair may be involved (Dai et al., 2003). The remaining patient had xeroderma pigmentosum (complementation group XP-C) but in addition showed severe sensitivity to IR, a possibility consistent with an additional mutation in a gene responsible for IR response i.e. XP patients are not normally sensitive to IR (Rogers et al., 2000). In almost all cases these novel cell lines showed accelerated telomere shortening in comparison to control cell lines (Figure 4.6).

Table 7.1 Summary of genetic defects that affect telomere maintenance and radiosensitivity in mammalian cells (adapted from Slijepcevic, 2004).

Defect	Species	Telomere dysfunction phenotype		Radiosensitive	Reference.
		Telomere length	Telomere fusion frequency		
ATM	Human	Short	High	yes	Hande et al., 2001
NBS	Human	Short	Unknown	yes	Ranganathan et al., 2001
FANC-A	Human	Short	High	yes	Callen et al., 2002
Ku	Mouse	Elongated	High	yes	Samper et al., 2000
DNA-PKcs	Mouse	Normal	Medium	yes	Goytisolo et al., 2002 Espejel et al., 2004
PARP1	Mouse	Short/Normal	High/Medium	yes	d'Adda di Fagagna et al., 1999 Samper et al., 2001
RAD54	Mouse	Short	Low	yes	Essers et al., 1997 Jaco et al., 2003
RAD51D	Mouse	Short	Medium	yes	Tarsounas et al., 2004
PARP2	Mouse	Normal	Low	yes	Dantzer et al., 2004 Ménissier-de Murcia et al., 2003
mTERC	Mouse	Short	Medium	yes	Goytisolo et al., 2000

We also observed accelerated telomere shortening in murine *BRCA1* deficient cells in comparison with a *BRCA1* proficient cell line (Figure 4.11 A). We also transiently depleted BRCA1 by siRNAs in two human mammary epithelial cell lines (Figures 5.1; 5.2; 5.3 and 5.4) but could not find changes in telomere length in comparison with control cells (Figure 5.8).

Given that some genes from the TERAGENE family have not been shown to play a direct role in telomere maintenance in the sense that they do not localise at telomeres (e.g. ATM), and the fact that this also applies to the proteins defective in our novel cell group (e.g. ligase I, ligase IV, Artemis) one of the implications of the TERAGENE hypothesis is that accelerated telomere shortening may be a general consequence of radiosensitivity. A theoretical framework that can explain this possibility already exists. For example, IR exerts its effects on cells through causing oxidative stress and telomeres are exceptionally sensitive to oxidative stress (von Zglinicki, 2002). In line with this possibility it was recently shown that *ATM* defective cells show telomere dysfunction largely as a result of oxidative stress (Tchirkov and Lansdorp, 2003).

Accelerated telomere shortening is usually associated with dysfunctional telomeres and these can be detected by several methods. For example, we have observed an increased incidence of chromosomes lacking detectable telomeric FISH signals in all the DNA damage response deficient cells in comparison to cells from normal individuals (Figure 4.9) a possibility which further suggests that telomeres shorten faster in DNA damage response defective cells. Chromosome ends that most frequently lack a FISH signal preferentially participate in end-to-end fusions, providing a direct link between short telomeres and end-to-end fusions (Hemann et al., 2001). Although we observed chromosomes lacking detectable telomere FISH signals in radiosensitive fibroblasts (Figure 4.9), chromosome end-to-end fusions were rare in

metaphase cells of radiosensitive fibroblast cell lines. In contrast, we observed elevated levels of anaphase bridges in these cells (Figure 4.8). Future work is required to explain these discrepancies.

We have also observed cytological evidence of telomere dysfunction in mouse *BRCA1* deficient cells. For example, elevated levels of end-to-end chromosome fusions, chromosomes lacking telomeric FISH signals and extra-chromosomal telomeric fragments were present in these cells in comparison with control cells (Figure 4.12). Extra-chromosomal telomeric fragments had a form of double minute chromosomes (Figure 4.12 B) and were similar to those recently reported in cells from *ERCC1/XPF* deficient mice (Zhu et al., 2003) suggesting that BRCA1 might play a similar role at telomeres as ERCC1/XPF. This enzyme, a well-known DNA repair enzyme that cleaves away portions of DNA strands that have been damaged by ultraviolet light, is responsible for removing the 3' overhang strand from uncapped telomeres. In addition we identified a lymphoblastoid cell line from a *BRCA1* carrier and a breast tumour cell line (HCC1937) with elevated levels of telomeric fusions (Al-Wahiby and Slijepcevic, in press). Thus overall, these cytogenetic analyses indicate that accelerated telomere shortening in mouse *BRCA1*$^{-/-}$ cells causes telomere dysfunction whereas telomeres remain functional in control cell lines. By using siRNA oligonucleotides against human *BRCA1* we have been able to significantly reduce expression of this gene in two mammary epithelial cell lines (Figures 5.1; 5.2; 5.3 and 5.4). We observed a significant increase in anaphase bridge frequency in one cell line compared with the mock-transfected counterpart (Figure 5.5 A). Future work is now required to examine in more detail whether mammary cells transfected with BRCA1 siRNA oligonucleotides show telomere dysfunction and we are currently exploring other techniques to determine whether mammary epithelial cells with reduced BRCA1 levels show impaired telomere maintenance (Figure 5.6).

Finally, we have been able to show that human ALT positive cell lines show

dysfunctional telomeres as detected by either the presence of DSBs at their telomeres or cytogenetic analysis. We believe that this is a particularly interesting observation from the perspective of cancer therapy. Anti-telomerase drugs have been suggested as a potentially promising anti-cancer therapeutic tool. However, cancer cells may use ALT mechanisms in the absence of telomerase (Henson et al., 2002). Our results suggest that ALT cells show dysfunctional telomeres and usually cells with dysfunctional telomeres are sensitive to IR (see above). If this is the case with human ALT cells than the problem of ALT activation as a result of exposing cancer cells to anti-telomerase drugs may be solved by exposing these cells to IR.

In conclusion, evidence from this study supports the hypothesis that the phenotypes of telomere dysfunction and altered DNA damage responses as revealed by IR sensitivity are linked in many cases. However, more work needs to be done to verify mechanisms underlying this link.

7.3 hTERT and telomerase activity in brain cancer

Brain tumours exhibit considerable chromosome instability (El-Zein et al., 1999; Hui et al., 2001; Sawyer et al., 2003), suggesting that DNA repair mechanisms may be impaired in these cells or that their genetic susceptibility may lead to defects in DNA damage response pathways. Since the development of the TRAP (telomeric repeat amplification protocol) assay, the number of reports investigating the association of telomerase activity with human cancer has increased exponentially. Nearly, all cancer types have been screened, and a strong association between the presence of telomerase and malignancy has been established. Importantly, high telomerase activity generally indicates aggressive potential, and frequently, but not always, high proliferation rates (reviewed in Dhaene et al., 2000). The latter observation inspired many researchers not only to regard telomerase as a new proliferation marker, but also to accept that cells are telomerase-negative only when TRAP results are negative after

excessive growth stimulation of cells (Greider, 1998; Wynford-Thomas, 1999). Since in most cancers and in stem cells of renewal tissues, telomerase activity levels generally correlate with the proliferation state of the cells (Greider, 1998), it seems appropriate to regard the enzyme's activity as a guarantee for indefinite cellular replicative capacity if there is a drive for proliferation and if nothing else arrests the cells.

At the time when we started this project no hTERT assessments were available in the literature. Only the standard PCR based TRAP was applied to assess telomerase activity in brain tumours and, particularly in meningiomas, an unclear picture emerged as to whether or not these tumours have telomerase activity (DeMasters et al., 1996; Langford et al., 1997; Hiraga et al., 1998; Sano et al., 1998; Carroll et al., 1999; Falchetti et al., 1999; Simon et al., 2000; Boldrini et al., 2003; Pistolesi et al., 2004). Although meningiomas are generally benign, i.e. encapsulated by a connective tissue and thus cells do not metastasise, they can grow to large sizes within the brain, which can be life threatening. We hoped by employing RT-PCR and immunocytochemistry to get a more informative view on telomerase in brain tumours. Since the presence of mRNA splicing was first suggested (Chow et al., 1977), alternative splicing was found to be a very important level of gene regulation (Lopez, 1998) and its existence is now predicted in one-third of the genes (Mironov et al., 1999). hTERT spliced variants were discovered in various tissues (KIlian et al., 1997) and are believed to be a limiting factor for the expression of telomerase activity (Kilian et al., 1997; Brenner et al., 1999; Ulaner et al., 1998; 2000). Therefore, we examined whether hTERT splicing variants were limiting components for the expression of telomerase activity in brain tumours, particularly in meningiomas.

Our results revealed for the first time hTERT mRNA and their spliced variants in brain tumours. hTERT mRNA was absent or expression levels were low in meningiomas and mostly high in malignant brain tumours, in agreement with telomerase activity in brain tumours. Although we found positive correlations between

telomerase activity, hTERT mRNA levels and proliferation (Figures 6.6 and 6.7), the presence of hTERT splice variants did not strictly correlate with the absence of telomerase activity (Figure 6.4; Table 6.1). We detected, in total, eight telomerase negative tumours (mainly meningiomas) out of 32 brain tumours with hTERT mRNA splicing variants and this opens up the possibility that hTERT splicing may contribute to activation of ALT mechanisms i.e. tumour cells need to maintain telomeres in the absence of telomerase activity. Elongated telomere lengths, for example, were detected in meningiomas with undetectable telomerase activity (Chen et al., 2000). We, therefore, speculate that alternative splicing of hTERT could be involved in telomerase and/or telomere length regulation in brain tumours. Furthermore, we detected the main component of telomerase, hTERT, by immunocytochemistry in TRAP-negative meningiomas *in vitro.* This suggests that low levels of telomerase activity, which are below detection of TRAP assay, might operate in meningiomas.

7.4 Future research

As discussed above, novel results generated by this thesis include:

- Discovery of TELEFLUCS
- Discovery of telomere dysfunction in ALT cells
- Potential implication of *BRCA1* in telomere maintenance
- Demonstration of accelerated telomere shortening in 5 novel human radiosensitive cell lines
- Discovery of splice variants of hTERT in brain tumours.

To explore the significance of these results several lines of research are now being pursued in our laboratory. First, it is of interest to determine whether the observed telomere dysfunction phenotype in ALT cells has any effect on survival of these cells after, for example, treatment with IR. It is well documented that telomere dysfunction causes organismal and cellular sensitivity to IR (Goytisolo et al., 2000;

Wang et al., 2000; McIlrath et al., 2001). If the same happens in ALT cells this may have significant clinical implications i.e. ALT cells, being sensitive to IR, should not be a problem in anti-telomerase cancer therapy as long as there is simultaneous exposure of these cells to IR during anti-telomerase treatment. Opposite results may also be important i.e. if ALT cells are not sensitive to IR this could mean that telomere dysfunction is a symptom of highly adaptable cells which simply use genomic rearrangements as a tool to survive and may therefore be the highest form of malignancy i.e. the most difficult cells to eradicate by any form of therapy. In this scenario functional telomeres would be an obstacle to cell survival. We have already irradiated an ALT cell line, its parental non-ALT cell line and the same ALT cell line transfected with hTERT with several doses of gamma rays to generate survival curves. Analysis of results is currently in progress and it is planned that several more ALT cell lines will be included in this analysis.

Second, we wish to examine mechanisms through which accelerated telomere shortening occurs in radiosensitive cell lines. We are currently assessing the level of oxidative stress in the panel of novel radiosensitive cell lines in comparison with control cells and also developing methods that will specifically detect damage at telomeres due to oxidative stress. One interpretation of our results is that accelerated telomere shortening in IR sensitive cells is caused by oxidative stress (see above). It is interesting in this regard that IR can generate high levels of telomeric sister chromatid exchanges (T-SCE) (W. Wright, Texas, a talk presented at XV International Chromosome Conference held at Brunel in September 2004) in contrast to SCEs in the rest of the genome which remain unchanged after IR. T-SCEs can be detected by a technique called chromosome orientation FISH (CO-FISH) (Bailey and Eberle, 2001; Bailey et al., 2004). We have already assessed two novel radiosensitive cell lines (Artemis and Ligase IV) using CO-FISH and our preliminary evidence indicates elevated levels of T-SCEs after IR in an Artemis cell line. A larger study along the lines

described above is planned in the near future.

Thirdly, to examine in more detail a potential role of BRCA1 in telomere function we are currently using immuno-FISH do detect the presence of DSBs at telomeres after BRCA1 depletion in two mammary epithelial cell lines. A pilot immuno-FISH experiment was successful (Figure 5.6). In addition, FISH slides are being analysed for chromosome aberrations in mammary epithelial cell lines. Although, we were successful in depleting BRCA1 by siRNA in mammary epithelial cells, the time duration of BRCA1 depletion is short and it may not be sufficient to detect effects of BRCA1 on telomeres if any. Therefore, we wish to incorporate our BRCA1 siRNAs into an appropriate plasmid and generate a vector that will prevent expression of BRCA1 in a more stable fashion. We also have access to *BRCA1*$^{-/-}$ *p53*$^{-/-}$ mice through collaboration with Dr. Beverly Koller (University of North Carolina at Chapel Hill) and wish to investigate telomere function in these mice. In a recent study *BRCA1*$^{-/-}$ *p53*$^{-/-}$ mice generated by another group were reported to have high incidence of end-to-end chromosome fusions (McPherson et al., 2004).

Finally, our analysis of hTERT expression and telomerase activity in brain tumours points to the possibility that hTERT splice variants may be involved in the regulation of telomerase enzyme activity. Therefore, further experiments are needed to clarify whether hTERT splicing is a limiting factor for the expression of telomerase activity in brain cancer or if it plays a role in telomere maintenance. Alternatively, lack of telomerase activity in some brain tumours may indicate active ALT mechanisms and this possibility could be examined in future experiments.

REFERENCES

Abbott DW, Thompson ME, Robinson-Benion C, Tomlinson G, Jensen RA, Holt JT, BRCA1 expression restores radiation resistance in BRCA1-defective cancer cells through enhancement of transcription-coupled DNA repair. J Biol Chem 1999; 274:18808-18812

Adelfalk C, Lorenz M, Serra V, von Zglinicki T, Hirsch-Kauffmann M, Schweiger M, Accelerated telomere shortening in Fanconi anemia fibroblasts--a longitudinal study. FEBS Letters 2001; 506:22-26

Ahmed S and Hodgkin J, MRT-2 checkpoint protein is required for germline immortality and telomere replication in *C. elegans*. Nature 2000; 403:159-164

Alexander P and Mikulski ZB, Mouse lymphoma cells with different radiosensitivities. Nature 1961; 192:572-573

Albanell J, Lonardo F, Rusch V, Engelhardt M, Langenfeld J, Han W, Klimstra D, Venkatraman E, Moore MAS, Dmitrovsky E, High telomerase activity in primary lung cancers: association with increased cell proliferation rates and advanced pathologic stage. J Nat Can Inst 1997; 89:1609-1615

Al-Wahiby S and Slijepcevic P, Chromosomal aberrations involving telomeres in BRCA1 deficient human and mouse cell lines. Cytogenetics and Genome Research, In press

Aprelikova O, Kuthiala A, Bessho M, Ethier S, Liu ET, BRCA1 protein level is not affected by peptide growth factors in MCF10A cell line. Oncogene 1996; 13:2487-2491

Bachand F, Triki I, Autexier C, Human telomerase RNA-protein interactions. Nucleic Acids Res 2001; 29:3385-3393

Bachor C, Bachor OA, Boukamp P, Telomerase is active in normal gastrointestinal mucosa and not up-regulated in precancerous lesions. J Can Res Clin Oncol 1999; 125:453-460

Baerlocher GM, Lansdorp PM. Telomere length measurements in leukocyte subsets by automated multicolor flow-FISH. Cytometry. 2003; 55:1-6

Baerlocher GM, Roth A, Lansdorp PM, Telomeres in hematopoietic stem cells. Ann N Y Acad Sci 2003; 996:44-48

Bailey SM, Meyne J, Chen DJ, Kurimasa A, Li GC, Lehnert BE, Goodwin EH, DNA double-strand break repair proteins are required to cap ends of mammalian chromosomes. Proc Natl Acad Sci USA 1999; 96:14899-14904

Bailey MN and Eberle RL, Termini of human chromosome display elevated rates of mitotic recombination. Mutagenesis 2001; 16:85-89

Bailey SM, Brenneman MA, Halbrook J, Nickoloff JA, Ullrich RL, Goodwin EH, The kinase activity of DNA-PK is required to protect mammalian telomeres. DNA Repair 2004; 3:225-233

Bailey SM, Goodwin EH, Cornforth MN, Strand-specific fluorescence in situ hybridization: the CO-FISH family. Cyt Gen Res 2004; 107:14-17

Bailey SM and Goodwin EH, DNA and telomeres: beginnings and endings. Cyt Gen Res 2004; 104:109-115

Baird DM, Rowson J, Wynford-Thomas D, Kipling D, Extensive allelic variation and ultrashort telomeres in senescent human cells. Nat Genet 2003; 33:203-207

Bakkenist CJ and Kastan MB, DNA damage activates ATM through intermolecular autophosphorylation and dimmer dissociation. Nature 2003; 421:499-506

Bakkenist CJ, Drissi R, Wu J, Kastan MB, and Dome JS. Disappearance of the telomere dysfunction-induced stress response in fully senescent cells. Cancer Research 2004; 64:3748-3752

Baldeyron C, Jacquemin E, Smith J, Jacquemont C et el., A single mutated BRCA1 allele leads to impaired fidelity of double strand break end-joining. Oncogene 2002; 21:1401-1410

Ball S, Gibson F, Rizzo S, Tooze J, Marsh J, and Gordon-Smith E, Progressive telomere shortening in anaplastic anemia. Blood 1998; 91:3582-3592

Barnes DE, Tomkinson AE, Lehmann AR, Webster ADB and Lindahl T, Mutations in the DNA ligase I gene of an individual with immunodeficiencies and cellular hypersensitivity to DNA-damaging agents. Cell. 1992; 69:495-503

Bassing CH, Chua KF, Sekiguchi J, Suh H, Increased ionising radiation sensitivity and genomic instability in the absence of histone H2AX. PNAS 2002; 99:8173-8178

Batliwalla FM, Rufer N, Lansdorp PM, Gregersen PK, Oligoclonal expansions in the CD8(+)CD28(-) T cells largely explain the shorter telomeres detected in this subset: analysis by flow FISH. Hum Immun 2000; 61:951-958

Baumann P, Benson FE, West SC, Human Rad51 protein promotes ATP-dependent homologous pairing and strand transfer reactions in vitro. Cell 1996; 87:757-766

Baur JA, Zou Y, Shay JW, and Wright WE, Telomere position effect in human cells. Science 2001; 292:2075-2077

Beattie TL, Zhou W, Robinson MO, Harrington L, Polymerization defects within human telomerase are distinct from telomerase RNA and TEP1 binding. Mol Biol Cell 2000; 11:3329-3340

Blackburn EH, Structure and function of telomeres. Nature 1991; 350:569-573

Blackburn EH, Telomere states and cell fates. Nature 2000; 408:53-56

Blagosklonny MV, An WG, Melillo G, Nguyen P, Trepel JB, and Neckers LM, Regulation of BRCA1 by protein degradation. Oncogene 1999; 18:6460-6468

Blasco MA, Lee HW, Hande MP, Samper E, Lansdorp PM, DePinho RA, Greider CW, Telomere shortening and tumor formation by mouse cells lacking telomerase RNA. Cell 1997; 91:25-34

Blasco MA, Hahn WC, Evolving views of telomerase and cancer. Trends Cell Biol 2003; 13:289-294

Bodnar AG, Ouellette M, Frolkis M, Holt SE, Chiu CP, Morin GB, Harley CB, Shay JW, Lichtsteiner S, Wright WE, Extension of life-span by introduction of telomerase into normal human cells. Science 1998; 279:349-352

Boldrini L, Pistolesi S, Gisfredi S, Ursino S, Lupi G, Caniglia M, Pingitore R, Basolo F, Parenti G, and Fontanini G, Telomerase in intracranial meningiomas. Int J Mol Med 2003; 12:943-947

Boulton SJ, Jackson SP, Identification of a Saccharomyces cerevisiae Ku80 homologue: roles in DNA double strand break rejoining and in telomeric maintenance. Nucleic Acids Res 1996; 24:4639-4648

Brenner CA, Wolny YM, Adler RR, Cohen J, Alternate splicing of the telomerase catalytic subunit in human oocytes and embryos. Mol Hum Reprod 1999; 5:845-850

Brummendorf TH, Holyoake TL, Rufer N, Barnett MJ, Schulzer M, Eaves CJ, Eaves AC, Lansdorp PM, Prognostic implications of differences in telomere length between normal and malignant cells from patients with chronic myeloid leukemia measured by flow cytometry. Blood 2000; 95:1883-1890

Brummendorf TH, Mak J, Sabo KM, Baerlocher GM, Dietz K, Abkowitz JL, and Lansdorp PM, Longitudinal studies of telomere length in feline blood cells: implications for hematopoietic stem cell turnover in vivo. Exp Hem 2002; 30:1147-1152

Bruun D, Folias A, Akkari Y, Cox Y, Olson S and Moses R, SiRNA depletion of BRCA1, but not BRCA2, causes increased genome instability in Fanconi anemia cells. DNA repair, 2003; 2:1007-1013

Bryan TM, Englezou A, Gupta J, Bachetti S, and Reddel RR, Telomere elongation in immortal human cells without detectable telomerase activity. EMBO 1995; 14:4240-4248

Bryan TM, Englezou A, Dalla-Pozza L, Dunham MA, Reddel RR, Evidence for an alternative mechanism for maintaining telomere length in human tumours and tumor-derived cell lines. Nat Med 1997; 3:1271-1274

Bryce LA, Morrison N, Hoare SF, Muir S, Keith WN, Mapping of the gene for the human telomerase reverse transcriptase, hTERT, to chromosome 5p15.33 by fluorescence in situ hybridization. Neoplasia 2000; 2:197-201

Cabuy E, de Ridder L, Telomerase activity and expression of telomerase reverse transcriptase correlated with cell proliferation in meningiomas and malignant brain tumors in vivo. Virchows Arch 2001; 439:176-184

Callen E, Samper E, Ramirez MJ, Creus A, Marcos R, Ortega JJ, Olive T, Badell I, Blasco MA and Surralles J, Breaks at telomeres and TRF2-independent end fusions in Fanconi anemia. Hum Mol Genet 2002; 11:439-444

Carney JP, Maser RS, Olivares H, Davis EM, Le Beau M, Yates JR 3rd, Hays L, Morgan WF, and Petrini JH, The hMre11/Rad50 protein complex and Nijmegen breakage syndrome: linkage of double-strand break repair to the cellular DNA damage response. Cell 1998; 93:477-486

Carroll T, Maltby E, Royds J, Timperley W, Jellinek D, Meningiomas, dicentric chromosomes, gliomas, and telomerase activity. J Pathol 1999; 188:395-399

Cawthon RM, Telomere measurement by quantitative PCR. Nucl Acid Res 2002; 30:e47

Cawthon RM, Smith KR, O'Brien E, Sivatchenko A, Kerber RA, Association between telomere length in blood and mortality in people aged 60 years or older. Lancet 2003 361:393-395

Celeste A, Fernandez-Capetillo O, Kruhlak MJ, Pilch DR, Histone H2AX phosphorylation is dispensable for the initial recognition of DNA breaks. Nat Cell Biol 2003; 5:675-679

Cesare AJ and Griffith JD, Telomeric DNA in ALT cells is characterised by free telomeric circles and heterogeneous t-loops. Mol Cell Biol 2004; 24:9948-9957

Cerone MA, Londono-Vallejo JA, Bacchetti S, Telomere maintenance by telomerase and by recombination can coexist in human cells. Hum Mol Gen 2001; 10:1945-1952

Chan SW, Blackburn EH, New ways not to make ends meet: telomerase, DNA damage proteins and heterochromatin. Oncogene 2002; 21:553-563

Chen HJ, Liang C-L, Lu K, Lin JW, Cho CL, Implication of telomerase activity and alterations of telomere length in the histologic characteristics of intracranial meningiomas. Cancer 2000; 89: 2092-2098

Chen JL, Opperman KK, Greider CW, A critical stem-loop structure in the CR4-CR5 domain of mammalian telomerase RNA. Nucleic Acids Res 2002; 30:592-597

Chong EYY, Pang JCS, Ko CW, Poon W-S, Ng HK, Telomere length and telomerase catalytic subunit expression in non-astrocytic gliomas. Pathol Res Pract 2000; 196:691-699

Chow LT, Gelinas RE, Broker TR, and Roberts RJ, An amazing sequence arrangement at the 5' ends of adenovirus 2 messenger RNA. Cell 1997; 12:1-8

Colgin LM, Wilkinson C, Englezou A, Kilian A, Robinson MO, and Reddel RR, The hTERTalpha splice variant is a dominant negative inhibitor of telomerase activity. Neoplasia 2000; 2:426-432

Cong YS, Wen J, Bacchetti S, The human telomerase catalytic subunit hTERT: organization of the gene and characterization of the promoter. Hum Mol Genet 1999; 8:137-142

Counter CM, Avilion AA, LeFeuvre CE, Stewart NG, Greider CW, Harley CB, Bacchetti S, Telomere shortening associated with chromosome instability is arrested in immortal cells which express telomerase activity. EMBO 1992; 11:1921-1929

Cruz S, Miquel R, Rossi ML, Figols J, Palacin A, Cardessa A, Clinico-pathological correlations in meningiomas: a DNA and immunohostochemical study. Histopathology 1993; 8:1-8

d'Adda di Fagagna F, Hande MP, Tong WM, Lansdorp PM, Wang ZQ, Jackson SP, Functions of poly(ADP-ribose) polymerase in controlling telomere length and chromosomal stability. Nat Genet 1999; 23:76-80

d'Adda di Fagagna F, Hande MP, Tong WM, Roth D, Lansdorp PM, Wang ZQ and Jackson SP, Effects of DNA nonhomologous end-joining factors on telomere length and chromosomal stability in mammalian cells. Cur Biol 2001; 11:1192-1196

d'Adda di Fagagna F, Reaper PM, Clay-Farrace L, Fiegler H, Carr P, Von Zglinicki T, Saretzki G, Carter NP, Jackson SP, A DNA damage checkpoint response in telomere-initiated senescence. Nature 2003; 426:194-198

d'Adda di Fagagna F, Teo SH, and Jackson SP, Functional links between telomeres and proteins of the DNA-damage response. Gen Dev 2004; 18:1781-1799

Dai Y, Kysela B, Hanakahi LA, Manolis K, Riballo E, Stumm M, Harville TO, West SC, Oettinger MA and Jeggo PA, Nonhomologous end joining and V(D)J recombination require an additional factor. Proc. Natl. Acad. Sci. U S A. 2003; 100:2462-2467

Dantzer F, Giraud-Panis MJ, Jaco I, Ame JC, Schultz I, Blasco M, Koering CE, Gilson E, Menissier-de Murcia J, de Murcia G, Schreiber V, Functional interaction between poly(ADP-Ribose) polymerase 2 (PARP-2) and TRF2: PARP activity negatively regulates TRF2. Mol Cell Biol 2004; 24:1595-1607

DeMasters BKK, Markham N, Lillehei KO, Shroyer KR, Differential telomerase expression in human primary intracranial tumors. AJCP 1997; 107:548-554

Deng CX and Scott F, Role of the tumor suppressor gene Brca1 in genetic stability and mammary gland tumor formation. Oncogene 2000; 19:1059-1064

Deng C-X and Brodie SG, Roles of BRCA1 and its interacting proteins. Bioessays 2000; 22:728-737

Deng C-X and Wang R-H, Roles of BRCA1 in DNA damage repair: a link between development and cancer. Hum Mol Gen 2003; 12:113-123

Derenzini M, Ceccarelli C, Santini D, Taffurelli M, Trere D, The prognostic value of the AgNOR parameter in human breast cancer depends on the pRb and p53 status. J Clin Pathol 2004; 57:755-761

de Thé H, Lavau C, Marchio A, Chomienne C, Degos L, and Dejean A, The PML-PAR alpha fusion mRNA generated by the t(15;17) translocation in acute promyelocytic leukaemia encodes a functionally altered RAR. Cell 1991; 66:675-684

Dhaene K, Van Marck E, and Parwaresch R, Telomeres, telomerase and cancer: an up-date. Virch Archive 2000; 437:1-16

Dhaene K, Vancoille G, Lambert J, Naeyaert JM, and E Van Marck, Absence of telomerase activity and telomerase catalytic subunit mRNA in melanocyte cultures. British Journal of Cancer 2000; 82:1051-1057

Ducrest A-L, Szutorisz H, Lingner J, and Nabholz M, Regulation of the human telomerase reverse transcriptase gene. Oncogene 2002; 21:541-552

Dunham MA, Neumann AA, Fasching CL, and Reddel RR, Telomere maintenance by recombination in human cells. Nat Gen 2000; 26:447-450

Ehemann V, Hashemi B, Lange A, and Otto HF, Flow cytometric DNA analysis and chromosomal aberrations in malignant glioblastomas. Cancer Letters 1999; 138:101-106

El-Zein R, Bondy ML, Wang L-E, de Andrade M, Increased chromosomal instability in peripheral lymphocytes and risk of human gliomas. Carcinogenesis 1999; 20:811-815

Epel ES, Blackburn EH, Lin J, Dhabhar FS, Adler NE, Morrow JD, Cawthon RM, Accelerated telomere shortening in response to life stress. Proc Natl Acad Sci U S A. 2004; 101:17312-17315

Espejel S, Franco S, Rodriguez-Perales S, Bouffler SD, Blasco MA, Mammalian Ku86 mediates chromosomal fusions and apoptosis caused by critically short telomeres. EMBO 2002; 21:2207-2219

Espejel S, Martin M, Klatt P, Martin-Caballero J, Flores JM, Blasco MA, Shorter telomeres, accelerated ageing and increased lymphoma in DNA-PKcs-deficient mice. EMBO Report 2004; 5:503-509

Essers J, Hendriks RW, Swagemakers SM, Troelstra C, de Wit J, Bootsma D, Hoeijmakers JH, Kanaar R, Disruption of mouse RAD54 reduces ionizing radiation resistance and homologous recombination. Cell 1997; 89:195-204

Etheridge KT, Banik SS, Armbruster BN, The nucleolar localization domain of the catalytic subunit of human telomerase. J Biol Chem 2002; 277:24764-24770

Falchetti ML, Pallini R, Larocca LM, D'Ambrosio E, Telomerase expression in intracranial tumours: prognostic potential for malignant gliomas and meningiomas. J Clin Pathol 1999; 52:234-236

Falchetti ML, Pallini R, D'Ambrosio E, Pierconti F, Martini M, Cimino-Reale G, Verna R, Maira G, Larocca LM, In situ detection of telomerase catalytic subunit mRNA in glioblastoma multiforme. Int J Cancer 2000; 88:895-901

Falchetti ML, Larocca LM, and Pallini R, Telomerase in brain tumors. Children's Nervous Systems 2002; 18:112-117

Feng J, Funk WD, Wang S-S, Weinrich SL, Avilion AA, Chiu C-P, Adams RR, Chang E, Allsopp RC, Yu J, Le S, Wast MD, Harley CB, Andrews WH, Greider CW, Villeponteau B, The RNA component of human telomerase. Science 1995; 269:1236-1241

Fernandez-Capetillo O, Chen HT, Celeste A, Ward I, Romanieko PJ, DNA damage-induced G2-M checkpoint activation by histone H2AX and 53BP1. Nat Cell Biol 2002; 4:993-997

Fernandez-Capetillo O, Lee A, Nussenzweig M, Nussenzweig A, H2AX: the histone guardian of the genome. DNA Repair 2004; 3:959-967

Filipowicz W and Pogacic V, Biogenesis of small nucleolar ribonucleoproteins. Cur Opinion Cell Biol 2002; 14:319-327

Finnon P, Wong HP, Silver AR, Slijepcevic P, Bouffler SD, Long but dysfunctional telomeres correlate with chromosomal radiosensitivity in a mouse AML cell line. International Journal of Rad Biol 2001; 77:1151-1162

Fischer U, Schütz N, Hemmer D, and Meese E, GAS64, the first and putative non-translated gene. Inter J Oncol 2002; 20:173-176

Foray N, Randrianarison V, Marot D, Perricaudet M, Lenoir G, and Feunteun J, Gamma-rays-induced death of human cells carrying mutations of BRCA1 or BRCA2. Oncogene 1999; 18:7334-7342

Ford LP, Zou Y, Pongracz K, Gryaznov SM, Shay JW, and Wright WE, Telomerase can inhibit the recombination-based pathway of telomere maintenance in human cells. J Biol Chem 2001; 276:32198-32203

Forstemann K, Hoss M, Lingner J, Telomerase-dependent repeat divergence at the 3' ends of yeast telomeres. Nucleic Acids Res 2000; 28:2690-2694

Franco S, Van De Vrught HJ, Fernandez P, Aracil M, Arwert F, and Blasco MA, Telomere dynamics in fancg-deficient mouse and human cells. Blood 2004; 104:3927-3935

Frank KM, Sekiguchi JM, Seidl KJ, Swat W, Rathbun GA, Cheng HL, Davidson L, Kangaloo L, and Alt FW, Late embryonic lethality and impaired V(D)J recombination in mice lacking DNA ligase IV. Nature 1998; 396:173-177

Freulet-Marriere MA, Potocki-Veronese G, Deverre JR, and Sabatier L, Rapid method for mean telomere length measurement directly from cell lysates. Biochem Biophys Res Com 2004; 314:950-956

Fujiwara M, Okayasu I, Takemura T, Tanaka I, Masuda R, Furuhata Y, Noji M, Oritsu M, Kato M, Oshimura M, Telomerase activity significantly correlates with chromosome alterations, cell differentiation, and proliferation in lung adenocarcinomas. Mod Pathol 2000; 13:723-729

Gan Y, Engelke KJ, Brown CA, and Au JLS, Telomere amount and length assay. Pharm Res 2001; 18:1655-1659

Gilley D, Blackburn EH, The telomerase RNA pseudoknot is critical for the stable assembly of a catalytically active ribonucleoprotein. Proc Natl Sci USA 1999; 96:6621-6625

Girard PM, Foray N, Stumm M, Waugh A, Riballo E, Maser RS, Phillips WP, Petrini J, Arlett CFand Jeggo PA, Radiosensitivity in Nijmegen Breakage Syndrome cells is attributable to a repair defect and not cell cycle checkpoint defects. Cancer Res 2000; 60:4881-4888

Girard PM, Riballo E, Begg AC, Waugh A, Jeggo PA, Nbs1 promotes ATM dependent phosphorylation events including those required for G1/S arrest. Oncogene 2002; 21:4191-4199

Goytisolo FA, Samper E, Martin-Caballero J, Finnon P, Herrera E, Flores JM, Bouffler SD and Blasco MA, Short telomeres result in organismal hypersensitivity to ionizing radiation in mammals. J Exp Med 2000; 192:1625-1636

Goytisolo FA, Samper E, Edmonson S, Taccioli GE and Blasco MA, The absence of the dna-dependent protein kinase catalytic subunit in mice results in anaphase bridges and in increased telomeric fusions with normal telomere length and G-strand overhang. Mol Cell Biol 2001; 21:3642-3651

Goytisolo FA and Blasco MA, Many ways to telomere dysfunction: in vivo studies using mouse models. Oncogene 2002; 21:5845-5891

Gowen, LC, Avrutskaya AV, Latour AM, Koller BH, Leadon SA, BRCA1 required for transcription-coupled repair of oxidative DNA damage. Science 1998; 281:1009-1012

Greenberg RA, O'Hagan RC, Deng H, Xia Q, Hann SR, Adams RR, Lichtsteiner S, Chin L, Morin GB, and DePinho RA, Telomerase reverse transcriptase gene is a direct target of c-Myc but is not functionally equivalent in cellular transformation. Oncogene, 1999; 18:1219-1226

Greider CW and Blackburn EH, Identification of a specific telomere terminal transferase activity in Tetrahymena extracts. Cell 1985; 43:405-413

Greider CW, Telomerase activity, cell proliferation, and cancer. Proc Natl Acad Sci USA 1998; 95:90-92

Griffith JD, Comeau L, Rosenfield S, Stansel RM, Bianchi A, Moss H, and de Lange T, Mammalian telomeres and in a large duplex loop. Cell 1999; 97:503

Grobelny JV, Godwin AK, Broccoli DJ, ALT-associated PML bodies are present in viable cells and are enriched in cells in the G(2)/M phase of the cell cycle. J Cell Sci 2000; 113: 4577-4585

Grobelny JV, Kulp-McEliece M, Broccoli D, Effects of reconstitution of telomerase activity n telomere maintenance by the alternative lengthening of telomeres (ALT) pathway. Hum Mol Gen 2001; 10:1953-1961

Gudas JM, Li T, Nguyen H, Jensen D, Rauscher FJ 3rd, Cowan KH, Cell cycle regulation of BRCA1 messenger RNA in human breast epithelial cells. Cell Growth Differ 1996; 7:717-723

Gupta J, Han L-P, Wang P, Gallie BL, Bacchetti S, Development of retinoblastoma in the absence of telomerase activity. J Natl Can Inst 1996; 88:1152-1157

Hackett JA, Feldser DM, Greider CW, Telomere dysfunction increases mutation rate and genomic instability. Cell 2001; 106: 275-286

Hakin-Smith V, Jellinek DA, Levy D, Caroll T, Teo M, Timperley WR, McKay MJ, Reddel RR and Royds JA Alternative lengthening of telomeres and survival in patients with glioblastoma multiforme. Lancet 2003; 361:836-838

Hande P, Slijepcevic P, Silver A, Bouffler S, van Buul P, Bryant P, Lansdorp P, Elongated telomeres in scid mice. Genomics 1999; 56:221-223.

Hande MP, Balajee AS, Tchirkov A, Wynshaw-Boris A and Lansdorp PM, Extra-chromosomal telomeric DNA in cells from Atm(-/-) mice and patients with ataxia-telangiectasia. Hum Mol Gen 2001; 10:519-528

Hanson H, Mathew CG, Docherty Z, and Mackie Ogilvie C, Telomere shortening in Fanconi anaemia demonstrated by a direct FISH approach. Cytogenet Cell Genet. 2001; 93:203-206

Harada K, Kurisu K, Tahara H, Tahara E, Ide T, and Tahara E, Telomerase activity in primary and secondary glioblastoma multiforme as a novel molecular tumor marker. Journal of Neurosurgery, 2000; 93:618-625

Harley CB, Futcher AB, and Greider CW, Telomeres shorten during ageing of human fibroblasts. Nature 1990; 345:458-460

Harrington L, Zhou W, McPhail T, Oulton R, Yeung DS, Mar V, Bass MB, and Robinson MO, Human telomerase contains evolutionarily conserved catalytic and structural subunits. Gen Dev 1997; 11:3109-3115

Heine B, Hummel M, Demel G, Stein H, Demonstration of constant upregulation of the telomerase RNA component in human gastric carcinomas using in situ hybridization. J Pathol 1998; 185:139-144

Hemann MT, Strong MA, Hao LY, Greider CW, The shortest telomere, not average telomere length, is critical for cell viability and chromosome stability. Cell 2001; 107:67-77

Henson JD, Neumann AA, Yeager TR, and Reddel RR, Alternative lengthening of telomeres in mammalian cells. Oncogene, 2002; 21: 598-610

Herbert B-S, Wright WE, and Shay JW, Telomerase and breast cancer. Breast Cancer Research 2001; 3:146-149

Herbig U, Jobling WA, Chen BPC, Chen DJ, and Sedivy JM, Telomere shortening triggers senescence of human cells through a pathway involving ATM, p53, and $p21^{CIP1}$, but not $p16^{INK4a}$. Mol Cell 2004; 14:501-513

Hiraga S, Ohnishi T, Izumoto S, Miyahara E, Kanemura Y, Matsumura H, Arita N, Telomerase activity and alterations in telomere length in human brain tumors. Cancer Research 1998; 58:2117-2125

Hiyama T, Yokozaki H, Kitadai Y, Haruma K, Yasui W, Kajiyama G, Tahara E, Overexpression of human telomerase RNA is an early event in oesophageal carcinogenesis. Virch Archive 1999; 434:483-487

Horikawa I, Cable PL, Afshari C, Barrett JC, Cloning and characterization of the promoter region of human telomerase reverse transcriptase gene. Cancer Res 1999; 59:826-830

Hou M, Xu D, Björkholm, and Gruber A, Real-time quantitative telomeric repeat amplification protocol assay for the detection of telomerase activity. Clin Chem 2001; 47:519-524

Huang F, Kanno H, Yamamoto I, Lin Y, and Kubota Y, Correlation of clinical features and telomerase activity in human gliomas. Journal of Neuro-Oncology 1999; 43:137-142

Hui AB, Lo KW, Yin XL, Poon WS, Ng HK, Detection of multiple gene amplifications in glioblastoma multiforme using array-based comparative genomic hybridization. Lab Invest 2001; 81:717-723

Huschtscha LI, Noble JR, Neumann AA, Moy EL, Barry P, Melki JR, Clark SJ, and Reddel RR, Loss of p16INK4 expression by methylation is associated with lifespan extension of human mammary epithelial cells. Cancer Res 1998; 58:3508-3512

Iijima K, Komatsu K, Matsuura S, Tauchi H, The Nijmegen breakage syndrome gene and its role in genome stability. Chromosoma 2004; 113:53-61

Jaco I, Munoz P, Goytisolo F, Wesoly J, Bailey S, Taccioli G, Blasco MA, Role of mammalian Rad54 in telomere length maintenance. Mol Cell Biol 2003; 23:5572-5580

Jeggo P and O'Neill P, The Greek goddess, Artemis reveals the secrets of her cleavage. DNA Repair 2002; 1:771-777

Jeggo PA and Concannon P, Immune diversity and genomic stability: opposite goals but similar paths. J Photochem Photobiol 2001; 65:88-96

Joenje H and Patel KJ, The emerging genetic and molecular basis of Fanconi anaemia. Nat Rev Gen 2001; 2:446-457

Johnson RD and Jasin M, Double-strand-break-induced homologous recombination in mammalian cells. Biochem Soc Trans 2001; 29:196-201

Kanaya T, Kyo S, Takakura M, Ito H, Namiki M, Inoue M, hTERT is a critical determinant of telomerase activity in renal-cell carcinoma. Int J Can 1998; 78:539-543

Kanoh J and Ishikawa F, Composition and conservation of the telomeric complex. CMLS Cel Mol Life Sci 2003; 60:2295-2302

Karlseder J, Broccoli D, Dai Y, Hardy S, de Lange T, p53- and ATM-dependent apoptosis induced by telomeres lacking TRF2. Science 1999; 283:1321-1325

Kastan MB and Lim D, The many substrates and functions of ATM. Nat Rev 2000; 1:179-186

Kickhoefer VA, Liu Y, Kong LB, Snow BE, Stewart PL, Harrington L, and Rome L, The telomerase/vault-associated protein TEP1 is required for vault RNA stability and its association with the fault particle. J Cell Biol 2001; 152:157-164

Kilian A, Bowtell DDL, Abud HE, Hime GR, Venter DJ, Keese PK, Duncan EL, Reddel RR, Jefferson RA, Isolation of a candidate human telomerase catalytic subunit gene, which reveals complex splicing patterns in different cell types. Hum Mol Gen 1997; 6:2011-2019

Kim NW, Piatyszek MA, Prowse KR, Harley CB, West MD, Ho PLC, Coviello GM, Wright WE. Weinrich SL, Shay JW, Specific association of human telomerase activity with immortal cells and cancer. Science 1994; 266:2011-2015

Kim NW, Wu F, Advances in quantification and characterization of telomerase activity by the telomeric repeat amplification protocol (TRAP). Nuc Acids Res 1997; 25:2595-2597

Kim SH, Kaminker P, Campisi J, TIN2, a new regulator of telomere length in human cells. Nat Genet 1999; 23:382-383

Kishi S, Zhou XZ, Ziv Y, Khoo C, Hill DE, Shiloh Y, and Lu KP, Telomeric protein Pin2/TRF1 as an important ATM target in response to double strand DNA breaks. J Biol Chem 2001; 276:29282-29291

Klapper W, Parwaresch R, Krupp G, Telomere biology in human aging and aging syndromes. Mech Ageing Dev 2001; 122:695-712

Kleihues P, Cavenee WK (ed), WHO Classification of tumours. Pathology and genetics. Tumours of the Nervous System. 2000; IARCPress, Lyon

Kleinschmidt D and Lillehei KO, Radiation-induced meningioma with a 63-year latency period. Case report. J Neur 1995; 82:487-488

Kleinschmidt-DeMasters BK, Hashizumi TL, Lillehei KO, Shroyer AL, Shroyer KR, Telomerase expression shows differences across multiple regions of oligodendroglioma versus high grade astrocytomas but shows correlation with Mib-1 labeling. J Clin Pathol 1998; 51:284-293

Kleinschmidt-Demasters BK, Evans LC, Bobak JB, Lopez-Uribe D, Hopper D, Shroyer AL, Shroyer KR, Quantitative telomerase expression in glioblastomas shows regional variation and down-regulation with therapy but no correlation with patient outcome. Hum Pathol 2000 31:905-913

Kubota Y, Nakada T, Sasagawa I, Yanai H, Itoh K, Elevated levels of telomerase activity in malignant pheochromocytoma. Cancer 1998; 82:176-179

Kyo S, Kanaya T, Takakura M, Tanaka M, Yamashita A, Inoue H, Inoue M, Expression of human telomerase subunits in ovarian malignant, borderline and benign tumors. Int J Can 1999; 80:804-809

Langford LA, Piatyszek MA, Xu R, Schold SC, Wright WE, Shay JW, Telomerase activity in ordinary meningiomas predicts pour outcome. Hum Pathol 1997; 28:416-420

Lansdorp PM, Poon S, Chavez E, Dragowska V, Zijlmans M, Bryan T, Reddel R, Egholm M, Bacchetti S, Martens U, Telomeres in the haemopoietic system. Ciba Foundation Symposium 1997; 211:209-218

Lansdorp PM, Repair of telomeric DNA prior to replicative senescence. Mech Ageing Dev 2000; 118:23-34

Lees-Miller SP and Meek K, Repair of DNA double strand breaks by non-homologous end joining. Biochimie 2003; 85:1161-1173

Le S, Zhu JJ, Anthony DC, Greider CW, and Black PM, Telomerase activity in human gliomas. Neurosurgery 1998; 42:1120-1124

Leuraud P, Dezamis E, Aguirre-Cruz L, Taillibert S, Lejeune J, Robin E, Mokhtari K, Boch AL, Cornu P, Delattre JY, Sanson M, Prognostic value of allelic losses and telomerase activity in meningiomas. J Neuro 2004; 100:303-309

Leteurtre F, Li X, Guardiola P, Le Roux G, Sergère JC, Richard P, Carosella ED and Gluckman E, Accelerated telomere shortening and telomerase activation in Fanconi's anaemia. British J haemat 1999; 105:883-893

Levy MZ. Allsopp RC, Futcher AB, Grieder CW, and Harley CB, Telomere end-replication problem and cell aging. J Mol Biol 1992; 225:951-960

Li B, Lustig AJ, A novel mechanism for telomere size control in Saccharomyces cerevisiae. Gen Dev 1996; 10:1310-1326

Li H, Zhao L, Yang Z, Funder JW, and Liu JP, Telomerase is controlled by protein kinase Calpha in human breast cancer cells. J Biol Chem 1998; 273:33436-33442

Li H, Lee TH, and Avraham H, A novel tricomplex of BRCA1, Nmi and c-Myc inhibits c-Myc induced hTERT promoter activity in breast cancer. J Biol Chem 2002; 277:20965-20973

Lieber MR, Ma Y, Pannicke U, and Schwarz K, The mechanism of vertebrate non-homologous DNA end joining and its role in V(D)J recombination. DNA repair 2004; 3:817-826

Lindsey J, McGill NI, Lindsey LA, Green DK, Cooke HJ, In vivo loss of telomeric repeats with age in humans. Mut Res 1991; 256:45-48

Lingner J, Hughes TR, Shevchenko A, Mann M, Lundblad V, Cech TR, Reverse transcriptase motifs in the catalytic subunit of telomerase. Science 1997; 276:561-567

Lippincott William and Wilkins, Clinical Anatomy for medical Students. 7th Edition

Liu K, Schoonmaker MM, Levine BL, June CH, Hodes RJ, Weng N-P, Constitutive and regulated expression of telomerase reverse transcriptase (hTERT) in human lymphocytes. Proc Nat Acad Sc USA 1999; 96:5147-5152

Liu D, O'connor MS, Qin J, Songyang Z, Telosome, a Mammalian Telomere-associated Complex Formed by Multiple Telomeric Proteins. J Biol Chem 2004; 279:51338-51342

Londoño-Vallejo AJ, Der-Sarkissian H, Cazes L, Bachetti S, Reddel RR, Alternative lengthening of telomeres is characterised by high rates of telomeric exchange. Cancer Res 2004; 64:2324-2327

Lopez AJ, Alternative splicing of pre-mRNA: Developmental consequences and mechanisms of regulation. Ann Rev Gen 1998; 32:279-305

Lundblad V and Blackburn EH, An alternative pathway for yeast telomere maintenance rescues est1-senescence. Cell 1993; 73:347-360

Lusis E and Gutmann DH, Meningioma: an update. Cur Opinion Neur 2004; 17:687-692

Lustig AJ, Clues to catastrophic telomere loss in mammals from yeast telomere rapid deletion. Nat Rev Genet 2003; 4: 916-923

Ma Y, Pannicke U, Schwarz K, Lieber MR, Hairpin opening and overhang processing by an Artemis:DNA-PKcs complex in V(D)J recombination and in non-homologous end joining. Cell 2002; 108:781-794

Magnani I, Guerneri S, Pollo B, Cirenei N, Colombo BM, Broggi G, Galli C, Bugiani O, Didonato S, Finocchiaro G, Conti AMF Increasing complexity of the karyotype in 50 human gliomas. Progressive evolution and de novo occurrence of cytogenetic alterations. Cancer Genet Cytogenet 1994; 75:77-89

Makarov VL, Hirose Y, and Langmore JP, Long G tails at both ends of human chromosomes suggest a C strand degradation mechanism for telomere shortening. Cell 1997; 88:657-666

Marcou J, Andrea AD, Jeggo PA and Plowman PN. Normal cellular radiosensitivity in an adult Fanconi anaemia patient with marked clinical radiosensitivity. Radiother. Oncol. 2001; 60:75-79

Martens UM, Brass V, Engelhardt M, Glaser S, Waller CF, Lange W, Schmoor C, Poon SS, Landsdorp PM, Measurement of telomere length in haematopoietic cells using in situ hybridization techniques. Biochem Soc Trans 2000; 28:245-250

Martens UM, Brass V, SEdlacek L, Pantic M, Exner C, Guo Y, Engelhardt M, Lansdorp PM, Waller CF, and Lange W, Telomere maintenance in human B lymphocytes. Brit J Haemat 2002; 119:810-818

Martin SG, Laroche T, Suka N, Grunstein M, Gasser SM, Relocalization of telomeric Ku and SIR proteins in response to DNA strand breaks in yeast. Cell 1999; 97:621-633

Mason JM and Biessmann H, The unusual telomeres of Drosphila. Trends Genet 1995; 11:58-62

Masutomi K, Yu EY, Khurts S, Ben-Porath I, Telomerase maintains telomere structure in normal human cells. Cell 2003; 114:241-253

Mazin AV, Alexeev AA, Kowalczykowski SC, A novel function of Rad54 protein. Stabilization of the Rad51 nucleoprotein filament. J Biol Chem 2003; 278:14209-14036

McClintock B, The stability of broken ends of chromosomes in Zea Mays. Genetics 1941; 26:58-62

McElligot R, and Wellinger RJ, The terminal DNA structure of mammalian chromosomes. EMBO 1997; 16:3705-3714

McIlrath J, Bouffler SD, Samper E, Cuthbert A, Wojcik A, Szumiel I, Bryant PE, Riches AC, Thompson A, Blasco MA, Newbold RF, Slijepcevic P, Telomere length abnormalities in mammalian radiosensitive cells. Cancer Res 2001; 61:912-915.

McPherson JP, Lemmers B, Hirao A, Hakem A, Abraham J, Migon E, Matysiak-Zablocki E, Tamblyn L, Sanchez-Sweatman O, Khokha R, Squire J, Hande MP, Mak TW, Hakem R, Collaboration of Brca1 and Chk2 in tumorigenesis. Gen Dev 2004; 18:1144-1153

Meeker AK, Coffey DS, Telomerase: a promising marker of biological immortality of germ, stem, and cancer cells. A review. Biochemistry 1997; 62:1323-1331

Mehle C, Piatyszek MA, Ljungberg B, Shay JW, Roos G, Telomerase activity in human renal cell carcinoma. Oncogene 1996; 13:161-166

Ménissier-de Murcia J, Ricoul M, Tartier L, Niedergang C, Huber A, Dantzer F, Schrieber V, Amé JC, Dierich A, LeMeur M, Sabatier L, Chambon P, de Murcia G, Functional interaction between PARP-1 and PARP-2 in chromosome stability and embryonic development in mouse. EMBO 2003; 22:2255-2263

Metcalfe JA, Parkhill J, Campbell L, Stacey M, Biggs P, Byrd PJ and Taylor AM, Accelerated telomere shortening in ataxia telangiectasia. Nat. Genet. 1996; 13:350-353

Meyerson M, Counter CM, Eaton EN, Ellisen LW, Steiner P, Caddle SD, Ziaugra L, Beijersbergen RL, Davidoff MJ, Liu Q, Bacchetti S, Haber DA, and Weinberg RA, hEST2, the putative human telomerase catalytic subunit gene, is up-regulated in tumor cells and during immortalization. Cell 1997; 90:785-795

Miki Y, Swensen J, Shattuck-Eidens D, Futreal P, A strong candidate for the breast and ovarian cancer susceptibility gene BRCA1. Science 1994; 266:66-71

Mills KD, Sinclair DA, Guarente L, MEC1-dependent redistribution of the Sir3 silencing protein from telomeres to DNA double-strand breaks. Cell 1999; 97:609-620

Miracco C, Pacenti L, Santopietro R, Biagioli M, Fimiani M, Perotti R, Rubegni P, Pirtoli L, Luzi P, Detection of telomerase activity and correlation with mitotic and apoptotic indices, Ki-67 and expression of cyclins D1 and A in cutaneous melanoma. Int J Cancer 2000; 88: 411-416

Mironov AA, Fickett JW, and Gelfand MS, Frequent alternative splicing of human genes. Genome Res 1999; 9:1288-1293

Mitchell JR, Cheng J, Collins K, A box H/ACA small nucleolar RNA-like domain at the human telomerase RNA 3' end. Mol Cell Biol 1999; 19:567-576

Mitchell JR, Collins K, Human telomerase activation requires two independent interactions between telomerase RNA and telomerase reverse transcriptase. Mol Cell 2000; 6:361-371

Morin GB, The human telomere terminal transferase enzyme is a ribonucleoprotein that synthesizes TTAGGG repeats. Cell 1089; 59:521-529

Morii K, Tanaka R, Onda K, Tsumanuma I, and Yoshimura J, Expression of telomerase RNA, telomerase activity, and telomere length in human gliomas. Biochemical and Biophysical Res Com 1997; 239:830-834

Motoyama N and Naka K, DNA damage tumor suppressor genes and genomic instability. Current Opinion in Gen Dev 2004; 14:11-16

Muniyappa K, Kironmai KM, Telomere structure, replication and length maintenance. Crit Rev Biochem Mol Biol 1998; 33:297-336

Munoz-Jordan JL, Cross GA, de Lange T, Griffith JD, t-loops at trypanosome telomeres. EMBO J 2001; 20:579-588

Murnane JP, Sabatier L, Marder BA, and Morgan WF, Telomere dynamics in an immortal human cell line. EMBO 1994; 13:4953-4962

Musa BS, Pople IK, and Cummins BH, Intracranial meningiomas following irradiation – a growing problem? Brit J Neuro 1995; 9:629-637

Myung K, Gosh G, Fattah FJ, Li G, Kim H, Dutia A, Pak E, Smith S, Hendrickson EA, Regulation of telomere length and suppression of genomic instability in human somatic cells by Ku86. Mol Cell Biol 2004; 24:5050-5059

Nabetani A, Yokoyama O, and Ishikawa F, Localisation of hRad9, hHus1, hRad1, and hRad17 and caffeine-sensitive DNA replication at the alternative lengthening of telomeres-associated promyelocytic leukemia body. J Biol Chem 2004; 279:25849-25857

Naka K, Ikeda K, and Motoyama N, Recruitment of NBS1 into PML oncogenic domains via interaction with SP100 protein. Bioch Biophys Res Com 2002; 29:863-871

Nakamura TM, Morin GB, Chapman KB, Weinrich SL, Andrews WH, Lingner J, Harley CB, Cech TR, Telomerase catalytic subunit homologs from fission yeast and human. Science 1997; 277:911-912

Nakamura TM, Cech TR, Reversing time: origin of telomerase. Cell 1998; 92:587-590

Nakamura Y, Hirose M, Matsuo H, Tsuyama N, Kamisango K, Ide T, Simple, rapid, quantitative, and sensitive detection of telomere repeats in cell lysate by a hybridization protection assay. Clin Chem 1999; 45:1718-1724

Nakayama J-I, Tahara H, Tahara E, Saito M, Ito K, Nakamura H, Nakanishi T, Thara E, Ide T, Ishikawa F, Telomerase activation by hTRT in human normal fibroblasts and hepatocellular carcinomas. Nat Genet 1998: 18:65-68

Nicoletti L, Migliorati G, Pagliacci MC, A rapid and simple method for measuring thymocyte apoptosis by propidium iodide staining and flow cytometry. J Immun Meth 1991; 139:271-279

Neidle S, Parkinson GN, The structure of telomeric DNA. Curr Opin Struct Biol 2003; 13:275-283

Oikawa S, and Kawanishi S, Site-specific DNA damage at GGG sequence by oxidative stress may accelerate telomere shortening. FEBS Letters 1999; 453:365-368

Okayasu I, Mitomi H, Yamashita K, Mikami T, Fujiwara M, Kato M, Oshimura M, Telomerase activity significantly correlates with cell differentiation, proliferation and lymph node metastasis in colorectal carcinomas. J Cancer Res Clin Oncol 1998; 124:444-449

Olovnikov AM, A theory of marginotomy. The incomplete copying of template margin in enzymic synthesis of polynucleotides and biological significance of the phenomenon. J Theor Biol 1973; 41:181-190

Pandita TK, Pathak S, Geard CR, Chromosome end associations, telomeres and telomerase activity in ataxi telangiectasia cells. Cytogenet Cell Genet 1995; 71:86-93

Pandita TK, Hall EJ, Hei TK, Piatyszek MA, Wright WE, Piao CQ, Pandita RK, Willey JC, Geard CR, Kastan MB, and Shay JW, Chromosome end-to-end associations and telomerase activity during cancer progression in human cells after treatment with alpha-particles simulating radon progeny. Oncogene 1996; 13:1423-1430

Pandita TK and Dhar S, Influence of ATM function on interactions between telomeres and nuclear matrix. Radiation Res 2000; 154:133-139

Paradis V, Dargere D, Laurendeau I, Benoit G, Vidaud M, Jardin A, Bedossa P, Expression of the RNA component of human telomerase (hTR) in prostate cancer, prostatic intraepithelial neoplasia, and normal prostate tissue. J Pathol 1999; 189:213-218

Park T-W, Riethdorf S, Riethdorf L, Löning T, Jänicke F, Differential telomerase activity, expression of the telomerase catalytic sub-unit and telomerase-RNA in ovarian tumors. Int J Cancer 1999; 84:426-431

Pasta E and Blasiak J, Non-homologous DNA end joining. Acta Biochemica Polonica 2003; 50:891-908

Paull TT, Rogakau EP, Yamazaki V, Kirchgessner CU, Gellert M, Bonner WM, A critical role for histone H2AX in recruitment of repair factors to nuclear foci after DNA damage. Curr Biol 2000; 10:886-895

Paull TT, Cortez D, Bowers B, Elledge SJ, Gellert M, Direct DNA binding by Brca1. Proc Nat Acad Sci USA 2001; 98:6086-6091

Perrem K, Colgin LM, Neumann AA, Yeager TR, and Reddel RR, Coexistence of alternative lengthening of telomeres and telomerase in hTERT-transfected GM847 cells. Mol Cell Biol 2001; 21:3862-3875

Petrini JH, The mammalian Mre11-Rad50-nbs1 protein complex: integration of functions in the cellular DNA-damage response. Amer J Hum Gen 1999; 64:1264-1269

Pistolesi S, Boldrini L, Gisfredi S, De Ieso K, Camacci T, Caniglia M, Lupi G, Pingitore R, Basolo F, Leocata P, Parenti G, Fontanini G, Immunohistochemical and molecular study of radiation-induced multiple meningiomas with pleural and pulmonary metastasis. Tumori 2004; 90:328-332

Ploton D, Ménager M, Adnet JJ Ultrastructural localization of NOR in nuclei of human breast cancer tissues using a one-step AgNOR staining method. Biol Cell 1982; 43:229-232

Poon SS, Martens UM, Ward RK, Lansdorp PM, Telomere length measurements using digital fluorescence microscopy. Cytometry 1999; 36:267-278

Presti LL, Cabuy E, Chirocolo M, and Dall'Olio F, Molecular cloning of the human β1,4 *N*-acetylgalactosaminyltransferase responsible for the biosynthesis of the Sd^a histo-blood group antigen: the sequence predicts a very long cytoplasmic domain. J Biochem 2003; 134:675-682

Ramakrishnan S, Eppenberger U, Mueller H, Shinkai Y, Narayanan R, Expression profile of the putative catalytic subunit of the telomerase gene. Cancer Res 1998; 58:622-625

Ranganathan V, Heine WF, Ciccone DN, Rudolph KL, Wu X, Chang S, Hai H, Ahearn IM, Livingston DM, Resnick I, Rosen F, Seemanova E, Jarolim P, DePinho RA, and Weaver DT, Rescue of a telomere length defect of Nijmegen breakage syndrome cells requires NBS and telomerase catalytic subunit. Curr Biol 2001; 11:962-966

Rattray AJ, and Symington LS, Multiple pathways for homologous recombination in Saccharomyces cerevisae. Genetics 1995; 139:45-56

Reddel RR, Bryan TM, Murnane JP, Immortalized cells with no detectable telomerase activity. A review. Biochemistry (Moscow) 1997; 62:1254-1262

Reddel RR, Bryan TM, Colgin LM, Perrem KT, and Yeager TR, Alternative lengthening of telomeres in human cells. Rad Res 2001; 155:194-200

Rhodes D, Fairall L, Simonsson T, Court R, and Chapman L, Telomere architecture. EMBO reports 2002; 3:1139-1145

Rhyu MS, Telomeres, Telomerase, and Immortality. J Natl Cancer Inst 1995; 87:884-894

Riballo E, Critchlow SE, Teo SH, Doherty AJ, Priestley A, Broughton B, Kysela B, Beamish H, Plowman N, Arlett CF, Lehmann AR, Jackson SP and Jeggo PA, Identification of a defect in DNA ligase IV in a radiosensitive leukaemia patient. Curr. Biol. 1999; 9:699-702

Rigolin GM, Porta MD, Bugli AM, Castagnari B, Mauro E, Bragotti LZ, Ciccone M, Cuneo A, Castoldi G. Flow cytometric detection of accelerated telomere shortening in myelodysplastic syndromes: correlations with aetiological and clinical-biological findings. Eur J Haemat 2004; 73:351-358

Rogers PB, Plowman PN, Harris SJ and Arlett CF, Four radiation hypersensitivity cases and their implications for clinical radiotherapy. Radiother. Oncol. 2000; 57:143-154

Roth CW, Kobeski F, Walter MF, and Biessmann H, Chromosome end elongation by recombination in the mosquito Anopheles gambiae. Mol Cell Biol 1997; 17:5176-5183

Rubio MA, Kim SH and Campisi J, Reversible manipulation of telomerase expression and telomere length. Implications for the ionizing radiation response and replicative senescence of human cells. J Biol Chem 2002; 277:28609-28617

Rufer N, Dragowska W, Thornbury G, Roosnek E, Lansdorp PM, Telomere length dynamics in human lymphocyte subpopulations measured by flow cytometry. Nat Biotech 1998; 16:743-747

Rufer N, Brummendorf TH, Kolvraa S, Bischoff C, Christensen K, Wadsworth L, Schulzer M, Lansdorp PM, Telomere fluorescence measurements in granulocytes and T lymphocyte subsets point to a high turnover of hematopoietic stem cells and memory T cells in early childhood. J Exper Med 1999; 190:157-167

Ruggero D, Wang ZG, and Pandolfi PP, The puzzling multiple lives of PML and its role in the genesis of cancer. Bioessays 2000; 22:827-835

Sallinen P, Miettinen H, Sallinen SL, Haapasalo H, Helin H, Kononen J, Increased expression of telomerase RNA component is associated with increased cell proliferation in human astrocytomas. Am J Pathol 1997; 150:1159-1164

Sambrook J, Fritsch E F, Maniatis T, Molecular cloning: A laboratory Manual, Cold Spring Harbor Laboratory Press, New York, 1989

Samper E, Goytisolo FA, Slijepcevic P, van Buul PP and Blasco MA, Mammalian Ku86 protein prevents telomeric fusions independently of the length of TTAGGG repeats and the G-strand overhang. EMBO Rep. 2000; 1:244-252

Samper E, Goytisolo FA, Menissier-de Murcia J, Gonzalez-Suarez E, Cigudosa JC, de Murcia G, Blasco MA, Normal telomere length and chromosomal end capping in poly(ADP-ribose) polymerase-deficient mice and primary cells despite increased chromosomal instability. J Cell Biol 2001; 154:49-60

Samper E, Fernandez P, Eguia R, Martin-Rivera L, Bernad A, Blasco MA, and Aracil M, Long-term repopulating ability of telomerase-deficient murine hematopoietic stem cells. Blood 2002; 99:2767-2775

Sano T, Asai A, Mishima K, Fujimaki T, Kirino T, Telomerase activity in 144 brain tumours. Br J Cancer 1998; 77:1633-1637

Sanson M, Cornu P, Biology of meningiomas. Acta Neurochir (Wien) 2000; 142:493-505

Sawyer JR, Husain M, Lukacs JL, Stangeby C, Binz RL, Al-Mefty O, Telomeric fusion as a mechanism for the loss of 1p in meningioma. Can Gen Cytogen 2003; 145:38-48

Schnapp G, Rodi HP, Rettig WJ, Schnapp A, Damm K, One-step affinity purification protocol for human telomerase. Nucleic Acids Res 1998; 26:3311-3313

Scheding S, Ersoz I, Hartmann U, Bartolvic K, Balabanov S, Salama A, Kanz L, and Brummendorf TH, Peripheral blood cell telomere length measurements indicate that hematopoietic stem cell turnover is not significantly increased in whole blood and apheresis PLT donors. Transfusion 2003; 48:1089-1095

Scheel C, Schaefer KL, Jauch A, Keller M, Wai D, Brinkschmidt C, van Valen F, Boecker W, Dockhorn-Dworniczak B, and Poremba C, Alternative lengthening of telomeres is associated with chromosomal instability in osteosarcomas. Oncogene 2001; 20:3835-3844

Scheel C and Poremba C, Telomere lengthening in telomerase-negative cells: the ends are coming together. Virch Archive 2002; 440:573-582

Scully R, Chen J, Plug A, Xiao Y, Weaver D, Association of BRCA1 with RAD51 in mitotic and meiotic cells. Cell 1997; 88:265-275

Seeler JS, and Dejean A, The PML nuclear bodies: actors or extras? Current Opinion in Gen Dev 1999; 9:362-367

Seal S, Barfoot R, Jayatilake H, Smith P, Evaluation of Fanconi Anemia Genes in Familial Breast Cancer Predisposition. Cancer Res 2003; 63:8596-8599

Sharan SK, Morimatsu M, Albrecht U, Lim DS, Embryonic lethality and radiation hypersensitivity mediated by Rad51 in mice lacking Brca2. Nature 1997; 386:804-810

Shen, SX, Weaver Z, Xu X, Li C, A targeted disruption of the murine Brca1 gene causes gamma-irradiation hypersensitivity and genetic instability. Oncogene 1998; 17:3115-3124

Shiloh Y, and Lehmann AR, Maintaining integrity. Nat Cell Biol 2004; 6:923-928

Simon M, Park T-W, Leuenroth S, Hans VHJ, Löning T, Schramm J, Telomerase activity and expression of the telomerase catalytic subunit, hTERT, in meningioma progression. J Neurosurg 2000; 92:832-840

Simon M, Park TW, Koster G, Mahlberg R, Hackenbroch M, Bostrom J, Loning T, Schramm J, Alterations of INK4a(p16-p14ARF)/INK4b(p15) expression and telomerase activation in meningioma progression. J Neurooncol 2001; 55:149-158

Sirri V, Roussel P, Hernandez-Verdun D, The AgNOR proteins: qualitative and quantitative changes during the cell cycle. Micron 2000; 31:121-126

Siwicki JK, Degerman S, Chrzanowska KH, Roos G, Telomere maintenance and cell cycle regulation in spontaneously immortalized T-cell lines from Nijmegen breakage syndrome patients. Exp Cell Res 2003; 287:178-189

Slijepcevic P, Hande MP, Bouffler S, Lansdorp P, and Bryant P, Telomere length, chromatin structure and chromosome fusigenic potential. Chromosoma 1997; 106:413-421

Slijepcevic P, Bryant PE, Chromosome healing, telomere capture and mechanisms of radiation-induced chromosome breakage. Int J Rad Biol 1998; 73:1-13

Slijepcevic P, Telomere length measurement by Q-FISH. Meth Cell Sci 2001; 23:17-22

Slijepcevic P, Telomeres and the control of cell division. In: Hughes D and Mehmet H, editors. Cell proliferation and apoptosis. Oxford: Bioscience Scientific Publishers; 2003; 123-145

Slijepcevic P, Is there a link between radiosensitivity and telomere maintenance? Rad Res 2004; 161:82-86

Smilenov LB, Morgan SE, Mellado W, Sawant SG, Kastan MB, and Pandita TK, Influence of ATM function on telomere metabolism. Oncogene 1997; 15:2659-2665

Smogorzewska A, van Steensel B, Bianchi A, Oelmann S, Schaefer MR, Schnapp G, de Lange T, Control of human telomere length by TRF1 and TRF2. Mol Cell Biol 2000; 20:1659-1668

Smogorzewska A, Karlseder J, Holtgreve-Grez H, Jauch A, and de Lange T, DNA ligase IV-dependent NHEJ of deprotected mammalian telomeres in G1 and G2. Curr Biol 2002; 12:1635-1644

Snouwaert JN, Gowen LC, Latour AM, Mohn AR, Xiao A, DiBiase L, Koller BH, BRCA1 deficient embryonic stem cells display a decreased homologous recombination frequency and an increased frequency of non-homologous recombination that is corrected by expression of a brca1 transgene. Oncogene 1999; 18:7900-7907.

Soder AI, Going JJ, Kaye SB, Keith WN, Tumour specific regulation of telomerase RNA gene expression visualized by in situ hybridization. Oncogene 1998; 16:979-983

Song K, Jung D, Jung Y, Lee SG, Lee I, Interaction of human Ku70 with TRF2. FEBS Letter 2000; 481:81-85

Sprung CN, Bryan TM, Reddel TM, and Murane JP, Normal telomere maintenance in immortal ataxia telangiectasia cell lines. Mut Res 1997; 379:177-184

Stewart GS, Wang B, Bignell CR, Taylor AM, and Elledge SJ, MDC1 is a mediator of the mammalian DNA damage checkpoint. Nature 2003; 421:961-966

Sugino T, Yoshida K, Bolodeoku J, Tarin D, Goodison S, Telomerase activity and its inhibition in benign and malignant breast lesions. J Pathol 1997; 183:57-61

Sugita Y, Nakashima A, Kato S, Sakata K, Morimatsu M, and Shigemori M, Telomerase activity in gliomas with the use of non-radioisotopic and semi-quantitative procedure for terminal repeat amplification protocol. Oncology Rep 2000; 7:1087-1092

Surrallés J, Jackson JP, Jasin M, Kastan MB, West SC, and Joenje H, Molecular cross-talk among chromosome fragility syndromes. Gen Dev 2004; 18:1359-1370

Symington LS, Role of RAD52 epistasis group genes in homologous recombination and double-strand break repair. Microbiol. Mol. Biol. Rev. 2002; 66:630-670

Thacker J, The RAD51 gene family, genetic instability and cancer. Cancer Letter 2004; xx:1-11

Takai H, Smogorzewska A, de Lange T, DNA damage foci at dysfunctional telomeres. Curr Biol 2003; 13:1549-1556

Takakura M, Kyo S, Kanaya T, Tanaka M, Inoue M, Expression of human telomerase subunits and correlation with telomerase activity in cervical cancer. Cancer Res 1998; 58:1558-1561

Takakura M, Kyo S, Kanaya T, Hirano H, Takeda J, Yutsudo M, Inoue M, Cloning of human telomerase catalytic subunit (hTERT) gene promoter and identification of proximal core promoter sequences essential for transcriptional activation in immortalized and cancer cells. Cancer Res 1999; 59:511-557

Takata M, Sasaki MS, Sonoda E, Morrison C, Hashimoto M, Utsimi H, Homologous recombination and non-homologous end-joining pathways of DNA double-strand repair have overlapping roles in maintenance of chromosomal integrity in vertebrate cells. EMBO 1998; 17:5497-5508

Tarsounas M, Munoz P, Claas A, Smiraldo PG, Pittman DL, Blasco MA, West SC, Telomere maintenance requires the RAD51D recombination/repair protein. Cell 2004; 117:337-347

Taylor AM, Harnden DG, Arlett CF, Harcourt SA, Lehmann AR, Stevens S and Bridges BA, Ataxia telangiectasia: a human mutation with abnormal radiation sensitivity. Nature 1975; 258: 427-429

Tchirkov A and Lansdorp PM, Role of oxidative stress in telomere shortening in cultured fibroblasts from normal individuals and patients with ataxia-telangiectasia. Hum. Mol. Genet. 2003; 12:227-32

Terasaki Y, Okumura H, Ohtake S, Nakao S, Accelerated telomere length shortening in granulocytes: a diagnostic marker for myeloproliferative diseases. Exper Hematol 2002; 30:1399-13404

Tischkowitz MD and Hodgson SV, Fanconi anaemia. J Med Gen 2003; 40:1-10

Teng SC and Zakian VA, Telomere-telomere recombination is an efficient bypass pathway for telomere maintenance in Saccharomyces cerevisiae. Mol Cell Biol 1999; 19:8083-8093

Thompson LH, Schild D, Recombinational DNA repair and human disease. Mut Res 2002; 509:49-78

Tomaska L, McEachern MJ, and Nosek J, Alternatives to telomerase: keeping linear chromosomes via telomeric circles. FEBS Letters 2004; 567:142-146

Tuteja R, Tuteja N, Nucleolin: a multifunctional major nucleolar phosphoprotein. Crit Rev Biochem Mol Biol 1998; 33:407-436

Ulaner GA, Guidice L, Developmental regulation of telomerase activity in human fetal tissues during gestation. Mol Hum Reprod 1997; 3:769-773

Ulaner GA, Hu J-F, Vu TH, Oruganti H, Giudice LC, Hoffman AR, Telomerase activity in human development is regulated by human telomerase reverse transcriptase (hTERT) transcription and by alternate splicing of hTERT transcripts. Cancer Res 1998; 58:4168-4172

Ulaner GA, Hu J-F, Vu TH, Oruganti H, Giudice LC, Hoffman AR, Regulation of telomerase by alternate splicing of human telomerase reverse transcriptase (hTERT) in normal and neoplastic ovary, endometrium and myometrium. Int J Cancer 2000; 85:330-335

Ulaner GA, Hu JF, Vu TH, Giudice LC, Hoffman AR, Tissue-specific alternate splicing of human telomerase reverse transcriptase (hTERT) influences telomere lengths during human development. Int J Cancer 2001; 91:644-649

van der Burgt I, Chrzanowska KH, Smeets D, and Weemaes C, Nijmegen breakage syndrome. J Med Gen 1996; 33:153-156

Varon R, Vissinga C, Platzer M, Cerosaletti KH, Chrzanoska KH, Sarr K, Beckmann G, Seemanova E, Cooper PR, Nowak NJ, and Reis A, Nibrin, a novel DNA double-strand break repair protein, is mutated in Nijmegen breakage syndrome. Cell 1998; 93:467-476

van Steensel B, de Lange T, Control of telomere length by the human telomeric protein TRF1. Nature 1997; 385:740-743

van Steensel B, Smogorzewska A, de Lange T, TRF2 protects human telomeres from end-to-end fusions. Cell 1998; 92:401-413

Van Ziffle JA, Baerlocher GM, and Lansdorp PM, Telomere length in subpopulations of human hematopoietic cells. Stem Cells 2003; 21:654-660

Venkitaraman AR, Cancer susceptibility and the functions of BRCA1 and BRCA2. Cell 2002; 108:171-182

von Zglinicki T, Pilger R, and Sitte N, Accumulation of single-strand breaks is the major cause of telomere shortening in human fibroblasts. Free Radic Biol Med 2000; 28:64-74

von Zglinicki T, Oxidative stress shortens telomeres. Trends Biochem Sci 2002; 27: 339-344.

Wang Y, Cortez D, Yazdi P, Neff N, Elledge SJ, and Qin J, BASC, a super complex of BRCA1-associated proteins involved in the recognition and repair of aberrant DNA structure. Gen Dev 2000; 14:927-939

Wang H, Zeng ZC, Bui TA, DiBiase SJ, Qin W, Xia F, Powell SN, and Iliakis G, Nonhomologous end-joining of ionising radiation-induced DNA double-stranded breaks in human tumor cells deficient in BRCA1 or BRCA2. Cancer Res 2001; 61:270-277

Wang RC, Smogorzewska A, and T de Lange, Homologous recombination generates T-loop-sized deletions at human telomeres. Cell 2004; 119:355-368

Wang S and Zhu J, The hTERT gene is embedded in a nuclease-resistant chromatin domain. JBC 2004 in press

Weaver Z, Montagna C, Xu X, Howard T, Gadina M, Brodie SG, Deng CX, Ried T, Mammary tumors in mice conditionally mutant for *Brca1* exhibit gross genomic instability and centrosome

amplification yet display a recurring distribution of genomic imbalances that is similar to human breast cancer. Oncogene 2002; 21:5097-5107

Weemaes CM, Hustinx TW, Scheres JM, van Munster PJ, Bakkeren JA, and Taalman RD, A new chromosomal instability disorder: the Nijmegen breakage syndrome. Acta Paediatr Scand 1981; 70:557-564

Weemaes CMR, Smeets DFCM, and van der Burgt CJAM, Nijmegen breakage syndrome: a progress report. Int J Rad Biol 1994; 66:S185-S188

Wei C, Skopp R, Takata M, Takeda S, and Price CM, Effects of double-strand break repair proteins on vertebrate telomere structure. Nucl Acids Res 2002; 30:2862-2870

Weinrich SL, Pruzan R, Ma LB, Ouellette M, Tesmer VM, Holt SE, Bodnar AG, Lichsteiner S, Kim NW, Trager JB, Taylor RD, Carlos R, Andrews WH, Wright WE, Shay JW, Harley CB, Morin GB, Reconstitution of human telomerase with the template RNA component hTR and the catalytic protein subunit hTRT. Nat Genet 1997; 17:498-502

Wellinger RJ, Ethier K, Labrecque P, Zakian VA, Evidence for a new step in telomere maintenance. Cell 1996; 85:423-433

Wege H, Chui MS, Le HT, Tran JM and Zern MA, SYBR Green real-time telomeric repeat amplification protocol for the rapid quantification of telomerase activity. Nucl Acids Res 2003; 31:e3

Whittle IR, Smith C, Navoo P, and Collie D, Meningiomas. The Lancet 2004; 363:1535-1543

Wick M, Zubov D, Hagen G, Genomic organization and promoter characterization of the gene encoding the human telomerase reverse transcriptase (hTERT). Gene 1999; 232:97-106

Wilson CA, Ramos L, Villasenor MR, Anders KH, Press MF, Localization of human BRCA1 and its loss in high-grade, non-inherited breast carcinomas. Nature 1999; 21:236-240

Wong KK, Chang S, Weiler SR, Ganesan S, Chaudhuri J, Zhu C, Artandi SE, Rudolph KL, Gottlieb GJ, Chin L, Alt FW and DePinho RA, Telomere dysfunction impairs DNA repair and enhances sensitivity to ionizing radiation. Nat. Genet. 2000; 26:85-88

Wong JM, Kusdra L, and Collins K, Subnuclear shuttling of human telomerase induced by transformation and DNA damage. Nat Cell Biol 2002; 4:731-736

Wong H-P and Slijepcevic P, Telomere length measurement in mouse chromosomes by a modified Q-FISH method. Cyt Gen Res 2004; 105:464-470

Wright WE, Shay JW, Piatyszek MA, Modifications of a telomeric repeat amplification protocol (TRAP) result in increased reliability, linearity and sensitivity. Nucl Acids Res 1995; 23:3794-3795

Wright WE, Piatyszek MA, Rainey WE, Byrd W, Shay JW, Telomerase activity in human germline and embryonic tissues and cells. Dev Gen 1996; 18:173-179

Wright WE, Tesmer VM, Huffman KE, Levene SD, Shay JW, Normal human chromosomes have long G-rich telomeric overhangs at one end. Gen Dev 1997; 11:2801-2809

Wu A, Ichihashi M, Ueda M, Correlation of the expression of human telomerase subunits with telomerase activity in normal skin and skin tumors. Cancer 1999; 86:2038-2044

Wu G, Lee WH. and Chen PL, NBS1 and TRF colocalize at promyelocytic leukaemia bodies during later S/G2 phases in immortalised telomerase negative cells: implication of NBS1 in alternative lengthening of telomeres. J Biol Chem 2000; 275:30618-30622

Wu G, jiang X, Lee WH, and Chen PL, Assembly of functional ALT-associated leukaemia bodies requires Nijmegen Breakage syndrome 1. Cancer Res 2003; 63:2589-2595

Wu X, Amos CI, Zhu Y, Zhao H, Grossman BH, Shay JW, Luo S, Hong WK and Spitz MR, Telomere dysfunction: a potential cancer predisposition factor. J Nat Can Inst 2003; 95:1211-1218

Wullich B, Rohde V, Oehlenschläger B, Bonkhoff H, Ketter R, Zwergel T, Sattler H-P, Focal intratumoral heterogeneity for telomerase activity in human prostate cancer. J Urol 1997; 161:1997-2001

Wynford-Thomas D, Cellular senescence and cancer. J Pathol 1999; 187:100-111

Xiong J, Fan S, Meng Q, Schramm L, Wang C, Bouzahza B, Zhou J, Zafonte B, Goldberg ID, Haddad BR, Pestell RG, and Rosen EM, BRCA1 inhibition of telomerase activity in cultured cells. Mol Cell Biol 2003; 23:8668-8690

Xu D, Gruber A, Bjorkholm M, Peterson C, and Pisa P, Suppression of telomerase reverse transcriptase (hTERT) expression in differentiated HL-60 cells: regulatory mechanisms. Brit J Can 1999; 80: 156-1161

Xu X, Wagner KU, Larson D, Weaver Z, Li C, Reid T, Hennighausen L, Wynsaw-Boris A, Deng C-X: Conditional mutation of *BRCA1* in mammary epithelial cells results in blunted ductal morphogenesis and tumor formation. Nat Gen 1999; 22:37-43

Yan P, Coindre J-M, Benhattar J, Bosman FT, Guillou L, Telomerase activity and human telomerase reverse transcriptase mRNA expression in soft tissue tumors: correlation with grade, histology, and proliferative activity. Cancer Res 1999; 59:3166-3170

Yan P, Saraga EP, Bouzourene H, Bosman FT, Benhattar J, Expression of telomerase genes correlates with telomerase activity in human colorectal carcinogenesis. J Pathol 2001; 193:21-26

Yang H, Jeffrey PD, Miller J, Kinnucan E, *BRCA2* function in DNA binding and recombination from a BRCA2-DSS1-ssDNA structure. Science 2002; 297:1837-1848

Yang Y, Cheng Y, Zhang C, Huang H, and Weissman SM, Nucleolar localization of hTERT protein is associated with telomerase function. Experim Cell Res 2002; 277:201-209

Ye JZ, de Lange T, TIN2 is a tankyrase 1 PARP modulator in the TRF1 telomere length control complex. Nat Genet 2004; 36:618-823

Yeager TR, Neumann AA, Englezou A, Huschtscha LI, Noble JR, and Reddel RR, Telomerase-negative immortalised human cells contain a novel type of promyelocytic leukaemia (PML) body. Cancer Res 1999; 59:4175-4179

Yi X, White DM, Aisner DL, Baur JA, Wright WE, and Shay JW, An alternative splicing variant of the human telomerase catalytic subunit inhibits telomerase activity. Neoplasia 2000; 2:433-440

Yi X, Shay JW, and Wright WE, Quantitation of telomerase components and hTERT mRNA splicing patterns in immortal human cells. Nucl Acids Res 2001;29: 4818-4825

Zhong Q, Chen CF, Li S, Chen Y, Wang CC, Xiao J, Chen PL, Sharp ZD, and Lee WH, Association of BRCA1 with the hRad50-hMre11-p95 complex and the DNA damage response. Science 1999; 285:747-750

Zhong Q, Boyer TG, Chen PL, and Lee WH, Deficient non-homologous end-joining activity in cell-free extracts from Brca1-null fibroblasts. Cancer Res 2002; 62:3966-3970

Zhong Q, Chen CF, Chen PL, and Lee WH, *BRCA1* facilitates microhomology-mediated end joining of DNA double strand breaks. J Biol Biochem 2002; 277:28641-28647

Zhou C and Liu J, Inhibition of human telomerase reverse transcriptase gene expression by BRCA1 in human ovarian cancer cells. Biochem Biophys Res Com 2003; 303:130-136

Zhu J, Wang H, Bishop JM, and Blackburn EH, Telomerase extends the lifespan of virus-transformed human cells without net telomere lengthening. Proc Natl Acad Sci USA 1999; 96:3339-3341

Zhu XD, Kuster B, Mann M, de Petrini JHJ, and de Lange T, Cell-cycle regulated association of RAD50/MRE11/NBS1 with TRF2 and human telomeres. Nat Gen 2000; 25:347-352

Zhu XD, Niedernhofer L, Kuster B, Mann M, Hoeijmakers JHJ and de Lange T, ERCC1/XPF removes the 3' overhang from uncapped telomeres and represses formation of telomeric DNA-containing double minute chromosomes. Mol. Cell 2003; 12:1489-1498

Zhu Y, Tomlinson RL, Lukowiak AA, Terns RM, and Terns MP, Telomerase RNA accumulates in Cajal bodies in human cancer cells. Mol Biol Cell 2004; 15:81-90

Zijlmans JM, Martens UM, Poon SS, Raap AK, Tanke HJ, Ward RK, Lansdorp PM, Telomeres in the mouse have large inter-chromosomal variations in the number of T2AG3 repeats. Proc Nat Acad Sci U S A 1997; 94:7423-7428